AD_________________

Award Number: W81XWH-07-2-0084

TITLE: Measurement of Forces and Moments Transmitted to the Residual Limb

PRINCIPAL INVESTIGATOR:
Edward S. Neumann, PhD, PE, CP
Woosoon Yim, PhD

CONTRACTING ORGANIZATION:
University of Nevada, Las Vegas
Las Vegas, NV 89154-1037

REPORT DATE: October 2010

TYPE OF REPORT: Final

PREPARED FOR: U.S. Army Medical Research and Materiel Command
Fort Detrick, Maryland 21702-5012

DISTRIBUTION STATEMENT:

Approved for public release; distribution unlimited

REPORT DOCUMENT PAGE

1. REPORT DATE *(DD-MM-YYYY)* 01-10-2010

2. REPORT TYPE Final

3. DATES COVERED *(From - To)* 24 AUG 2007-20 SEP 2010

4. TITLE AND SUBTITLE

Measurement of Forces and Moments Transmitted to the Residual Limb

5a. CONTRACT NUMBER

5b. GRANT NUMBER W81XWH-07-2-0084

5c. PROGRAM ELEMENT NUMBER

6. AUTHOR(S)

Edward S. Neumann, PhD, PE, CP; Kartheek Yalamanchili, MSE, EI; Justin Brink, BS Kin; Joon Lee, PhD

5d. PROJECT NUMBER

5e. TASK NUMBER

5f. WORK UNIT NUMBER

7. PERFORMING ORGANIZATION NAME(S) AND ADDRESS(ES)

University of Nevada, Las Vegas

Las Vegas, NV 89154-1037

8. PERFORMING ORGANIZATION REPORT NUMBER

9. SPONSORING / MONITORING AGENCY NAME(S) AND ADDRESS(ES)

U.S. Army Medical Research aand M Fort Detrick, Maryland 21702-5012

10. SPONSOR/MONITOR'S ACRONYM(S)

11. SPONSOR/MONITOR'S REPORT NUMBER(S)

12. DISTRIBUTION / AVAILABILITY STATEMENT

Approved for public release; distribution unlimited

13. SUPPLEMENTARY NOTES

4. ABSTRACT Forces and moments are measured using a tri-axial transducer and compared across different feet, activities, and subjects. Regression models estimate intra-socket pressures as a function of the forces, moments, and alignments.

15. SUBJECT TERMS

Amputees, prosthesis alignment, socket pressure, gait, force and moment sensors

16. SECURITY CLASSIFICATION OF: U			17. LIMITATION OF ABSTRACT	18. NUMBER OF PAGES	19a. NAME OF RESPONSIBLE PERSON USAMRMC
a. REPORT U	b. ABSTRACT U	c. THIS PAGE U	UU	184	19b. TELEPHONE NUMBER *(include area code)*

Standard Form 298 (Rev. 8-98)
Prescribed by ANSI Std. Z39.18

Table of Contents

Introduction

The purpose of the project entitled "Measurement of the Forces and Moments Transmitted to the Residual Limb" was to evaluate the feasibility of using a tri-axial transducer mounted to the pylon of a lower limb prosthesis directly below the socket to a.) Characterize and evaluate the performance of prosthetic components such as feet, and b.) Estimate the pressures occurring on the residual limb as a result of these components. Success in achieving these two goals would mean that off-the-shelf instrumentation is available that could be used in prosthetic clinics to assist in prescribing components, to evaluate amputee rehabilitation progress, and to develop specifications for components capable of battle-field use or use in other activities for which conventional prosthetic components may not perform adequately. The project obtained a commercially available transducer used in robotics applications (45E15A4 made by JR3, Inc), developed a GUI for processing the data, developed a wireless system for transmitting the data remotely to a laptop, and employed a convenience sample of four transtibial amputee subjects for data collection. Tekscan's F-Socket pressure sensing system was used to record intra-socket pressures. Experimental data were collected from the subjects as they walked in a variety of environments including level walking at a self-selected comfortable speed, walking up and down a ramp, walking up and down steps, walking across a grassy slope with the prosthetic foot uphill and downhill, and walking in a circle with a diameter of ten feet with the prosthetic foot on the inside and outside. The body of this report describes in more detail the transducer (Chapter 1), the GUI (Chapter 2), and the design of the experiment (Chapter 3). Analyses of the data to assess the achievement of goal a. are presented in Chapter 4 which compares activities and feet, and Chapter 5, which compares the performance of a SACH foot of identical design across three different subjects. Analyses of pressure data to assess achievement of goal b. are presented in Chapter 6, which evaluates use of the data to develop pressure models by means of regression analysis. Results are compared for an acceptable alignment and two perturbations which move the foot anterior and posterior by 5mm. Chapter 7 examines the use of subjective measures of discomfort that subjects reported for the alignment perturbations. Chapter 8 briefly discusses potential clinical applications of the research. Key Research Outcomes are discussed following Chapter 8, and the Conclusions section describes the contributions of the research to clinical practice as well as to research on prosthetic component design.

1. Transducer Instrumentation

Transducer Electronics

A tri-axial transducer, model OTESTSENSOR 45E15A4 with digital output, was ordered from JR3, Inc on 10 September 2007 and received on 21 December 2007. A data processing board and related electronic instrumentation also was ordered on 13 September 2007. The top and bottom of the transducer were machined by JR3 to have four bolt holes in the standard pattern used in prosthetics so that standard prosthetic adaptors could be attached. The heart of the force sensing system is a tri-axial transducer, model 1000N125 from JR3, Inc. The data recording components for the JR3 tri-axial transducer require portability and wireless operation so that it can be carried by a research subject in a variety of environments outside of the laboratory. To satisfy the required conditions, the research team developed the force sensing system by using a PC104/Plus bus-based compact system with a battery power pack and Wi-Fi wireless network access. Figure 1 shows the block diagram of the force sensor system. A PC104/Plus bus based 32bit AMD single board computer comprises the master computer, and the embedded operating system features Windows XP Embedded. The force sensor is connected to the single board computer and DSP processing interface board via a high speed interface cable. The force sensor system is remotely controlled from the operator computer using a Wi-Fi wireless network featuring up to 50Mbytes speed. Table 1 describes the specifications of the force sensor system. The figure 2 is a picture of the force sensor system.

The force sensor system software was developed using Microsoft Windows XP Embedded which allows a compact size Windows XP operating system to be installed on the single board computer. The operating system enables flexible component selection from thousands of existing Windows applications and drives. Figure 3 shows the Windows dialog developed for displaying instantaneous forces and moments at the operator computer interface. The program reads the force and moment data from the force sensor and saves it to a data file on the single board computer every 10 msec. A test that the system was functioning correctly was made by applying force manually to the transducer and observing the data reported in the display.

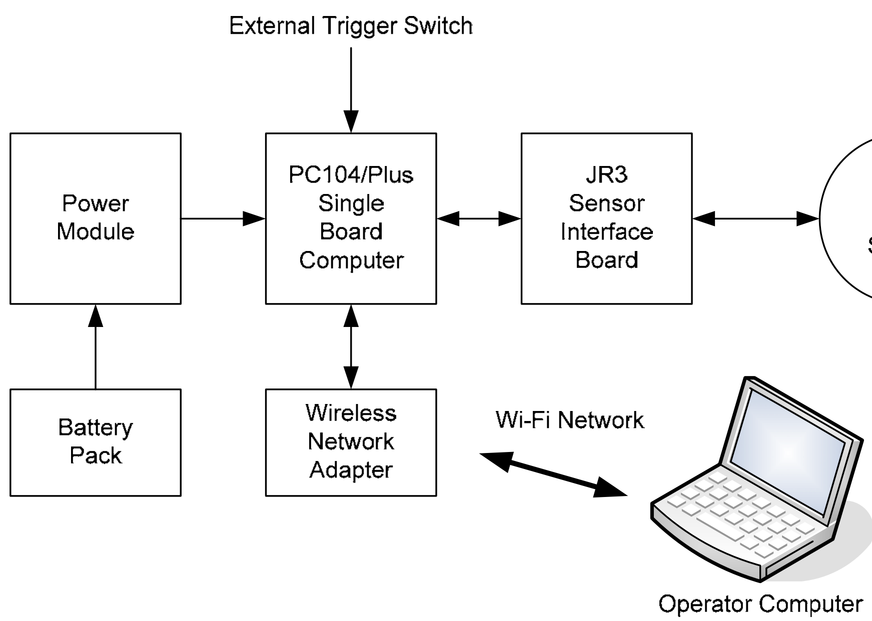

Figure 1-1. Force Sensor System Block Diagram

Table 1-1. Force Sensor System Specification

Item	Specification
Size	8.25 x 5 x 3 inch
Power Battery	14.8V 4400mAh
Computer	Industrial PC/104 Single Board Computer
SBC Operating System	Windows XP Embedded
Wi-Fi Network	Wireless-G with Speed Booster
Operator Computer	Windows XP with Remote Desktop Connection
Force Sensor	JR3 1000N125
Operating Time	above 60 min after complete charge
Minimum Sampling Time	10msec

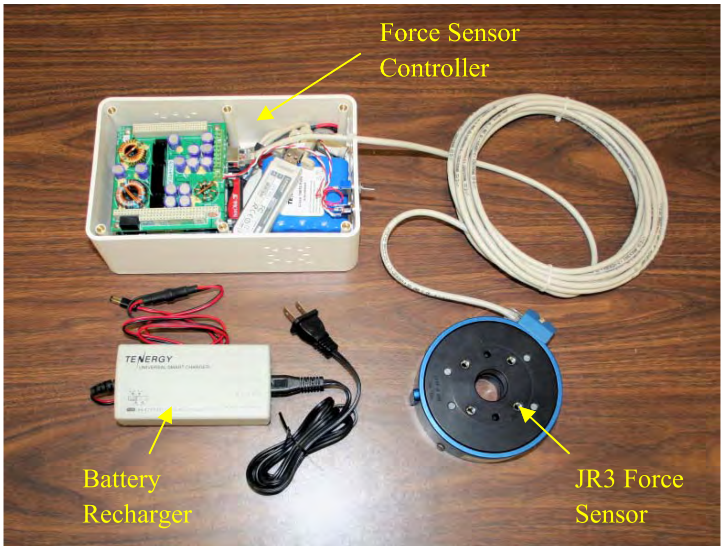

Figure 1-2. Picture of Force Sensor System

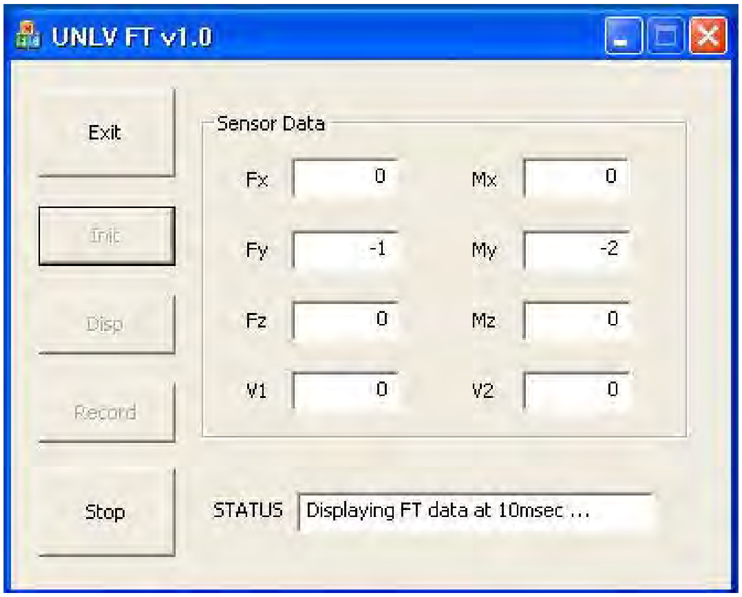

Figure 1-3. Dialog Box of Windows Program

Transducer Accuracy

The table below indicates the accuracy of the transducer along with other characteristics, as published by JR3. The transducer is sufficiently accurate for measuring the gait characteristics of subjects weighing up to nearly 500lbs, or activities which involve deceleration or acceleration forces of up to 500 lbs along the pylon of a prosthesis.

Diameter 4.50	in
Thickness 1.	50 in
Material A	L 2024
Mass 1.	75 lb
Nominal Accuracy, all axes	$\pm$ 0.25 % of measuring range
Operating Temperature Range, non-condensing	-40 to +150 F
Fx, Fy	
Standard Measurement Range	$\pm$ 250 lb
Standard Resolution	0.031 lb
Stiffness 0.	36e6 lb/in
Single-axis Overload	1550 lb
Fz	
Standard Measurement Range	$\pm$ 500 lb
Standard Resolution	0.063 lb
Stiffness 2.	83e6 lb/in
Single-axis Overload	4800 lb
Mx, My	
Standard Measurement Range	$\pm$1125 in-lb
Standard Resolution	0.14 in-lb
Stiffness 4.	79e6 in-lb/rad
Single-axis Overload	4400 in-lb
Mz	
Standard Measurement Range	$\pm$1125 in-lb
Standard Resolution	0.14 in-lb
Stiffness 1.	49e6 in-lb/rad
Single-axis Overload	3750 in-lb

.**Table 1-2. Transducer Accuracy**

Load Limits of the Transducer

The overload capabilities of the transducer actually allow loads greater than the standard measurement range. The following two equations can be used to determine whether multi-axis overloads will exceed the limits of the transducer:

$Fx/a + Fy/b + Fz/c + My/d + Mz/e \leq 1$, and

$Fx/b + Fy/a + Fz/c + My/d + Mz/e \leq 1$ where

a=1 700 lb
b =1550 lb
c=4 800 lb
d =4400 in-lb
e=3 750 in-lb

These limits make it unlikely that the transducer would be overloaded in activities deemed safe for humans. Examination of results for walking down steps revealed actual loads to be less than 25% of the load limits. The graphs below show the results of applying each equation. Numbers in the denominators are in English units, which should be converted into ISO units for computations. To convert pounds into Newtons a multiplier of 4.4 was used and to convert in-lbs into Newton-meters a multiplier of 0.112985 was used.

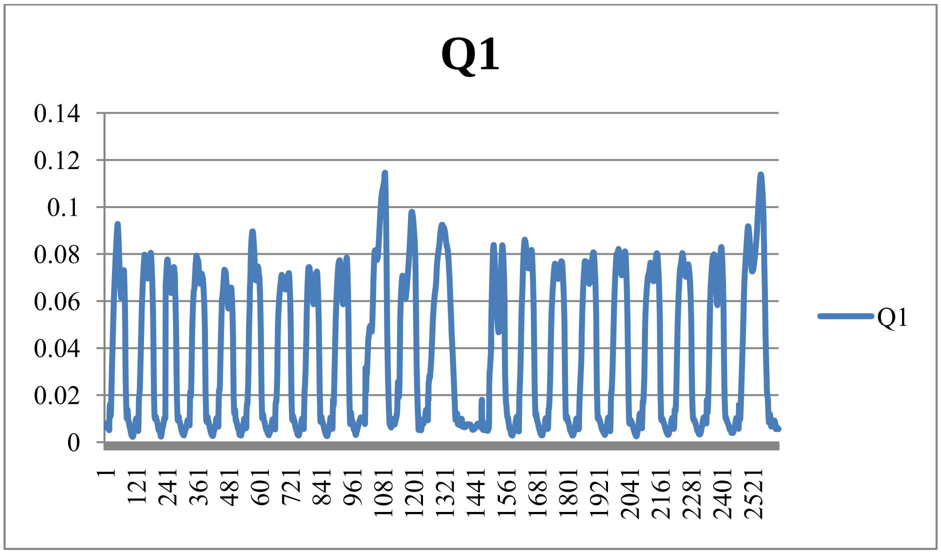

Figure 1-4. Values Obtained by Applying the First Overload Equation to Going Down Steps.

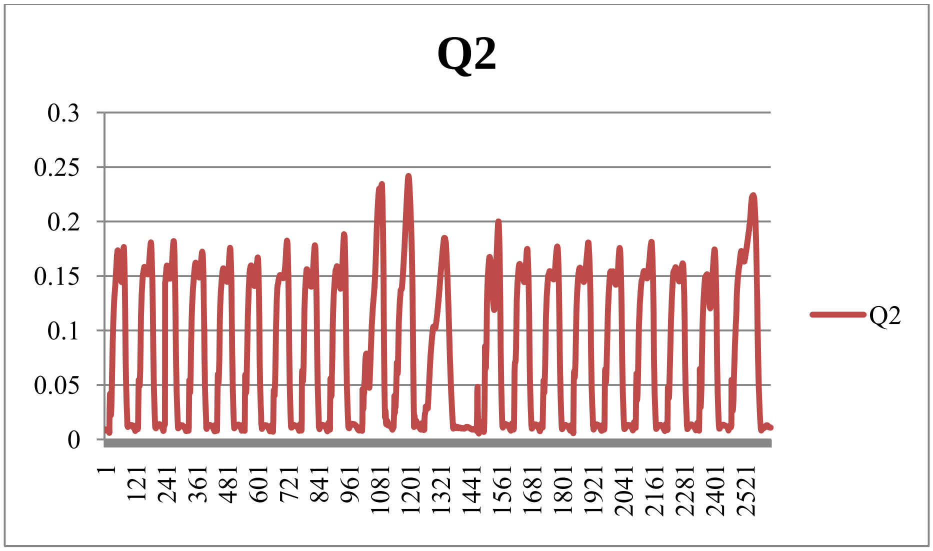

Figure 1-5. Values Obtained by Applying the Second Overload Equation to Going Down Steps.

The first picture below illustrates the orientation of the XYZ axes when the transducer is mounted in the configuration used for data collection, and the orientation used in this report. A right-handed orthogonal system, the Z axis is parallel to the pylon, the X axis is pointed toward the toes, and the Y axis is perpendicular to the pylon Z axis and the X axis. The second picture illustrates the transducer with standard prosthetic modular components attached (female adaptors) to allow attachment to the base of the socket. Build height is approximately 2.75 inches, or XX inches between the Allen screws. The third illustration below depicts the transducer with the Hosmer

Spectrum Alignment System attached, which was used for the alignment perturbation studies. Build height is approximately 4.25 inches. The third picture illustrates the computer and battery pack and the packpack for them.

NOTE: The transducer outputs force in Newtons (N) and moments in Newton-decimeters, or Newton meters X 10. All measurements except those in the graphs on pages 32-35 present data in Nm X 10. The graphs on pages 32-35 present moments in Nm.

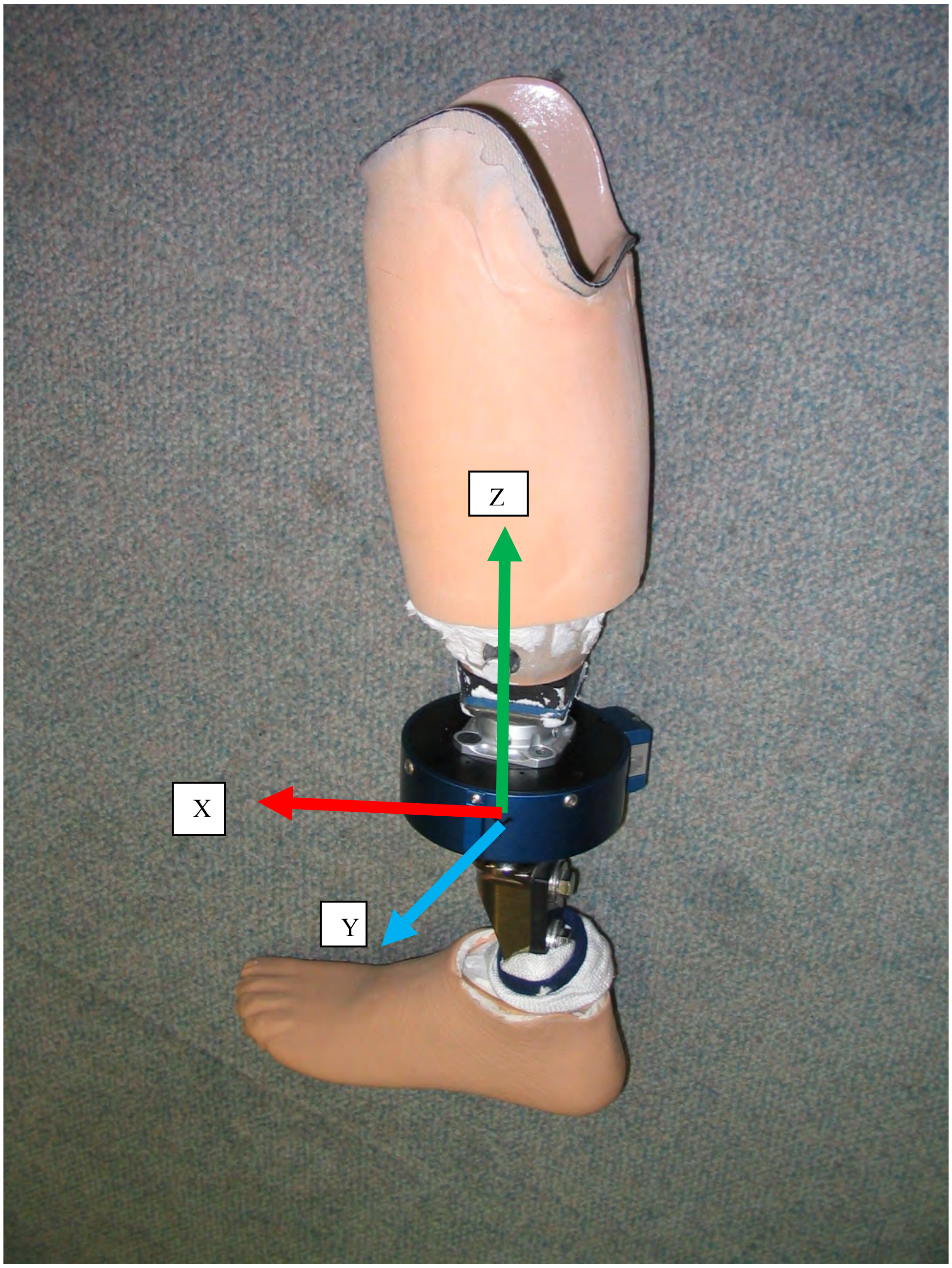

Figure 1-6. Orientation of Transducer Axes

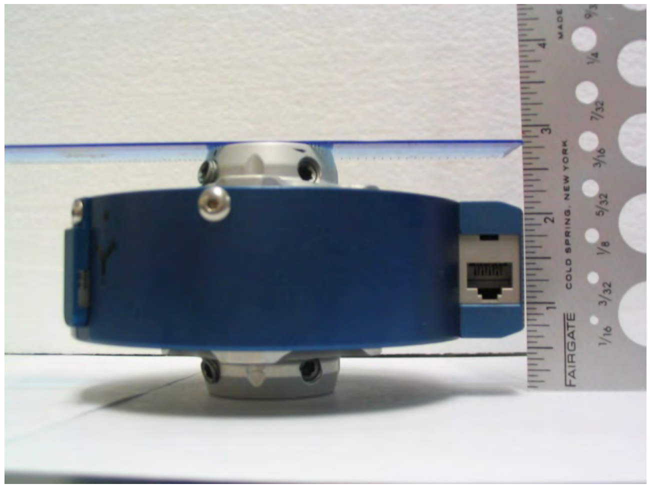

Figure 1-7. Transducer with Female Adaptors attached

Figure 1-8. Transducer with Hosmer Spectrum Alignment System Attached

Figure 1-9. Computer, Battery Pack, and Backpack

2. GUI for the Transducer and Pressure Data

Four main steps involved in the development of GUI software were: 1) the development of code for displaying and analyzing the data collected from the JR3 tri-axial transducer, which can measure forces and moments in three dimensions at the base of the socket; 2) the development of code for displaying and analyzing the data on pressure occurring inside the socket measured by means of the Tekscan pressure measurement system; 3) the development of code for merging data from the two previously mentioned sources in to one GUI display and, 4) the development of code that allows exporting the processed data in an EXCEL file format, which can be used in statistical analysis packages such as SPSS, and SYSTAT.

GUI Transducer Software

This section discusses the development and operation of software for analyzing the forces and moments data collected by the JR3 tri-axial transducer. A requirement existed for two separate methods of analyzing the transducer data: Requirement A called for normalized gait cycle which enabled steps of different duration to be compared, and Requirement B called for analysis of the actual (non-normalized) gait cycle which enabled loading rates and impulse to be calculated.

Requirement A: The goals of software design for data normalized in the time domain were to:

1. Display via the GUI, the continuous stream of data produced by the transducer during one walking trial for any of the three forces and three moments.

2, Convert the continuous flow of data during one walking trial into discrete gait cycles for analysis, and also display the discrete gait cycles by means of the GUI.

3. Normalize each discrete gait cycle so that gait cycles during the trial could be compared in the time domain;

    A. Subdivide each step into 50 discrete time intervals, so that each interval represents 2% of the gait cycle

    B. Assign sampling data points from the transducer into the correct time interval.

    C. Compute the mean and standard deviation of the 50 normalized intervals for the trial and display using the GUI.

    D. Compute the resultant mean force and mean moment for the trial, and the angle of the force with respect to the pylon axis.

    E. Copy the processed data into an EXCEL compatible file format for export.

Requirement B: The goals of software design for data not normalized in the time domain were to:

1. Compute the average loading rate beginning at heel contact over the trial and display the results.

2. Compute the average impulse for three separate stance phases (heel contact to first maximum, first maximum to second maximum, and second maximum to toe off) and the total stance phase and display the results.

3. Copy the processed data into an EXCEL compatible file format for export.

To achieve these goals the following decisions were made during the design phase of software development.

1. Prior to the use of transducer software and GUI, the raw data produced by the transducer should be opened and saved in an EXCEL file format. Data saved in the Excel file should then be fed into the transducer software.

2. Among the various variables that could be used to identify heel strike and to-off, the vertical force parallel to the pylon (Z-direction) should be used. The Z-direction force data should be displayed to show the continuous stream of all the steps together.

3, Individual gait cycles should be selected by inspection of the plot, rather than by an algorithm. For ease of selecting individual gait cycles, zoom-in, zoom-out and pointer options should be included in the window. For finding the exact heel contact and toe-off points the zoom- in option should be used, and for identifying the sample points the software pointer should be used. The location of the tip of the pointer over the point should provide the time of occurrence of the sample points that identify the beginning and end of the gait cycle. The end time for one gait cycle can be the start time for the next gait cycle unless it is preferred to examine only the stance phase. In this case the start and end times of stance should be determined.

4. After inputting the start and end points of individual gait cycles (or stance), the transducer force and moment data associated with each step should be divided into 50 intervals. For example if there are 350 transducer sample points associated with a single step, the software should calculate that there will be 7 sample points in each interval (350/5) and sort every 7 consecutive points into each of the 50 intervals in sequence. Then the software should compute the

average force or moment value of those 7 points in each interval and the GUI should display the plots of the mean values of each of the 50 intervals for each step (gait cycle).
5. After displaying the mean value of each step for each of the 50 intervals of the individual gait cycle, the software should calculate the means and standard deviations over all of the steps in the trial for each of the 50 intervals and plot them in a separate window.
6. The same procedure should be followed for calculating the means, standard deviations, loading rates and impulses of remaining forces in the other two directions and the moments in all three directions. The start and finish times of each gait cycle should be automatically brought forward from the definitions supplied by the user for the Z direction force, so that the same time points are used for forces and moments along the other two dimensions.
7. The resultant force and moment for the average of all the steps in the trial should be computed for each of the 50 intervals using the Pythagorean Theorem and displayed.
8. The angle of the resultant with the pylon should be calculated as the arctan of X/Z and Y/Z and displayed.
9. After calculation of means and standard deviation, the software should calculate the loading rate and impulse using actual times rather than normalized times.
10. After calculation of all these parameters, the resulting data should be exported into an Excel file format which can be used for input into statistical software such as SPSS, or SYSTAT.

GUI Software for Tekscan Data

This section discusses the goals for the development and operation of the software for merging and analyzing data collected using the Tekscan F-socket software to measure pressure on the residual limb at its interface with the socket. Requirements of the software interface design were to:
1. Utilize analysis capabilities inherent in the Tekscan software to the extent possible.
2. Create a visual display that allows the user to simultaneously inspect both transducer data and Tekscan data for correlation.
3. Develop Tekscan output files that can be merged with transducer software output files and used in statistical regression packages where the pressure data serve as the dependent variable and the transducer data serve as the independent variables.

Decisions made during the design of the Tekscan GUI follow:
1. The Tekscan F-socket data should be collected following the normal procedures that Tekscan recommends and make use of the software Tekscan provides. Using the Tekscan software, the user should open the downloaded movie and add a box or polygon to the window to extract pressure data from the region of the sensor that is of interest and prepare a plot of pressure versus time for the box or polygon using the data analysis capability within the Tekscan software.
2. Raw data from the Tekscan F-socket will be in matrix form (cell value versus time) with one entry for each cell of the sensor (92 cells in the case of the F-Socket); the raw sensor array, cannot be used in the software to analyze pressure unless it is calibrated and windowed using the Tekscan software. However, the data from the box or polygon described above will exist as a single value versus time. This data should be saved in ASCII format and exported from the Tekscan software after plotting the window or polygon. A Tekscan feature allows this.
3. This exported file should be opened in Excel and saved as an Excel file, so it can be inputdirectly into the software.
4. After the Tekscan data have been input into the GUI, the processing of it should follow the same steps used for the transducer data. For each gait cycle, the result should be 50 intervals, and the GUI should compare the means of the pressure data falling within the interval. Then the means and standard deviations over all the gait cycles in the trial should be computed so there are 50 means and standard deviations, one for each normalized interval.
5. At the end of processing the Tekscan data, a file should be created in Excel format that contains the values of the 50 means and standard deviations computed over all the gait cycles in the trial, which can be exported from the GUI and input into statistical software for further analysis.

In order to assist the user, additional decisions were made concerning the data display options to be made available in the GUI. It was the opinion of the research team that too many display options may make the software unwieldy and the data difficult to view. This section describes decisions made with respect to some constraints that were built into the GUI.
1. Curves showing the mean values of pressures inside the box or polygon should be displayed on the screen in a manner that allows the user to visually compare them to on the curves of the mean forces and moments computed over the trial. This would facilitate visual inspection of the data for potential correlations between pressure and the forces and moments.

2. Depending on the plane of the residual limb in which pressure measurement was undertaken with the Tekscan equipment, the forces and moments most likely to be related to pressure variation should be displayed. For pressures acting primarily on the frontal plane of the residual limb, the most likely sources of gait-related pressures were assumed to be forces acting in the X and Z directions and moments about the Y and Z axes. For pressures acting primarily on the sagittal plane of the residual limb, the most likely sources of gait-related pressures were assumed to be forces acting in the Y and Z directions and moments about X and Z axes.
3. In order to merge data from Tekscan with data from the tri-axial transducer and display both simultaneously, the pressure data should be sorted into 50 intervals following the same normalizing procedure used for the transducer data.
4. The two sources of data should be merged into one combined file in EXCEL format to facilitate export into available statistical packages. Regression analysis should not be carried out within the GUI software.

MATLAB
Different software packages and programming languages were evaluated for attaining the objectives including LabVIEW, Visual Basic, Mathcad., and MATLAB. Based on compatibility and ease of programming, Matlab was chosen. MATLAB is a fourth generation programming language and numerical computing environment. MATLAB can be used for plotting functions and data, implementation of algorithms, creations of user interfaces, matrix manipulation, and interfacing with programs in other languages. It is very easy working with MATLAB executable code, which doesn't require a second separate software package. A program written in MATLAB can be installed on a laptop without the need for installation of a comprehensive MATLAB background package. This made it desirable to choose MATLAB for developing the software.

Ten "Good Steps" Design
It was decided that the GUI should be designed to analyze the data from ten good steps that would be collected by having the subject walk continuously without the need to stop. Ten steps allowed collection of a large enough sample of gait cycles to compute means and standard deviations and conduct tests of significance on the means and standard deviations. It also allowed the design of an interactive GUI interface requiring only one window in which the starting and ending points of the steps could be entered. More than ten steps would require multiple windows on the laptop and make it difficult to use the GUI. If more than ten steps of data were needed, the data could still be collected continuously as the transducer collected and transmitted it, but the long file that resulted would need to be broken into multiple files prior to processing and the out EXCEL output files from the GUI merged. The experimental protocol called for approximately fifteen steps during a trial, which would allow several non-representative steps at the beginning and end of gait to be discarded. The design of the GUI also allowed other non-representative steps that occurred in the middle of a trial to be discarded, for example if the subject had to stop and turn around.

Problems Encountered and Solved
Problems encountered during the development of the GUI software using MATLAB and described below.
1. Clipping of a continuous stream of data into discrete steps: Initial plans were to develop a GUI that employed a pointer which could be positioned over a desired point on the raw data plot, and by clicking a mouse the starting and ending point of a step could be selected. In other words, the initial design concept was to develop software with which discrete steps could be selected manually (clipping) just by clicking on the desired start and end points. But restrictions in the MATLAB code prevented being able to do this, and it also was found to be impossible to use different colors to identify the curves of different individual gait cycles. To overcome this difficulty the use of a pointer was retained, but the means for identifying the start and end points was designed to utilize 10 edit boxes into which the values of the graph coordinates of the start and end points of each step could be entered manually.
2. Pointer: For entering the values for start and end points the user would need to know the exact values of the coordinates, which can be accomplished only by looking at the raw data plot. But it was difficult to determine exact values in a plot containing thousands of sample pints just by inspecting it with the naked eye. It took several months to find a solution to this problem. By looking at different options and asking for help on internet forums the problem was resolved successfully. To solve this problem, a pointer which displays the x and y values of the plot was incorporated into the GUI. These values are entered into the ten pairs of edit boxes described above.
3. One way mapping: Initially total data from the transducer file was plotted. But once plotted, it was not possible to go from the plot back into specific regions of the data file on which the plot was based. In other words, while individual gait cycles could be identified, it was not possible to pull those data out from the original transducer file and recover the values of the forces and moments recorded from the transducer. This made it impossible to further

process data and plot individual gait cycles or calculate means. To solve this problem, code was completely changed and rewritten using a different logic. Internet forum groups were called upon to help solve this problem.
4. Executable file: Problems occurred in converting the .m file of Matlab into an executable file that would work as a stand-alone application without any need of the original Matlab version installed on the target system. To solve this problem several websites, forum groups, and requested help online from MATLAB programmers was used.

The figures below illustrate the GUI windows for defining steps for the transducer and pressure variables. The GUI is described in the Appendix. During analysis of the data for this project, the EXCEL output files for the normalized data were used to prepare the graphs and undertake statistical analyses. While the GUI displays were essential for the initial processing of the data and the disaggregation of the stream of data into discrete steps, the EXCEL output files were of most use for analysis of the data. Several features of the GUI including the loading rate and impulse computations using the real-time data were not used due to time and resource limitations. Although the GUI also produced files of non-normalized real-time transducer data on the steps, these also were not examined due to time constraints.

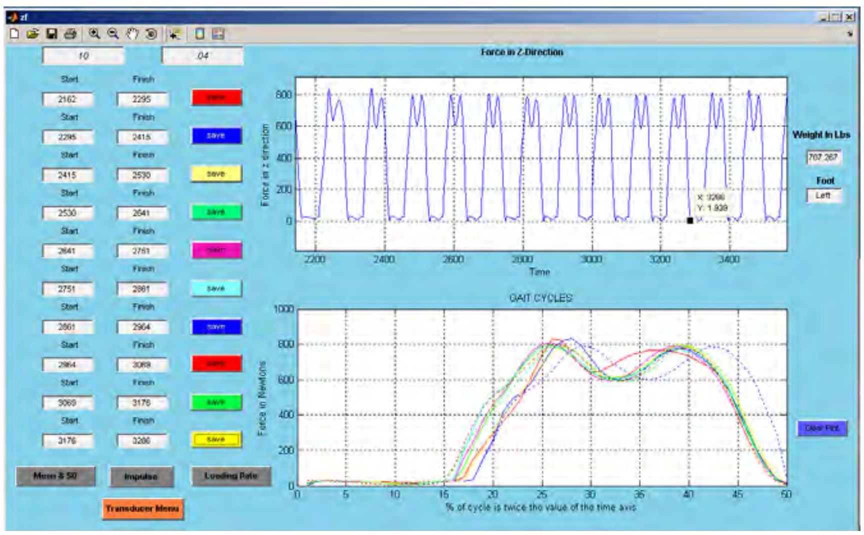

Figure 2-1. GUI Display of Transducer Data for Identifying Steps

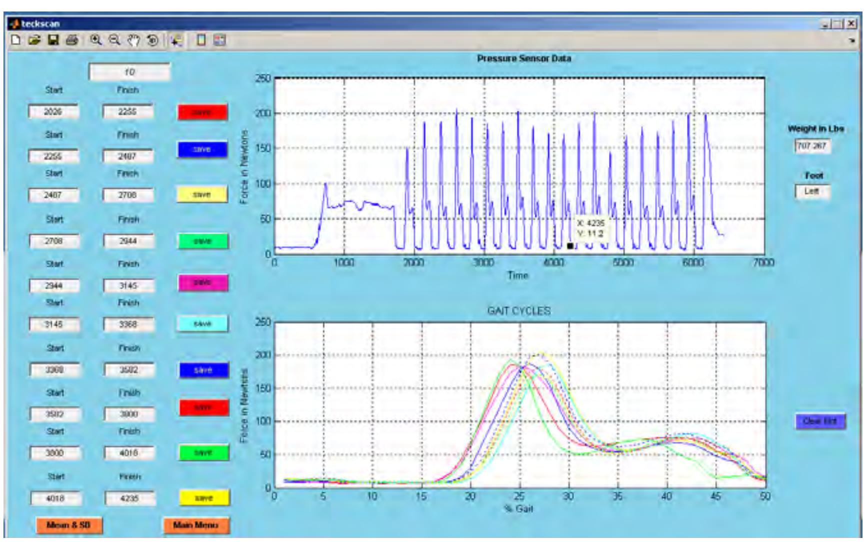

Figure 2-2. GUI Display of Pressure Data for Identifying Steps

3. Experimental Methods and Data Collection

IRB Approval and Subject Recruitment

A sample of convenience subjects was utilized. The experiments were designed and data collection forms, a Call for Subjects, and Letters of Informed Consent were prepared. The research protocol was submitted to the Army for an IRB pre-review on 25 September 2007 and a response was received from AMDEX on 13 November 2007 with suggested changes. The protocol was modified based on these suggestions and submitted to the IRB at UNLV on 20 November 2007. It was approved by UNLV on 22 April 2008. The protocol was then submitted to USAMRMC and was approved on 8 May 2008. A Call for Subjects was prepared and distributed to local clinics. Hanger Prosthetics & Orthotics, Inc. also was contacted and asked for help with recruiting subjects. Hanger reviewed the protocol and offered to help recruit subjects from its Las Vegas clinic. Two subjects were recruited with the help of Hanger. One additional subject heard about the study and asked to participate. The fourth subject was recruited with the help of BioQuest, Inc., who wished to see the data for two feet it manufactures, the PerfectStride and the BioStride. The first subject was recruited in November of 2009 and data collection for this subject was completed in January of 2010. Data collection for the last subject was obtained at the end of March, 2010. Pressure sensitivity was measured using Semmes Weinstein monofilaments at several regions on the residual limb. Characteristics of the subjects are shown in Table 3-1.

Phase 1 of Data Collection – Comparison of Activities and Feet

Data collection consisted of two sessions. Both sessions were conducted on the campus of the University of Nevada, Las Vegas in or near the Thomas Beam Engineering Building. One session involved the use of two different feet and the transducer. One of the feet was selected by the principle investigator. The pylon of the subject's prosthesis was replaced with a shortened pylon that allowed the transducer to be attached as well as the foot that was chosen. Subjects wore their own preferred shoes. The prosthesis was donned and the subject was accompanied to the site of data collection. A cable was inserted into the transducer that ran up to a backpack that the subject was wearing. The backpack contained the controller and batteries that powered the transducer as well as the transmitter, which also was in the backpack. The receiver was plugged into a nearby electrical outlet. The transducer was turned on and initialized by having the subject lift their prosthetic foot slightly so that the transducer would initialize bearing none of the loads associated with gait. Thus, the initial reading from the transducer was approximately zero when the foot was lifted. The subject was then instructed to undertake one of the five activities: level walking at a self-selected comfortable speed, walking up and down a 7% to 8% wheelchair ramp by the entrance to the Engineering Building, walking across a grassy slope in front of the engineering building with the prosthetic foot on both the uphill and downhill side of the slope, walking in a circle of ten foot diameter that had been drawn with chalk on the sidewalk in front of the Engineering Building, and ascending and descending a flight of 38 steps that leads from the ground floor to the second floor of the Engineering Building. The subject was instructed to continue the activity until approximately fifteen good steps were observed. The sites chosen were sufficiently long enough that the fifteen steps could be taken without the subject having to stop and turn around. As the data were produced for an activity they were transmitted to the laptop and stored in a file. At the end of the activity, the file was named and stored. While this was taking place, the Principle Investigator collected subjective data on the intra-socket pressures experienced by the subjects. These data are described in Chapter 7. The subject was then asked to undertake another of the activities and the procedures were repeated until data had been collected for all five activities. One activity, ascending and descending of the steps in the Engineering Building, required that the power source for the receiver be changed from one electrical outlet to another in the Engineering Building, which necessitated a shut-down and re-initialization of the transducer. After all five activities were completed, the subject doffed their prosthesis and the Principle Investigator exchanged feet and pylons. The prosthesis was donned with the second foot attached, and the experiment repeated. Transducer data collection was at 100 Hz.

	Subject 1	Subject 2	Subject 3	Subject 4
Age	30 38		29	63
Sex	M M		F	M
Weight, kg	93 95	.3	70.8	94.4
Height, cm	170 1	83	170	180
Reason for Amputation	Trauma Traum	a	Cancer	Trauma
Side of Amputation	Left Left		Left	Right
Years Since Amputation	5 yrs 6 mos	14 yrs 7 mos	9 yrs 5 mos	40 yrs
Foot Size	27 cm	27 cm	24 cm	27 cm
K Level	4 4		4	4
Suspension	Gel Liner & Sleeve	Gel Liner & Pin Lock	Gel Liner & Pin Lock	Pelite Liner, Socks & Cuff
Residual Limb Length, cm	15.2 19	.1	14.3	9.8
Sensation, g				
Distal Tibia	9.6 9.	6	2.4	20
Distal Lateral	20 2.	4	2.4	2.4
Distal Medial	9.6 2.	4	2.4	2.4
Distal Gastrocnemius	>20 2	.4	2.4	2.4
Patella Tendon	>20 2	.4	2.4	9.6
Fibula Head	20 2.	4	2.4	2.4
Popliteal	>20 2	.4	2.4	2.4

Table 3-1. Subject Characteristics

Subject 1 provided a spare socket and foot that did not cause any discomfort problems. Subject 2 provided a socket that was not frequently used anymore but was not as comfortable as their current socket. The subject found it acceptable for data collection, though not for long term use. The socket supplied by Subject 3 was used for more athletic activities such as hiking, and had an acceptable fit for long term use. Subject 4 used their current socket, which reportedly was worn for many hours a day for non-sedentary work and used in activities that included climbing ladders.

Subject 1 provided both feet used in the study, a TruStep manufactured by College Park, Inc., and a Renegade manufactured by Freeedom Innovations, Inc. The subject had prior experience with both feet. Subject 2 did not provide any feet, and the research team selected a SACH foot manufactured by Ohio Willow Wood and a Carbon Copy 2 foot, also manufactured by Ohio Willow Wood. The subject reported having prior experience with a SACH foot, but not a Carbon Copy 2. Subject 3 provided a FlexFoot, which is produced by Ossur, Inc., and a SACH foot manufactured by Ohio Willow Wood was selected by the research team for the second foot. The Flexfoot was the foot used by the subject on their spare prosthesis, and the subject had prior experience with it. The subject did not have prior experience with the SACH foot. Subject 4 provided both the PerfectStride and BioStride feet, and had experience with both. A SACH foot produced by Ohio Willow Wood was selected by the research team for the third foot so that a comparison could be made of the same foot design across three different subjects. Subject 4 had prior experience using a SACH foot.

Phase 2 of Data Collection – Pressure Measurement

The second session involved collection of pressure data in addition to the transducer measurements and was carried out on a separate day for Subjects 1, 2, and 3. Both sessions were carried out on the same day for Subject 4 due to travel constraints for the subject, who came from out-of-town. Pressure data were collected for level walking at a self-selected comfortable speed for three different alignment conditions: the neutral acceptable alignment, a 5 mm anterior shift of the foot (+5 mm), and a 5 mm posterior shift of the foot (-5 mm). The socket flexion angle was not changed. The perturbations were accomplished with a Hosmer Spectrum Alignment System, which had the desirable feature of providing 1 mm of travel per revolution of the adjustment screw, making it easy to perform perturbations of $\pm$5 mm. The Hosmer component which facilitated anterior-posterior movement of the foot was attached to the distal side of the transducer using the four standard bolt holes, and the pylon was attached to the component. The feet used in the perturbation experiments were the TruStep for Subject 1, the SACH foot for Subjects 2, 3, and 4, and the PerfectStride and BioStride for Subject 4.

The F-Socket sensor model 9811E was used for collecting pressure data. It is an FSR type of pressure sensing device which measures pressure by detecting voltage changes that occur when an electric current is passed through an ink. The F-Socket sensor is rectangular (21.5 X 7.5 cm), consists of 96 individual cells arranged in 16 rows and 6 columns, and has a lower spatial resolution than the in-shoe sensor. It is approximately 0.28mm thick and very flexible. The sensor can be trimmed to fit inside the curved surface of a prosthetic socket to minimize distortion. Cells can be removed from the end of the strip and vertical slits created between the columns of sensors. F-Socket specification details are provided in Figure 3-1 and Table 3-1. The F-Socket sensor employs force sensing resistors for measuring the pressures developed in the socket. These force sensing resistors measure pressures based on piezoelectric ink sandwiched between two Mylar layers. As pressure increases, the contact area between ink particles increases, and resistance to current flows through the ink changes. The voltage drop across the cell changes, and when the sensor has been properly calibrated, this change in voltage can be used to estimate the pressure applied to the sensor.

Overall length L	Overall width W	Tab Length A	Matrix Width MW	Matrix Height MH	Columns CW	CS	QTY	Rows RW	RS	QTY	Total No.of Sensels
(in) 14.48	(in) 3.00	(in) 5.61	(in) 3.00	(in) 8.00	(in) 0.25	(in) 0.5	6	(in) 0.31	(in) 0.5	16	96
(mm) 367.8	(mm) 76.2	(mm) 142.5	(mm) 76.2	(mm) 203.2	(mm) 6.4	(mm) 12.7	6	(mm) 7.9	(mm) 12.7	16	96

Table 3-2. Dimensions of the F-Socket Sensor Array

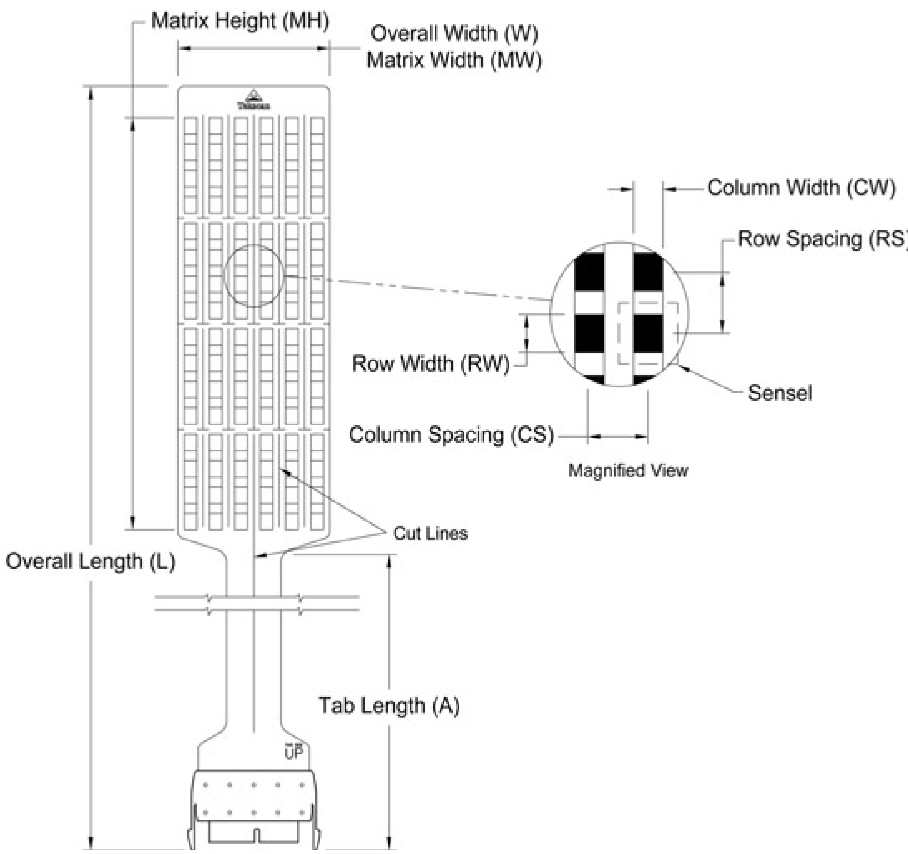

Figure 3.3: F-Socket sensor 9811E

(Source: Tekscan, Inc.)

Experiments were conducted in a hallway in the Engineering Building, which was sufficiently long to allow more than 10 good steps to be taken without having to turn around. The columns of the Tekscan sensors were slit with a pen knife to allow them to conform to the curved wall of the socket, the ends of the cuts were reinforced with transparent tape to prevent tearing, and the entire sensor was wrapped in a clear plastic food wrap to keep the columns of sensors from overlapping and also to further prevent tearing. Sensors had to be calibrated prior to the collection of data. Calibration involved placing the sensor between thin sheets of Pelite cut to the dimensions of the sensor and then placing the resulting assembly in between two large blocks of aluminum which were machined to just cover the sensor. The Principle Investigator the stood on the upper aluminum block while calibration took place using Tekscan's software. The weight of the Principle Investigator plus the weight of the aluminum block were entered into the Tekscan software to provide the known weights necessary for calibration. This approach was developed following experimentation with different methods of calibration, and was found to be the best one for distributing weight evenly over all the cells of the sensor. The sensors for Subject 4 had to be shortened because of the short length of the Subject's residual limb.

Following calibration, the sensor arrays were placed into the anterior and posterior sides of the laminated socket so that they would lie between the socket wall and liner. It was not possible to locate the sensors next to the skin of the subjects because they would have to pass underneath the sleeve or liner, and where they crossed the knee joint, they either would have restricted flexion of the subject's knee or they would have been damaged. The prosthesis, containing the transducer and alignment system was then donned by the subject and the sensor handles attached to the sensors. The cables from the handles ran up to a data logger on the subject's waist. The logger captured and stored data from the sensors, which had to be downloaded after each walking trial to Tekscan software installed on the laptop. Downloading of the data required that a cable be attached to both the data logger and the laptop. To initiate data collection, the data logger was turned on and checked to make sure that it was recording data properly. The transducer was then turned on and initialized. The data logger was triggered to begin data collection, and the subject was instructed to walk to the end of the hallway at a self-selected comfortable speed. At the end of the hallway, the data logger was turned off along with the transducer, and the data were downloaded to the laptop. If, as sometimes occurred, the data logger failed to record data, the trial was repeated. When it was determined that pressure data had been successfully captured and downloaded, the subject was asked to sit in a chair while a perturbation was made to the alignment of the foot, which could be done easily without having to doff the prosthesis. Transducer and pressure files were labeled and saved. The order of alignments was the initial neutral alignment followed by a +5 mm perturbation and then a -5 mm perturbation. In the case of Subject 4, the prosthesis was doffed following the last perturbation so that feet could be changed and the pylon length adjusted. Data were captured at 200 Hz. The Tekscan data were processed using Tekscan F-Scan Mobile 5.72 software and exported as files containing the average pressures in each of the socket windows. Later, the pressure and transducer data were processed using the GUI as described in the following paragraph.. The illustrations on the last page depicts data collection activities. Statistical methods used to analyze the data collected included the t-test, one way ANOVA, and regression analysis, which are described in more detail in the following chapters.

Selection of Starting and Ending Points for Steps – Transducer Data

1. The Fz data recorded for each activity was observed in the GUI to determine which steps were to be used. The ten steps selected were those displaying the most consistent vertical ground reaction force profiles. Profile consistency and quality were derived from visually inspecting the Force VS Time plot in the GUI. Steps displaying similar maxima and minima values in force during midstance were chosen.

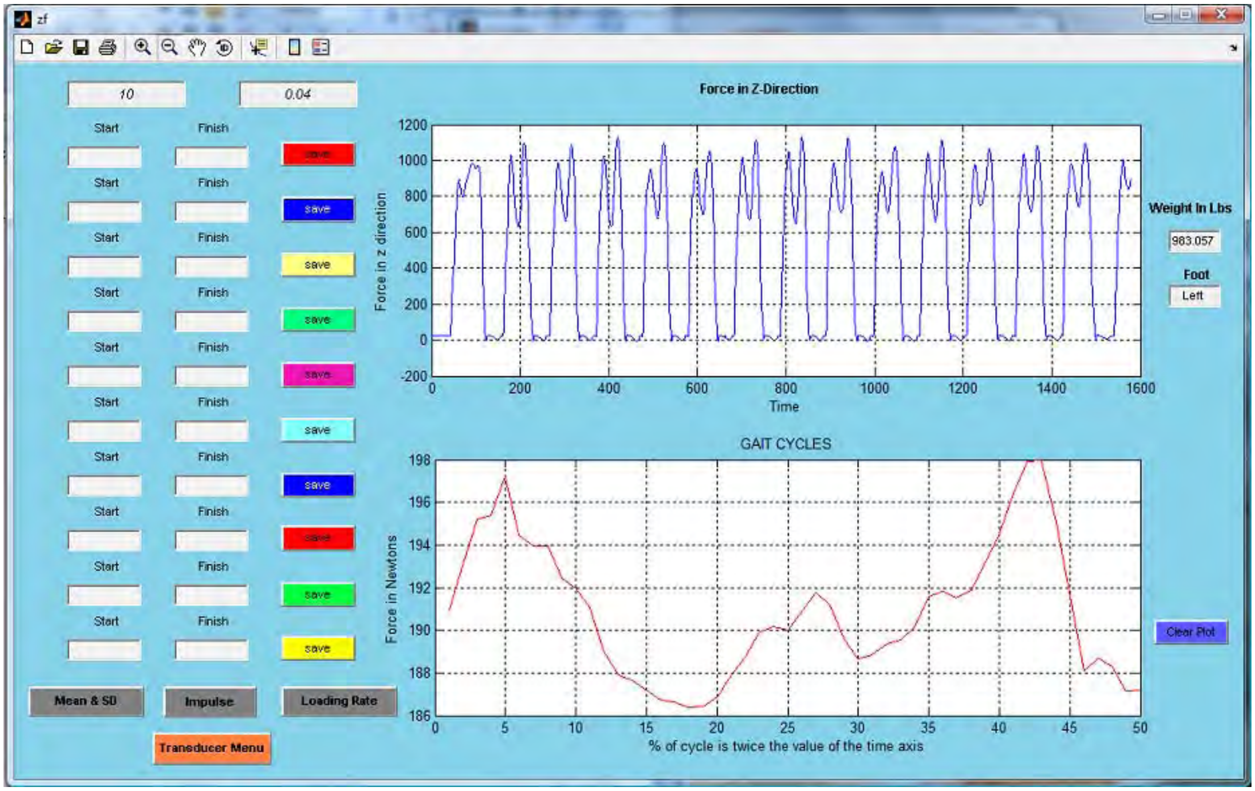

Figure 3-4 . Appearance of GUI as Used to Select Steps Based on Maximum and Minimum Values Associated with Midstance

2. After identifying the first step, the zoom feature in the GUI was used to maximize the profiles for two steps within the Force VS Time plot window. This sufficiently exposed the plot characteristics to be visually scrutinized for stance initiation and termination.

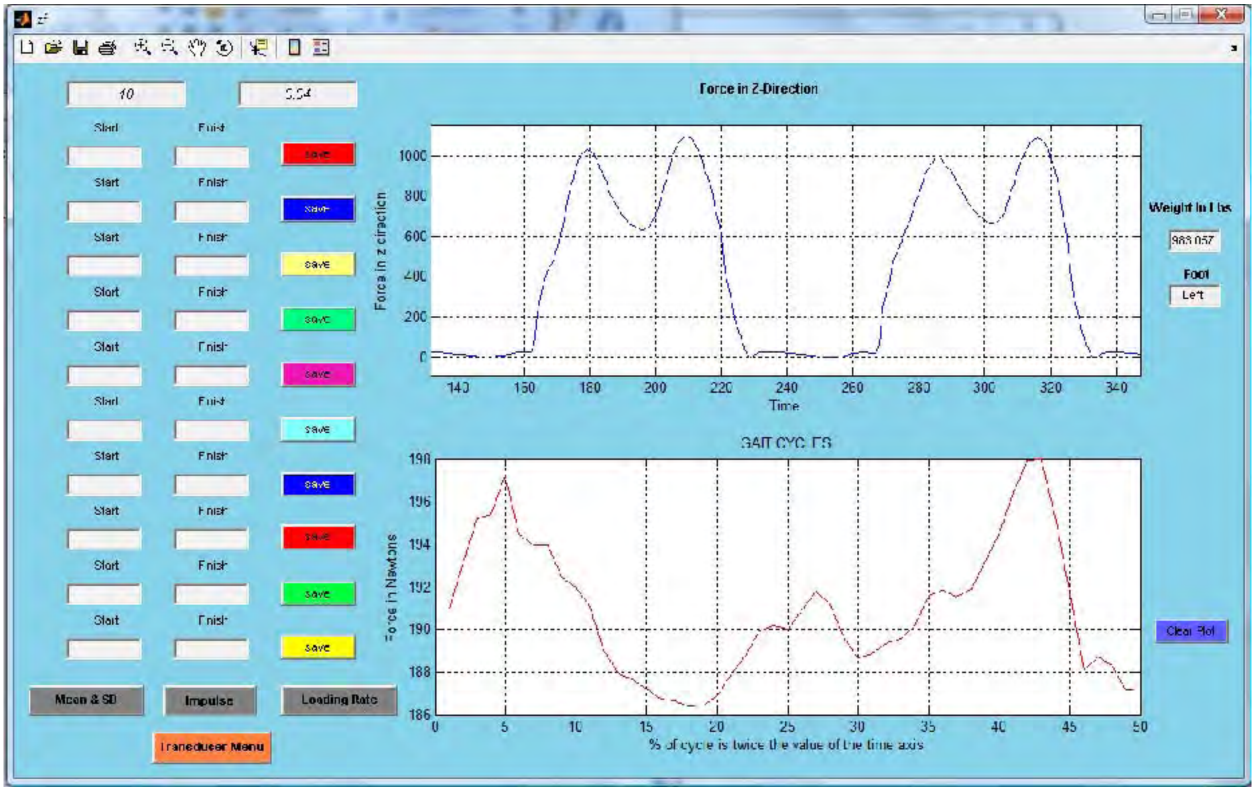

Figure 3-5. Magnification of Individual Steps in the GUI

3. The loading portion of stance was easily identified by a sharp positive increase in the plot's slope. This slope led into one of the maxima of a bimodal curve representing midstance. The second maxima preceded a sharp negative slope which represented unloading prior to toe-off. Between stances, the swing phase was readily observed to be a nearly flat line with values of approximately zero Newtons.

4. Toward the end of the swing-phase, the subject’s leg would decelerate in preparation for stance. Consequently, the transducer would record a slight drop in magnitude. This created a “U” in the plot consisting of three data points. Having the first data point in the swing phase and the third in the loading of stance, the middle value was identified as heel strike. Using the GUI’s data cursor and toggling between adjacent points, this lowest value in the “U” (heel strike) was indentified, and its position in time was recorded.

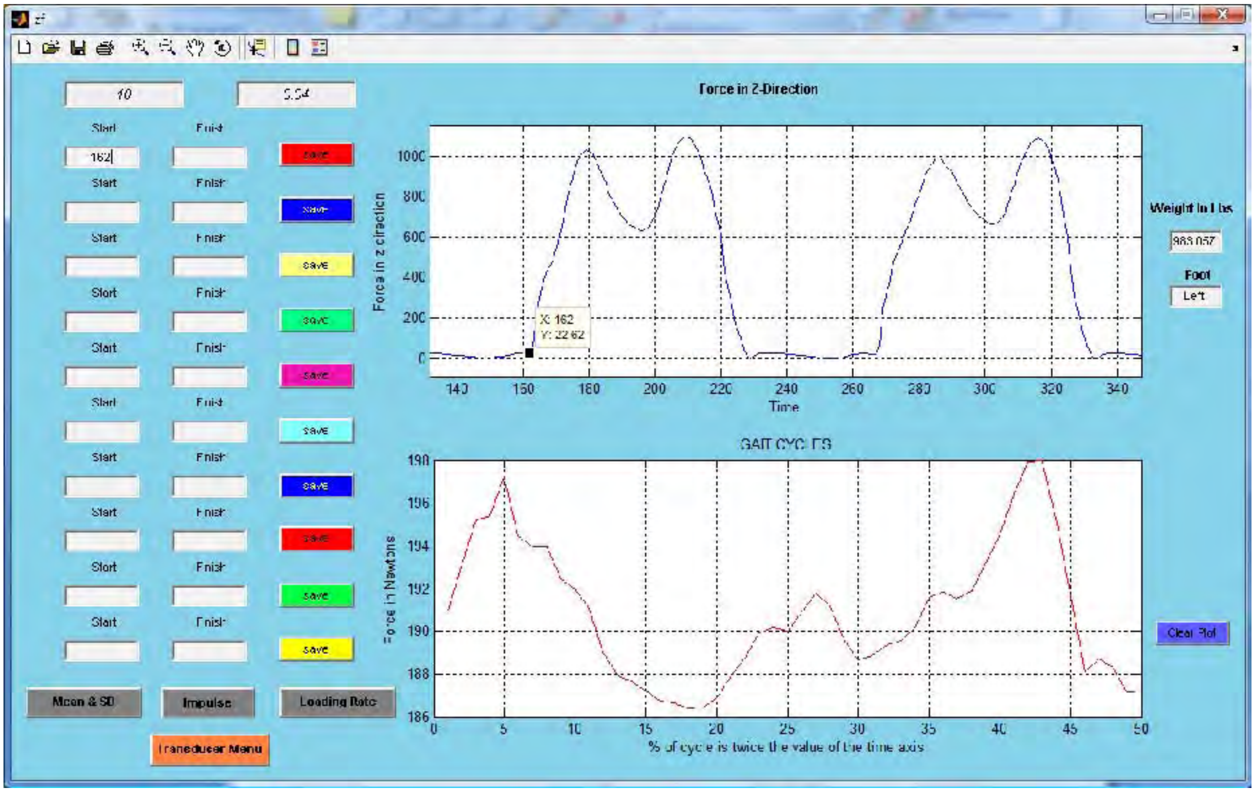

Figure 3-6. Identification of Points Representing Heel Strike

Similar to the initiation of stance, the transition from stance termination into swing delivered a three point "U" shape in the plot. Like the selection for heel strike, toe-off was termed as the lowest force value of the three points.

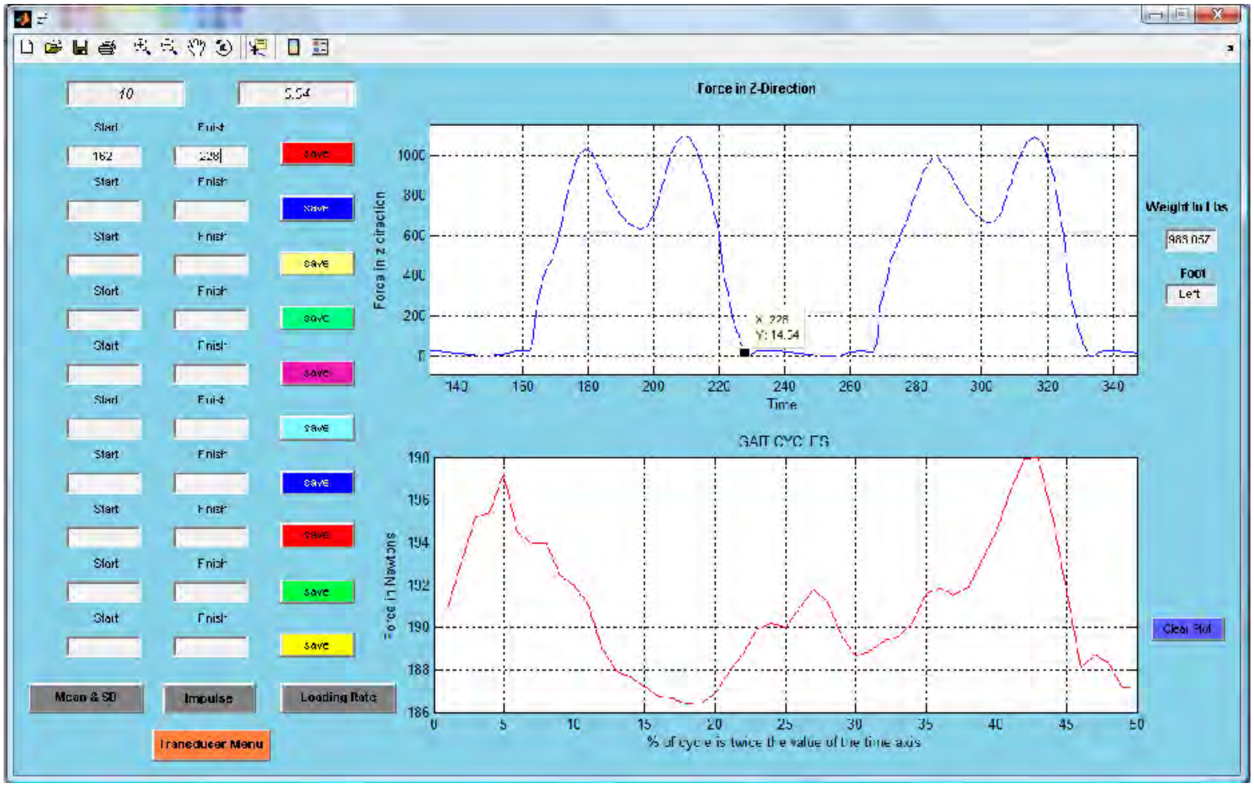

Figure 3-7. Selection of Points Representing Toe-Off

* Some exceptions in data characteristics required some alterations to Step 4. See below for Step 4 Alternative Approaches.

5. Steps 4 and 5 were repeated for the remaining 9 steps. All starting and stopping points for each step were recorded. The positions found in the Fz plot were then applied to Fx and Fy. After opening the Fx and Fy data within the GUI, the starting and stopping points were entered in the appropriate spaces.

Step 4 Alternative Approaches:

- In cases where more than three points comprised the "U" portions before and/or after stance (two middle values of equal magnitude), the middle "U" value closest to the start or stop of stance was chosen.
- Some instances occurred in which a distinct "U" could not be identified before and/or after stance. In these cases, the data cursor was positioned toward the end of swing. It was then toggled toward stance until it reached the first point on the loading slope that was much greater than the previous point; approximately 200% larger. The cursor was then toggled back to the previous position and marked as the "Start" of the step. The selection of the "Stop" position was found in the same way except substituting the unloading slope for the loading.
- Due to the centrifugal force of the prosthetic, there were instances when the transducer experienced a relatively small negative Fz force during swing. When this occurred, the start/stop of the step was identified as the first point on the loading/unloading slope with a positive force magnitude adjacent to a negative magnitude.

* It should be noted, that when a step required and alternative approach to start/stop selection the other nine steps typically required the same approach. Therefore, there was consistency in point selection throughout the activity.

Selection of Starting and Ending Points for Steps – Pressure Data

6. Using Tekscan's software, a pressure window was drawn to include every pressure sensor cell of the Tekscan placed in the anterior portion of the socket - the entire sensor array. The overall pressure data produced a pressure verusus time plot similar to a vertical ground reaction force profile. The ten steps selected were those displaying the most consistent profiles characteristic of vertical ground reaction force profiles. Profile consistency and quality were derived from visually inspecting the pressure versus time plot. Steps displaying similar maxima and minima values in pressure during midstance were chosen.

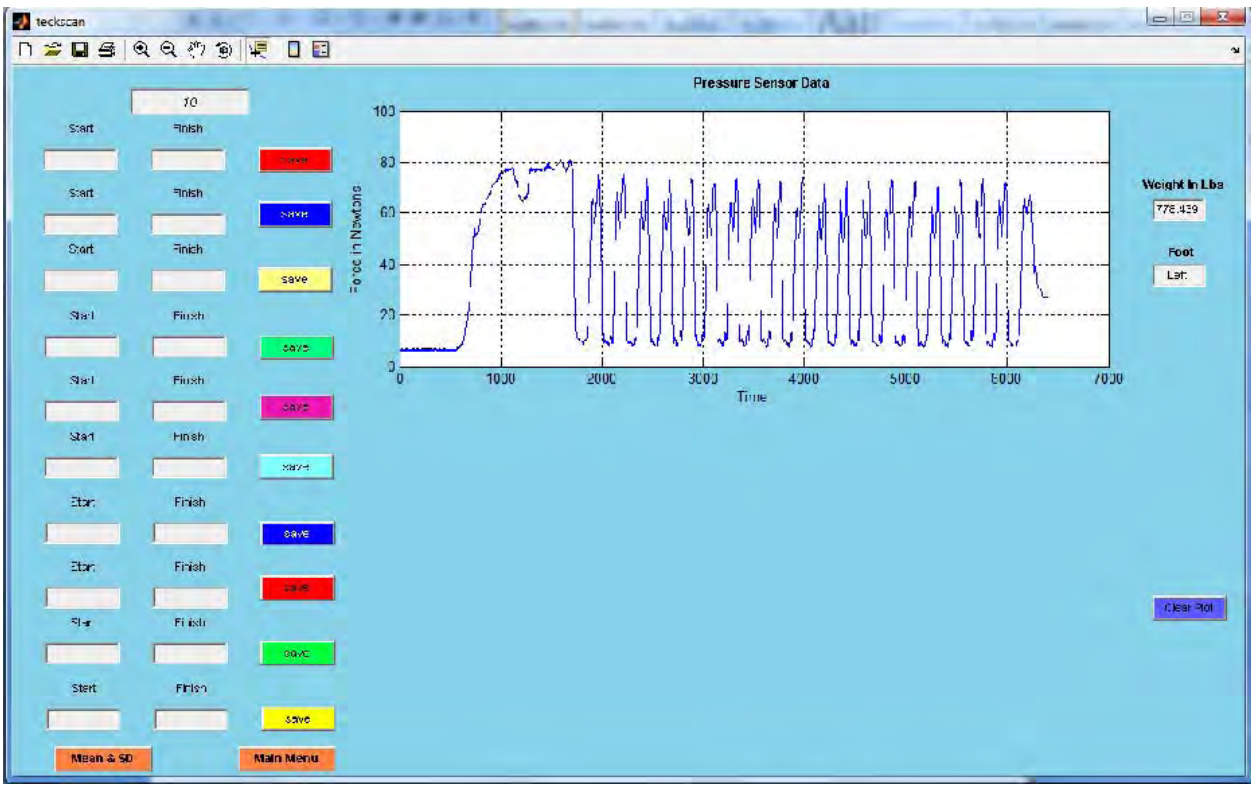

Figure 3-8 . Appearance of GUI when Tekscan Data for a Pressure Window are Imported. In this case data represent the entire array consisting of 96 cells. The Y axis reports average pressure for the window.

7. After identifying the first step, the zoom feature in the GUI was used to maximize the profiles for two steps within the pressure versus time plot window. This sufficiently exposed the plot characteristics to allow them to be visually scrutinized for stance initiation and termination.

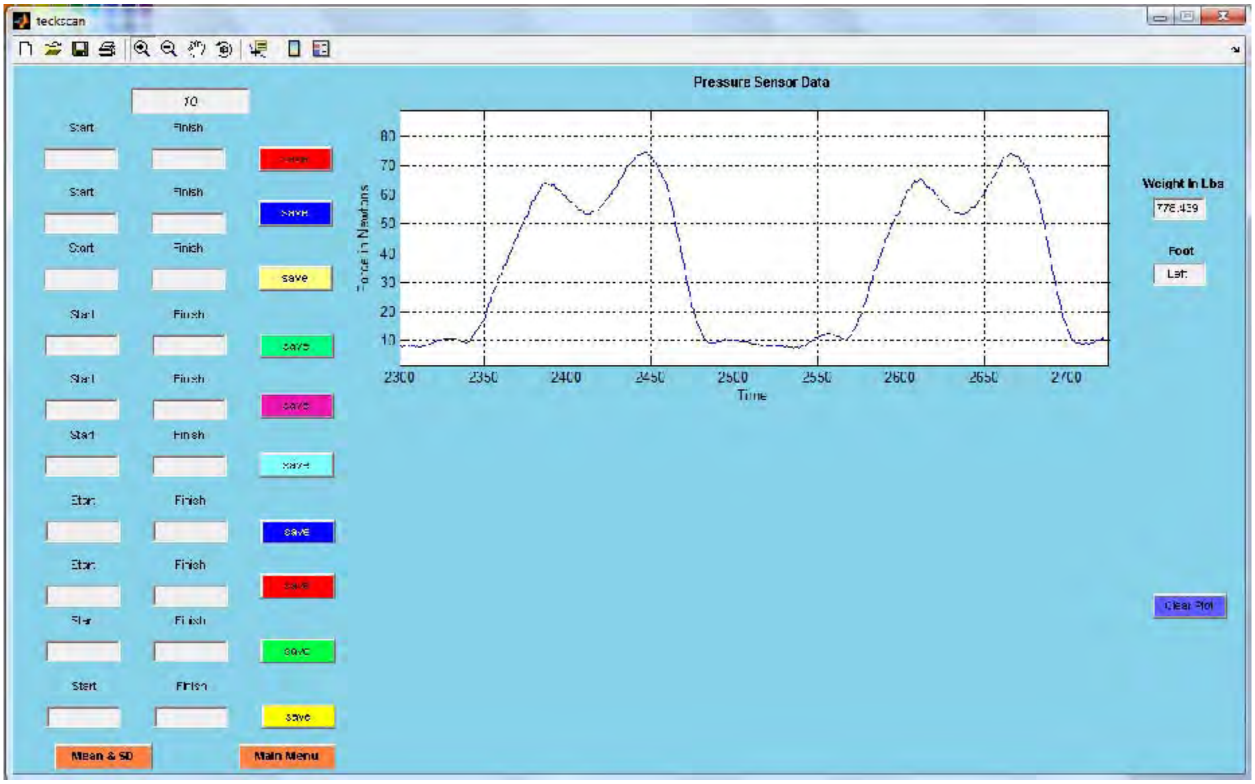

Figure 3-9. Magnification of Individual Steps in the GUI

8. The loading portion of stance was easily identified by a sharp positive increase in the plot's slope. This slope led into one of the maxima of a bimodal curve representing midstance. The second maxima preceded a sharp negative slope which represented unloading prior to toe-off. Between stances, the swing phase was readily observed to be a nearly flat line with relatively low values of pressure.

9. Toward the end of the swing-phase, the subject's leg would decelerate in preparation for stance. Consequently, the overall pressure within the socket would slightly drop in magnitude. This created a "U" in the plot consisting of three data points. Having the first data point in the swing phase and the third in the loading of stance, the middle value was identified as heel strike. Using the GUI's data cursor and toggling between adjacent points, this lowest value in the "U" (heel strike) was indentified, and its position in time was recorded.

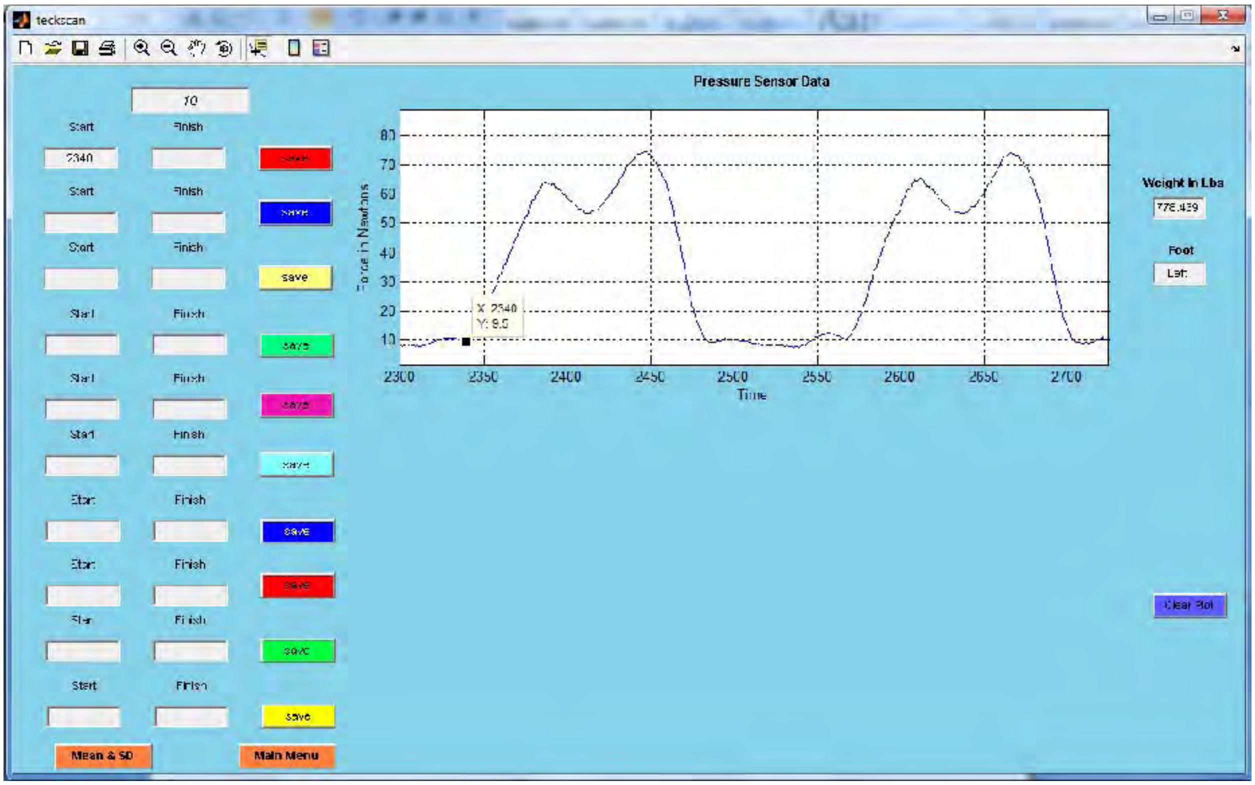

Figure 3-10. Identification of Points Representing Heel Strike

Similar to the initiation of stance, the transition from stance termination into swing delivered a three point "U" shape in the plot. Like the selection for heel strike, toe-off was defined as the lowest pressure value of the three points.

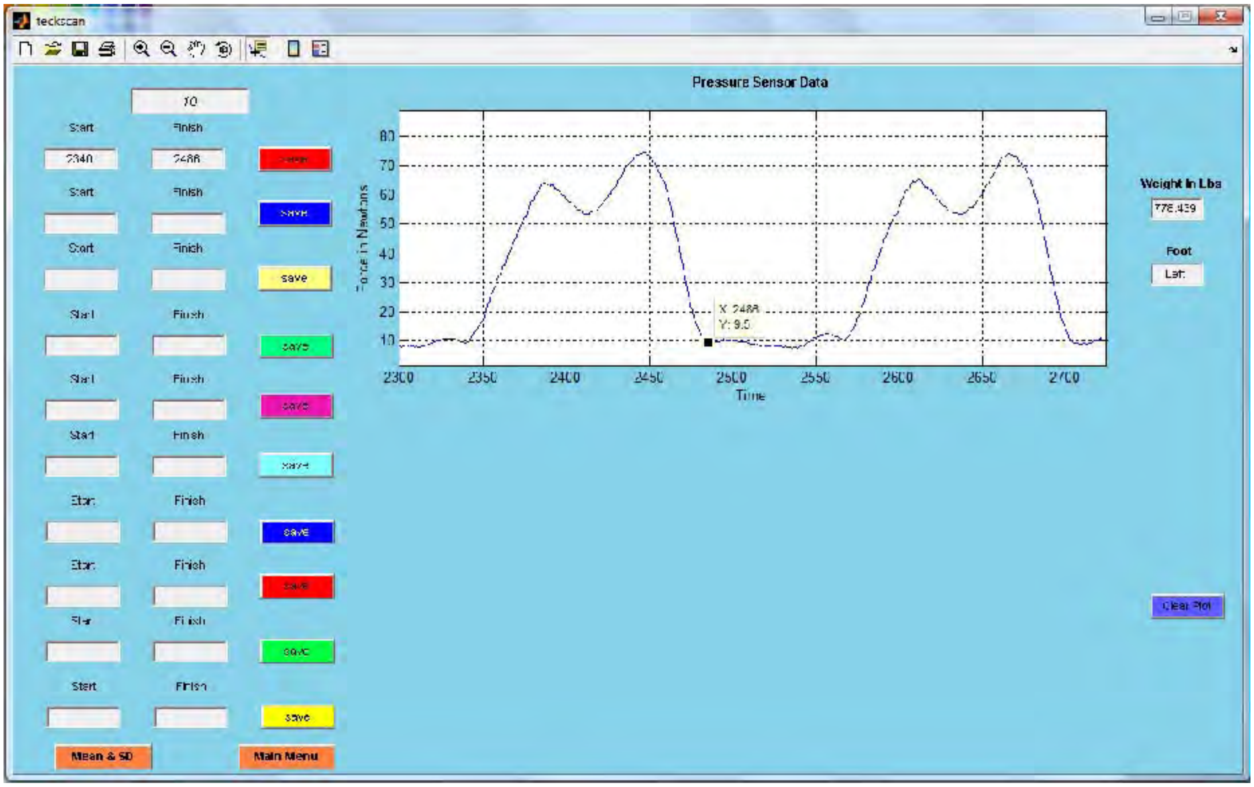

Figure 3-11. Selection of Points Representing Toe-Off

* Some exceptions in data characteristics required some alterations to Step 4. See below for Step 4 Alternative Approaches.

10. Steps 4 and 5 were repeated for the remaining 9 steps. All starting and stopping points for each step were recorded. The positions found on the overall anterior pressure plot were then applied to the other pressure windows (anterior and posterior). After opening each pressure window's data within the GUI, the starting and stopping points were entered in the appropriate windows of the GUI.

Step 4 Alternative Approaches:

- In cases where more than three points comprised the "U" portions before and/or after stance (e.g., two middle values of equal magnitude), the middle "U" value closest to the start or stop of stance was chosen.
- Some instances occurred in which a distinct "U" could not be identified before and/or after stance. In these cases, the data cursor was positioned toward the end of swing. It was then toggled toward stance until it reached the first point on the loading slope that was much greater than the previous point; approximately 200% larger. The cursor was then toggled back to the previous position and marked as the "Start" of the step. The selection of the "Stop" position was found in the same way except that the unloading slope for the stance phase was substituted for loading curve at the beginning of stance.

* It should be noted that when a step required an alternative approach to start/stop selection, the other nine steps typically required the same approach. Therefore, there was consistency in point selection throughout the activity.

A.

B.

C.

D.

E.

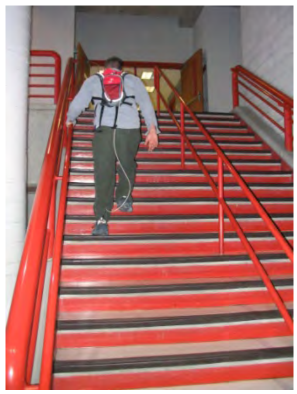

F.

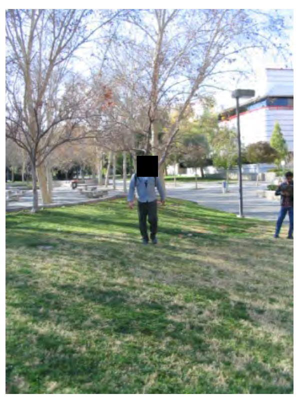

G.

H.

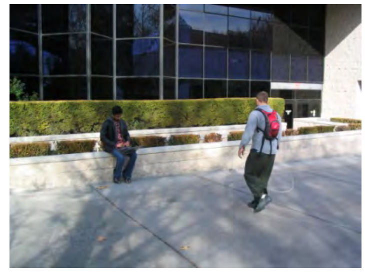

I.

Figure 3-8. Data Collection.
A. Instrumentation for pressure measurements.
B. Initializing the transducer.
C. Pressure data collection.
D. Level walking at a self-selected comfortable speed.
E. Walking up and down a ramp.
F. Walking up and down steps.
G. Walking across a grassy slope.
H. Laying out a circle of 10 foot diameter.
I. Walking around a circle of 10 foot diameter.

5. Comparison of Feet across Subjects

The SACH foot was used by three of the four subjects, which permits a demonstration of how the output from the transducer can be used to compare feet across subjects. The same design of SACH foot was used for all three subjects, and only the size, side (two left feet and one right foot), and heel plug that controls heel stiffness varied. The feet were produced by Ohio Willow Wood and were a right 27 cm with a firm heel plug (Subject 4), a left 27 cm with a medium heel plug (Subject 2), and a left 24 cm with a medium heel plug (Subject 3). In order to compare the subjects, the force and moment data from the transducer had to be normalized. Force data were divided by the subject's weight in Newtons, and moment data were divided by the subject's mass in kg. The subjects' weights were obtained by having the subject stand on the prosthetic foot alone for 3 to 5 seconds following transducer initialization and prior to walking. Subjects were allowed to touch the wall to help with balance, but were monitored to ensure that they did not try to support their weight. Data for level walking at a self-selected comfortable speed were used to compare the peak forces and moments reported by the transducer along all three axes. The intervals when the maximum occurred were determined by inspection of the output from the GUI. A one-way ANOVA was used to compare each maximum of the mean value using the three subjects as groups, and the values of the ten steps as observations for each group. In order to compare the right foot of Subject 4 with the left feet of Subjects 2 and 3, forces along the Y axis and moments about the X and Z axes for Subject 4 had to be multiplied by -1.

Figure 5-1 graphs the force and moment values versus per cent of the stance phase for the three subjects when the data have been normalized and the data for Subject 4 had been corrected to make the right foot comparable to the left feet of the other subjects. The maximum values for each force and moment for each subject are shown in Table 5-1, where the results of the one-way analysis of variance are also shown. The intervals during which the maximum occurred are shown in the table. These can be converted to the per cent of the stance phase if the numbers are multiplied by two and one is subtracted from the result (2 X interval – 1); the graphs in Figure 5-1 present results in terms of per cent of the stance phase. The graphs indicate that the force and moment curves appeared different for the different subjects. Differences were evident for Fx, Fy, Mx and Mz. Since the feet were all of identical design, this could only be attributable to differences in either the gait patterns of the individual subjects or the alignment of the prostheses. Analysis of variance results indicated that for only two of the transducer measurements, Fy+ and Mz+ was there a strong likelihood of no significant differences between the three subjects. All of the other measurements had probabilities less than 0.05 that the maximum values came from the same distributions.

Looking at the individual curves and the table, it can be seen that the maximum values for the means of Fy+ are relatively low when compared to the means for the other forces and occur early in stance, which suggests a phenomenon related to heel strike. The low values suggest that this force may not have much clinical importance. The curves for Mz+ indicate very striking dissimilarities between Subject 3 and the other subjects. For Subject 3, the maximum value of Mz+ occurred late in stance (85%), and negative Mz values occurred early in stance (20%). In contrast, Subjects 2 and 4 exhibited small positive moments early in stance and much larger negative moments late in stance. This suggests something fundamentally different is occurring in the gait of Subject 3, but it cannot be determined what is happening from the data. Subject 3 also exhibited strong dissimilarities to the other subjects for Mx and Fy. It could be related to alignment.

It is interesting to note that although the first and second peaks of Fz appear similar, the ANOVA revealed them to be significantly different. This is due to the very small variance in the data among the ten steps used to compute means. Force in the Z direction parallel to the pylon is analogous to the vertical ground reaction force, and generally of clinical importance since it reveals what portion of body weight is being transmitted to the residual limb. However, for the first peak which occurs during loading response the statistically significant difference is likely of little clinical significance because the mean values are very close together. For the second peak, the mean value for Subject 2 is noticeably greater than for Subjects 3 and 4, and this could be of clinical interest. It is also interesting to note that in most cases the force along the direction of the pylon is rarely greater than body weight; the values for the first peak are only 0.9% and 5% greater than body weight for subjects 2 and 4 respectively. For the second peak the values are 11% greater for Subject 2. All the other subjects have values less than 1.00 for both peaks, though they are very close at approximately 99.5% to 99.9% of body weight. This is a phenomenon that has been observed in many studies of the gait of amputees. The weight and vertical ground reaction force on the prosthetic side is significantly less than the weight on the anatomically intact contra-lateral side (61). No one has been able to explain this, but the transducer data suggest the same phenomenon occurs directly below the socket, which implies that shock absorption of some type must be occurring within the socket or at the anatomic joints of the leg above the socket. It should be noted that the resultant force will always be greater than the force along the pylon, and thus should always be greater than body weight. This may help explain why amputees are able to progress in the forward direction since if the resultant force were less than body weight, it would be impossible to impart the acceleration to the body that is necessary for forward motion.

The forces and moments showing the greatest relative differences among subjects were Fx, Fy, Mx, and Mz. However, these were relatively small forces and moments compared to Fz and My, which showed more similarity in the graphs although the maximum values were significantly different when the means were compared using ANOVA. Heel plug stiffness could be one reason why Subject 4, who had the firmest heel plug, also exhibited the greatest My+ moment during loading whereas the Subjects 2 and 3, who both had medium stiffness heel plugs, exhibited similar means for My+. Subject 4 also exhibited higher mean values for the first peak of Fz. Subject 4 did not exhibit the largest Fz second peak forces or My- moments associated with propulsion, however. In summary, the data from the transducer indicate that feet having identical design may produce significantly different forces and moments that are transmitted to the residual limb. Whether the differences are caused the size of the foot, heel plug stiffness, alignment, or the gait preferences of the individual is not known. It might be that some but not all of the differences could be due to heel plug stiffness and foot size, or the alignment setup. Adaptation time also could be a factor since subjects had less than 30 minutes to adapt to the SACH foot used in the study. Some of the differences may be due to the gait preferences of the subject. The gait preferences could be affected by intra-socket pressures. The next chapter examines the relationship between the transducer measurements and pressures that are generated between the wall of the socket and the residual limb.

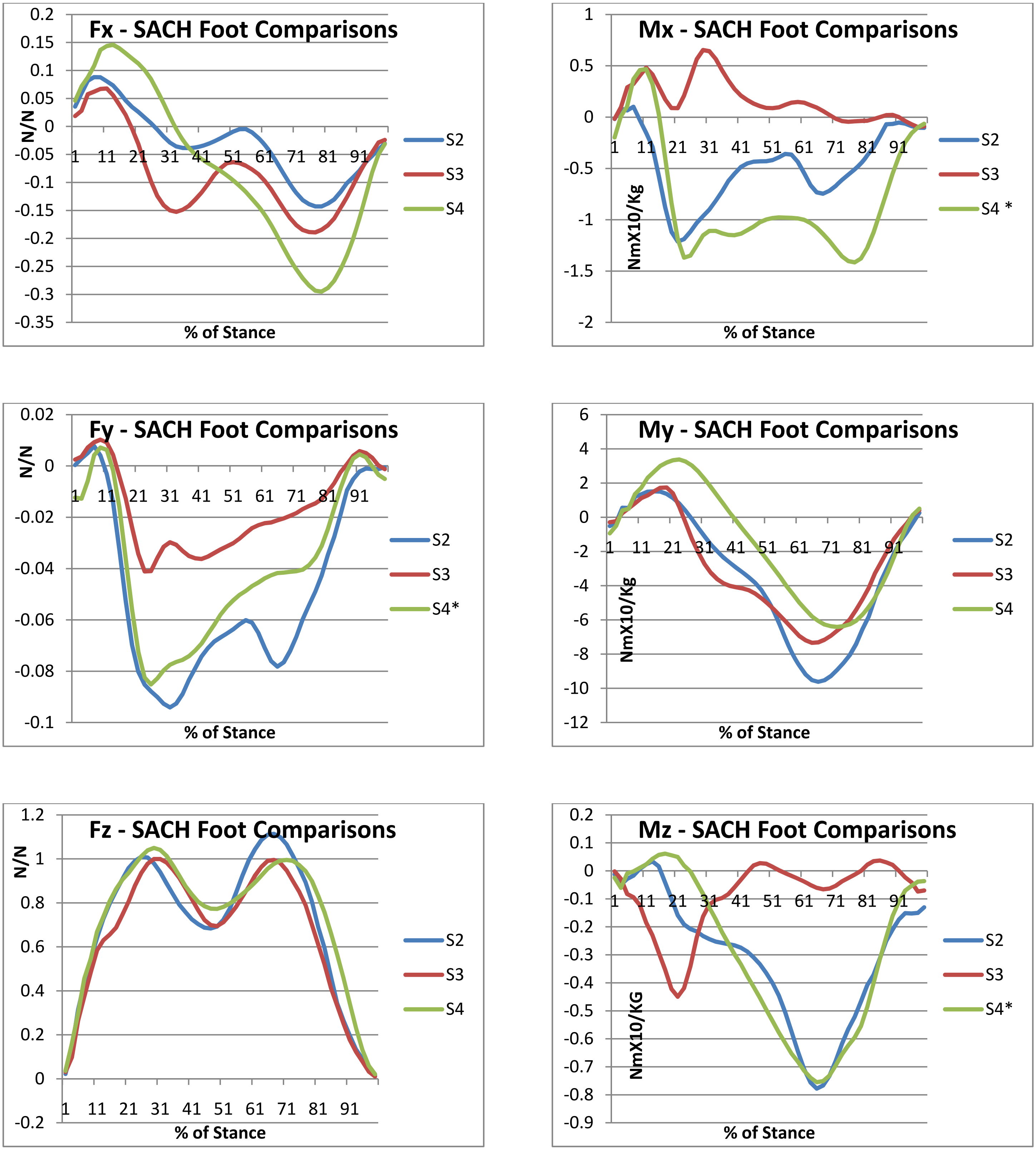

Figure 5-1. Normalized Forces and Moments for the SACH foot. An asterisk (*) indicates that the transducer data were multiplied by -1 to allow a comparison of left and right feet.

Table 5-1. ANOVA of SACH Foot Maximum Moments and Forces for Three Subjects								
Fx+	**Groups**	**Interval**	**Count**	**Sum**	**Average**	**Variance**		
S2		4	10	0.880696	0.08807	6.23E-05		
	S3	6	10	0.679326	0.067933	0.000173		
	S4	7	10	1.457931	0.145793	0.000153		
	ANOVA							
	Source of Variation		SS df		MS	F	**P-value**	F crit
	Between Groups		0.032666	2	0.016333	126.1233	2.01E-14	3.354131
	Within Groups		0.003496	27	0.000129			
	Total		0.036162	29				
Fx-	**Groups**		**Count**	**Sum**	**Average**	**Variance**		
S2		40	10	-1.4293	-0.14293	2.52E-05		
S3		39	10	-1.89154	-0.18915	2.25E-05		
S4		40	10	-2.94995	-0.29499	3.21E-05		
	ANOVA							
	Source of Variation		SS df		MS	F	**P-value**	F crit
	Between Groups		0.121542	2	0.060771	2287.951	7.46E-31	3.354131
	Within Groups		0.000717	27	2.66E-05			
	Total		0.122259	29				
Fy+	**Groups**		**Count**	**Sum**	**Average**	**Variance**		
S2		4	10	0.077637	0.007764	2.04E-05		
S3		5	10	0.102324	0.010232	3.48E-05		
S4	neg	5	10	0.071768	0.007177	4.38E-05		
	Source of Variation		SS df		MS	F	**P-value**	F crit
	Between Groups		5.26E-05	2	2.63E-05	0.797237	0.460895	3.354131
	Within Groups		0.00089	27	3.3E-05			
	Total		0.000943	29				
Fy-	**Groups**		**Count**	**Sum**	**Average**	**Variance**		
S2		16	10	-0.94138	-0.09414	7.48E-05		
S3		12	10	-0.41115	-0.04112	9.03E-05		
S4	neg	13	10	-0.85169	-0.08517	0.000188		
	Source of Variation		SS df		MS	F	**P-value**	F crit
	Between Groups		0.016109	2	0.008054	68.50522	2.65E-11	3.354131
	Within Groups		0.003175	27	0.000118			
	Total		0.019283	29				

Fz 1st Peak	**Groups**	**Interval**	**Count**	**Sum**	**Average**	**Variance**		
	S2	13	10 1	0.09701 1	.009701	0.001864		
	S3	15	10 9	.995356 0	.999536	0.000263		
	S4	15	10 1	0.4953 1	.04953	0.001394		
	Source of Variation		SS df		MS	F	**P-value**	F crit
	Between Groups		0.013964	2 0	.006982	5.947471 0	.007242 3	.354131
	Within Groups		0.031696 2	7	0.001174			
	Total		0.04566	29				
Fz 2nd Peak	**Groups**		**Count**	**Sum**	**Average**	**Variance**		
	S2	34	10 1	1.13793 1	.113793	0.000695		
S3		34	10	9.95308	0.995308	0.000134		
	S4	36	10 9	.951612 0	.995161	0.000352		
	Source of Variation		SS df		MS	F	**P-value**	F crit
	Between Groups		0.093708	2 0	.046854	118.9314	4.1E-14 3	.354131
	Within Groups		0.010637 2	7	0.000394			
	Total		0.104345	29				
Mx+	**Groups**		**Count**	**Sum**	**Average**	**Variance**		
	S2	2	10 0	.839042 0	.083904	0.009694		
	S3	15	10 6	.536968 0	.653697	0.040267		
	S4 neg	6	10 4	.669085 0	.466909	0.011912		
	Source of Variation		SS df		MS	F	**P-value**	F crit
	Between Groups		1.687486	2 0	.843743	40.9099	6.73E-09 3	.354131
	Within Groups		0.556859 2	7	0.020624			
	Total		2.244345	29				
Mx-	**Groups**		**Count**	**Sum**	**Average**	**Variance**		
	S2	11	10 -	12.1241 -	1.21241	0.040185		
S3		49	10	-0.96402	-0.0964	0.00269		
	S4 neg	39	10 -	14.151 -	1.4151	0.031386		
	ANOVA							
	Source of Variation		SS df		MS	F	**P-value**	F crit
	Between Groups		10.08512	2 5	.042561	203.7079	5.15E-17 3	.354131
	Within Groups		0.668355 2	7	0.024754			
	Total		10.75348	29				

My+	**Groups**		**Count**	**Sum**	**Average**	**Variance**		
	S2	8	10 1	5.13202 1	.513202	0.085594		
	S3	10	10 1	7.42759 1	.742759	0.153026		
	S4	12	10 3	3.79612 3	.379612	0.099863		
	Source of Variation		SS df		MS	F	**P-value**	F crit
	Between Groups		20.71824	2 1	0.35912	91.81346	9.04E-13 3	.354131
	Within Groups		3.046353 2	7	0.112828			
To	tal		23.76459	29				
My-	**Groups**		**Count**	**Sum**	**Average**	**Variance**		
	S2	34	10 -	96.1857 -	9.61857	0.048206		
	S3	33	10 -	73.4224 -	7.34224	0.021041		
	S4	37	10 -	64.1314 -	6.41314	0.075613		
	Source of Variation		SS df		MS	F	**P-value**	F crit
	Between Groups		54.39903	2 2	7.19951	563.2877	9.68E-23 3	.354131
	Within Groups		1.303751 2	7	0.048287			
To	tal		55.70278	29				
Mz+	**Groups**		**Count**	**Sum**	**Average**	**Variance**		
	S2	7	10 0	.336788 0	.033679	0.004295		
	S3	43	10 0	.370747 0	.037075	0.004885		
	S4 neg	9	10 0	.616373 0	.061637	0.023432		
	Source of Variation		SS df		MS	F	**P-value**	F crit
	Between Groups		0.004655	2 0	.002328	0.214116	0.808612 3	.354131
	Within Groups		0.293504 2	7	0.010871			
To	tal		0.298159	29				
Mz-	**Groups**		**Count**	**Sum**	**Average**	**Variance**		
	S2	33	10 -	7.77852 -	0.77785	0.019357		
S3		11	10	-4.49696	-0.4497	0.003373		
	S4 neg	33	10 -	7.54926 -	0.75493	0.008334		
	Source of Variation		SS df		MS	F	**P-value**	F crit
	Between Groups		0.671257	2 0	.335629	32.41241	6.66E-08 3	.354131
	Within Groups		0.279583 2	7	0.010355			
To	tal		0.950841	29				

6. Pressure Models

Background

The transducer makes it possible to examine the relationship between the forces and moments in the pylon and those exerted on the residual limb inside the socket. As mentioned above, a previous study conducted in 1987 was able to estimate the pressures inside a transtibial socket using measurements of the forces and moments in the pylon (46). Strain gauges were glued to the pylon of a prosthesis and holes drilled in the socket to insert transducers and measure pressures at a limited number of locations. As part of the study, the alignment of the prosthesis was varied, and the sensitivity of pressures to changes in alignment was modeled as a function of the alignment changes. The theoretical models proposed were

$$\begin{vmatrix} \sigma_p(\theta,t) \\ \sigma_g(\theta,t) \end{vmatrix} = |W(\theta)| * \begin{vmatrix} F_z(\theta,t) \\ M_x(\theta,t) \end{vmatrix}$$

Where:
$\sigma_p(\theta,t)$= pressure on the patellar tendon region
$\sigma_g(\theta,t)$ = pressure on the gastrocnemius region
$W(\theta)$ = matrix of coefficients that relate pylon forces and moments to socket pressures
$F_z(\theta,t)$ = axial force in the pylon
$M_x(\theta,t)$ = flexion-extension moment in the pylon
θ = socket flexion-extension perturbation with respect to an acceptable alignment
t = time during the gait cycle
And

$$|W(\theta)| = \begin{vmatrix} W_{11} + \left(\frac{dW_{11}}{d\theta}\right) * \theta & W_{12} + \left(\frac{dW_{12}}{d\theta}\right) * \theta \\ W_{21} + \left(\frac{dW_{21}}{d\theta}\right) * \theta & W_{22} + \left(\frac{dW_{22}}{d\theta}\right) * \theta \end{vmatrix}$$

The model added the pressure effects created by pylon axial forces to the pressure effects created by pylon flexion-extension moments. It was calibrated using regression analysis by entering pressure as the dependent variable and force and moment and socket alignment perturbation as the independent variables. Two subjects were examined who were using a SACH foot. Observations consisted of variable values sampled at uniform intervals during the gait cycle over multiple steps. The authors reported correlation R values of 0.937 in the patellar region and 0.984 in the gastrocnemius region for the first subject in the study, and values of 0.938 and 0.989 respectively for a second subject. Using technology that was not available in 1987, the forces and moments represented in the above model can be measured with tri-axial transducer instrumentation when the transducer is mounted distal to the socket and a subject walks. The model can be extended to multiple sites inside the socket by the use of arrays of force sensing resistors (FSRs) inserted into the socket. This avoids the need to drill holes in the socket wall and install force sensors. In this study, pressures have been measured by Tekscan's F-Socket, which employs a matrix of 96 force-sensing resistors (FSR). The sensor strip is 21.5 X 7.5 cm and approximately 0.28 mm thick, and allows pressures to be measured simultaneously over a number of regions inside a socket.

The study cited above and several others provided evidence at a moderate level of confidence that peak pressure on the residual limb increases at the distal tibia and decreases at the patella tendon as socket alignment changes from acceptable to one of greater flexion, whereas it deceases at the distal tibia and increases at the patella tendon as socket alignment changes from acceptable to one of greater extension (7, 23, 31, 35, 36, 46, 52). Flexion of a socket produces results similar to movement of the foot back, and extension of the socket produces results similar to movement of the foot forward. However, small linear shifts of the foot backward and forward may not produce perceived pressure changes of the same magnitude as small angular changes in the orientation of the socket. Changes in the angle of the socket that are not compensated for by changing the alignment of the foot at the ankle basically lift the heel or the toe off the floor such that weight is redistributed toward the part of the foot still in contact with the floor. In contrast, anterior and posterior shifting of the foot does not lift the heel or toe off the floor, but only changes the length of the heel and toe lever arms.

Additional evidence statements and the associated levels of confidence developed as a result of the State-of-the-Science review are presented below (61):

1. The times of occurrence of intra-socket peak pressures are significantly affected when an acceptable socket flexion-extension alignment is perturbed (31, 52)-*Insufficient Evidence*.
2. The times of occurrence of intra-socket peak shear stresses are significantly affected when an acceptable socket flexion-extension alignment is perturbed (31)-*Insufficient Evidence.*
3. The patterns and durations of intra-socket shear stresses are significantly affected when an acceptable socket flexion-extension alignment is perturbed (52)-*Insufficient Evidence.*
4. Pressure on the distal tibia increases with posterior translation of the foot and decreases with anterior translation of the foot with respect to an acceptable alignment (7, 23, 35)-*Moderate Confidence.*
5. Intra-socket peak shear stresses on the residual limb are significantly affected with anterior and posterior translation of the foot with respect to an acceptable alignment (35)-*Insufficient Evidence.*
6. Intra-socket peak pressures on the residual limb are increased significantly on the lateral distal tibia and decreased on the medial distal tibia when the socket is abducted from an acceptable alignment (7, 23, 35)-*Insufficient Evidence*.
7. Intra-socket peak shear stresses are significantly affected when the socket is perturbed by abduction or adduction from an acceptable alignment (35)-*Insufficient Evidence*.
8. Intra-socket pressures at the lateral distal tibia increase when the foot is translated medial and decrease when the foot is translated lateral from an acceptable alignment (7, 23, 35)-*Moderate Confidence*.
9. Intra-socket pressures at the lateral tibial condyle decreae when the foot is translated medial and increase when the foot is translated lateral from an acceptable alignment (23)-*Moderate Confidence.*
10. Intra-socket peak shear stresses are significantly affected when the foot is translated medial or lateral from an acceptable alignment (35)-*Insufficient Evidence*.
11. Heel wedging increases peak pressure at the distal end of the tibia, and forefoot wedging increases pressure in the subpatellar region (41)-*Moderate Confidence*.
12. Heel wedging increases the time to occurrence of peak pressure in the subpatellar region (41)-*Moderate Confidence*.
13. Heel wedging decreases signal power in the subpatellar region and increases signal power at the distal end of the tibia, and forefoot wedging increases signal power in the subpatellar region and decreases signal power in the distal end of the tibia (41)-*Moderate Confidence*.

Many of the evidence statements deal with shear forces, which cannot be measured with arrays of FSR sensors. For this reason, shear forces could not be examined in this study, which considers only pressures which are normal to the residual limb. Some evidence statements concern medial and lateral pressures, which could be examined by experimentally varying the inset and outset of the foot or abducting and adducting the socket. However due to time and resource limitations of the grant and subject availability, only pressures related to movements of the foot anterior and posterior were examined.

Table 6-1 indicates the theoretical relationship between transducer measurements and impact on the residual limb. These relationships are based on the static analysis of a standing amputee using accepted principles of engineering mechanics, and some reflect paradigms that are taught to prosthetists during training to learn alignment procedures. The table takes into account the force or moment transmitted from the socket to the transducer first, and then the force or moment that would need to be generated by the residual limb to produce this effect on the socket. The latter is interpreted as being equal but opposite in direction to the force exerted by the socket on the residual limb and it is the force or moment transmitted to the residual limb that is presented in the third column. This table can be used to relate parts of the transducer curves (e.g., positive and negative portions) directly to pressures on different regions of the residual limb, and can be used to form hypotheses about how perturbations of a prosthetic foot should affect transducer and pressure measurements. One of the most important variables in the table is the moment about the Y axis, My, which can be either positive or negative. The Y axis on the transducer is directed to the left at right angles to the Z and Y axes, and moments about the Y axis represent forces in the sagittal plane defined by axes Z and X. It is positive early in stance (My+) when the heel strikes the ground, creating a moment that should, according to the hypothesis, produce pressure on the distal tibia and popliteal region. Later in stance as the foot rolls over and the forefoot begins developing the moment due to body weight, the moment becomes negative (My-). A negative moment should produce pressure at the notch and in the gastrocnemius region. Both moments are influenced by the weight of the subject, which appears as a ground reaction force when measurements are carried out using a forceplate, and as Fz when measurements are taken using the transducer. Both moments are also influenced by foot design which determines the stiffness of the heel and forefoot and may influence the location of the center of pressure on the foot. Moment about the Y axis is strongly influenced by the cross product of force (Fz being the dominant force and Fx being a relatively small force in comparison) and the moment arm through which the force is applied.

For Subjects 2, 3, and 4, pressures created by perturbations of the SACH foot were examined. For Subject 1, only the College Park Tru Step foot was examined, and for Subject 4, the BioQuest PerfectStride and BioStride feet were examined in addition to the SACH foot. Tekscan F-Socket arrays were calibrated, inserted in the anterior and posterior regions of the transtibial socket between the socket wall and the liner or wool sock worn by the subject, and secured with tape. The prosthesis was then donned, the transducer initialized, the Tekscan remote data logger turned on, and the subject was instructed to walk straight down a hallway at a self-selected comfortable speed until ten good steps were recorded. Pressures were recorded simultaneously for both sensors. For each foot, pressures associated with the initial acceptable alignment were measured first, and then the foot was moved anterior 5 mm and posterior 5 mm with respect to the socket and pressure measurements were taken again. The initial alignment (referred to as the "Neutral" alignment in tables and figures) replicated the original alignment of the prosthesis as closely as could be established during the set-up of the instrumentation. Set up required replacing the original pylon with a new one shortened to accommodate the thickness of the transducer and Spectrum Alignment System used to achieve the perturbations. The Hosmer Spectrum Alignment System was attached to the distal side of the transducer using the four machined bolt holes. The Spectrum is designed such that the amount of movement of the foot can be determined easily – each revolution of the alignment screw moves the foot by 1 mm. Up to 14 mm of travel is possible in each direction. For each alignment, ten good steps of data were taken, which were recorded and subsequently processed by the GUI for analysis. The perturbations were then carried out without the need to doff and don the prosthesis. Doffing and donning became necessary only in the case of Subject 4, for whom pressure measurements were taken for three different feet. The processing of data by the GUI allowed 50 intervals of pressure and transducer data to be matched in the time domain for regression analysis.

The same procedures were used to fit regression equations for all subjects, feet, and alignments. This was done to ensure consistency and facilitate an examination of results across subjects, feet and alignments. The transducer variables hypothesized *a priori* to be affected by the anterior and posterior perturbation of the foot were Fz, Fx+, Fx-, My+ and My-. These were defined as the independent variables in the regression model, with each of the pressure windows constituting an independent variable. A model that incorporated just these transducer variables

Reported by GUI	Effect from Socket	Effect on Residual Limb as Transmitted Through Socket Interface	Biomechanical Correlate
Force X	Anterior-Posterior Force Perpendicular to Pylon	Anterior-Posterior Force on Limb	Braking and Propulsion Force on Foot
+	Press	ure on Posterior	
-		Pressure on Anterior	
Force Y	Medial-Lateral Force Perpendicular to Pylon	Medial-Lateral Force on Limb	
+		Pressure on Right Side	
-		Pressure on Left Side	
Force Z	Force Parallel to Pylon	Vertical Force on Limb	Vertical Ground Reaction Force Related to Loading Response, Propulsion, and Vertical Movement of body Center of Mass, and/or linear shock absorption
+	Up	ward Pressure	
-	Do	wnward Pressure	Not expected during stance
Moment about X	Abduction or Adduction Rotation Moment on Socket in Frontal Plane of Socket	Moment Creating a Varus or Valgus Moment at the Knee	Moment in Frontal Plane Related to Foot Inversion and Eversion Resistance and/or Foot Inset or Outset and/or Socket Abduction-Adduction
+		Pressure on Distal Right and Proximal Left	
-		Pressure on Distal Left and Proximal Right	
Moment about Y	Flexion or Extension Rotation Moment on Socket in Sagittal Plane of Socket	Moment Creating a Flexion or Extension Moment at the Knee	Moment in Sagittal Plane Related to Heel and Toe Resistance and/or Foot Anterior or Posterior Placement and/or Socket Flexion-Extension
+		Pressure on Distal Anterior and Proximal Posterior	
-		Pressure on Distal Posterior and Proximal Anterior	
Moment about Z	Internal or External Rotation Moment on Socket in Transverse Plane of Socket	Moment Creating an Inward or Outward Rotation Moment at the Knee	Moment in Transverse Plane Related to Foot Rotation Resistance or Foot Internal-External Rotation and/or torsion moment absorption
+		Pressure to Rotate Counter-Clockwise as Viewed from Above	
-		Pressure to Rotate Clockwise as Viewed from Above	

Table 6-1 Interpretation of GUI variables and hypotheses relating to socket pressures.

and no others was termed an *a prioi* model, and was fitted to the data using step-wise regression with the probability for an independent variable to enter set at $p \leq 0.005$. This somewhat high level of significance was adopted to prevent the stepwise regression analysis procedure from bringing in additional variables unless there was a very strong probability that the variable had a significant influence on pressure. The pressure windows examined included the distal tibia, regions lateral and medial to the distal tibia, the notch region, the gastrocnemius region posterior to the distal tibia, and the popliteal region. The sizes of the windows were established by visually inspecting the Tekscan pressure data for each array and bounding those areas exhibiting the highest pressures. Tekscan software that displayed each array as a movie was used to do this. The average pressures for each window were exported using the Tekscan software and imported into the GUI for processing. Figure ZZZ shows the windows for each subject and each sensor. Altogether, 122 regression curves were fitted.

In the case of Subject 1, the middle columns of pressure sensors on the anterior array were damaged sometime during or after the first walking trial, making it impossible to determine pressures at the distal tibia and notch for subsequent perturbations. Instead, windows on the lateral side of the notch area and distal tibia were used to develop models. In the case of Subject 4, examination of the pressure data during processing revealed a somewhat unusual pattern in the popliteal region. The lateral and medial sensors in the popliteal area had distinctly different pressure patterns that suggested much of the force normally being taken by the gastrocnemious region in the latter part of stance was instead being absorbed by the region lateral to the popliteal area. The gastrocnemius region appeared to show no major pressure variations. Because of this, the area lateral to the popliteal region was windowed and used as a substitute for measurements of distal gastrocnemius pressures.

General Results

Peak Moments about the Y Axis and Peak Pressures. General results will be presented first, followed by results for specific subjects. Tables 6-2 and 6-3 indicate how the perturbations affected the transducer measurements of peak moment about the Y axis (My+ and My-) and the peak pressures of the variables used as the dependent variables in the regression analyses. Only results found to be significant at $p \leq 0.05$ (t-test) are presented. According to the theory presented in the table, moment about the Y axis should be affected by the length of the moment arms for the heel and forefoot as determined by the anterior and posterior position of the foot. This relationship can be used to develop a series of hypotheses. As the foot is perturbed anterior, the moment arm of the forefoot should increase in length, and the moment arm of the heel should shorten. As the moment arm increases in length, the magnitude of the moment should increase if the vertical load placed on the forefoot remains the same. The opposite effects should occur if the moment arm decreases in length. Thus, movement of the foot anterior from the neutral alignment should cause an increase the peak My- moment and a decrease in the peak My+ moment, and vice versa if the foot is moved posterior. If the moment increases, then peak pressure should also increase under this paradigm (or decrease if the moment decreases). Thus, perturbation of the foot +5 mm from neutral should increase peak My- values and pressures that are related to My- at the notch and gastrocnemius and decrease peak My+ values and pressures that are related to My+ at the distal tibia and popliteal region. Perturbation of the foot by -5 mm from neutral should increase peak My+ values and pressures at the distal tibia and popliteal region and decrease peak My- values and pressures at the notch and gastrocnemius. If the foot is moved from +5 mm anterior to -5 mm posterior, peak My+ values should show a relatively large increase compared to a perturbation from neutral, peak My- values should exhibit a relatively large decrease, and with this should be associated increases in peak pressures at the distal tibia and popliteal region and decreases in the peak pressures at the notch and gastrocnemius. Table 6-2 presents significant changes in peak values of My and pressure when alignments of +5 mm are compared to alignments of -5 mm, and presents the results of tests of these hypotheses.

For all of the feet and subjects except Subject 4 when using the PerfectStride, peak My+ values exhibited a significant increase when the foot was perturbed from +5 mm to – 5mm, and behaved in accordance with the hypothesis. For all of the feet and subjects except Subject 1 who used the TruStep, peak My- values exhibited a

Change in Moment or Pressure with Change in Alignment from +5 mm to -5 mm			
Variable	**Significant Increase↑[1]**	**Significant Decrease↓[1]**	**No Significant Change**
My+	***S1 TruStep*** ***S2 SACH*** ***S3 SACH*** ***S4 SACH*** ***S4 BioStride***		*S4 PerfectStride*
My-		***S2 SACH*** ***S3 SACH*** ***S4 SACH*** ***S4 PerfectStride*** ***S4 BioStride***	*S1 TruStep*
Distal Tibia Pressure	**<u>S4 SACH</u>** **S4 PerfectStride** **<u>S4 BioStride</u>**	S1 TruStep[2] S2 SACH	S3 SACH
Notch Pressure		**S1 TruStep[3]** **<u>S3 SACH</u>** **<u>S4 SACH</u>** **<u>S4 PerfectStride</u>** **<u>S4 BioStride</u>**	S2 SACH
Popliteal 1st Pressure Peak	**<u>S4 SACH</u>**	S1 TruStep S4 PerfectStride	S2 SACH S3 SACH S4 BioStride
Popliteal 2nd Pressure Peak	S4 SACH	**S1 TruStep** **<u>S3 SACH</u>** **<u>S4 PerfectStride</u>** **<u>S4 BioStride</u>**	S2 SACH
Gastrocnemius Pressure	S4 SACH[4]	**S1 TruStep** **<u>S4 PerfectStride[4]</u>** **<u>S4 BioStride[4]</u>**	S2 SACH S3 SACH

Table 6-2 Comparison of Predictions to Results for 1 cm of Perturbation. Notes: 1. Significant at $p \leq 0.05$. 2. Lateral to distal tibia. 3. Lateral to notch. 4. Lateral to popliteal. Entries in bold indicate changes expected under the apriori hypothesis. Underlined entries for pressure variables show agreement between significant changes in pressures as predicted by the theoretical apriori model and significant changes in My.

<table>
<tr><th colspan="5">Change in Moment or Pressure with Change in Alignment from Neutral to +5 mm and -5 mm</th></tr>
<tr><th>Variable</th><th>Perturbation</th><th>Significant Increase↑[4]</th><th>Significant Decrease↓[4]</th><th>No Significant Change</th></tr>
<tr><td rowspan="2">My+</td><td>+5 mm</td><td>S1 TruStep</td><td>S2 SACH
S3 SACH</td><td>S4 SACH
S4 PerfectStride
S4 BioStride</td></tr>
<tr><td>-5 mm</td><td>S1 TruStep
S4 BioStride</td><td></td><td>S2 SACH
S3 SACH
S4 SACH
S4 PerfectStride</td></tr>
<tr><td rowspan="2">My-</td><td>+5 mm</td><td>S4 BioStride</td><td></td><td>S1 TruStep
S2 SACH
S3 SACH
S4 SACH
S4 PerfectStride</td></tr>
<tr><td>-5 mm</td><td></td><td>S2 SACH
S3 SACH
S4 SACH</td><td>S1 TruStep
S4 Perfect Stride
S4 BioStride</td></tr>
<tr><td rowspan="2">Distal Tibia Pressure</td><td>+5 mm</td><td>S2 SACH</td><td>S4 SACH
S4 PerfectStride</td><td>S1 TruStep[1]
S3 SACH
S4 BioStride</td></tr>
<tr><td>-5 mm</td><td><u>S4 BioStride</u></td><td>S1 TruStep[1] S2</td><td>SACH
S3 SACH
S4 SACH
S4 PerfectStride</td></tr>
<tr><td rowspan="2">Notch Pressure</td><td>+5 mm</td><td>S1 TruStep[2]
S4 BioStride</td><td>S3 SACH
S4 PerfectStride</td><td>S2 SACH
S4 SACH</td></tr>
<tr><td>-5 mm</td><td></td><td>S1 TruStep[2]
<u>S3 SACH</u>
<u>S4 SACH</u>
S4 PerfectStride
S4 BioStride</td><td>S2 SACH</td></tr>
<tr><td rowspan="2">Popliteal 1st Pressure Peak</td><td>+5 mm</td><td></td><td><u>S2 SACH</u>
<u>S3 SACH</u>
S4 SACH
S4 PerfectStride
S4 BioStride</td><td>S1 TruStep</td></tr>
<tr><td>-5 mm</td><td></td><td>S3 SACH
S4 PerfectStride</td><td>S1 TruStep
S2 SACH
S4 SACH</td></tr>
<tr><td rowspan="2">Popliteal 2nd Pressure Peak</td><td>+5 mm</td><td>S1 TruStep</td><td>S3 SACH
S4 SACH
S4 PerfectStride</td><td>S2 SACH
S4 BioStride</td></tr>
<tr><td>-5 mm</td><td></td><td><u>S3 SACH</u>
<u>S4 SACH</u>
S4 PerfectStride</td><td>S1 TruStep
S2 SACH
S4 BioStride</td></tr>
<tr><td rowspan="2">Gastrocnemius Pressure</td><td>+ 5 mm</td><td>S1 SACH
S4 BioStride[3]</td><td>S4 PerfectStride[3] S2</td><td>SACH
S3 SACH
S4 SACH[3]</td></tr>
<tr><td>-5 mm</td><td></td><td>S4 PerfectStride[3]</td><td>S1 TruStep
S2 SACH
S3 SACH
S4 SACH[3]
S4 BioStride[3]</td></tr>
</table>

Table 6-3 Comparison of Predictions to Results for ±5 mm of Perturbation. Notes: 1 Lateral to distal tibia; 2 Lateral to notch; 3 Lateral popliteal and gastrocnemius; 4. Significant at $p \leq 0.05$. Entries in bold indicate changes expected under the apriori hypothesis. Underlined entries for pressure variables show agreement between significant changes in pressures as predicted by the theoretical apriori model and significant changes in My.

significant decrease when the foot was moved from + 5 mm to -5 mm and behaved in accordance with the hypothesis. Resulting peak pressures, however, did not always agree with the hypotheses. Peak notch pressure was consistent with the hypothesis and exhibited significant decreases for all feet and subjects except Subject 2 when using a SACH foot when the foot was moved posterior, and did not exhibit any significant increases. Subject 2 data exhibited no significant change in peak notch pressure. Conversely, this could be rephrased to state that peak notch pressures exhibited significant increases when the foot was moved from -5 mm posterior to +5 mm anterior for all but Subject 2 when using a SACH foot. [The other hypothesis can similarly be restated in terms of movement from a -5 mm position to a +5 mm position.] Peak popliteal pressures (2nd peak) were consistent with the hypothesis and exhibited significant decreases for all feet and subjects except Subjects 2 and 4 when using the SACH foot. Subject 4 actually exhibited a significant increase in peak pressure, which was contrary to the hypothesis. Subject 2 exhibited no significant change in peak pressure when the two positions of the foot were compared. For pressure in the gastrocnemius region, there was still less agreement with the hypothesis. Three feet worn by two of the subjects exhibited results in agreement with the hypothesis, whereas one foot and subject exhibited peak pressures that changed in a direction opposite to the hypothesis, and two feet and two subjects exhibited no significant changes in peak pressure. For the distal tibia, which is perhaps the most critical region of a socket for amputee comfort, peak pressure changes were in agreement with the hypothesis for only one subject and the three feet that the subject used during testing; the peak pressures increased significantly as the foot was moved 1 cm posterior. For two subjects and two feet, the peak pressures decreased significantly, which was opposite to the direction of change hypothesized. For one subject and foot, there was no significant change in peak pressure. It is noted that because the distal tibia region is critical to amputee comfort, it often is provided relief in the socket and extra pressure absorbing materials in gel liners. The one subject who exhibited pressure increases in agreement with the hypothesis used wool socks and a Pelite liner whereas all the other subjects used gel liners. Results may be due in part to differences in the interface (wools socks versus gel liners), or other factors not fully explained.

The table also indicates for which trials there was consistent agreement between significant differences in peak transducer measurements of moments about the Y axis and significant differences in peak pressures. These trials are underlined. Given the design of the experiment (six feet used by four subjects) the maximum number of consistent trials possible was six. The greatest number of consistent trials occurred for the notch peak pressure. Four feet used by two subjects exhibited consistency. Next in number of consistent trials was the maximum value of the 2nd peak popliteal pressure which occurred for three feet used by two different subjects. Following this were the peak gastrocnemius pressure and peak distal tibia pressure with two consistent trials each. It is noted that Subject 4, the subject who used wool socks and a Pelite liner, accounted for eight of the ten trials exhibiting consistency. This subject had the shortest residual limb and the longest experience with prosthesis use.

Table 6-3 presents significant differences for perturbations of $\pm$ 5 mm from the neutral alignment and reveals that small perturbations about the acceptable alignment produced results that, in many cases, would not be predicted from the hypothesis. Twelve trials were examined for each variable; six representing movement of the foot + 5 mm and six representing movement of the foot -5 mm. In only four out of the twelve trials the measured maximum My+ agreed with the changes predicted from the hypothesis; for seven of the trials there were no significant changes in maximum measured My+ and for one trial the change that occurred was in the opposite direction. For My- four trials were in agreement with the hypothesis, and eight showed no significant differences. SACH feet appeared to be the only ones that were in agreement with the hypothesis concerning shifts in alignment that should decrease the maximum moment about the Y axis, primarily that My- should decrease if the foot were shifted posterior. All three SACH feet exhibited changes that were in agreement with this. Two SACH feet exhibited significant decreases in My+ when the foot was shifted anterior, which was in agreement with the hypothesis. Two of the energy storing feet (TruStep and BioStride) were the only feet to show significant increases in moment that were in agreement with the hypothesis. Overall, for fifteen out of twenty-four trials there were no significant changes in moment about the Y axis, but for only one trial was the change in a direction opposite to the hypothesis.

Among the pressure windows, peak notch pressure agreed with the hypothesis seven out of twelve times, the greatest number of any of the pressure windows. Changes for two of the trials were in the opposite direction, and three trials exhibited no significant changes. The maximum of the first peak popliteal pressure was in agreement with the hypothesis five out of twelve times, showed no significant change four times, and changed in a direction opposite to the hypothesis two times. The maximum of the second peak popliteal pressure exhibited agreement with the hypothesis four out of twelve trials, exhibited no significant differences on five trials, and changed in a direction opposite to the hypothesis three times. Change in maximum pressure on the gastrocnemius was in agreement with the hypothesis for three trials, exhibited no significant difference for eight trials, and changed in a direction opposite to the hypothesis once. Results for the maximum distal tibia pressure were similar to the gastrocnemius. Three trials agreed with the hypothesis, seven exhibited no significant change, and two changed in a direction opposite to the hypothesis.

No particular type of foot appeared to be related to consistency of agreement with the hypothesis as it concerned the pressure consequences of perturbation. The SACH and energy storing feet appeared in all categories of results – change in agreement with the hypothesis, no significant change, and change in the opposite direction. However, the number of trials associated with correctly predicted significant decreases in maximum pressure was much greater than the number of trials associated with correctly predicted significant increases in maximum pressure – sixteen trials versus six trials out of a total of sixty trials (5 maximum pressure variables X 2 perturbation directions X 6 feet). To repeat an earlier statement, the results were defined with respect to a shift, in this case from the neutral alignment to one that was either $\pm$ 5 mm anterior or posterior. If results were instead defined as a shift from the perturbed position to a neutral acceptable alignment, these decreases would be defined as increases. This leads to the somewhat counter-intuitive conclusion that at an acceptable alignment, significant changes in pressure are more often in the direction of *greater* pressure rather than *less* pressure compared to a nearby alignment, particularly for the notch and popliteal regions. Due to the small size of the sample and limited amount of data this is a very tentative conclusion. An explanation for it can be proposed: greater pressure implies greater control over the prosthesis and the ability to generate larger moments about the Y axis.

Regression Analysis Results. One hundred twenty-two step-wise regression models were fitted to the data using the procedures described earlier. Each was based on 50 observations representing the intervals developed in the GUI along the time domain. A $p \leq 0.005$ was used to allow into the regression models only those variables that had a very low probability of having no significant relationship with pressure. Only Fx+, Fx-, Fz, My+ and My- were used as candidate independent variables. The general form of the regression model was

$P = \alpha + \beta_1*(Fz) + \beta_2*(Fx+) + \beta_3*(Fx-) + \beta_4*(My+) + \beta_5*(My-)$ where

P is pressure measured in kPa; Fz, Fx+ and Fx- are forces measured in N; and My+ and My- are moments measured in Nm X 10.

The regression coefficients obtained are shown in tables 6-4, 6-5, and 6-6 for four pressure windows – the distal tibia, popliteal region, gastrocnemius region, and the notch. While other pressure windows were analyzed, only these four are reported in the tables. These windows represent 84 regressions, or 68.8% of the total regressions. Table 6-7 reports the R-square values. Over 84% of the multiple correlation coefficients were higher than 0.900, 51% were 0.950 or higher, and 12% were 0.990 or higher. The lowest value was 0.692 for the distal tibia pressure window of Subject 1 for a perturbation of -5 mm. Thus, the degree of fit of the data to the models was extremely high. Tables 6-8, 6-9, and 6-10 provide statistics on the model regression coefficients including the total number of regressions in which they appeared, the number of times they were added to or deleted from the regression for the neutral alignment, and the direction in which the regression coefficient changed (increase or decrease) with perturbation. These tables provide results for additional pressure windows that are not reported in tables 6-4, 6-5, and 6-6. The individual equations are given for each subject, foot, and alignment perturbation in matrix form at the end of the chapter along with graphs of the variables and predicted versus actual values of pressures.

Tables 6-8, 6-9, and 6-10 indicate that Fz, or the vertical force along the pylon analogous to ground reaction force, appeared in 80 regressions, or 95% of the total for the four windows. The other independent variables appeared in fewer regressions. My- appeared in 52 regressions (62%), Fx- appeared in 46 regressions (55%), Fx+ appeared in 31 regressions (37%), and My+ appeared in 29 regressions (35%). These results suggest that Fz, or force parallel to the pylon, played a major and pervasive role in producing and influencing intra-socket pressure. The negative My moment that occured toward the end of stance had the second most pervasive effect, and negative Fx, or force directed toward the anterior of the residual limb, had the third most pervasive effect across the subjects and feet included in the study. Positive Fx and My were present in only about one third of the models.

In the tables, values of the coefficients for the neutral acceptable alignment are printed in bold to make them easier to see, and asterisks (*) indicate that the stepwise algorithm did not include the independent variable. Examination of the number of times a variable appeared in the equation for the neutral alignment reveals that Fz (Table 6-8) appeared in the models for all four pressure windows for all feet, subjects, and perturbations with only one exception – the notch of Subject 3. Magnitudes of the coefficients for Fz varied from a low of 0.019 (Subject 4, BioStride foot, notch) up to 0.173 (Subject 3, SACH foot, popliteal region). In only five cases of perturbation were the resulting coefficients within $\pm$ 1 standard deviation of the value for the neutral alignment.

The regression coefficients for moment about the Y axis varied across subjects, feet, and perturbations (Table 6-9). Negative My was present in six out of six equations for neutral alignment for the distal tibia, and five out of six equations for neutral alignment for the notch and gastrocnemius. At the distal tibia, the negative signs of all the coefficients indicated that it served to decrease pressure. At the other three sites in the socket, the positive signs indicated that My- increased pressure. At the distal tibia, My- was present in the equations for all the perturbations with the exception of the -5 mm shift for Subject 1. At the notch, My- was not present in the neutral alignment model for Subject 1, but did appear in the models for the perturbations with a negative sign, indicating that in these models it correlated with a decrease in pressure for Subject 1. It appeared in the notch neutral alignment and perturbation models of all the other subjects with the exception of the + 5 mm perturbation for Subject 4 when using the BioStride foot. For the gastrocnemius window pressures, My- disappeared from the perturbation equations for four of the ten models.

The positive My moment appeared in three of the neutral alignment models for the distal tibia, but the coefficient for the BioStride foot had a negative sign, whereas the working hypothesis calls for a positive sign. Within the logical framework of the regression model, the negative sign implies that at heel contact the moment generated about the Y axis due to the design of the foot actually reduces, rather than increases, pressure at the distal tibia. Additional research would be needed to verify this. The positive My moment also appeared in three models each for the popliteal and gastrocnemius regions, though for different subjects and feet. It appeared in only one model for the notch. Positive My failed to appear in 43 models, or more than half of the total. Examining the data in table 6-9 column by column facilitates a non-statistical analysis of the interaction between foot type and the inclusion of the independent variable in the models. The moment about the Y axis appears in all but four of the twenty-four possible models for the SACH foot used by Subject 4, suggesting that the moment influences pressure in many regions of the socket in a variety of alignments. In contrast, moment about the Y axis appears in only nine of the twenty-four possible models for the TrusStep foot used by Subject 1, suggesting that it influences pressure in fewer regions of the socket and pressure appears not to be influenced significantly in many regions if the foot is perturbed slightly. In general, the SACH feet in the study tend to exhibit the involvement of moment about the Y axis in a greater number of regressions than do the energy storing feet: 15, 12, and 20 models for the SACH feet for Subjects 2, 3, and 4 respectively versus 9, 14, and 11 models for the TruStep, PerfectStride, and BioStride, respectively (Subjects 1 and 4).

Fz Regression Coefficients								
			Subject 1[1]	Subject 2	Subject 3	Subject 4[2]		
	Model	**Alignment**	**TruStep**	**SACH**	**SACH**	**SACH**	**PerfectStride**	**BioStride**
Fz	**Distal Tibia**	+5mm	0.057 0.	031	0.176 0.	030 0.	041	0.033
		Neutral	**0.063 ± 0.001**	**0.029 ± 0.001**	**0.163 ± 0.006**	**0.052 ± 0.004**	**0.061 ± 0.004**	**0.056 ± 0.002**
		-5 mm	0.043 0.	033	0.176 0.	041 0.	066	0.076
	Popliteal	+5mm	0.080 0.	096	0.127 0.	030 0.	037	*0.043*
		Neutral	**0.097 ± 0.001**	**0.079 ± 0.001**	**0.173 ± 0.004**	**0.045 ± 0.001**	**0.065 ± 0.004**	**0.043 ± 0.001**
		-5 mm	0.056 0.	091	0.122 0.	035 0.	054	*0.043*
	Gastrocnemius	+5mm	*0.043*	*0.029*	0.076 0.	020 0.	026	0.022
		Neutral	**0.043 ± 0.001**	**0.028 ± 0.001**	**0.083 ± 0.001**	**0.032 ± 0.001**	**0.040 ± 0.002**	**0.021 ± 0.001**
		-5 mm	0.020 0.	031	0.078 0.	034 0.	033	0.022
	Notch	+5mm 0	.023	0.044	*	*0.014*	0.025 0.	020
		Neutral	**0.040 ± 0.001**	**0.026 ± 0.004**	*****	**0.014 ± 0.001**	**0.042 ± 0.002**	**0.019 ± 0.001**
		-5 mm	*	0.034	*	*0.015*	0.024 0.	013

Table 6-4. Fz Regression Coefficients for Neutral Alignment and ± 5 mm Pertubations

1. Dsital tibia = lateral to the distal tibia; Popliteal = proximal gastrocnemius; Notch=lateral to anterior
2. Gastrocnemius=lateral gastrocnemius

Coefficients for perturbations within ± 1 standard deviation of the coefficient for the neutral regression are shown in italics.

My Regression Coefficients								
			Subject 1[1]	Subject 2	Subject 3	Subject 4[2]		
	Model	**Alignment**	**TruStep**	**SACH**	**SACH**	**SACH**	**PerfectStride**	**BioStride**
My+	**Distal Tibia**	+5mm	0.036 *		*	0.077 0	.091 0	.084
		Neutral	*****	*****	**0.191 ± 0.037**	**0.101 ± 0.014**	*****	**-0.084 ± 0.025**
		-5 mm	*	-0.024	*	*0.099*	* *	
	Popliteal	+5mm *		-0.105	*	*	0.077	*-0.075*
		Neutral	**-0.043 ± 0.005**	*****	*****	**-0.032 ± 0.003**	*****	**-0.075 ± 0.020**
		-5 mm	*	-0.038 *		*	-0.083 *	
	Gastrocnemius	+5mm *		-0.036	*	-0.039	*-0.080*	*
		Neutral	*****	*****	**-0.026 ± 0.008**	**-0.054 ± 0.004**	**-0.090 ± 0.015**	*****
		-5 mm	*	-0.016 *		-0.062 *		*
	Notch	+5mm	0.058	* *		-0.028	* *	
		Neutral	*****	*****	*****	**-0.021 ± 0.002**	*****	*****
		-5 mm	* * *			*-0.023*	* *	
My-	**Distal Tibia**	+5mm	-0.055 -	0.014 -	0.182	-0.037 -	0.042 -	0.024
		Neutral	**-0.020 ± 0.002**	**-0.009 + 0.001**	**-0.172 ± 0.009**	**-0.057 ± 0.006**	**-0.077 ± 0.009**	**-0.051 ± 0.004**
		-5 mm	*	-0.017	-0.208	-0.035	*-0.071*	-0.078
	Popliteal	+5mm	-0.053 -	0.020 *		*	0.077	*
		Neutral	*****	**0.021 + 0.002**	**0.054 ± 0.007**	**0.042 ± 0.002**	*****	*****
		-5 mm	* -	0.009	*	* * *		
	Gastrocnemius	+5mm *		*	*0.047*	0.063 0	.110 *	
		Neutral	*****	**0.009 + 0.001**	**0.047 ± 0.002**	**0.068 ± 0.003**	**0.121 ± 0.004**	**0.070 ± 0.006**
		-5 mm	-0.030	* 0	.052	0.079	* 0	.040
	Notch	+5mm	-0.034	0.026 0	.194	0.025 0	.117 *	
		Neutral	*****	**0.117 + 0.005**	**0.227 ± 0.011**	**0.032 ± 0.001**	**0.134 ± 0.005**	**0.012 ± 0.001**
		-5 mm	-0.040	0.065 0	.142	0.022 0	.012 0	.015

Table 6-5. My Regression Coefficients for Neutral Alignment and ±5 mm Perturbations

1. Dsital tibia = lateral to the distal tibia; Popliteal = proximal gastrocnemius; Notch=lateral to anterior
2. Gastrocnemius=lateral gastrocnemius

Coefficients for perturbations within ± 1 standard deviation of the coefficient for the neutral regression are shown in italics.

			Fx Regression Coefficients					
			Subject 1[1]	Subject 2	Subject 3	Subject 4[2]		
	Model	**Alignment**	**TruStep**	**SACH**	**SACH**	**SACH**	**PerfectStride**	**BioStride**
Fx+	**Distal Tibia**	+5mm *		-0.166	_-0.709_	-0.130 *		_-0.262_
		Neutral	**0.130 ± 0.032**	**-0.054 ± 0.008**	**-0.692 ± 0.092**	**-0.297 ± 0.026**	*****	**-0.288 ± 0.026**
		-5 mm	*	_-0.060_	_-0.616_	-0.246 -	0.294	-0.352
	Popliteal	+5mm	*	* * 0		.103	0.246	*
		Neutral	*****	**-0.066 ± 0.015**	*****	**0.038 ± 0.007**	*****	**0.135 ± 0.021**
		-5 mm	*	* * 0		.102	0.203	*
	Gastrocnemius	+5mm	*	* * 0		.046	0.160	0.129
		Neutral	*****	*****	*****	*****	**0.112 ± 0.015**	*****
		-5 mm	0.140	* * *			* *	
	Notch	+5mm	*	* * -		0.036	* *	
		Neutral	*****	*****	*****	*****	*****	**0.047 ± 0.008**
		-5 mm	-0.349	* * 0		.012	*	_0.042_
Fx-	**Distal Tibia**	+5mm 0.	135	0.146	_0.222_	0.051 0	.097	*
		Neutral	**0.053 ± 0.009**	**0.106 ± 0.007**	**0.222 ± 0.051**	*****	**0.143 ± 0.028**	*****
		-5 mm	*	0.141	0.341	*	*	*
	Popliteal	+5mm 0	.232	0.365	*	*	-0.249	*
		Neutral	*****	**-0.070 ± 0.012**	**-0.326 ± 0.030**	**-0.170 ± 0.008**	*****	*****
		-5 mm	*	0.221	* *		* *	
	Gastrocnemius	+5mm *		0.156	*	-0.115	-0.284	0.172
		Neutral	*****	**0.048 ± 0.005**	**-0.056 ± 0.011**	**-0.183 ± 0.008**	**-0.257 ± 0.011**	**-0.099 ± 0.016**
		-5 mm	0.140	0.123	*	_-0.182_	* *	
	Notch	+5mm 0	.247	0.530	-0.377	-0.046	_-0.331_	0.042
		Neutral	**0.082 ± 0.004**	**-0.236 ± 0.035**	**-0.483 ± 0.052**	**-0.057 ± 0.004**	**-0.323 ± 0.017**	*****
		-5 mm	0.238	0.234 -	0.209	-0.048	0.072 *	

Table 6-6. Fx Regression Coefficients for Neutral Alignment and ±5 mm Perturbations.

1. Dsital tibia = lateral to the distal tibia; Popliteal = proximal gastrocnemius; Notch=lateral to anterior

2. Gastrocnemius=lateral gastrocnemius

Coefficients for perturbations within ± 1 standard deviation of the coefficient for the neutral regression are shown in italics.

Multiple Correlation Coefficients –R^2							
		Subject 1[1]	**Subject 2**	**Subject 3**	**Subject 4[2]**		
	Alignment	**TruStep**	**SACH**	**SACH**	**SACH**	**PerfectStride**	**BioStride**
Distal Tibia	+5mm 0.	954	0.891	0.978	0.944	0.936	0.703
	Neutral	**0.990**	**0.987**	**0.969**	**0.946**	**0.875**	**0.944**
	-5 mm	0.692	0.957	0.983	0.952	0.920	0.909
Popliteal	+5mm 0.	974	0.984	0.954	0.867	0.990	0.916
	Neutral	**0.995**	**0.995**	**0.985**	**0.988**	**0.829**	**0.952**
	-5 mm	0.785	0.995	0.966	0.828	0.953	0.940
Gastrocnemius	+5mm 0.	920	0.949	0.986	0.990	0.985	0.893
	Neutral	**0.992**	**0.994**	**0.996**	**0.977**	**0.992**	**0.965**
	-5 mm	0.888	0.990	0.989	0.967	0.851	0.914
Notch	+5mm 0.	970	0.978	0.911	0.987	0.953	0.895
	Neutral	**0.980**	**0.974**	**0.929**	**0.980**	**0.980**	**0.940**
	-5 mm	0.977	0.950	0.907	0.968	0.881	0.918

Table 6-7. Multiple Correlation Coefficients for Neutral Alignment and ±5 mm Perturbations.

1. Dsital tibia = lateral to the distal tibia; Popliteal = proximal gastrocnemius; Notch=lateral to anterior
2. Gastrocnemius=lateral gastrocnemius

Regression Coefficient Summary for Fz								
		Subject 1	**Subject 2**	**Subject 3**	**Subject 4**			
		TruStep	**SACH**	**SACH**	**SACH**	**PerfectStride**	**BioStride**	Total
	Total Regressions	23	18	18 21		21	21 122	
Fz	Regressions with Fz	21	18	15	21	20	21	116
	Added to Neutral Regr	0	0	0	0	0	0	0
	Deleted from Neutral Regr	2	0	0	0	0	0	2
	Max. non-zero value	+0.97	+0.096	+0.176	+0.052	+0.081	+0.076	
	Regression	Neut prox gas	+5 popliteal	± 5 dist tib	Neut dist tib	Neut lat dist tib	-5 dist tib	
	Min. non-zero value	+0.20	+0.026	+0.059	+0.010	+0.003	+0.003	
	Regression	-5 dist gas	Neut notch	+5 med dist tib	-5 med dist tib	Neut med dist tib	+5 med dist tib	
	Changes with +5mm*							
	Distal tibia	NA	↑	↑	↓	↓	↓	
	Popliteal	↓	↑	↓	↓	↓	↑	
	Gastrocnemius	0	↑	↓	↓	↓	↑	
	Notch	NA	↑ *		0	↓	↑	
	Changes with -5mm*							
	Distal tibia	NA	↑	↑	↓	↑	↑	
	Popliteal	↑	↑	↓	↓	↓ 0		
	Gastrocnemius	↓	↑	↓	↑	↓	↑	
	Notch	NA	↑ *		↑	↓	↓	

Table 6-8. Fz Regression Coefficient Summary

No change in value is reported as 0; **A** means added to regression for neutral alignment and **D** means deleted from regression for neutral alignment, and an asterisk (*) means it was not included in the regression. NA means not applicable due to sensor malfunction

Regression Coefficient Summary for My								
		Subject 1	**Subject 2**	**Subject 3**	**Subject 4**			
		TruStep	**SACH**	**SACH**	**SACH**	**PerfectStride**	**BioStride**	Total
Total	Regressions	23	18	18	21	21	21	122
My+	Regressions with My+	6	5	3	16	9	7	47
	Added to Neutral Rg	3	0	0	1	3	0	7
	Deleted from Neutral Rg	3	1	6	4	2	5	21
	Max. non-zero value	+0.058	-0.105	+0.191 +0.101		-0.108	-0.195	
	Regression	+5 lat anterior[2]	+5 popliteal	Neut dist tib	Neut dist tib	+5 med gastroc	-5 dist tib	
	Min. non-zero value	-0.043	-0.024 -0.026		-0.017	0.058	-0.010	
	Regression	Prox gastroc	-5 dist tib	Neut gastroc	-5 lat dist tib	Neut lat dist tib	+5 med gastroc	
	Changes with +5mm*							
	Distal tibia	NA[3] *		D	↓ A		D	
	Popliteal	D	A	*	D	A	D	
	Gastrocnemius	*	A	D	↓	↓↑ *		
	Notch	NA[3] *		*	↑ *		*	
	Changes with -5mm*							
	Distal tibia	NA[3] A		D	↓ *		↑	
	Popliteal	D	A	*	D	*	D	
	Gastrocnemius	*	A	D	↓	D↓ *		
	Notch	NA[3] *		*	↑ *		*	
My-	Regressions with My-	9	16	16	17	16	12	86
	Added to Neutral	4	0	0	0	1	0	5
Deleted	from Neutral	1	0	2	4	1	5	13
	Max. non-zero value	-0.053	+0.117	+0.227 +0.079		+0.134	-0.115	
	Regression	+5 prox gast	Neut notch	Neut notch	-5 lat gastroc	Neut notch	+5 med gastroc	
	Min. non-zero value	+0.017	± 0.009	+0.007	-0.004	-0.003	-0.005	
	Regression	Neut ant med prox	Neut gastroc[1]	Neut med dist tib	-5 med dist tib	-5 med dist tib	+5 med dist tib	
	Changes with +5mm							
	Distal tibia	NA[3]	↑	↑	↓	↓	↓	
	Popliteal	*	↑ D		D	↓ *		
	Gastrocnemius	*	D	0	↓	↑	↓	
	Notch	NA[3]	↓	↓	↓	↓ D		
	Changes with -5mm							
	Distal tibia	NA[3]	↑	↑	↓	↓	↑	
	Popliteal	*	↓ D		D	*	*	
	Gastrocnemius	*	D	↑	↑ D		↓	
	Notch	NA[3]	↓	↓	↓	↓	↑	

Table 6-9 My Regression Coefficient Summary

No change in values is reported as 0; **A** means added to regression for neutral alignment and **D** means deleted from regression for neutral alignment, and an asterisk (*) means it was not included in the regression. Notes: 1. Also neutral medial distal tibia and -5 popliteal. 2. also -5 med anterior.
3. not applicable due to sensor malfunction

	Regression Coefficient Summary for Fx							
		Subject 1	**Subject 2**	**Subject 3**	**Subject 4**			
		TruStep	**SACH**	**SACH**	**SACH**	**PerfectStride**	**BioStride**	Total
	Total Regressions	23 18		18	21 21		21	122
Fx+	Regressions with Fx+	6	9	5	18	13	13	64
	Added to Neutral Rg	2	0	0	3	3	1	9
	Deleted from Neutral Rg	5	3	5	0	0	4	17
	Max. non-zero value	-0.938	-0.215	-0.709 -0.297		-0.294	-0.352	
	Regression	-5 prox gastroc	+5 lat dist tibia	+5 dist tibia	Neut dist tib	-5 dist tibia	-5 dist tibia	
	Min. non-zero value	+0.085	+0.044 -0.055		+0.012	+0.016	+0.042	
	Regression	Neut Mid gas	Neut med dist tib	Neut med dist tib	-5 notch	-5 dist lat tib	-5 notch	
	Changes with +5mm*							
	Distal tibia	NA	↑	↑	↓ *		↓	
	Popliteal	*	D	*	↑ A		*	
	Gastrocnemius	*	*	*	*A	↑	↑	
	Notch	NA	*	*	*A	*	*A	
	Changes with -5mm*							
	Distal tibia	NA	↑	↓	↓ A		↑	
	Popliteal	*A	D	*	↑ A		D	
	Gastrocnemius	*A	*	*	*	D	*	
	Notch	NA	*	*	*A	*	↓	
Fx-	Regressions with Fx-	11	18	12	13	14	10	78
	Added to Neutral Rg	3	0	0	1	2	2	8
	Deleted from Neutral Rg	1	0	4	3	1	3	12
	Max. non-zero value	+0.266	+0.530	-0.483 -0.183		-0.331	+0.172	
	Regression	-5 med notch	+5 notch	Neut notch	Neut gas	-5 notch	+5 Lat gastroc	
	Min. non-zero value	+0.053	-0.070 -0.056		-0.034	+0.013	0.029	
	Regression	Neut Lat dist tib	Neut popliteal	Neut gastroc	Neut Lat dist tib	-5 med dist tib	Neut Med dist tib	
	Changes with +5mm							
	Distal tibia	NA	↑ 0		*	↓ *		
	Popliteal	*	↑ D		D	↑ *		
	Gastrocnemius	*	↓ D		↓	↑	↑	
	Notch	NA	↑	↓	↓	↑ *A		
	Changes with -5mm							
	Distal tibia	D	↑	↑ *		D	*	
	Popliteal	*	↑ D		D	*	*	
	Gastrocnemius	*A	↑ D		↓ D		D	
	Notch	NA	↑	↓	↓	↓ *		

Table 6-10. Fx Regression Coefficient Summary

No change in values is reported as 0; **A** means added to regression for neutral alignment and **D** means deleted from regression for neutral alignment, and an asterisk (*) means it was not included in the neutral regression. NA means not applicable due to sensor malfunction.

Along the X axis, the regression coefficients for Fx+ and Fx- varied across subjects, feet, and perturbations (Table 6-10). Negative Fx, or force directed toward the anterior of the residual limb, appeared in more models (46 out of 84) than positive Fx, or force directed toward the posterior of the residual limb (31 out of 84 models). Negative Fx appeared in four neutral alignment models of pressure for the distal tibia with a positive sign indicating that it increased pressure. It appeared five out of six times in neutral alignment models for the notch, four times with a negative sign indicating that it correlated with a decrease in pressure. This is counter-intuitive since pressure on the anterior of the limb would be expected to increase pressure. Fx becomes negative after about 20% -35% of stance and its curve has a shape similar to the negative moment about Y. One possibility is that pressure at the notch is traded off for pressure elsewhere on the anterior of the residual limb such as the distal tibia, possibly through rotation of the socket, which would be possible if there were sufficient relief at the distal tibia or thick gel material in the liner which allowed compression. Of the four trials exhibiting a role for Fx- in the models in which it decreased pressure at the notch, three also had models exhibiting a role for Fx- in which it increased pressure at the distal tibia. Negative Fx also appeared five times in neutral alignment models for the gastrocnemius region, four with a negative sign indicating that it correlated with a decrease in pressure.

Positive force along the X axis directed toward the posterior region of the residual limb or in the forward direction, Fx+, appeared in fewer models than Fx-. It appeared with a negative sign in four out of six equations for neutral alignment for the distal tibia, indicating that an increase in force in the positive X direction on the posterior of the residual limb correlated with a decrease in pressure at the distal tibia. This seems consistent with theory if the residual limb is pressing into the posterior wall of the socket and thereby relieving the distal tibia. Fx+ appeared with a positive sign for Subject 1. It appeared with a positive sign in two models for the popliteal region for neutral alignment, and with a negative sign for Subject 2. It appeared in one model each with a positive sign for the gastrocnemius region and the notch, indicating a correlation between the magnitude of Fx+ and pressure at both the distal posterior region of the residual limb, which is consistent with the hypothesis, and at the notch, which would require an explanation similar but opposite to the one for the distal tibia and Fx-; positive pressure on the posterior of the residual limb could mean that the socket is rotating such that pressure increases on the notch. Fx+ did not enter 41of the 84 equations. With perturbations, it disappeared from five of the models for neutral alignment. It appeared in 9 perturbation models for which it was not present in the model for neutral alignment. Looking down the columns of Table Z Fx tended to appeared more times in the models for the SACH feet rather than the energy storing feet. It appeared in 16, 11, and 17 models for Subjects 2, 3, and 4, respectively, who were using SACH feet. It appeared in 10, 13, and 10 models involving energy storing feet for Subjects 1 and 4.

In summary, most of the regression models appeared to have coefficients unique to the subject, foot, and alignment. The R-square values were very high, however, and the pressure estimates made with the majority of the models were extremely accurate. Examination of the results suggests that force parallel to the pylon correlated significantly with pressure for nearly every trial and pressure window that was examined. The negative moment about the Y axis that tends to occur after approximately 25% of stance appeared to have the strongest relationship to a reduction of pressure at the distal tibia. The negative My moment also appeared to have a strong relationship with an increase in pressure at the notch. Positive My moment did not appear to have a strong relationship to an increase of pressure at the distal tibia, although theory states that it should. Reasons may be the use of gel liners or relief in the socket. Force along the X axis appeared to have mixed and often ambiguous relationships with pressures that required making additional untested assumptions to reconcile results with theory. In terms of the feet themselves, the SACH feet overall employed more variables in the regressions than the energy storing feet, an average of 3.51 variables per model compared to 2.91 variables per model (significant at $p = 0.0043$, t-test). However, the models for the energy storing feet did not predict maximum values as well as the models for the SACH feet. There were no significant differences in the average number of variables per model between the neutral alignment and the perturbations among the SACH or energy storing feet. An important finding was that the regression coefficients did not appear to vary smoothly or predictably with perturbations of $\pm$ 5 mm as implied in the model by Winarski.*et al* at the beginning of the chapter. With perturbation, independent variables frequently dropped out of the models. Use of a lower level of significance to enter the models, such as 0.05, might have resulted in fewer variables dropping out. Sometimes the values of the regression coefficients for the neutral alignment were greater than the values for both perturbations, sometimes they were smaller, and sometimes they lay in between. The large number of coefficients made it challenging to discern any patterns in the shifts and additional analysis would be necessary to examine this. Also, the timing of the maximum values of both the dependent and independent variables frequently changed with alignment perturbation, which might have influenced the values of the regression coefficients. These changes are reported in the tables for individual models, which are discussed in the next section. Additional analysis would be necessary to determine how these changes influenced results.

Individual Regression Models

At the end of the chapter are presented for each subject and foot the figures showing the pressure windows (Figure A), graphs of variables (Figure B), tests of statistical significance for maximum values (Table A), a summary of regression coefficient patterns of change as a result of perturbations of alignment (Table B), the coefficient matrices for each alignment (Table C), and graphs of predicted versus actual pressures (Figure C). Results for subjects 1, 2, 3, and 4 are presented in tables labeled 6-11, 6-12, 6-13, and 6-14, respectively ant figures labeled 6-1, 6-2, 6-3, and 6-4, respectively.

Subject 1. The residual limb of Subject 1 was protected with a thick distal end pad and thick gel liner, and had pressure sensitivity thresholds of 9.6 g at the distal tibia, and greater than 20 g at the distal gastrocnemius, patella tendon, and popliteal areas. There were relatively many areas on the limb having low pressure sensitivity. The foot tested was the TruStep, which was a spare foot that had been used previously by the subject and with which the subject was familiar. The TruStep foot features small elastomeric bumpers placed between rigid components to absorb and release energy. The cells in the middle two columns of the anterior sensor became damaged during the first walking trial, making it impossible to compare distal tibia and notch pressures with the perturbation trials. This was due to the subject using a sleeve instead of a pin suspension system, and the inability of the sensor array to accommodate flexing of the knee when underneath the sleeve. Because of the loss of data from these cells, analysis used the sensor cells lateral to the notch and distal tibia for all conditions. The subject used a spare socket with no reported fit problems. The maximum values of Fx-, Fz, and My- occurred earlier for the perturbations than for the neutral alignment, but the pressure maximums did not show time shifts as great. There were significant differences in maximum values for the neutral alignment compared to the perturbations ($p \leq 0.05$) for Fx+, the 1st peak of Fz, and My- for the +5 mm perturbation; and for Fx+, the 2nd peak of Fz, and My+ for the – 5mm perturbation. With the – 5mm perturbation the increase in My+ was 19.4%., indicating the effect of an increase in the length of the heel lever arm. The other significant changes were all less than 10% of the absolute values of the forces and moments. Significant differences in maximum pressures occurred with the +5 mm perturbation for the lateral anterior (notch substitute), 2nd peak of Fz, and 2nd peak of the distal gastrocnemius windows. With the -5mm perturbation, significant pressure differences occurred for the anterior lateral, 1st peak of the distal gastrocnemius, and lateral to the distal tibia (substitute for the distal tibia) windows. The differences for these windows were all less than 6 kPa, and thus may not be of clinical importance. The models containing the most variables were for the regions lateral to the distal tibia (neutral) and lateral anterior (+5mm) with four independent variables each. The distal gastrocnemius models for the neutral and +5mm alignments were simple and contained only Fz. The regression coefficients for Fz were of approximately the same magnitude as those for Subjects 3 and 4. The My+ coefficients were zero for the neutral alignment for all pressure windows except the popliteal, suggesting that the initial Y moment at heel contact did not affect pressure in most regions of the socket. However, the My+ variable entered the models for the foot was moved forward +5 mm, which contradicts the initial hypothesis. Similarly, the My- regression coefficients were zero for the neutral alignment for the gastrocnemius region, the popliteal region, and the notch. However, it entered the models for the popliteal and notch when the foot was perturbed +5mm, and for the notch when the foot was perturbed – 5mm. The My- regression coefficient was negative for the distal tibia and the other windows, indicating that it served to relieve pressure in late stance during the propulsion phase. Fx+ and Fx- also did not appear in a majority of the models for the neutral alignment. Multiple correlation coefficients (R^2) were all above 0.980 for the neutral alignment, and tended to decrease for the perturbations. Model accuracy for the neutral alignment was high as indicated in the plots of actual versus predicted pressure. The 0.692 value for the distal tibia at the -5mm alignment was the lowest in the study, and the values for the -5mm models at the popliteal, and gastrocnemius regions were also among the lowest in the study. The acceptable alignment for Subject 1 could be characterized as one which allowed the subject to minimize the pressure effects of moments about the Y axis and forces along the X axis, and allowed Fz to be the source of much of the pressure.

Subject 2. Subject 2 had a residual limb with pressure sensation of 2.4 g at all locations except the distal tibia, where it was 9.6 g. The subject used a gel liner with a pin lock and reported using a SACH foot, the foot used in the experiment, previously at some time during the 14 years since amputation had occurred. A medium stiffness heel plug was used. The subject used a spare socket which was due for replacement. The maximum values of Fx-, Fz, and My- tended to occur earlier for the +5 mm perturbation than for the neutral alignment. The maximum values of Fx- and My+ were significantly lower than those of the neutral alignment for the +5mm perturbation, and the peak value of My- was significantly lower for the -5mm perturbation. The differences were all less than 10% of the values for the neutral alignment with one exception; the value of My+ was approximately 23% lower with the +5 mm perturbation. With the +5 mm perturbation there was a significant pressure increase at the distal tibia, and a significant decrease for the 1st peak pressure at the popliteal region. With the – 5 mm perturbation, there were no significant changes in pressure at any of the four windows. The magnitudes of the significant pressure changes were around 3 kPa, which probably were not of clinical importance. The models containing the most variables were, in the neutral alignment the distal tibia (4 variables); at +5 mm the distal tibia and popliteal (4 variables); and at -5 mm the distal tibia (5 variables). With perturbation, two models added independent variables, and only one model lost a variable. No model had fewer than 3 independent variables. The magnitude of the regression coefficient of Fz for the distal tibia at neutral alignment was the lowest of any of the subjects, but was within the range of values spanned by the other subjects for the remaining windows. The My+ variable did not enter the models for any of the windows at neutral alignment, though it appeared for the -5 mm perturbation at the distal tibia, popliteal, and gastrocnemius regions, and also appeared for the +5 mm perturbation at the popliteal and gastrocnemius regions. In all cases it reduced estimated pressure. The My- variable was present in the models for all four windows for the neutral alignment. In the models, the sign of the regression coefficient indicated that it decreased pressure at the distal tibia, and increased it at the popliteal and gastrocnemius regions and the notch. The magnitudes of the coefficients for My- were the lowest of any subject for the distal tibia, popliteal, and gastrocnemius regions and within the range of values of the other subjects at the notch. The variable Fx+ appeared in the models for neutral alignment at the distal tibia and popliteal regions, acting to decrease pressure. The variable Fx- appeared in all four models, acting to decrease pressure in the popliteal region and the notch, and to increase pressure at the distal tibia and gastrocnemius region. With perturbation, the signs of the regression coefficients were all positive, indicating that for all four windows Fx- would increase pressure in the models. The values of the multiple correlation coefficients were all above 0.970 for the neutral alignment and were close to or above 0.950 for both perturbations and models with one exception – at +5 mm for the distal tibia the value was 0.891. Examination of the graphs of predicted versus actual pressures revealed very high accuracy for all models at the neutral alignment. The acceptable alignment for Subject 2 appeared to be influenced by My- and Fx-, and an attempt to minimize pressure at the distal tibia. As a result, pressure was maximized at the notch.

Subject 3. Threshold pressure sensitivity for the residual limb of Subject 3 was 2.4 g or less for all regions. The subject used a gel liner with a pin lock, and had not used a SACH foot prior to data collection. A medium stiffness heel plug was used. The subject used a spare socket that was worn for outdoor activities such as hiking, and was satisfied with its fit. Compared to the neutral alignment, the time interval of occurrence for the maximum values of Fz, Fx+, Fx-, and My- for the perturbations changed by no more than one time interval, or 2% of stance. The time interval for the maximum My+ value was 4% earlier with foot perturbation of $\pm$ 5 mm. With a +5 mm perturbation there was a significant decrease (33%) in the maximum value of My+, and with a –5 mm perturbation there was a significant decrease in Fx+ (30%) and My- (15%0. The time intervals for pressure maximums changed only 2% or did not change at all for all windows except the 1st peak popliteal pressure, which occurred 4% later when the foot was perturbed -5 mm. With perturbation the pressures decreased by a large amount at the notch (44% when the foot was moved -5mm and 20% when the foot was moved +5 mm), and popliteal region for the 1st peak (25% when the foot was moved -5 mm and 26% when the foot was moved +5 mm) and popliteal region for the 2nd peak (29% when the foot was moved -5 mm and 25% when the foot was moved +5 mm). Changes of this magnitude would possibly be of clinical relevance. The force along the pylon, Fz, did not appear in the model for notch pressure, but the regression coefficients for Fz for the other models had the highest numerical values of any of the subjects. The value of the coefficient for the distal tibia was approximately three times as large as those for the other subjects, and the values for the popliteal and gastrocnemius regions were approximately two to two-and-a-half times as large. With perturbation, the values of the regression coefficients for Fz increased at the notch and decreased at the popliteal and gastrocnemius regions. The My+ variable entered the model for the distal tibia neutral alignment where its coefficient had the highest positive value of any subject for any alignment, and was approximately twice as large as the only other subject who produced a model for the distal tibia that included My+. Moment My+ entered the neutral alignment model for the gastrocnemius, but with the smallest magnitude of any of the three subjects who produced a model containing this variable. With perturbation, My+ disappeared from all models. Moment My- entered the neutral alignment models for the notch, distal tibia, popliteal and gastrocnemius regions. At the notch, the regression coefficient was the largest of any subject, and was almost twice as large as the next smallest coefficient produced by a subject. The regression coefficient at the distal tibia was over twice as large as the coefficient next closest in magnitude produced by a subject. With perturbation, My- disappeared from the model for the popliteal region, and exhibited a mixture of increases and decreases for the other pressure windows. Force Fx+ was absent from all regressions except the distal tibia, where the value of the regression coefficient for the neutral alignment was over twice as large in magnitude as the next largest neutral alignment coefficient among the subjects. The negative sign for the coefficient indicated that it reduced pressure at the distal tibia. Force Fx- was present in all four models for the neutral alignment. For the distal tibia, popliteal, and gastrocnemius regions the regression coefficients were the largest of any subject, and the cases of the popliteal and gastrocnemius regions, the sign indicated that Fx- reduced pressure. The positive sign for the distal tibia model indicated a relationship in which Fx- increased pressure. With perturbation the regression coefficients for the popliteal and gastrocnemius regions disappeared from the models. At the notch the regression coefficients decreased in magnitude with perturbatioin, and at the distal tibia posterior movement of the foot left the coefficient unchanged whereas forward movement of the foot caused it to increase. For the neutral alignments, the multiple correlation coefficients for Subject 3 varied from 0.929 at the notch to 0.996 at the gastrocnemius. For the perturbations the values were lower, except in the case of the distal tibia, where they increased slightly. Graphs showing the accuracy of the models indicates that at the distal tibia and popliteal region maximum values were under-predicted by a small amount, and by a larger amount at the notch (approximately 18%). The acceptable alignment for Subject 3 appeared to be characterized by substantially higher pressures at the notch and popliteal regions than with the perturbed alignments, due to Fx- and My-, which were the only variables to appear in the notch model for any of the alignments. Subject 3 was the only subject for whom Fz did not appear in the neutral model for the notch. This may reflect the subject's lack of experience with the SACH foot, or it could reflect a socket design which minimized pressure on the notch. It may imply that at other than the neutral acceptable alignment, the combination of foot characteristics and socket design did not produce optimum control of the prosthesis as manifest by lower pressures in areas important for control.

***Subject 4*.** Pressure thresholds for Subject 4 were 9.6 g at the patella tendon (notch), 20 g at the distal tibia, and 2.4 g at the other locations where touch sensitivity was measured. The subject had the shortest residual limb among the subjects at 9.8 cm. The subject's socket was the one used daily with a Pelite liner, wool socks for volume control, and cuff suspension. Three feet were examined: a SACH foot with a high stiffness heel insert (requested by the subject), the BioQuest PerfectStride, and the BioQuest BioStride. The subject, an amputee for forty years, had prior experience with all three types of feet. To conduct experiments involving the different feet, the prosthesis had to be doffed between trials and the pylon length changed to accommodate the different build heights of the feet. Examination of the pressure sensor data revealed a pattern in the popliteal region that was visibly different from the other subjects. There was a pronounced peaking pattern on the lateral side of the popliteal region that was similar to that for the gastrocnemius region of the other subjects, and distinct from the pattern of peaking in the center of the popliteal region. At the same time, there were no strong pressure peaking patterns in the gastrocnemius region of the socket. It was concluded that the region lateral to the popliteal region was absorbing the loads during the propulsion phase that normally would be absorbed by the gastrocnemius. This region, and the region medial to the popliteal were windowed separately. The lateral region was used to represent the gastrocnemius region for data analysis. Results for each foot will be discussed separately.

Subject 4 – SACH Foot. For the +5 mm perturbation the only significant change in magnitude of the maximum value of a transducer measurement occurred for the 1st peak of Fz, which increased by approximately 4%. Only My- decreased significantly, by approximately 8%, for the – 5 mm perturbation. With respect to shifts in timing of the peaks, the second peak of Fz and the maximum of My- occurred 4% earlier with a perturbation of + 5mm, and there were no changes greater than 2% with the -5 mm perturbation. Examination of pressures revealed that for the +5 mm perturbation maximum pressure at the distal tibia decreased by approximately 51%, maximum pressure for the 1st peak at the popliteal region decreased by approximately 20%, and maximum pressure for the 2nd peak at the popliteal region decreased by approximately 10%. For the -5 mm perturbation maximum pressure at the notch decreased by 20% and the maximum pressure for the 2nd peak at the popliteal region decreased by approximately 6%. Of these changes in maximum pressures, the difference for the distal tibia was 36.0 kPa and potentially of clinical relevance, especially since the subject tested as relatively insensate at this location. The change for the 1st peak in the popliteal region was 12.0 kPa, which might be of clinical relevance. The remaining differences were 5 kPa or less, and likely not of clinical relevance. The timing shifts of maximum pressure events were to an earlier time for the +5 mm perturbation, with 4% of stance differences at the distal tibia, notch, and 1st popliteal peak. The timing shifts for -5 mm perturbations were all 2% earlier, or in the case of the notch, no change. The regression models for Subject 4 and the SACH foot at neutral alignment contained four or five variables, with five being the maximum number that could be in the models. When the foot was perturbed, variables tended to drop out of the models. Regression coefficients for Fz were present in all four models with values that lay inside the range of values for the other subjects and feet, except at the notch, where the model for Subject 4's SACH foot had the lowest value. Subject 4 with the SACH foot was the only subject (and foot) for whom moment My+ appeared in all four models for the neutral alignment. The values of the regression coefficients lay inside the ranges for the other subjects and feet where My+ entered their models. The signs of the coefficients were in accordance with the hypothesis for the distal tibia, the region substituting for the gastrocnemius region, and the notch, but in contradiction for the popliteal region, which, as has been discussed previously, exhibited anomalous pressure patterns. With a perturbation of +5 mm, the regression coefficients decreased at the distal tibia and the region representing the gastrocnemius, and increased at the notch. With a perturbation of -5 mm, regression coefficients increased at the region representing the gastrocnemius. Moment My+ dropped out of the model for the popliteal region when the alignment was perturbed. Moment My- also entered all four models for the neutral alignment with regression coefficient values that lay inside the ranges of the other subjects. Again, the signs of the coefficients were in agreement with the hypothesis for all but the popliteal region. Perturbation of the foot resulted in the loss of My- in the models for the popliteal region, and a decrease in the magnitude of the regression coefficients at the distal tibia and region representing the gastrocnemius. At the notch, movement of the foot +5 mm decreased the magnitude of the regression coefficient and movement -5 mm increased the magnitude of the coefficient. Force Fx+ appeared in the neutral alignment models for the distal tibia and popliteal region with signs indicating that it decreased pressure for the former, and increased it for the latter, which would agree with the hypothesis. Perturbation of the foot in either direction resulted in a decrease in the magnitude of the regression coefficient at the distal tibia and an increase at the popliteal region. Force Fx- appeared in the neutral alignment models for all windows except the distal tibia. The sign of the regression coefficients associated it with decreases in pressure at the notch, popliteal region, and region representing the gastrocnemius. The signs would agree with the hypothesis for the popliteal region and region representing the gastrocnemius, which are on the posterior of the limb. The negative sign at the notch would contradict the hypothesis; however it is noted that Fx+ did not appear in the neutral model for the notch and that negative signs for Fx- appeared in the models for two other subjects and four of the six feet examined. Force Fx- occurs during the propulsion phase when My- occurs, and thus could not be associated with a positive moment about the Y axis, which would tend to increase pressure at the distal tibia and decrease pressure at the notch. It may instead reflect the way in which the anterior wall of the socket interacts with the residual limb; as My- increases, if there is intimate contact between the wall of the socket and the stiff bone and tissue of the tibia, then the anatomic structures below the notch may absorb some of the effect of the moment via an increase in pressure, which reduces pressure at the notch. This is a tentative hypothesis that would have to be investigated further. Coefficients of multiple correlation were all close to or above 0.950 for the neutral models. Values of the coefficients of multiple correlation for the perturbations were close to those for the neutral alignment, except for the popliteal region, where coefficient values dropped from 0.988 to 0.867 and 0.828 for the +5 mm and -5 mm perturbations, respectively. Graphs of model accuracy indicated all pressures including maximum pressures were being predicted with very high accuracy. The acceptable alignment of the SACH foot for Subject 4 appeared to be characterized by the most complex models of the study, with most of the candidate independent variables included. Most of the regression coefficients in the models were in agreement with the hypothesis. It is noted that this subject used a Pelite liner and wool socks, rather than a gel liner, and also was the subject whose years of experience were nearly three times that of the next longest use of a prosthesis among the subjects.

Subject 4 – PerfectStride Foot. The PerfectStride foot is an ESAR foot that features a coil spring design rather than a leaf spring design. The titanium spring represents an anterior facing curved calf shank. The carbon graphite foot keel is a convex plate that arches upward like a leaf spring and replicates the arch of the foot. Significant changes in maximum forces and moments occurred only for -5 mm posterior translation of the foot and consisted of decreases of approximately 18% for Fx+, 4% for Fx-, and 6% for the 1st peak of Fz. With the -5 mm perturbation the interval associated with the maximum value occurred 6% earlier during stance for Fx-, 10% earlier for the 2nd peak of Fz, and 8% earlier for My-. These were large shifts compared to the SACH and TruStep feet, and close to those for the BioStride. Significant decreases in pressure occurred for the +5 mm perturbation for all the pressure windows: approximately 31% at the distal tibia, 23% at the notch, 9% for the 1st peak at the popliteal region, 14% for the 2nd peak at the popliteal region, and 20% for the region representing the gastrocnemius. The changes in pressure ranged from 8.1 to 24.6 kPa which might have clinical relevance for the higher values. The intervals during which the maximum values occurred did not shift more than 2% of stance. For a -5 mm perturbation, maximum pressures decreased significantly at the notch, for the 1st peak at the popliteal region, for the 2nd peak at the popliteal region, and the region representing the gastrocnemius by approximately 48%, 20%, 31%, and 52%, respectively. The magnitudes of the changes ranged from 18.2 to 62.5 kPa which were large and of probable clinical relevance for the higher values. The intervals during which the maximum values occurred shifted to later times during stance by 8% for the distal tibia and by 4% for the notch, and 1st and 2nd peak at the popliteal region. The interval did not shift for the region representing the gastrocnemius. The models for the neutral alignment contained only one variable, Fz, for the popliteal region, three variables for the distal tibia and notch. and all five variables for the region representing the gastrocnemius. The values of the regression coefficients were higher than those for the SACH foot used by Subject 4, and within the range of values for the other subjects. For neutral alignment, the positive My+ moment associated with loading response appeared only in the model for the region representing the gastrocnemius. The maximum My+ moment was 155. 9 Nm X 10, which was only 40% of the maximum value of My+ obtained from the SACH foot used by the same subject, 388. 8 Nm X 10, and probably reflects the coil spring design of the PerfectStride together with the use of a heel plug of high stiffness in the SACH foot. With perturbation of the foot, the My+ variable appeared for all of the windows except the notch. The moment My- appeared in all the neutral alignment models except the popliteal region. The magnitudes of the regression coefficients associated with My- for the notch and region representing the gastrocnemius were the largest of any of the subjects. With perturbation, the regression coefficients for My- tended to decrease in magnitude or were deleted from the models. The Force Fx+ was present only in the model for the region representing the gastrocnemius, which was the only time Fx+ appeared in the neutral alignment model for this pressure window among any of the subjects and feet. Force Fx- appeared in the neutral alignment model for the distal tibia with a positive sign, with agrees with the hypothesis, in the neutral alignment model for the region representing the gastriocnemius with a negative sign, which agrees with the hypothesis, but in similar to the other subjects, Fx- appeared in the model of the notch with a negative sign. For the region representing the gastrocnemius, the regression coefficient had the largest magnitude of any of the subjects and feet. With perturbation of the foot, the magnitudes of the regression coefficients exhibited a mix of increases and decreases, and the models tended to contain more variables; nine variables entered the regressions and four were deleted. Multiple correlation coefficients for neutral alignment models for the distal tibia and popliteal region were lower than typical for the models for other subjects and feet – 0.875 and 0.829, respectively, but were 0.980 and 0.992 at the notch and region representing the gastrocnemius. The data indicate that the multiple correlation coefficients for models of the distal tibia and popliteal region increased in magnitude with perturbation of the foot, but they decreased for the other two pressure windows, creating a relationship that was dissimilar to many of the other feet and subjects in which the coefficients decreased with perturbation. The increase in the multiple correlation coefficient for models of the distal tibia and popliteal region appeared to be related to the increase in the number of variables that entered the models when the foot alignment was perturbed from neutral. In particular, My+ entered the models, which is agreement with the hypothesis that My+ contributes to pressure at the distal tibia and popliteal regions. Examination of the accuracy of the models for the distal tibia and popliteal regions indicated that at the distal tibia the predicted maximum pressures were lower and less sharply peaked than the actual pressures, and at the popliteal region the prediction of the 1st peak was high, the predicton of the 2nd peak was low, and the predicted time of occurrence of the peaks was at a later interval than actually occurred. Reasons for this can only be put forth tentatively. One possibility is that the design of the foot keel tends to reduce the magnitude of accelerations created by the foot and transmitted to the residual limb and vice versa. Moment My+, which occurs during loading response, was relatively low at neutral alignment due to the coil or keel design and did not enter the model. The only remaining variable that correlated well with distal tibia pressure was Fz, which did not exhibit as rapid a rise and as sharp a peak as distal tibia pressure during loading response. Comparison of the Fz graphs of Subject 4 for the SACH and PerfectStride feet reveals how the PerfectStride both reduces the maximum value of Fz and the sharpness of peaking of Fz that occurs with the SACH foot. A question then appears concerning why the distal tibia pressure peaks more sharply. The following reasoning attempts to identify a possible cause. The pressure at the distal tibia could be the result of knee extensor activity initiated by the subject to stabilize the knee. The rotational energy associated with the moment created at the socket as a result of the knee extensor activity could be absorbed by the or keel design spring design of the foot and does not appear as a sharply peaked My+ moment at the transducer, much in the same way that peaking of the Fz force is muted. The acceptable alignment of the PerfectStride foot on Subject 4 appeared to be related to a position in which My+ did not enter the models for the distal tibia or the popliteal regions, which tentatively suggests that the length of the heel lever arm may be important for alignment and related to the coil or keel design.

<u>Subject 4 – BioStride Foot</u>. The BioStride foot is also an ESAR foot that was developed by the same firm subsequent to the PerfecStride. It features a multilayer carbon graphite anterior facing convexly curved and layered calf shank. The carbon graphite foot keel arches upward to replicate the arch of the foot and acts like a leaf spring. The maximum moment of My+ at neutral alignment was only 101.8 Nm X 10 and was the lowest value for any subject and foot. The maximum moment of My- at neutral alignment was 543.7 Nm X 10 and also the lowest value for any subject and foot. Forces Fx+ and Fx- showed no significant changes with perturbation. With +5 mm of perturbation the 1st and 2nd peaks of Fz exhibited a decrease of approximately 3% and an increase of approximately 6% , respectively, and moment My- exhibited an increase of approximately 15%. Intervals during which the maximum values occurred shifted earlier by 8% of stance for My-, 6% for Fx-, and 4% for the 1st and 2nd peaks of Fz and My+. With -5 mm perturbation, moment My+ increased by approximately 37%. The interval of occurrence of maximum values shifted 6% earlier for My-, and 4% earlier for Fx- and the 2nd peak of Fz. A forward perturbation of +5 mm increased pressure at the notch by approximately 15% and at the region representing the gastrocnemius by approximately 10%, and decreased the 1st peak of pressure at the popliteal region by approximately 2%. All of the changes were less than approximately 6 kPa and probably not of clinical relevance. Posterior perturbation of -5 mm increased maximum pressure at the distal tibia by approximately 37%, and decreased pressure at the notch and the 1st peak of the popliteal region by approximately 13% and 7%, respectively. The increase at the distal tibia was 18.7 kPa and possibly of clinical relevance, whereas the decreases at the notch and 1st peak of the popliteal region were less than 4 kPa and probably not of clinical relevance. The neutral alignment models for +5 mm contained more variables than the PerfectStride. All the neutral alignment models contained at least three variables with the model for the distal tibia containing four variables. Moment My+ was included in the neutral alignment models for the distal tibia and popliteal region. However the regression coefficient for My+ at the distal tibia had a negative sign indicating that the moment acted to decrease pressure at the distal tibia during loading response, rather than increase it as the hypothesis predicted. The reason is that moment My+ reached its maximum value at 18% of stance whereas the distal tibia did not reach maximum pressure until 38% of stance when My+ had decreased to almost zero. Force Fx+ also had a negative sign for its neutral alignment regression coefficient in the model for the distal tibia, indicating that it, along with My+, also acted to reduce the effects of Fz during early stance. This can be verified by examining the graphs of model variables for Subject 4. My- was included in the neutral alignment models for the distal tibia, notch, and region representing the gastrocnemius. With the +5 mm perturbation, Fx- entered two models, and My+ was deleted from the models for the distal tibia and popliteal region; My- was deleted from the models for the notch and region representing the gastrocnemius. With the -5 mm perturbation Fx+ and My+ were deleted from the model for the popliteal region and only Fz remained. The values of the regression coefficients for Fz lay within the range of the values of the other subjects. The values of the regression coefficients for My+, as mentioned above, indicated that it served to reduce pressure at the distal tibia, amd the negative sign for the popliteal region indicated that its effect of reducing pressure was similar to the findings for Subject 1 and for the SACH foot for Subject 4. The regression coefficients at the neutral alignment for My- were similar in sign to those of the other subjects and fell inside the ranges exhibited by them. Force Fx+ entered neutral model equations for the distal tibia, popliteal region,and notch. This was the greatest number of neutral alignment models that Fx+ appeared in for any subject or foot. Subject 4 was the only subject to have Fx+ in a neutral alignment model for the notch, where the sign of the coefficient indicated that it increased pressure. At the same time, the BioStride had the fewest neutral alignment models for which Fx- appeared among any of the subjects and feet. The only model in which force Fx- appeared was the neutral alignment model for the region representing the gastrocnemius, where it appeared with a negative sign, which was consistent with results for Subject 3, and the other two feet used by Subject 4. It appeared in the models for two perturbations. The magnitude of the regression coefficient for Fx- fell within the range of those for the other subjects and feet. The multiple correlation coefficients were all at or above 0.940 for the neutral alignment and decreased for the perturbations. Examining the accuracy of the neutral alignment models revealed a small over-prediction at the distal tibia and small under-prediction at the notch, region representing the gastrocnemius, and 2nd peak for the popliteal region. The actual pressures showed sharper peaks and tighter curves at the notch, popliteal region, and region representing the gastrocnemius in a manner similar to the maximum pressure predictions for the PerfectStride. The possible reason may be the same – energy absorption by the shank or keel design of the foot, which mutes maximum pressures developed at the socket. However, the sharp peak of actual pressure at the distal tibia was actually made sharper by the model, in contrast to the results of the distal tibia model for the PerfectStride which produced estimates that were less sharply peaked than the actual pressure. Based on the magnitude of the regression coefficients, the acceptable alignment of the BioStride on Subject 4 appeared to be influenced more strongly by the effects of My+ at the distal tibia and popliteal regions than the PerfectStride and less strongly by the effects of My-. At the neutral alignment, the magnitudes of My+ and My- were substantially less for the BioStride (approximately 65% of the My+ and 75% of My- moments of the PerfectStride moments) as were the maximum distal tibia pressure (74% of the PerfectStride pressure) and popliteal pressure (64% for the 1st peak and 61% for the 2nd peak of the PerfectStride Pressure). The smaller moments of the BioStride were in agreement with the lesser pressures. However, differences in design appear to have made the BioStride pressures at these two socket locations more closely related to moments about the Y axis and perturbation of the foot, primarily through the reduction of pressure at the distal tibia and popliteal region early in stance.

Discussion

The combined use of the measurements of the triaxial transducer and pressure sensors facilitated the development of models that estimate pressures, including maximum pressures, with great accuracy in all of the feet for all of the subjects. The value of the models is that they indicate which transducer measurements appear to explain the pressures, and whether the forces and moments are associated with increases or decreases of the pressures. The models were very complex, however, and require interpretation, which can be challenging. There were major variations among the models for different subjects, feet, and perturbations. Comparison of results to the apriori hypothesis revealed the following:

1. The hypothesis proposed that the My+ moment would be related to pressure and the distal tibia and popliteal region. Results showed this relationship to exist for the SACH foot at the neutral alignment for two different subjects. For the remaining subjects and feet, the My+ moment did not appear in the neutral alignment models for three trials, and in one model it appeared with a negative sign, which was opposite to the causal direction hypothesized. However, examination of the data revealed why the sign was negative. At the popliteal region, My+ appeared in three models and was missing from three models. For those models in which it appeared it had a negative sign, indicating that it was associated with a decrease in pressure, which was in contradiction to the hypothesis. Further examination of the data would be needed to determine an explanation for this.
2. The hypothesis proposed that the My- moment would be related to pressure at the notch and gastrocnemius region. At the notch, the hypothesis was confirmed by five out of six models by the presence of the variable and a sign of that indicated an increase in My+ would be associated with an increase in pressure. For the sixth model, My+ did not enter the equation. The hypothesis was correct for five out of six possible models at the gastrocnemius; My- did not enter the equation for the sixth model.
3. The hypothesis proposed that Fx+ would be associated with pressure increases on the posterior of the residual limb, including the popliteal region and gastrocnemius region. Two neutral alignment models of the popliteal region supported the hypothesis by inclusion of Fx+ with positive signs for the regression coefficients. One neutral alignment model included Fx+ with a negative sign, which was opposite to the hypothesis, and three neutral alignment models did not include Fx+. Only one model at the gastrocnemius region included Fx+, and it had a sign that was in agreement with the hypothesis.

$. The hypothesis proposed that Fx- would be associated with pressure increases on the anterior of the residual limb, including the distal tibia and notch. At the distal tibia, this was confirmed by four out of six possible models for the neutral alignment. For the other two neutral alignment models of the distal tibia, Fx- did not enter the regression relationships. At the notch, Fx- entered five regression neutral alignment relationships, but with a negative sign for four of the models indicating it was associated with a decrease in pressure. Further examination of the data would be needed to determine an explanation for this.

Other results revealed relationships that were not anticipated in the hypothesis. These are identified below.

1. The hypothesis proposed that Fz, force parallel to the pylon, would be associated with upward pressure and did not elaborate further. Results revealed Fz to enter twenty-three out of twenty-four neutral alignment models; it was present in the models for every subject, pressure window, and foot except for the notch of Subject 3. It also was present in all the models for the perturbations except the notch of Subject 3 and the -5 mm perturbation for Subject 1.
2. The hypothesis did not take into account the possibility that a force or moment could be associated with a decrease in pressure.
    A. Moment My+ was associated with a decrease in pressure at the gastrocnemius in three neutral alignment models. The other three models did not include My+. This is consistent with the hypothesis but had not been considered.
    B. Moment My- was associated with a decrease in pressure at the distal tibia in all six models for neutral alignment. This is consistent with the hypothesis, but had not been considered.

C. Force Fx+ acting on the posterior of the residual limb was found to decrease pressure on the distal tibia in four out of five neutral alignment models. This could be consistent with the hypothesis if the socket plus liner or Pelite/sock interface had room sufficient to allow the force to compress the posterior fleshy tissues or gel liner and thereby decrease contact pressure on the anterior of the residual limb. This might be the case in situations when the knee is actively flexing. In the fifth neutral alignment model Fx+ was associated with an increase of pressure on the distal tibia.
D. Force Fx- acting on the anterior of the residual limb was associated with a decrease in pressure for the gastrocnemius region on the posterior in four out of five neutral alignment models. This could also be consistent with the hypothesis if the socket plus liner or Pelite/sock interface had room sufficient to allow the force to compress the anterior of the interface and thereby decrease pressure on the posterior of the residual limb. This might be the case in situations when the knee is actively extending. Since the anterior of the residual limb is bony, tissue compression is less likely to be involved. In the fifth model the sign of the regression coefficient indicated an increase in pressure.

The results suggest that of the four pressure windows examined, the notch may be the region of the socket that is most indicative of alignment acceptability through its relationship with My-. A regression coefficient for My- appeared in five of the six possible models of the notch with the correct sign. It did not appear in the sixth model, for Subject 1, but the array of sensor cells representing the notch was lost for Subject 1 and the true notch could not be modeled. The neutral alignment regression coefficient for My- at the notch had a value higher than the values of the coefficients for the perturbations for eight out of the ten perturbations associated with these five models. This suggests that at the neutral alignment, as opposed to the perturbations, My- had the strongest direct association with notch pressure. An alignment paradigm can be advanced that incorporates this observation, as follows: to obtain the maximum contribution to gait from a prosthetic foot, the moment generated during the propulsion phase is crucial. The source of this moment is a function of the forefoot lever arm length and its stiffness. The moment is controlled by pressure at the notch, with the amputee seeking an alignment which provides optimum control of the foot by means of this pressure. While heel contact can have a major influence on comfort at the distal tibia during loading response, the effectiveness of the propulsive moment influences forward progression. An analogy may be made to driving an automobile. Different individuals have different driving styles. Major influences on how a car is driven are the steering ratio and responsiveness of the engine to signals from the accelerator along with the driving style or preferences of the individual. Some drivers seek low steering ratios and good acceleration in their autos, while others prefer higher steering ratios and engines that do not offer maximum responsiveness to acceleration. Drivers who have vehicles which do not match their driving preferences may not exhibit performance as good as with a vehicle which does match their driving preference. The notch and anterior of the socket adjacent to it is like the steering wheel and accelerator of a vehicle; it is where the amputee generates the inputs necessary to achieve the performance desired. The foot itself has properties analogous to the steering ratio and responsiveness of the engine to signals from the accelerator.

Summary

There appeared to be internal consistency among the relationships in the models, but the relationships have not been transparent due to the large number of variables and complexity of the resulting regressions. It is noted that this study represents the first attempt to develop comprehensive models of socket pressure using state-of-the-art measurement systems, and it may take a number of studies using these methods to develop improved methods for interpreting the results. Based on the results of this first study, it does not appear possible to predict the effect of a particular foot on a particular subject prior to use of the foot; rather, the foot needs to be used and measurements taken to understand how it is functioning and affecting the residual limb of a specific individual. Key intervening variables are the design and quality of the socket and the gait preferences of the subject. The measurements allow an analysis of the response characteristics of feet at a level not previously examined and open up possibilities for a more rational selection of particular feet for individuals who plan to use them in particular situations. The time of occurrence of the maximum forces and moments may be a key to understanding the response characteristics of feet. Time and study resources did not permit further examination of this. Nor did resources allow further examination of the changes in the forces and moments associated with perturbation, or analyses of forces and moments normalized by body mass and weight. One of the major limitations of this study was that a convenience sample was used, and three of the subjects utilized spare sockets that may have reached the end of their useful life. With the careful design of experiments to test hypotheses about different feet, different socket designs, or different liners and suspension methods, much useful information could be gained about how different designs influence the pressures experienced inside of sockets. The following pages present the data on each subject.

Figure 6-1A. Subject 1: TruStep Foot Pressure Sensor Windows

Anterior:

Notch:-Green (<u>No Data for Trials 2&3</u>)
Lateral to Distal Tibia-Red (Substitute for Distal Tibia)
Medial to Distal Tibia-Magenta
Distal Tibia-Cyan (<u>No Data for Trials 2&3</u>)
Anterior Lateral Proximal-Yellow (Substitute for Notch)
Anterior Medial Proximal-Blue
Anterior Proximal-Dark Green (<u>No Data for Trials 2&3</u>)

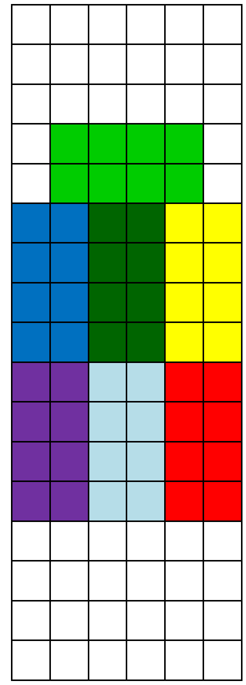

Posterior:

Popliteal-Green (<u>No Data</u>)
Proximal Gastrocnemius (Substitute for Popliteal) -Red
Middle Gastrocnemius-Magenta
Distal Gastrocnemius -Cyan

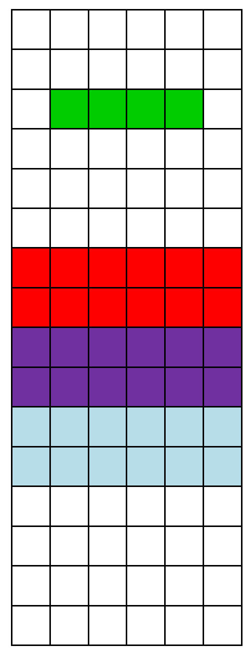

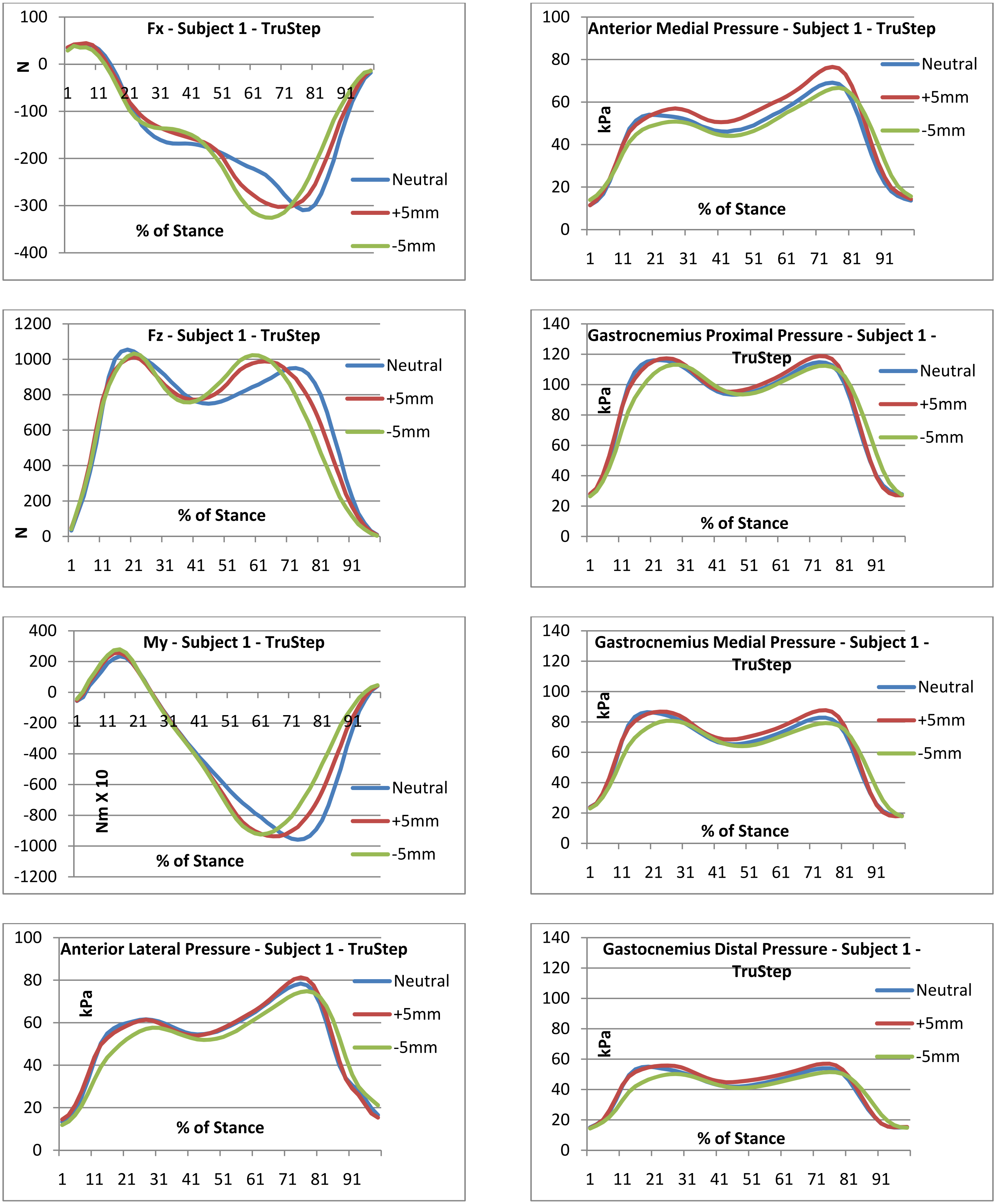

Figure 6-1B. Forces, Moments, and Pressures for Subject 1

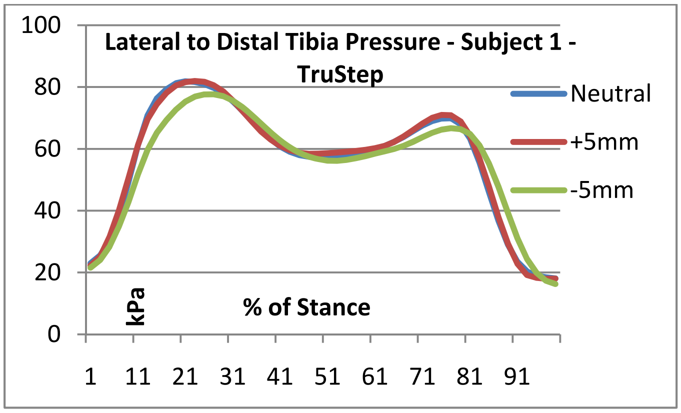

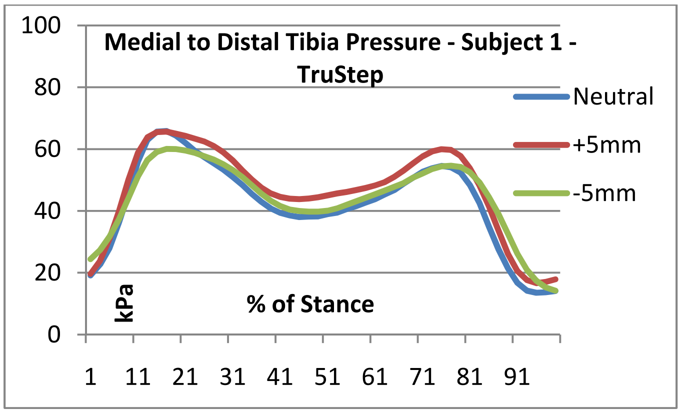

Figure 6-1B, Continued

SUBJECT 1 - TruStep			
	-5 mm	**Neutral Alignment**	**+ 5mm**
Fx+ (N)			
Interval of Maximum Value	4	4	4
Maximum Value	35.5	40.5	44.5
Difference from Neutral Alignment	-5.0	XXXX	4.0
Significance of Difference from Neutral Alignment	0.0039	XXXX	0.0302
Significance of Difference between +5 mm and -5mm		0.0000	
Fx- (N)			
Interval of Maximum Value	34	39	35
Maximum Value	325.8	309.6	302.6
Difference from Neutral Alignment		XXXX	
Significance of Difference from Neutral Alignment	NS	XXXX	NS
Significance of Difference between +5 mm and -5mm		NS	
Fz 1st Peak (N)			
Interval of Maximum Value	11	10	11
Maximum Value	1032.5	1054.8	1012.5
Difference from Neutral Alignment		XXXX	-42.3
Significance of Difference from Neutral Alignment	NS	XXXX	0.0082
Significance of Difference between +5 mm and -5mm		NS	
Fz 2nd Peak (N)			
Interval of Maximum Value	30	37	32
Maximum Value	1023.0	950.7	988.3
Difference from Neutral Alignment	72.3	XXXX	
Significance of Difference from Neutral Alignment	0.0525	XXXX	NS
Significance of Difference between +5 mm and -5mm		NS	
My+ (NmX10)			
Interval of Maximum Value	8	8	8
Maximum Value	279.4	234.0	257.3
Difference from Neutral Alignment	45.4	XXXX	23.3
Significance of Difference from Neutral Alignment	0.0001	XXXX	0.0176
Significance of Difference between +5 mm and -5mm		0.0017	
My- (NmX10)			
Interval of Maximum Value	31	37	33
Maximum Value	925.3	958.3	936.7
Difference from Neutral Alignment		XXXX	
Significance of Difference from Neutral Alignment	NS	XXXX	NS
Significance of Difference between +5 mm and -5mm		NS	
Anterior Lateral Pressure (kPa)			
Interval of Maximum Value	39	38	38
Maximum Value	74.8	78.4	81.3
Difference from Neutral Alignment	-3.6	XXXX	2.9
Significance of Difference from Neutral Alignment	0.0226	XXXX	0.0107
Significance of Difference between +5 mm and -5mm		0.0002	
Anterior Medial Pressure (kPa)			
Interval of Maximum Value	39	38	38
Maximum Value	66.7	69.1	79.3
Difference from Neutral Alignment		XXXX	10.2
Significance of Difference from Neutral Alignment	NS	XXXX	0.0000
Significance of Difference between +5 mm and -5mm		0.0000	

SUBJECT 1 - TruStep			
	-5 mm	**Neutral Alignment**	**+ 5mm**
Proximal Gastrocnemius Pressure 1st Peak (kPa)			
Interval of Maximum Value	14	12	13
Maximum Value	113.1	116.1	117.3
Difference from Neutral Alignment		XXXX	
Significance of Difference from Neutral Alignment	NS	XXXX	NS
Significance of Difference between +5 mm and -5mm		0.0389	
Proximal Gastrocnemius Pressure 2nd Peak (kPa)			
Interval of Maximum Value	38	37	37
Maximum Value	112.4	114.7	118.8
Difference from Neutral Alignment		XXXX	4.1
Significance of Difference from Neutral Alignment	NS	XXXX	0.0455
Significance of Difference between +5 mm and -5mm		0.0103	
Medial Gastrocnemius Pressure 1st Peak (kPa)			
Interval of Maximum Value	13	10	12
Maximum Value	80.8	86.4	86.0
Difference from Neutral Alignment	-5.6	XXXX	
Significance of Difference from Neutral Alignment	0.0258	X XXX	NS
Significance of Difference between +5 mm and -5mm		0.0125	
Medial Gastrocnemius Pressure 2nd Peak (kPa)			
Interval of Maximum Value	38	37	38
Maximum Value	79.2	82.7	87.7
Difference from Neutral Alignment		XXXX	5.0
Significance of Difference from Neutral Alignment	NS	XXXX	0.011
Significance of Difference between +5 mm and -5mm		0.0029	
Distal Gastrocnemius Pressure 1st Peak (kPa)			
Interval of Maximum Value	14	10	13
Maximum Value	50.1	55.0	55.8
Difference from Neutral Alignment	-4.9	XXXX	
Significance of Difference from Neutral Alignment	0.0390	X XXX	NS
Significance of Difference between +5 mm and -5mm		0.0158	
Distal Gastrocnemius Pressure 2nd Peak (kPa)			
Interval of Maximum Value	38	38	38
Maximum Value	51.5	54.0	57.0
Difference from Neutral Alignment		XXXX	3.0
Significance of Difference from Neutral Alignment	NS	XXXX	0.0240
Significance of Difference between +5 mm and -5mm		0.0168	
Lateral to Distal Tibia Pressure (kPa)			
Interval of Maximum Value	14	11	12
Maximum Value	77.6	81.8	81.9
Difference from Neutral Alignment	-4.2	XXXX	
Significance of Difference from Neutral Alignment	0.0378	X XXX	NS
Significance of Difference between +5 mm and -5mm		0.0499	
Medial to Distal Tibia Pressure (kPa)			
Interval of Maximum Value	9	9	9
Maximum Value	60.1	65.9	65.6
Difference from Neutral Alignment	-5.8	XXXX	
Significance of Difference from Neutral Alignment	0.0055	X XXX	NS
Significance of Difference between +5 mm and -5mm		0.0075	

Table 6-11A. Significant Differences for Subject 1 Forces, Moments, and Pressures

Significant Differences Between Neutral Alignment and Plus and Minus 5 mm – Subject 1 - TruStep																		
			Pressure Measurements															
			Lat Dist Tib		**Med Dist Tib**		**Prox Gast 1st Pk**		**Prox Gast 2nd Pk**		**Med Gast 1st Pk**		**Med Gast 2nd Pk**		**Dist Gast 1st Pk**		**Dist Gast 2nd Pk**	
			+5mm	**-5mm**	**+5mm**	**-5mm**	**+5mm**	**-5mm**	**+5mm**	**-5mm**	**+5mm**	**-5mm**	**+5mm**	**-5mm**	**+5mm**	**-5mm**	**+5mm**	**-5mm**
Transducer Measurements		**Difference N, NmX10, kPa**		↓ -4.2		↓ -5.8			↑ 4.1			↓ -5.6	↑ +5.0			↓ -4.9	↑ 3.0	
Fx+	**+5mm**	↑ +4.0							↑↑				↑↑				↑↑	
	-5mm	↓ -5.0		↓↓		↓↓						↓↓				↓↓		
Fx-	**+5mm**																	
	-5mm																	
Fz 1st Pk	**+5mm**	↓ -42.3							↓↑				↓↑				↓↑	
	-5mm																	
Fz 2nd Pk	**+5mm**																	
	-5mm	↑ +72.3		↑↓		↑↓						↑↓				↑↓		
My+	**+5mm**	↑ +23.3							↑↑				↑↑				↑↑	
	-5mm	↑ +45.4		↑↓		↑↓						↑↓				↑↓		
My-	**+5mm**																	
	-5mm																	

Note: In the cells of the matrix, the first arrow indicates a significant change in the transducer variable, and the second arrow indicates a significant change in the peak pressure measurement (t-test, $p \leq 0.05$); upward pointing arrows represent an increase in the magnitude of the variable with the perturbation compared to the initial neutral alignment, and downward pointing arrows represent a decrease in the magnitude of the variable with the perturbation.

Subject 1 – TruStep, Table Continued						
			Pressure Measurements			
			Ant Lateral		**Ant Medial**	
			+5mm	**-5mm**	**+5mm**	**-5mm**
Transducer Measurements		**Difference N, NmX10, kPa**	↑ +2.9	↓ -3.6	↑ +10.2	
Fx+	**+5mm**	↑ +4.0	↑↑		↑↑	
	-5mm	↓ -5.0		↓↓		
Fx-	**+5mm**					
	-5mm					
Fz 1st Pk	**+5mm**	↓ -42.3	↓↑		↓↑	
	-5mm					
Fz 2nd Pk	**+5mm**					
	-5mm	↑ +72.3		↑↓		
My+	**+5mm**	↑ +23.3	↑↑		↑↑	
	-5mm	↑ +45.4		↑↓		
My-	**+5mm**					
	-5mm					

Table 6-11B. Summary of Significant Differences for Subject 1

Subject 1 - TruStep						
Alignment	**Pressure Window**	**Variables in Regression**	**Variables Added to Regression for Neutral Alignment at p ≤ 0.005 to enter**	**Variables Removed from Regression for Neutral Alignment at p ≤ 0.005 to enter**	**Maximums Separated by 2 or More Time Intervals**	
Neutral	Lat Dist Tibia	Fz, My-, Fx-, Fx+				
	Med Dist Tibia	Fz, My+, Fx+				
	Prox Gastroc	Fz, My+				
	Med Gastroc	Fz, Fx+				
	Dist Gatroc	Fz				
	Lat Ant Prox	Fz, Fx-				
	Med Ant Prox	Fz, My-				
+5 mm	Lat Dist Tibia	Fz, My-, Fx-		*Fx+↑ Fz,	Fx-,My-	
	Med Dist Tibia	Fz, My+		*Fx+↑ Fz,		
	Prox Gastroc	Fz, Fx-, My-	Fx-, My-	*My+↑	Fz, Fx-, My-	
	*Med Gastroc↑ Fz			*Fx+↑ P,	Fz	
	*Dist Gatroc↑ Fz				P, Fz	
	Lat Ant Prox	Fz, Fx-, My-, *My+↑ *M	y+↑, My-		Fz, Fx-, My-	
	*Med Ant Prox↑	Fz, Fx-, My-, *My+↑ Fx-,	*My+↑		Fz, Fx-, My-	
-5 mm	*Lat Dist Tibia↓ *Fz	↑ *F	x+↓ *F	x+↓, Fx-, My-	P, *Fz↑, My-	
	*Med Dist Tibia↓ *Fz	↑		*Fx+↓, *My+↑ *Fz	↑	
	Prox Gastroc	*Fz↑, Fx+	*Fx+↓ *M	y+↑ P,	*Fz↑	
	*Med Gastroc↓ *Fz	↑, Fx+			P, *Fz↑	
	*Dist Gatroc↓ *Fz	↑, Mx-, My-	Mx-, My-		P, *Fz↑, My-	
	Lat Ant Prox	*Fx+↓, My-, Fx-	Mx-, My-	*Fz↑ *Fz	↑, Fx-, My-	
	Med Ant Prox	*Fx-↓, My-, *My+↑ Fx-,	*My+↑ *Fz	↑ *Fz	↑, Fx-, My-	

Table 6-11C Model Structural Changes with Perturbation for Subject 1

Note: An asterisk (*) indicates a statistically significant difference in maximum values from neutral alignment at $p \leq 0.05$ and a difference that is at least 5% of the value for the neutral alignment and therefore of possible clinical relevance; an upward arrow (↑) indicates an increase in the magnitude of the maximum value and a downward arrow (↓) indicates a decrease in the magnitude of the maximum value. There are 50 time intervals during stance, and 2 intervals represent 4% of stance. P stands for maximum pressure in the column indicating 2 or more intervals between maximum values

Subject 1 TruStep Neutral

Apriori Model (Fz, Fx(+), Fx(-), My(+), My(-))

Pressure Region	R^2	Y(hat)	Const.	Fz	Fx(+)	Fx(-)	My(+)	My(-)
Distal Tib. Lateral	0.990	P(DistTibLat)	12.015	0.063	0.130	0.053	0.000	-0.020
Distal Tib. Medial	0.964	P(DistTibMed)	8.651	0.044	0.189	0.000	0.051	0.000
Ant Lateral Prox	0.980	P(AntLat)	11.765	0.040	0.000	0.082	0.000	0.000
Ant Medial Prox	0.979	P(AntMed)	9.117	0.042	0.000	0.000	0.000	0.017
Gastroc Prox	0.995	P(GastrProx)	21.449	0.097	0.000	0.000	-0.043	0.000
Gastroc Mid	0.992	P(GastrMed)	13.677	0.070	0.085	0.000	0.000	0.000
Gastroc Dist	0.985	P(GastrDist)	10.875	0.043	0.000	0.000	0.000	0.000

Subject 1 TruStep +5mm

Apriori Model (Fz, Fx(+), Fx(-), My(+), My(-))

Pressure Region	R^2	Y(hat)	Const.	Fz	Fx(+)	Fx(-)	My(+)	My(-)
Distal Tibia[1]	0.957	P(DistTib)	13.843	0.047	0.000	0.176	0.036	-0.055
Distal Tib. Lateral	0.954	P(DistTibLat)	15.309	0.057	0.000	0.135	0.000	-0.047
Distal Tib. Medial	0.851	P(DistTibMed)	18.046	0.039	0.000	0.000	0.046	0.000
Ant Lateral Prox	0.970	P(AntLat)	11.206	0.023	0.000	0.247	0.058	-0.034
Ant Medial Prox	0.972	P(AntMed)	8.609	0.023	0.000	0.231	0.055	-0.030
Anterior Proximal[1]	0.971	P(AntProx)	8.095	0.020	0.000	0.286	0.052	-0.041
Gastroc Prox	0.974	P(GastrProx)	20.627	0.080	0.000	0.232	0.000	-0.053
Gastroc Mid	0.912	P(GastrMed)	18.850	0.067	0.000	0.000	0.000	0.000
Gastroc Dist	0.920	P(GastrDist)	13.110	0.043	0.000	0.000	0.000	0.000

Note 1: Sensor failure prevented data collection for neutral and -5mm alignments; equations were not used in subsequent comparisons.

Subject 1 TruStep -5mm

Apriori Model (Fz, Fx(+), Fx(-), My(+), My(-))

Pressure Region	R^2	Y(hat)	Const.	Fz	Fx(+)	Fx(-)	My(+)	My(-)
Distal Tib. Lateral	0.692	P(DistTibLat)	26.949	0.043	0.000	0.000	0.000	0.000
Distal Tib. Medial	0.605	P(DistTibMed)	25.382	0.028	0.000	0.000	0.000	0.000
Ant Lateral Prox	0.877	P(AntLat)	30.766	0.000	-0.349	0.238	0.000	-0.040
Ant Medial Prox	0.876	P(AntMed)	19.342	0.000	0.000	0.266	0.058	-0.045
Gastroc Prox	0.785	P(GastrProx)	53.526	0.056	-0.938	0.000	0.000	0.000
Gastroc Mid	0.765	P(GastrMed)	35.850	0.042	-0.464	0.000	0.000	0.000
Gastroc Dist	0.888	P(GastrDist)	16.660	0.020	0.000	0.140	0.000	-0.030

Table 6-11D Regression Models for Subject 1

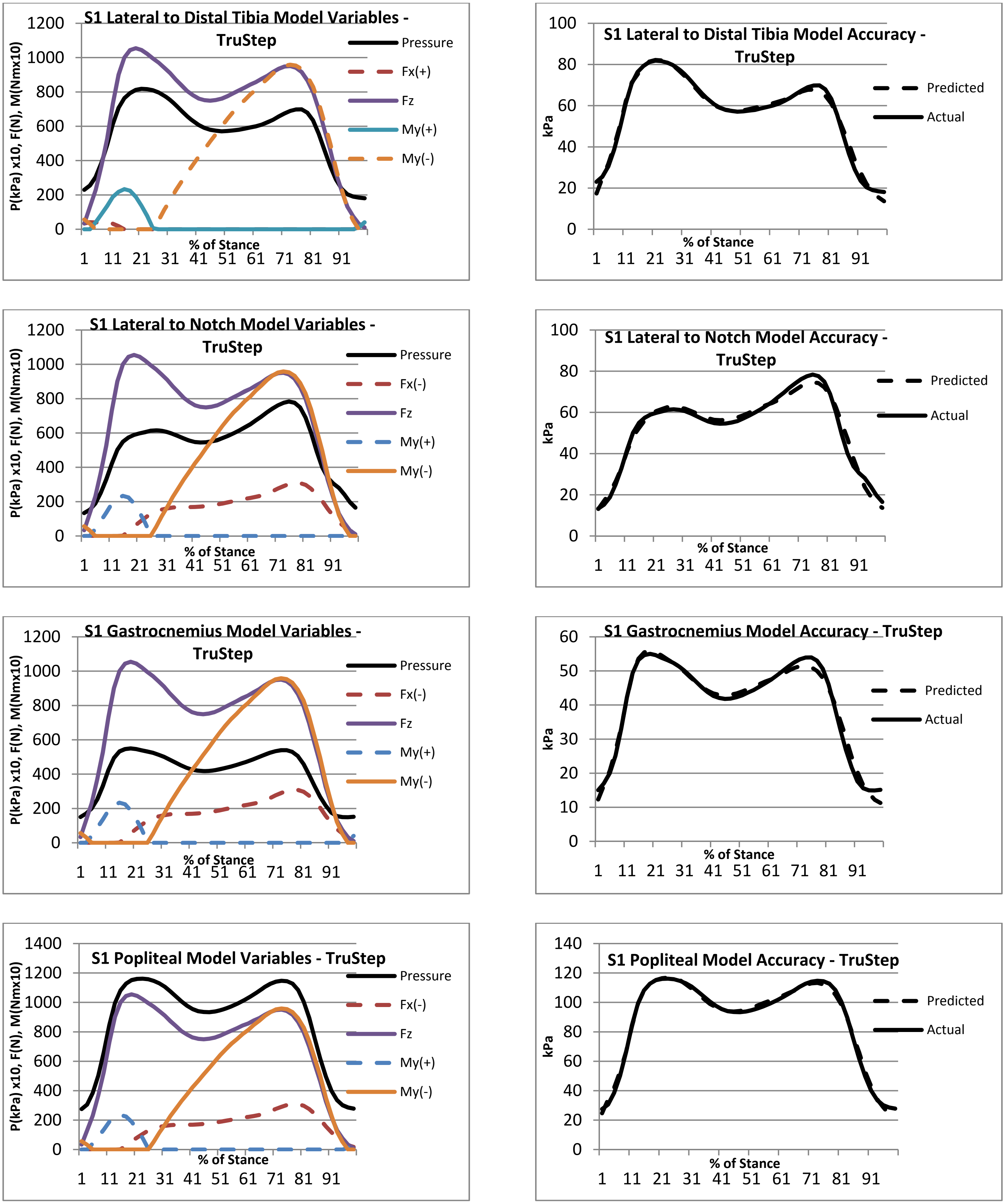

Figure 6-1C. Subject 1 Model Variables and Accuracy

Figure 6-2A. Subject 2: SACH Foot Pressure Sensor Windows

Anterior:
Notc h-Green
An terior Lateral-Red
Ante rior Medial-Magenta
Distal Tibia-Cyan

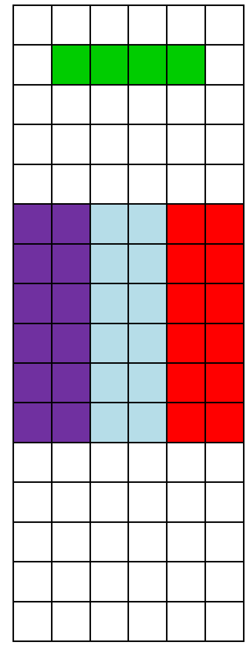

Posterior:
Po pliteal-Green
Distal Gastrocnemius-Red

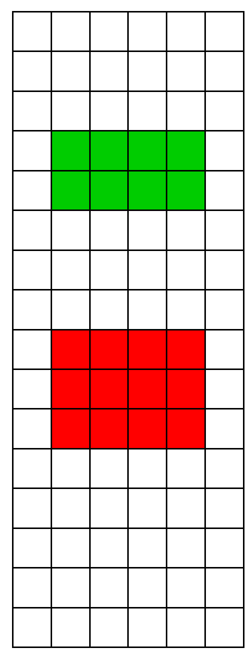

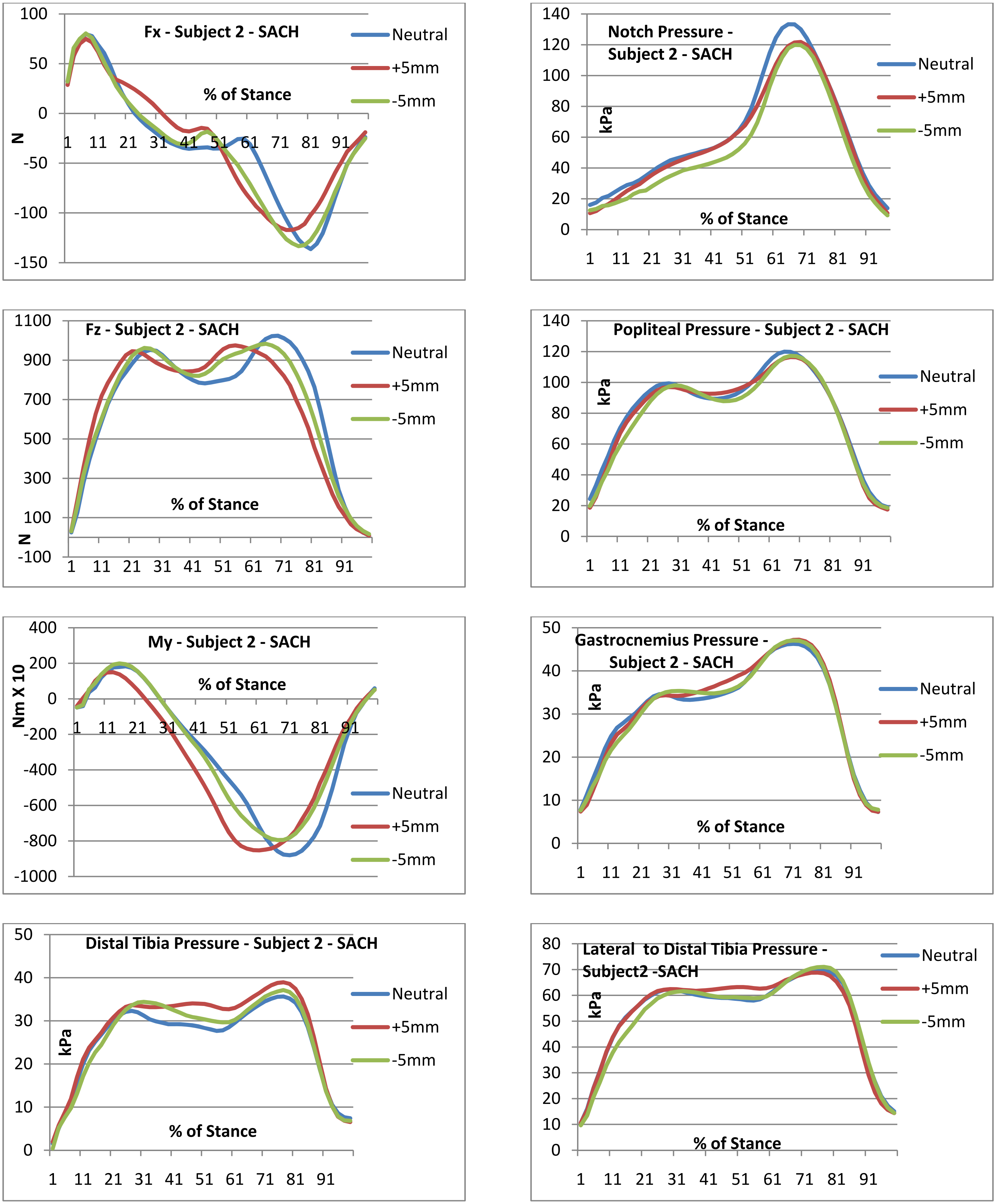

Figure 6-2B. Forces, Moments, and Pressures for Subject 2

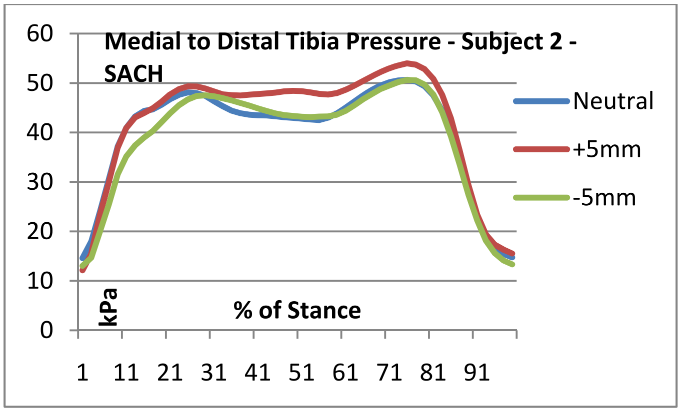

Figure 6-2B, Continued

SUBJECT 2 -SACH			
	-5 mm	**Neutral Alignment**	**+ 5mm**
Fx+ (N)			
Interval of Maximum Value	4	4	4
Maximum Value	80.4	79.7	74.9
Difference from Neutral Alignment		XXXX	
Significance of Difference from Neutral Alignment	NS	XXXX	NS
Significance of Difference between +5 mm and -5mm		NS	
Fx- (N)			
Interval of Maximum Value	39	41	37
Maximum Value	133.4	136.4	117.2
Difference from Neutral Alignment		XXXX	-19.2
Significance of Difference from Neutral Alignment	NS	XXXX	0.0077
Significance of Difference between +5 mm and -5mm		0.0173	
Fz 1st Peak (N)			
Interval of Maximum Value	13	14	11
Maximum Value	962.1	952.2	945.3
Difference from Neutral Alignment		XXXX	
Significance of Difference from Neutral Alignment	NS	XXXX	NS
Significance of Difference between +5 mm and -5mm		NS	
Fz 2nd Peak (N)			
Interval of Maximum Value	33	35	28
Maximum Value	983.1	1024.0	975.0
Difference from Neutral Alignment		XXXX	
Significance of Difference from Neutral Alignment	NS	XXXX	NS
Significance of Difference between +5 mm and -5mm		NS	
My+ (NmX10)			
Interval of Maximum Value	8	9	7
Maximum Value	199.1	183.0	149.1
Difference from Neutral Alignment		XXXX	-33.9
Significance of Difference from Neutral Alignment	NS	XXXX	0.0185
Significance of Difference between +5 mm and -5mm		0.0001	
My- (NmX10)			
Interval of Maximum Value	34	36	31
Maximum Value	795.0	880.3	853.1
Difference from Neutral Alignment	-85.3	XXXX	
Significance of Difference from Neutral Alignment	0.0002	X XXX	NS
Significance of Difference between +5 mm and -5mm		0.0351	
Distal Tibia Pressure (kPa)			
Interval of Maximum Value	39	39	39
Maximum Value	37.1	35.6	38.9
Difference from Neutral Alignment		XXXX	3.3
Significance of Difference from Neutral Alignment	NS	XXXX	0.0008
Significance of Difference between +5 mm and -5mm		0.0170	
Notch Pressure (kPa)			
Interval of Maximum Value	34	33	35
Maximum Value	119.9	133.3	121.8
Difference from Neutral Alignment		XXXX	
Significance of Difference from Neutral Alignment	NS	XXXX	NS
Significance of Difference between +5 mm and -5mm		NS	

SUBJECT 2 - SACH			
	-5 mm	**Neutral Alignment**	**+ 5mm**
Popliteal Pressure 1st Peak (kPa)			
Interval of Maximum Value	15	14	15
Maximum Value	98.1	99.4	96.8
Difference from Neutral Alignment		XXXX	-2.6
Significance of Difference from Neutral Alignment	NS	XXXX	0.0474
Significance of Difference between +5 mm and -5mm		NS	
Popliteal Pressure 2nd Peak (kPa)			
Interval of Maximum Value	34	33	34
Maximum Value	117.2	120.0	116.4
Difference from Neutral Alignment		XXXX	
Significance of Difference from Neutral Alignment	NS	XXXX	NS
Significance of Difference between +5 mm and -5mm		NS	
Gastrocnemius Pressure (kPa)			
Interval of Maximum Value	36	36	37
Maximum Value	47.0	46.3	47.2
Difference from Neutral Alignment		XXXX	
Significance of Difference from Neutral Alignment	NS	XXXX	NS
Significance of Difference between +5 mm and -5mm		NS	
Lateral to Distal Tibia Pressure (kPa)			
Interval of Maximum Value	38	39	38
Maximum Value	70.9	69.5	68.8
Difference from Neutral Alignment		XXXX	
Significance of Difference from Neutral Alignment	NS	XXXX	NS
Significance of Difference between +5 mm and -5mm		0.0394	
Medial to Distal Tibia Pressure (kPa)			
Interval of Maximum Value	38	38	38
Maximum Value	50.6	50.6	54.0
Difference from Neutral Alignment		XXXX	3.4
Significance of Difference from Neutral Alignment	NS	XXXX	0.0000
Significance of Difference between +5 mm and -5mm		0.0021	

Table 6-12A. Significant Differences for Subject 2 Forces, Moments, and Pressures.

Significant Differences Between Neutral Alignment and Plus and Minus 5 mm – Subject 2 - SACH																
			Pressure Measurements													
			Distal Tibia		**Notch**		**Popliteal 1st Peak**		**Popliteal 2nd Peak**		**Gastrocnemius**		**LatDist Tib**		**MedDist Tib**	
			+5mm	**-5mm**	**+5mm**	**-5mm**	**+5mm**	**-5mm**	**+5mm**	**-5mm**	**+5mm**	**-5mm**	**+5mm**	**-5mm**	**+5mm**	**-5mm**
Transducer Measurements		**Difference** **N, NmX10, kPa**	↑ +3.3				↓ -2.6								↑ +3.4	
Fx+	**+5mm**															
	-5mm															
Fx-	**+5mm**	↓ -19.2	↓↑				↓↓								↓↑	
	-5mm															
Fz 1st Pk	**+5mm**															
	-5mm															
Fz 2nd Pk	**+5mm**															
	-5mm															
My+	**+5mm**	↓ -33.9	↓↑				↓↓								↓↑	
	-5mm															
My-	**+5mm**															
	-5mm	↓ -85.3														

Table 6-12B. Summary of Significant Differences for Subject 2

Note: In the cells of the matrix, the first arrow indicates a significant change in the transducer variable, and the second arrow indicates a significant change in the peak pressure measurement (t-test, $p \leq 0.05$); upward pointing arrows represent an increase in the magnitude of the variable with the perturbation compared to the initial neutral alignment, and downward pointing arrows represent a decrease in the magnitude of the variable with the perturbation.

Subject 2 - SACH						
Alignment	**Pressure Window**	**Variables in Regression**	**Variables Added to Regression for Neutral Alignment at p < 0.005 to enter**	**Variables Removed from Regression for Neutral Alignment at p < 0.005 to enter**	**Maximums Shifted by 2 or More Time Intervals**	
Neutral	Distal Tibia	Fz, Fx-, My-, Fx+				
	Notch	My-, Fz, Fx-				
	Popliteal	Fz, Fx-, My-				
	Gastrocnemius	Fz, Fx-, My-				
	Lat to Dist Tibia	Fz, Fx-, My-, Fx+				
	Med to Dist Tibia	Fz, Fx-, My-, Fx+				
+5 mm	*Distal Tibia↑ Fz,	*Fx-↓, Fx+, My-			*Fx-↓, Fz, My-	
	Notch My-	, *Fx-↓, Fz			P,*Fx-↓, Fz, My-	
	Popliteal Fz,	*Fx-↓, *My+↓, My-	*My+↓		*Fx-↓, Fz, *My+↓, My-	
	Gastrocnemius Fz,	*Fx-↓, *My+↓			*Fx-↓, Fz, *My+↓	
	Lat to Dist Tibia	Fz, *Fx-↓, Fx+, My-			*Fx-↓, Fz, My-	
	*Med to Dist Tibia	Fz, *Fx-↓, My-, Fx+			*Fx-↓, Fz, My-	
-5 mm	Distal Tibia	Fz, Fx-, *My-↓, My+, Fx+			Fx-, Fz, *My-↓	
	Notch	My-, Fz, Fx-			Fx-, Fz, *My-↓	
	Popliteal	Fz, Fx-, My+, *My-↓ My+			Fx-, Fz, *My-↓	
	Gastrocnemius	Fz, Fx-, My+,			Fx-, Fz	
	Lat to Dist Tibia	Fz, Fx-, *My-↓, Fx+			Fx-, Fz, *My-↓	
	Med to Dist Tibia	Fz, Fx-, *My-↓		Fx+	Fx-, Fz, *My-↓	

Table 6-12C. Model Structural Changes with Perturbations for Subject 2.

Note: An asterisk (*) indicates a statistically significant difference in maximum values from neutral alignment at $p \leq 0.05$ and a difference that is at least 5% of the value for the neutral alignment and therefore of possible clinical relevance; an upward arrow (↑) indicates an increase in the magnitude of the maximum value and a downward arrow (↓) indicates a decrease in the magnitude of the maximum value. There are 50 time intervals during stance, and 2 intervals represent 4% of stance. P stands for maximum pressure in the column indicating 2 or more intervals between maximum values. Variables in a regression are listed in the order in which they entered the equation.

Subject 2 SACH Neutral

Apriori Model (Fz, Fx(+), Fx(-), My(+), My(-))

Pressure Region	R^2	Y(hat)	Const.	Fz	Fx(+)	Fx(-)	My(+)	My(-)
Distal Tibia	0.987	P(DistTib)	4.469	0.029	-0.054	0.106	0.000	-0.009
Notch	0.974	P(Notch)	14.844	0.026	0.000	-0.236	0.000	0.117
GastrocDist	0.994	P(GastrDist)	6.897	0.028	0.000	0.048	0.000	0.009
Popliteal	0.995	P(Popliteal)	24.223	0.079	-0.066	-0.070	0.000	0.021
AntLateral	0.975	P(Lateral)	14.612	0.050	-0.061	0.179	0.000	-0.011
AntMedial	0.986	P(Medial)	12.299	0.037	0.044	0.101	0.000	-0.009

Subject 2 SACH +5mm

Apriori Model (Fz, Fx(+), Fx(-), My(+), My(-))

Pressure Region	R^2	Y(hat)	Const.	Fz	Fx(+)	Fx(-)	My(+)	My(-)
Distal Tibia	0.891	P(DistTib)	7.949	0.031	-0.166	0.146	0.000	-0.014
Notch	0.978	P(Notch)	-4.183	0.044	0.000	0.530	0.000	0.026
GastrocDist	0.949	P(GastrDist)	6.583	0.029	0.000	0.156	-0.036	0.000
Popliteal	0.984	P(Popliteal)	11.726	0.096	0.000	0.365	-0.105	-0.022
AntLateral	0.914	P(Lateral)	17.696	0.053	-0.215	0.223	0.000	-0.020
AntMedial	0.913	P(Medial)	15.439	0.040	-0.093	0.176	0.000	-0.017

Subject 2 SACH -5mm

Apriori Model (Fz, Fx(+), Fx(-), My(+), My(-))

Pressure Region	R^2	Y(hat)	Const.	Fz	Fx(+)	Fx(-)	My(+)	My(-)
Distal Tibia	0.957	P(DistTib)	3.811	0.033	-0.060	0.141	-0.024	-0.017
Notch	0.950	P(Notch)	-3.181	0.034	0.000	0.234	0.000	0.065
GastrocDist	0.990	P(GastrDist)	4.701	0.031	0.000	0.123	-0.016	0.000
Popliteal	0.995	P(Popliteal)	10.289	0.091	0.000	0.221	-0.038	-0.009
AntLateral	0.948	P(Lateral)	13.754	0.049	-0.109	0.240	0.000	-0.017
AntMedial	0.961	P(Medial)	10.377	0.038	0.000	0.149	0.000	-0.015

Table 6-12D. Regression Models for Subject 2

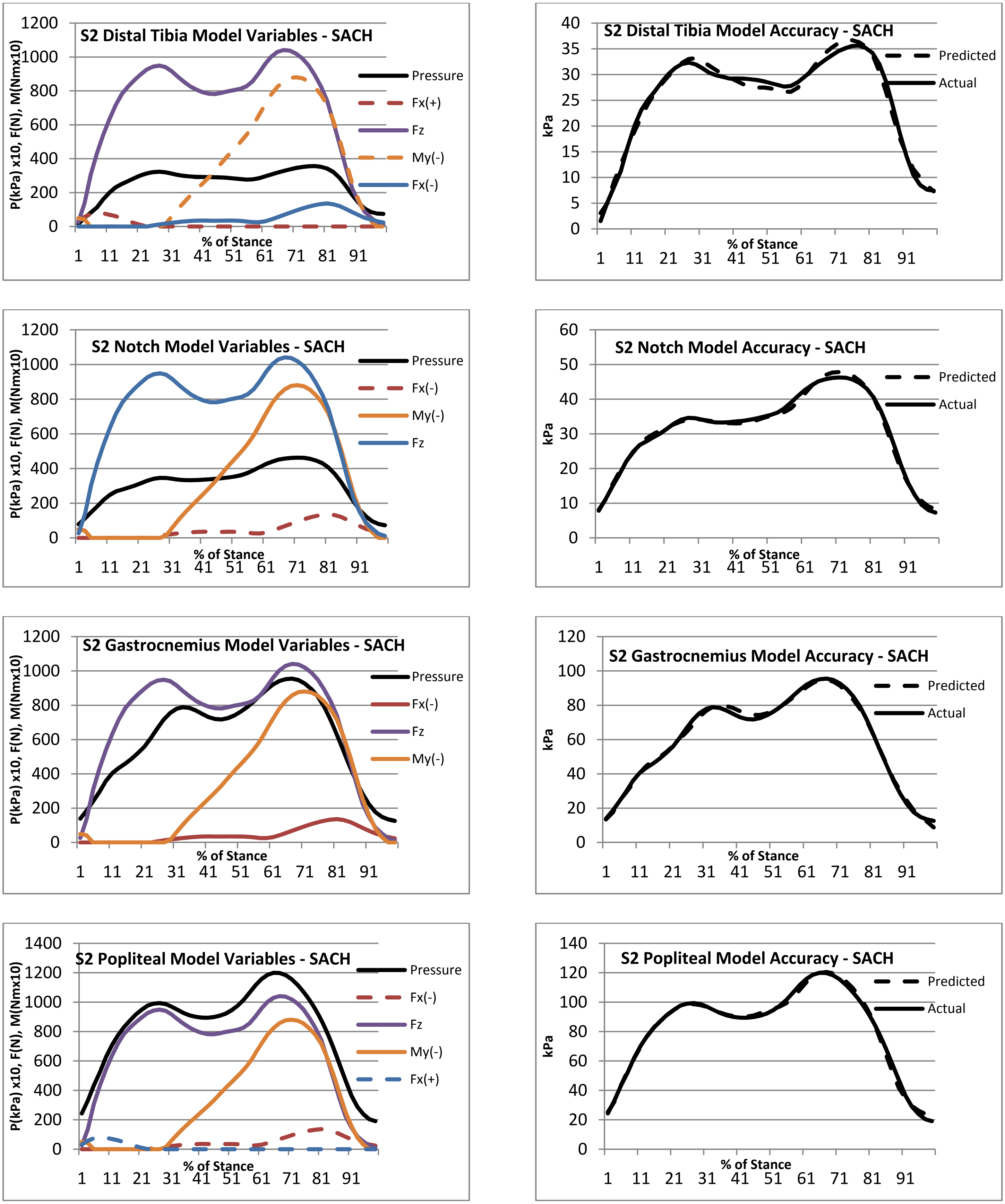

Figure 6-2C. Subject 2 Model Variables and Accuracy

Figure 6-3A: Subject 3: SACH Foot Pressure Sensor Windows

Anterior:
Notc h-Green
An terior Lateral-Red
Ante rior Medial-Magenta
Distal Tibia-Cyan

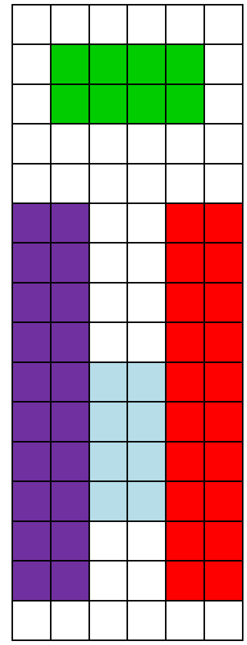

Posterior:
Po pliteal-Green
Distal Gastrocnemius-Red

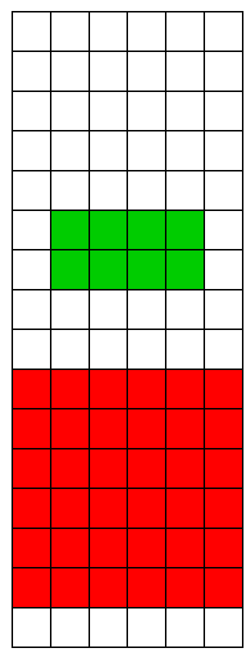

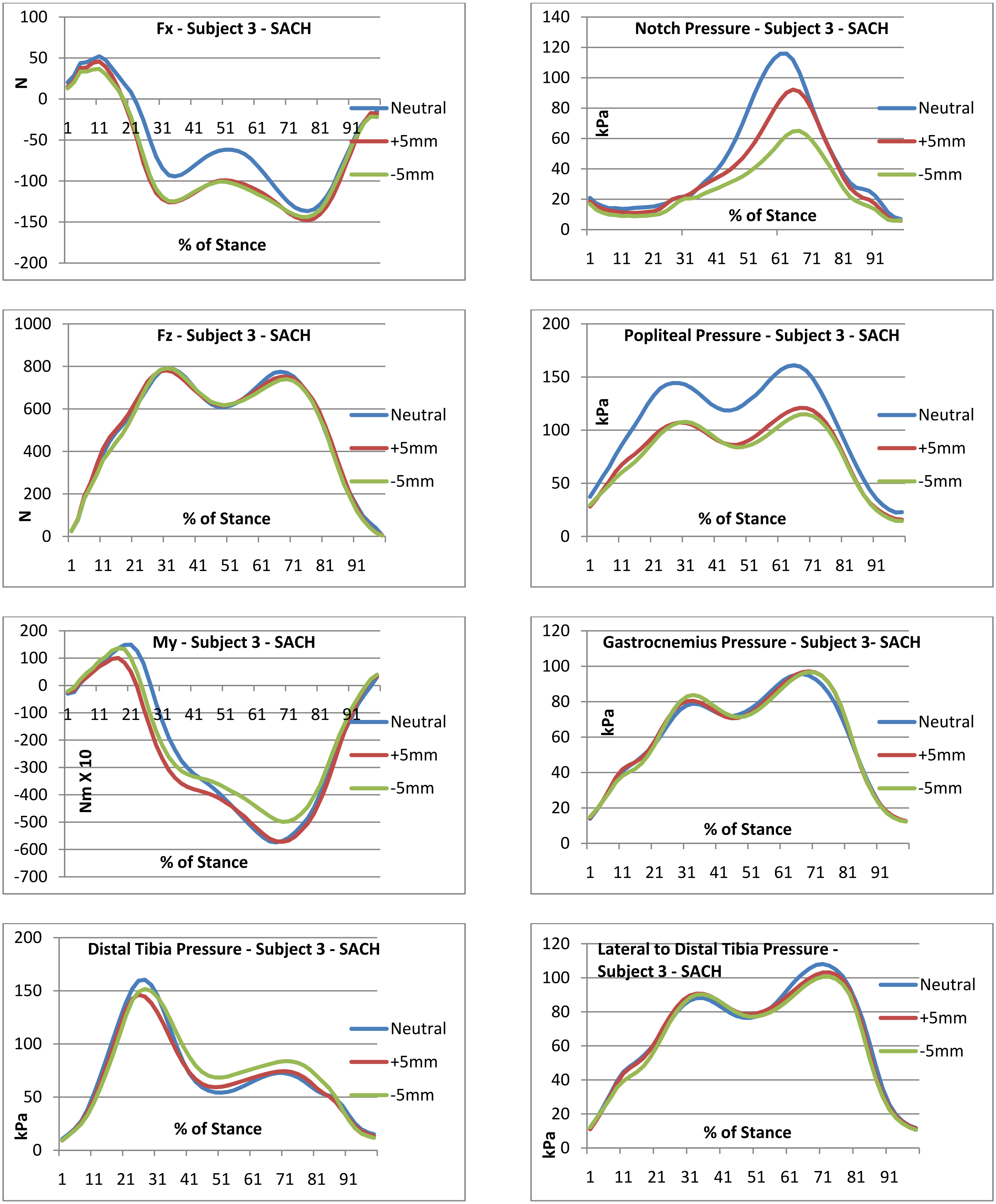

Figure 6-3B. Forces, Moments, and Pressures for Subject 3

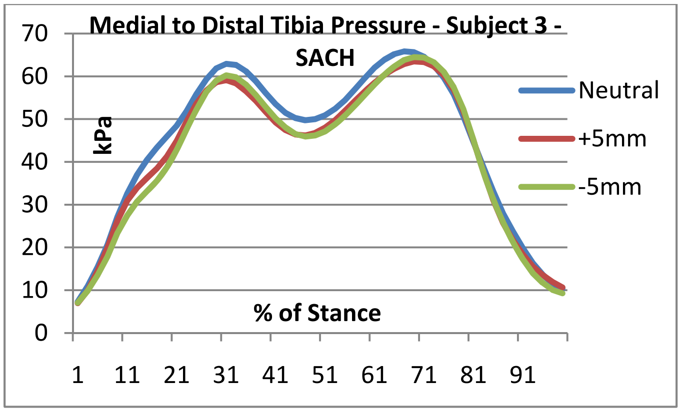

Figure 6-3B, Continued

SUBJECT 3 -SACH			
	-5 mm	**Neutral Alignment**	**+ 5mm**
Fx+ (N)			
Interval of Maximum Value	6	6	6
Maximum Value	36.7	52.2	45.8
Difference from Neutral Alignment	-15.5	XXXX	
Significance of Difference from Neutral Alignment	0.0012	X XXX	NS
Significance of Difference between +5 mm and -5mm		0.0023	
Fx- (N)			
Interval of Maximum Value	39	39	39
Maximum Value	143.9	136.7	148.0
Difference from Neutral Alignment		XXXX	11.3
Significance of Difference from Neutral Alignment	NS	XXXX	0.0340
Significance of Difference between +5 mm and -5mm		NS	
Fz 1st Peak (N)			
Interval of Maximum Value	16	17	16
Maximum Value	790.3	788.8	780.8
Difference from Neutral Alignment		XXXX	
Significance of Difference from Neutral Alignment	NS	XXXX	NS
Significance of Difference between +5 mm and -5mm		NS	
Fz 2nd Peak (N)			
Interval of Maximum Value	35	34	35
Maximum Value	740.0	774.6	751.1
Difference from Neutral Alignment		XXXX	
Significance of Difference from Neutral Alignment	NS	XXXX	NS
Significance of Difference between +5 mm and -5mm		NS	
My+ (NmX10)			
Interval of Maximum Value	9	11	9
Maximum Value	136.6	149.5	100.6
Difference from Neutral Alignment		XXXX	-48.9
Significance of Difference from Neutral Alignment	NS	XXXX	0.0000
Significance of Difference between +5 mm and -5mm		0.0004	
My- (NmX10)			
Interval of Maximum Value	35	34	35
Maximum Value	498.8	573.8	571.8
Difference from Neutral Alignment	-75.0	XXXX	-2.0
Significance of Difference from Neutral Alignment	0.0000	X XXX	NS
Significance of Difference between +5 mm and -5mm		0.0005	
Distal Tibia Pressure (kPa)			
Interval of Maximum Value	14	14	13
Maximum Value	151.7	160.4	146.1
Difference from Neutral Alignment	-8.7	XXXX	-14.3
Significance of Difference from Neutral Alignment	NS	XXXX	NS
Significance of Difference between +5 mm and -5mm		NS	
Notch Pressure (kPa)			
Interval of Maximum Value	34	32	33
Maximum Value	65.0	115.9	92.2
Difference from Neutral Alignment	-50.9	XXXX	-23.7
Significance of Difference from Neutral Alignment	0.0000	X XXX	0.0224
Significance of Difference between +5 mm and -5mm		0.0145	

SUBJECT 3 - SACH			
	-5 mm	**Neutral Alignment**	**+ 5mm**
Popliteal Pressure 1st Peak (kPa)			
Interval of Maximum Value	16	14	15
Maximum Value	107.8	144.3	107.2
Difference from Neutral Alignment	-36.5	XXXX	-37.1
Significance of Difference from Neutral Alignment	0.0000	XXXX	0.0000
Significance of Difference between +5 mm and -5mm		NS	
Popliteal Pressure 2nd Peak (kPa)			
Interval of Maximum Value	35	33	34
Maximum Value	115.0	161.0	120.9
Difference from Neutral Alignment	-46.0	XXXX	-40.1
Significance of Difference from Neutral Alignment	0.0000	XXXX	0.0000
Significance of Difference between +5 mm and -5mm		0.0330	
Gastrocnemius Pressure (kPa)			
Interval of Maximum Value	35	34	35
Maximum Value	96.7	95.5	97.1
Difference from Neutral Alignment		XXXX	
Significance of Difference from Neutral Alignment	NS	XXXX	NS
Significance of Difference between +5 mm and -5mm		NS	
Lateral to Distal Tibia Pressure (kPa)			
Interval of Maximum Value	37	36	37
Maximum Value	100.7	108.1	103.2
Difference from Neutral Alignment	-7.4	XXXX	-4.9
Significance of Difference from Neutral Alignment	0.0001	XXXX	0.0043
Significance of Difference between +5 mm and -5mm		NS	
Medial to Distal Tibia Pressure (kPa)			
Interval of Maximum Value	35	34	35
Maximum Value	64.5	65.9	63.5
Difference from Neutral Alignment		XXXX	-2.4
Significance of Difference from Neutral Alignment	NS	XXXX	0.0053
Significance of Difference between +5 mm and -5mm		NS	

Table 6-13A. Significant Differences for Subject 3 Forces, Moments, and Pressures

Significant Differences Between Neutral Alignment and Plus and Minus 5 mm – Subject 3 - SACH																
			Pressure Measurements													
			Distal Tibia		**Notch**		**Popliteal 1st Peak**		**Popliteal 2nd Peak**		**Gastrocnemius**		**LatDist Tib**		**MedDist Tib**	
			+5mm	**-5mm**	**+5mm**	**-5mm**	**+5mm**	**-5mm**	**+5mm**	**-5mm**	**+5mm**	**-5mm**	**+5mm**	**-5mm**	**+5mm**	**-5mm**
Transducer Measurements		**Difference** **N, NmX10, kPa**			↓ -23.7	↓ -50.9	↓ -37.1	↓ -36.5	↓ -40.1	↓ -46.0			↓ -7.4	↓ -4.9	↓ -2.4	
Fx+	**+5mm**															
	-5mm	↓ -15.5				↓↓		↓↓		↓↓				↓↓		
Fx-	**+5mm**	↑ +11.3			↑↓		↑↓		↑↓				↑↓		↑↓	
	-5mm															
Fz 1st Pk	**+5mm**															
	-5mm															
Fz 2nd Pk	**+5mm**															
	-5mm															
My+	**+5mm**	↓ -48.9			↓↓		↓↓		↓↓				↓↓		↓↓	
	-5mm															
My-	**+5mm**															
	-5mm	↓ -75.0				↓↓		↓↓		↓↓				↓↓		

Table 6-13B. Summary of Significant Differences for Subject 3

Note: In the cells of the matrix, the first arrow indicates a significant change in the transducer variable, and the second arrow indicates a significant change in the peak pressure measurement (t-test, $p \leq 0.05$); upward pointing arrows represent an increase in the magnitude of the variable with the perturbation compared to the initial neutral alignment, and downward pointing arrows represent a decrease in the magnitude of the variable with the perturbation.

Subject 3 - SACH						
Alignment	**Pressure Window**	**Variables in Regression**	**Variables Added to Regression for Neutral Alignment at p ≤ 0.005 to enter**	**Variables Removed from Regression for Neutral Alignment at p ≤ 0.005 to enter**	**Maximums Shifted by 2 or More Time Intervals**	
Neutral	Distal Tibia	Fz, My-, Fx+, My+, Fx-				
	Notch M	y- ,Fx-				
	Popliteal	Fz, Fx-, My-				
	Gastrocnemius	Fz, My-, Fx-, My+				
	Lat to Dist Tibia	Fz, Fx-, My-, My+, Fx+				
	Med to Dist Tibia	Fz, My-, Fx+				
+5 mm	Distal Tibia	Fz, My-, Fx+, *Fx-↑		*My+↓ *M	y+↓	
	*Notch↓ My-	, *Fx-↑				
	*Popliteal↓ Fz			*Fx-↑, My-		
	Gastrocnemius Fz,	My-		*Fx-↑, *My+↓ *M	y+↓	
	*Lat to Dist Tibia	Fz, My-, *Fx-↑		Fx+, *My+↓ *M	y+↓	
	*Med to Dist Tibia	Fz, My-		Fx+		
-5 mm	Distal Tibia	Fz, *My-↓, Fx-, *Fx+↓		My+	My+	
	*Notch↓ *M	y-↓, Fx-			P	
	*Popliteal↓ Fz			Fx-, *My-↓ P		
	Gastrocnemius Fz,	*My-↓		Fx-, My+	My+	
	*Lat to Dist Tibia	Fz, *My-↓, Fx-		*Fx+↓, My+	My+	
	Med to Dist Tibia	Fz, *My-↓		*Fx+↓		

Table 6-13C. Model Structural Changes with Perturbations for Subject 3

Note: An asterisk (*) indicates a statistically significant difference in maximum values from neutral alignment at $p \leq 0.05$ and a difference that is at least 5% of the value for the neutral alignment and therefore of possible clinical relevance; an upward arrow (↑) indicates an increase in the magnitude of the maximum value and a downward arrow (↓) indicates a decrease in the magnitude of the maximum value. There are 50 time intervals during stance, and 2 intervals represent 4% of stance. P stands for maximum pressure in the column indicating 2 or more intervals between maximum values. Variables in a regression are listed in the order in which they entered the equation.

Subject 3 SACH Neutral

Apriori Model (Fz, Fx(+), Fx(-), My(+), My(-))

Pressure Region	R^2	Y(hat)	Const.	Fz	Fx(+)	Fx(-)	My(+)	My(-)
Distal Tibia	0.969	P(DistTib)	14.915	0.163	-0.692	0.222	0.191	-0.172
Notch	0.929	P(Notch)	18.098	0.000	0.000	-0.483	0.000	0.227
GastrocDist	0.996	P(GastrDist)	9.910	0.083	0.000	-0.056	-0.026	0.047
Popliteal	0.985	P(Popliteal)	23.857	0.173	0.000	-0.326	0.000	0.054
AntLateral	0.993	P(Lateral)	4.004	0.078	0.113	0.219	0.065	0.029
AntMedial	0.994	P(Medial)	8.344	0.067	-0.055	0.000	0.000	0.007

Subject 3 SACH +5mm

Apriori Model (Fz, Fx(+), Fx(-), My(+), My(-))

Pressure Region	R^2	Y(hat)	Const.	Fz	Fx(+)	Fx(-)	My(+)	My(-)
Distal Tibia	0.978	P(DistTib)	11.295	0.176	-0.709	0.222	0.000	-0.182
Notch	0.911	P(Notch)	14.659	0.000	0.000	-0.377	0.000	0.194
GastrocDist	0.986	P(GastrDist)	9.071	0.076	0.000	0.000	0.000	0.047
Popliteal	0.954	P(Popliteal)	14.109	0.127	0.000	0.000	0.000	0.000
AntLateral	0.989	P(Lateral)	7.985	0.082	0.000	0.089	0.000	0.033
AntMedial	0.981	P(Medial)	7.056	0.059	0.000	0.000	0.000	0.017

Subject 3 SACH -5mm

Apriori Model (Fz, Fx(+), Fx(-), My(+), My(-))

Pressure Region	R^2	Y(hat)	Const.	Fz	Fx(+)	Fx(-)	My(+)	My(-)
Distal Tibia	0.983	P(DistTib)	7.612	0.176	-0.616	0.341	0.000	-0.208
Notch	0.907	P(Notch)	11.252	0.000	0.000	-0.209	0.000	0.142
GastrocDist	0.989	P(GastrDist)	9.529	0.078	0.000	0.000	0.000	0.052
Popliteal	0.966	P(Popliteal)	15.272	0.122	0.000	0.000	0.000	0.000
AntLateral	0.988	P(Lateral)	8.832	0.080	0.000	0.089	0.000	0.037
AntMedial	0.978	P(Medial)	6.672	0.060	0.000	0.000	0.000	0.021

Table 6-11D. Regression Models for Subject 3

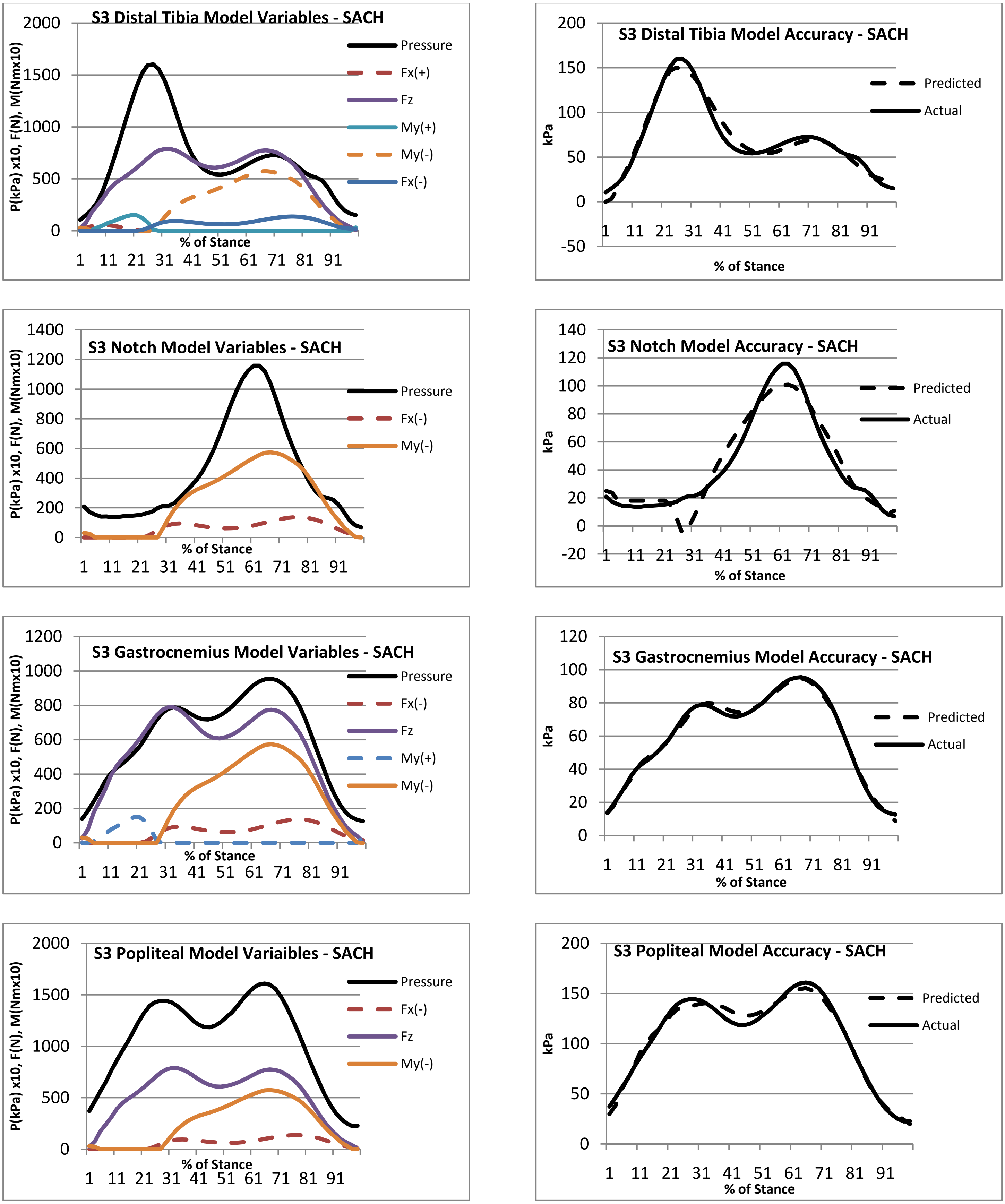

Figure 6-3C Subject 3 Model Variables and Accuracy

Figure 6-4A. Subject 4: PerfectStride, BioStride, SACH Foot Pressure Sensor Windows

Anterior:
Notch-Green

Anterior Lateral-Red
Anterior Medial-Magenta
Distal Tibia-Cyan

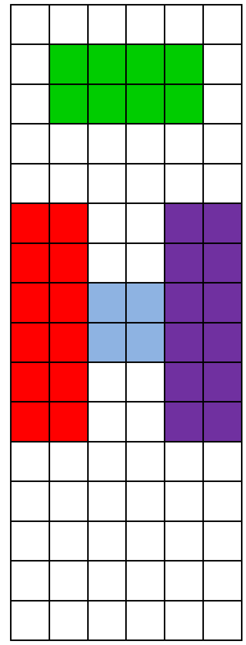

Posterior:
Popliteal-Green
Lateral Gastrocnemius-Red
Medial Gastrocnemius-Magenta

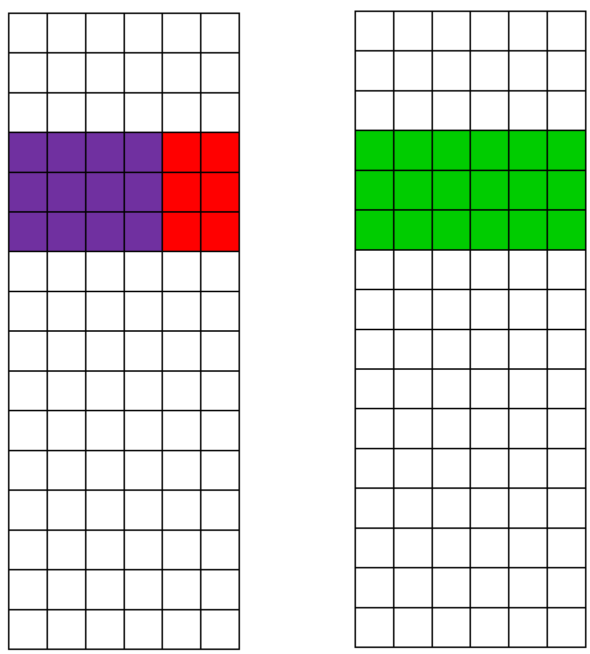

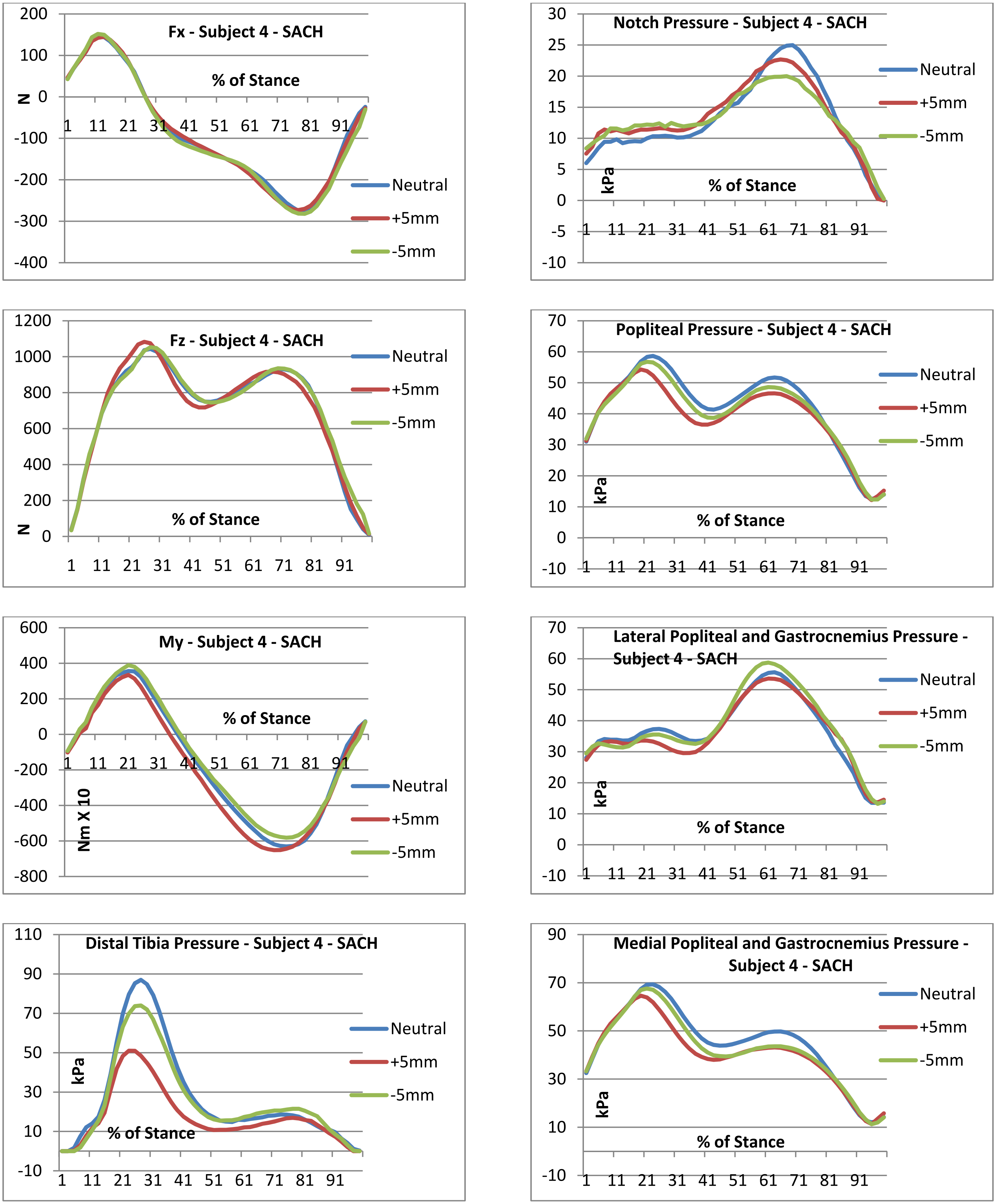

Figure 6-4B-S. Forces, Moments, and Pressures- S4 SACH

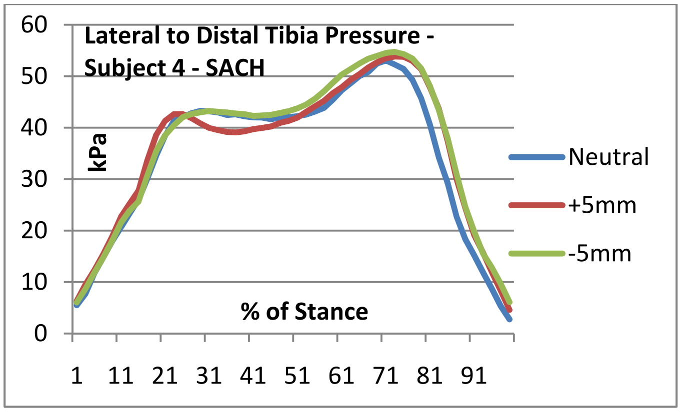

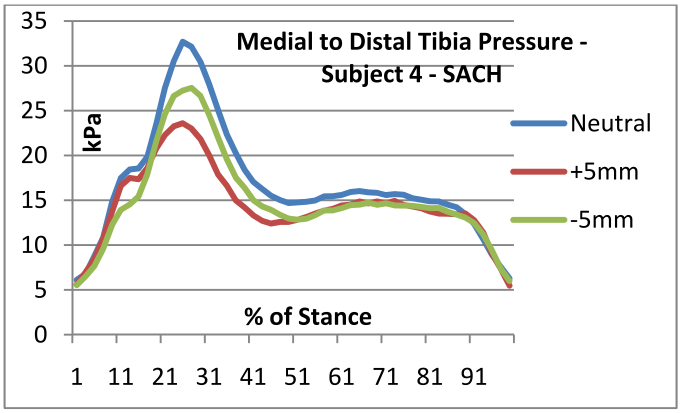

Figure 6-4B-S, Continued

SUBJECT 4 - SACH			
	-5 mm	Neutral Alignment	+ 5mm
Fx+ (N)			
Interval of Maximum Value	6	6	7
Maximum Value	151.7	144.8	145.0
Difference from Neutral Alignment		XXXX	
Significance of Difference from Neutral Alignment	NS	XXXX	NS
Significance of Difference between +5 mm and -5mm		NS	
Fx- (N)			
Interval of Maximum Value	40	40	39
Maximum Value	282.2	277.3	273.1
Difference from Neutral Alignment		XXXX	
Significance of Difference from Neutral Alignment	NS	XXXX	NS
Significance of Difference between +5 mm and -5mm		NS	
Fz 1st Peak (N)			
Interval of Maximum Value	14	14	13
Maximum Value	1052.5	1043.7	1082.9
Difference from Neutral Alignment		XXXX	39.2
Significance of Difference from Neutral Alignment	NS	XXXX	0.0372
Significance of Difference between +5 mm and -5mm		NS	
Fz 2nd Peak (N)			
Interval of Maximum Value	35	36	34
Maximum Value	935.5	930.3	917.5
Difference from Neutral Alignment		XXXX	
Significance of Difference from Neutral Alignment	NS	XXXX	NS
Significance of Difference between +5 mm and -5mm		NS	
My+ (NmX10)			
Interval of Maximum Value	11	11	11
Maximum Value	388.8	355.8	334.4
Difference from Neutral Alignment		XXXX	
Significance of Difference from Neutral Alignment	NS	XXXX	NS
Significance of Difference between +5 mm and -5mm		0.0153	
My- (NmX10)			
Interval of Maximum Value	37	37	35
Maximum Value	581.9	630.8	652.1
Difference from Neutral Alignment	-48.9	XXXX	
Significance of Difference from Neutral Alignment	0.0089	X XXX	NS
Significance of Difference between +5 mm and -5mm		0.0000	
Distal Tibia Pressure (kPa)			
Interval of Maximum Value	14	14	12
Maximum Value	74.0	87.0	51.0
Difference from Neutral Alignment		XXXX	-36.0
Significance of Difference from Neutral Alignment	NS	XXXX	0.0001
Significance of Difference between +5 mm and -5mm		0.0225	
Notch Pressure (kPa)			
Interval of Maximum Value	34	35	33
Maximum Value	20.0	25.0	22.7
Difference from Neutral Alignment	-5.0	XXXX	
Significance of Difference from Neutral Alignment	0.0018	X XXX	NS
Significance of Difference between +5 mm and -5mm		0.0057	

SUBJECT 4 - SACH			
	-5 mm	**Neutral Alignment**	**+ 5mm**
Popliteal Pressure 1st Peak (kPa)			
Interval of Maximum Value	11	12	10
Maximum Value	56.8	58.6	46.6
Difference from Neutral Alignment		XXXX	-12.0
Significance of Difference from Neutral Alignment	NS	XXXX	0.0057
Significance of Difference between +5 mm and -5mm		0.0910	
Popliteal Pressure 2nd Peak (kPa)			
Interval of Maximum Value	31	32	32
Maximum Value	48.6	51.7	46.6
Difference from Neutral Alignment	-3.1	XXXX	-5.1
Significance of Difference from Neutral Alignment	0.0057	X XXX	0.0000
Significance of Difference between +5 mm and -5mm		0.0365	
Lateral Popliteal and Gastrocnemius Pressure (kPa)			
Interval of Maximum Value	31	32	31
Maximum Value	58.8	55.6	53.6
Difference from Neutral Alignment		XXXX	
Significance of Difference from Neutral Alignment	NS	XXXX	NS
Significance of Difference between +5 mm and -5mm		0.0102	
Medial Popliteal and Gastrocnemius Pressure (kPa)			
Interval of Maximum Value	11	12	10
Maximum Value	67.6	69.3	64.6
Difference from Neutral Alignment		XXXX	-4.7
Significance of Difference from Neutral Alignment	NS	XXXX	0.0204
Significance of Difference between +5 mm and -5mm		NS	
Lateral to Distal Tibia Pressure (kPa)			
Interval of Maximum Value	37	36	37
Maximum Value	54.7	53.0	53.8
Difference from Neutral Alignment		XXXX	
Significance of Difference from Neutral Alignment	NS	XXXX	NS
Significance of Difference between +5 mm and -5mm		NS	
Medial to Distal Tibia Pressure (kPa)			
Interval of Maximum Value	14	13	13
Maximum Value	27.6	32.7	23.6
Difference from Neutral Alignment		XXXX	-9.1
Significance of Difference from Neutral Alignment	NS	XXXX	0.0030
Significance of Difference between +5 mm and -5mm		NS	

Table 6-14A-S. Significant Differences for Subject 4 Forces, Moments, and Pressures (SACH).

Significant Differences Between Neutral Alignment and Plus and Minus 5 mm – Subject 4 - SACH																		
			Pressure Measurements															
			Distal Tibia		**Notch**		**Popliteal 1st Peak**		**Popliteal 2nd Peak**		**Lateral Pop**		**Medial Pop**		**LatDist Tib**		**MedDist Tib**	
			+5mm	**-5mm**	**+5mm**	**-5mm**	**+5mm**	**-5mm**	**+5mm**	**-5mm**	**+5mm**	**-5mm**	**+5mm**	**-5mm**	**+5mm**	**-5mm**	**+5mm**	**-5mm**
Transducer Measurements		**Difference** **N, NmX10, kPa**	↓ -36.0			↓ -5.0		↓ -12.0	↓ -3.1	↓ -5.1			↓ -4.7				↓ -9.1	
Fx+	**+5mm**																	
	-5mm																	
Fx-	**+5mm**																	
	-5mm																	
Fz 1st Pk	**+5mm**	↑ +39.2	↑↓						↑↓				↑↓				↑↓	
	-5mm																	
Fz 2nd Pk	**+5mm**																	
	-5mm																	
My+	**+5mm**																	
	-5mm																	
My-	**+5mm**																	
	-5mm	↓ -48.9				↓↓		↓↓		↓↓								

Table 6-14B-S. Summary of Significant Differences for Subject 4 (SACH).

Note: In the cells of the matrix, the first arrow indicates a significant change in the transducer variable, and the second arrow indicates a significant change in the peak pressure measurement (t-test, $p \leq 0.05$); upward pointing arrows represent an increase in the magnitude of the variable with the perturbation compared to the initial neutral alignment, and downward pointing arrows represent a decrease in the magnitude of the variable with the perturbation.

Subject 4 - SACH						
Alignment	**Pressure Window**	**Variables in Regression**	**Variables Added to Regression for Neutral Alignment at $p \leq 0.005$ to enter**	**Variables Removed from Regression for Neutral Alignment at $p \leq 0.005$ to enter**	**Maximums Shifted by 2 or More Time Intervals**	
Neutral	Distal Tibia	My+, Fx+, Fz, My-				
	Notch	My-, Fz, Fx-, My+				
	Popliteal	Fz, Fx-, My-, My+, Fx+				
	Lateral Pop & Gas	Fz, My-, Fx-, My+				
	Medial Pop & Gas	Fz, Fx-, My-, Fx+, My+				
	Lat to Dist Tibia	Fz, My+, Fx+, My-, Fx-				
	Med to Dist Tibia	Fz, My-, My+, Fx+				
+5 mm	*Distal Tibia↓	Fz, My-, Fx+, My+, Fx-	Fx-		P, Fz, My-	
	Notch	My-, Fz, Fx-, My+, Fx+	Fx+		P, Fz, My-	
	*Popliteal↓	Fz, Fx+		Fx-, My-, My+	P, Fz	
	Lateral Pop & Gas	My-, Fx-, Fz, My+, Fx+	Fx+		Fz, My-	
	*Med Pop & Gas↓	Fz, Fx+, Fx-, My-	My+		P, Fz, My-	
	Lat to Dist Tibia	Fz, Fx-, Fx+		My+, My-	Fz	
	*Med to Dist Tibia	Fz, My+, Fx+		My-	Fz	
-5 mm	Distal Tibia	Fz, *My-↓, Fx+, My+				
	*Notch↓ Fz,	*My-↓, Fx-, My+, Fx+	Fx+			
	*Popliteal↓ Fz,	Fx+		Fx-, *My-↓, My+		
	Lateral Pop & Gas	*My-↓, Fz, Fx-, My+				
	Medial Pop & Gas	Fz, Fx-, Fx+, *My-↓		My+		
	Lat to Dist Tibia	Fz, Fx+, *My-↓, My+		Fx-		
	Med to Dist Tibia	Fz, My+, Fx+, *My-↓				

Table 6-14C-S. Model Structural Changes and Perturbations for Subject 4 (SACH)

Note: An asterisk (*) indicates a statistically significant difference in maximum values from neutral alignment at $p \leq 0.05$ and a difference that is at least 5% of the value for the neutral alignment and therefore of possible clinical relevance; an upward arrow (↑) indicates an increase in the magnitude of the maximum value and a downward arrow (↓) indicates a decrease in the magnitude of the maximum value. There are 50 time intervals during stance, and 2 intervals represent 4% of stance. P stands for maximum pressure in the column indicating 2 or more intervals between maximum values. Variables in a regression are listed in the order in which they entered the equation.

Subject 4 SACH Neutral
Apriori Model (Fz, Fx(+), Fx(-), My(+), My(-))

Pressure Region	R^2	Y(hat)	Const.	Fz	Fx(+)	Fx(-)	My(+)	My(-)
Distal Tibia	0.946	P(DistTib)	3.240	0.052	-0.297	0.000	0.101	-0.057
Notch	0.980	P(Notch)	4.135	0.014	0.000	-0.057	-0.021	0.032
Gastroc (Lateral)	0.977	P(GastrLateral)	23.292	0.032	0.000	-0.183	-0.054	0.068
Gastroc (Medial)	0.985	P(GastrMedial)	20.749	0.050	0.051	-0.164	-0.019	0.030
Popliteal	0.988	P(Popliteal)	21.358	0.045	0.038	-0.170	-0.032	0.042
AntLateral	0.984	P(Lateral)	4.838	0.047	-0.069	-0.034	-0.026	0.018
AntMedial	0.947	P(Medial)	7.992	0.014	-0.055	0.000	0.030	-0.008

Subject 4 SACH +5mm
Apriori Model (Fz, Fx(+), Fx(-), My(+), My(-))

Pressure Region	R^2	Y(hat)	Const.	Fz	Fx(+)	Fx(-)	My(+)	My(-)
Distal Tibia	0.944	P(DistTib)	-1.072	0.030	-0.130	0.051	0.077	-0.037
Notch	0.987	P(Notch)	3.703	0.014	0.024	-0.046	-0.028	0.025
Gastroc (Lateral)	0.990	P(GastrLateral)	20.118	0.020	0.046	-0.115	-0.039	0.063
Gastroc (Medial)	0.972	P(GastrMedial)	19.690	0.034	0.107	-0.108	0.000	0.026
Popliteal	0.867	P(Popliteal)	15.059	0.030	0.103	0.000	0.000	0.000
AntLateral	0.982	P(Lateral)	3.210	0.037	-0.036	0.064	0.000	0.000
AntMedial	0.902	P(Medial)	7.535	0.009	-0.020	0.000	0.024	0.000

Subject 4 SACH -5mm
Apriori Model (Fz, Fx(+), Fx(-), My(+), My(-))

Pressure Region	R^2	Y(hat)	Const.	Fz	Fx(+)	Fx(-)	My(+)	My(-)
Distal Tibia	0.952	P(DistTib)	1.938	0.041	-0.246	0.000	0.099	-0.035
Notch	0.968	P(Notch)	5.009	0.015	0.012	-0.048	-0.023	0.022
Gastroc (Lateral)	0.967	P(GastrLateral)	23.184	0.034	0.000	-0.182	-0.062	0.079
Gastroc (Medial)	0.969	P(GastrMedial)	19.939	0.042	0.065	-0.129	0.000	0.026
Popliteal	0.828	P(Popliteal)	12.707	0.035	0.102	0.000	0.000	0.000
AntLateral	0.986	P(Lateral)	4.102	0.044	-0.055	0.000	-0.017	0.017
AntMedial	0.951	P(Medial)	7.736	0.010	-0.050	0.000	0.028	-0.004

Table 6-14D-S. Regression Models for Subject 4 (SACH).

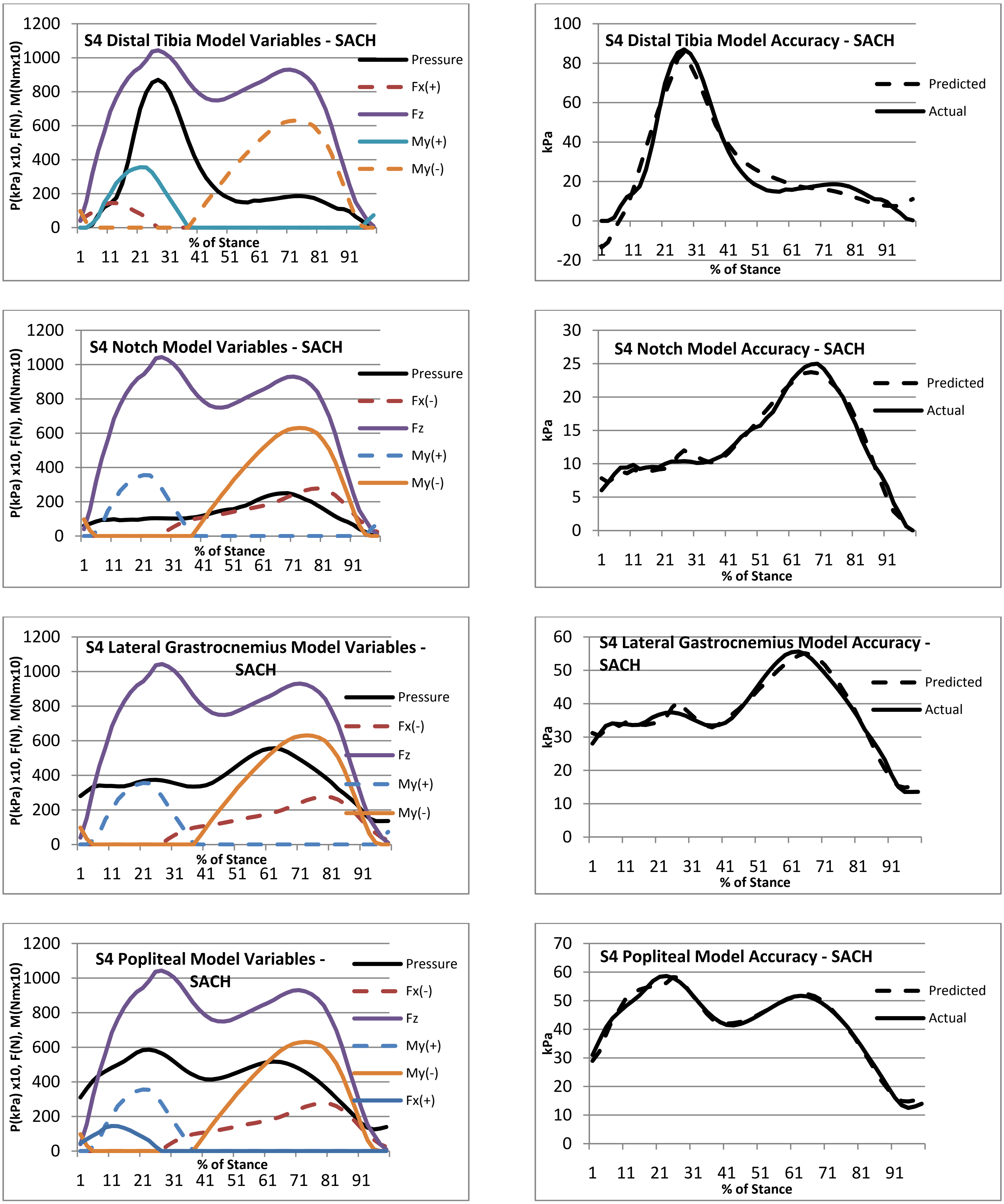

Figure 6-4C-S. Subject 4 Model Variables and Accuracy (SACH)

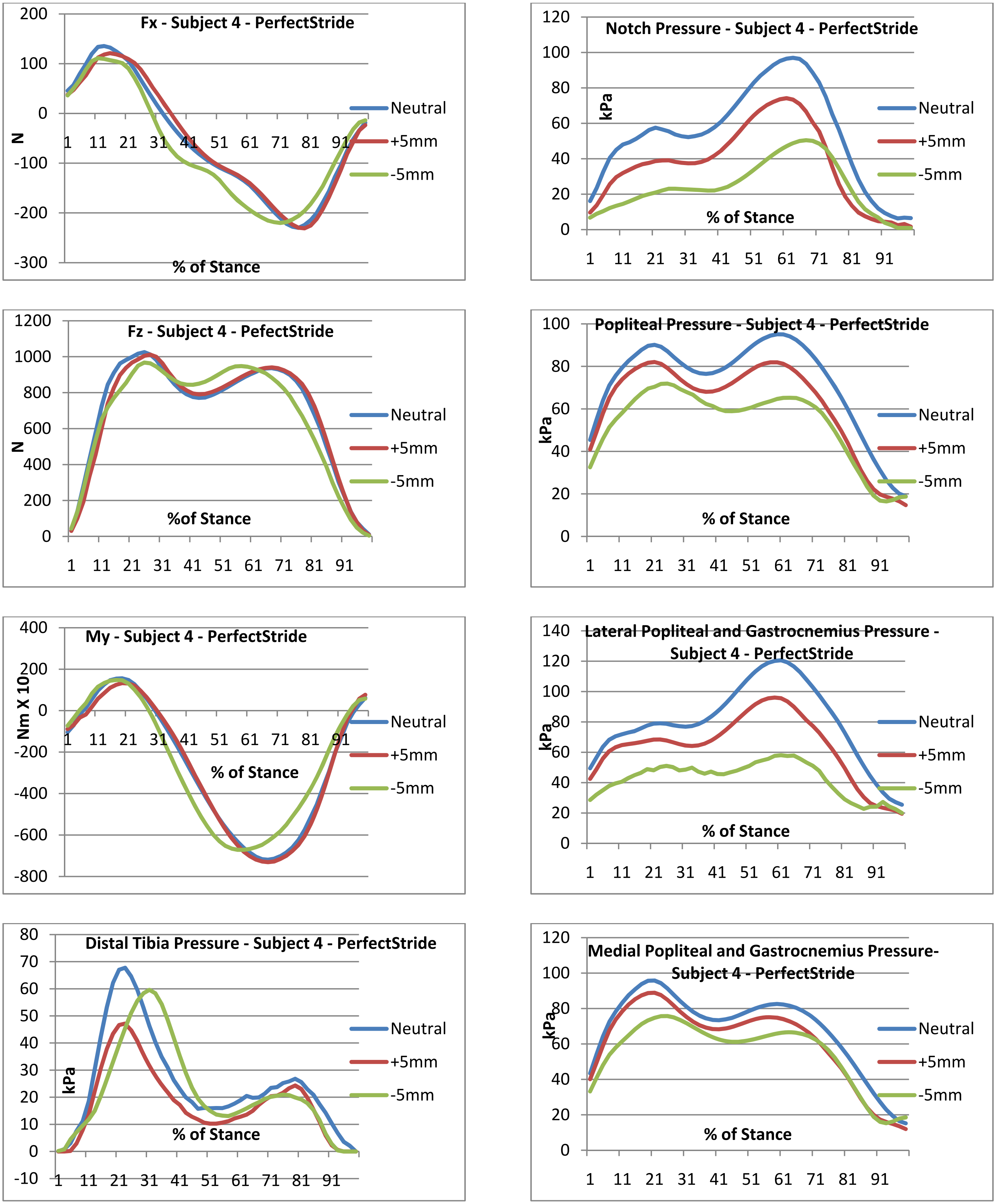

Figure 6-4B-P. Forces, Moments, and Pressures - S4 PerfectStride

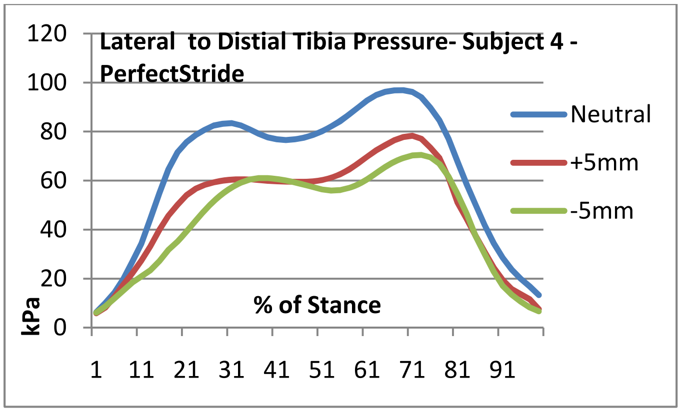

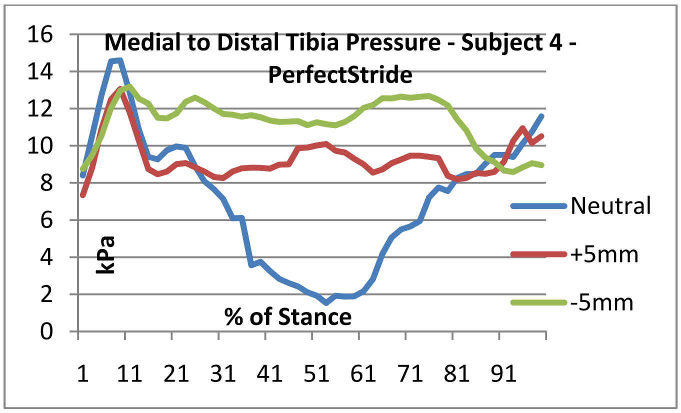

Figure 6-4B-P, Continued.

SUBJECT 4 - PerfectStride			
	-5 mm	**Neutral Alignment**	**+ 5mm**
Fx+ (N)			
Interval of Maximum Value	6	7	8
Maximum Value	111.1	135.4	121.1
Difference from Neutral Alignment	-24.3	XXXX	
Significance of Difference from Neutral Alignment	0.0121 X	XXX	NS
Significance of Difference between +5 mm and -5mm		NS	
Fx- (N)			
Interval of Maximum Value	36	39	40
Maximum Value	220.2	229.8	231.0
Difference from Neutral Alignment	-9.6	XXXX	
Significance of Difference from Neutral Alignment	0.0106 X	XXX	NS
Significance of Difference between +5 mm and -5mm		0.0132	
Fz 1st Peak (N)			
Interval of Maximum Value	13	13	14
Maximum Value	967.4	1026.0	1011.8
Difference from Neutral Alignment	-58.6	XXXX	
Significance of Difference from Neutral Alignment	.0054 X	XXX	NS
Significance of Difference between +5 mm and -5mm		0.0131	
Fz 2nd Peak (N)			
Interval of Maximum Value	29	34	34
Maximum Value	947.7	936.3	940.5
Difference from Neutral Alignment		XXXX	
Significance of Difference from Neutral Alignment	NS	XXXX	NS
Significance of Difference between +5 mm and -5mm		NS	
My+ (NmX10)			
Interval of Maximum Value	9	10	9
Maximum Value	148.2	155.9	132.3
Difference from Neutral Alignment		XXXX	
Significance of Difference from Neutral Alignment	NS	XXXX	NS
Significance of Difference between +5 mm and -5mm		NS	
My- (NmX10)			
Interval of Maximum Value	30	34	34
Maximum Value	671.6	719.4	730.7
Difference from Neutral Alignment		XXXX	
Significance of Difference from Neutral Alignment	NS	XXXX	NS
Significance of Difference between +5 mm and -5mm		0.0423	
Distal Tibia Pressure (kPa)			
Interval of Maximum Value	16	12	12
Maximum Value	59.6	67.8	47.1
Difference from Neutral Alignment		XXXX	-20.7
Significance of Difference from Neutral Alignment	NS	XXXX	0.0226
Significance of Difference between +5 mm and -5mm		0.0298	
Notch Pressure (kPa)			
Interval of Maximum Value	34	32	31
Maximum Value	50.5	96.9	74.2
Difference from Neutral Alignment	-46.4	XXXX	-22.7
Significance of Difference from Neutral Alignment	0.0000 X	XXX	0.0000
Significance of Difference between +5 mm and -5mm		0.0000	

SUBJECT 4 - PerfectStride			
	-5 mm	**Neutral Alignment**	**+ 5mm**
Popliteal Pressure 1st Peak (kPa)			
Interval of Maximum Value	13	11	11
Maximum Value	71.9	90.1	82.0
Difference from Neutral Alignment	-18.2	XXXX	-8.1
Significance of Difference from Neutral Alignment	0.0000	XXXX	0.0000
Significance of Difference between +5 mm and -5mm		0.0002	
Popliteal Pressure 2nd Peak (kPa)			
Interval of Maximum Value	32	30	29
Maximum Value	65.2	95.1	81.9
Difference from Neutral Alignment	-29.9	XXXX	-13.2
Significance of Difference from Neutral Alignment	0.0000	XXXX	0.0000
Significance of Difference between +5 mm and -5mm		0.0000	
Lateral Popliteal and Gastrocnemius Pressure (kPa)			
Interval of Maximum Value	31	31	30
Maximum Value	58.1	120.6	96.0
Difference from Neutral Alignment	-62.5	XXXX	-24.6
Significance of Difference from Neutral Alignment	0.0000	XXXX	0.0000
Significance of Difference between +5 mm and -5mm		0.0000	
Medial Popliteal and Gastrocnemius Pressure (kPa)			
Interval of Maximum Value	13	11	13
Maximum Value	75.7	95.8	88.9
Difference from Neutral Alignment	-20.1	XXXX	-6.9
Significance of Difference from Neutral Alignment	0.0000	XXXX	0.0000
Significance of Difference between +5 mm and -5mm		0.0000	
Lateral to Distal Tibia Pressure (kPa)			
Interval of Maximum Value	37	35	36
Maximum Value	70.5	96.8	78.3
Difference from Neutral Alignment	-26.3	XXXX	-18.5
Significance of Difference from Neutral Alignment	0.0000	XXXX	0.0003
Significance of Difference between +5 mm and -5mm		NS	
Medial to Distal Tibia Pressure (kPa)			
Interval of Maximum Value	6	5	5
Maximum Value	13.2	14.6	13.6
Difference from Neutral Alignment		XXXX	
Significance of Difference from Neutral Alignment	NS	XXXX	NS
Significance of Difference between +5 mm and -5mm		NS	

Table 6-14A-P. Significant Differences for Subject 4 Forces, Moment, and Pressures (PerfectStride)

Significant Differences Between Neutral Alignment and Plus and Minus 5 mm - Subject 4 - PerfectStride																		
			Pressure Measurements															
			Distal Tibia		Notch		Popliteal 1st Peak		Popliteal 2nd Peak		Lateral Pop		Medial Pop		LatDist Tib		MedDist Tib	
			+5mm	-5mm	+5mm	-5mm	+5mm	-5mm	+5mm	-5mm	+5mm	-5mm	+5mm	-5mm	+5mm	-5mm	+5mm	-5mm
Transducer Measurements		Difference N, NmX10, kPa	↓ -20.7		↓ -46.4	↓ -22.7	↓ -8.1	↓ -18.2	↓ -13.2	↓ -29.9	↓ -24.6	↓ -62.5	↓ -6.9	↓ -20.1	↓ -26.3	↓ -18.5		
Fx+	+5mm																	
	-5mm	↓ -24.2				↓↓		↓↓		↓↓		↓↓		↓↓		↓↓		
Fx-	+5mm																	
	-5mm	↓ -9.6				↓↓		↓↓		↓↓		↓↓		↓↓		↓↓		
Fz 1st Pk	+5mm																	
	-5mm	↓ -58.6				↓↓		↓↓		↓↓		↓↓		↓↓		↓↓		
Fz 2nd Pk	+5mm																	
	-5mm																	
My+	+5mm																	
	-5mm																	
My-	+5mm																	
	-5mm																	

Table 6-14B-P. Summary of Significant Differences for Subject 4 (PerfectStride)

Note: In the cells of the matrix, the first arrow indicates a significant change in the transducer variable, and the second arrow indicates a significant change in the peak pressure measurement (t-test, $p \leq 0.05$); upward pointing arrows represent an increase in the magnitude of the variable with the perturbation compared to the initial neutral alignment, and downward pointing arrows represent a decrease in the magnitude of the variable with the perturbation.

Subject 4 – PerfectStride						
Alignment	**Pressure Window**	**Variables in Regression**	**Variables Added to Regression for Neutral Alignment at p $\leq$ 0.005 to enter**	**Variables Removed from Regression for Neutral Alignment at p $\leq$ 0.005 to enter**	**Maximums Separated by 2 or More Time Intervals**	
Neutral	Distal Tibia	Fz, My-, Fx-				
	Notch	Fz, My-, Fx-				
	Popliteal Fz,					
	Lat Gastrocnemius	Fz, My-, Fx-, Fx+ , My+				
	Med Gastrocnemius	Fz, Fx+, My+, Fx-, My-				
	Lat Dist Tibia	Fz, Fx+, My-, My+				
	Med Dist Tibia	Fz, Fx-, Fx+, My-				
+5 mm	*Distal Tibia↓	Fz, My+, My-, Fx-	My+			
	*Notch↓	Fz, My-, Fx-				
	*Popliteal↓	Fz, Fx-, My-, Fx+, My+	Fx+, Fx-, My+, My-			
	*Lat Gastroc↓	Fz, My-, Fx-, Fx+, Fx-, My+				
	*Med Gastroc↓	Fz, Fx-, My-, Fx+, My+			P	
	Lat Dist Tibia	Fz, Fx+, My-		My+		
	Med Dist Tibia	No variables				
-5 mm	Distal Tibia	*Fz↓, My-, *Fx+↓ *F	x+↓ Fx-		P, *Fz↓, Fx-, My-	
	*Notch↓ *Fz	↓, Fx-, My-			P, *Fz↓, Fx-, My-	
	*Popliteal↓ *Fz	↓, *Fx+↓, My+	*Fx+↓, My+		P, *Fz↓	
	*Lat Gastroc↓ *Fz	↓			*Fz↓	
	*Med Gastroc↓ *Fz	↓, *Fx+↓, My+,Fx-		My-	P, *Fz↓, Fx-	
	*Lat Dist Tibia	*Fz↓, Fx-, *Fx+↓, My-	Fx-	My+	*Fz↓, Fx-, My-	
	Med Dist Tibia	*Fz↓, *Fx+↓, Fx-, My-			*Fz↓, Fx-, My-	

Table 6-14C-P. Model Structural Changes with Perturbations for Subject 4 (PerfectStride)

Note: An asterisk (*) indicates a statistically significant difference in maximum values from neutral alignment at $p \leq 0.05$ and a difference that is at least 5% of the value for the neutral alignment and therefore of possible clinical relevance; an upward arrow (↑) indicates an increase in the magnitude of the maximum value and a downward arrow (↓) indicates a decrease in the magnitude of the maximum value. There are 50 time intervals during stance, and 2 intervals represent 4% of stance. P stands for maximum pressure in the column indicating 2 or more intervals between maximum values

Subject 4 PerfectStride Neutral
Apriori Model (Fz, Fx(+), Fx(-), My(+), My(-))

Pressure Region	R^2	Y(hat)	Const.	Fz	Fx(+)	Fx(-)	My(+)	My(-)
Distal Tibia	0.875	P(DistTib)	-8.102	0.061	0.000	0.143	0.000	-0.077
Notch	0.980	P(Notch)	13.062	0.042	0.000	-0.323	0.000	0.134
Gastroc (Lateral)	0.992	P(GastrLateral)	37.936	0.040	0.112	-0.257	-0.090	0.121
Gastroc (Medial)	0.991	P(GastrMedial)	25.915	0.057	0.227	-0.164	-0.104	0.043
Popliteal	0.829	P(Popliteal)	26.562	0.065	0.000	0.000	0.000	0.000
AntLateral	0.992	P(Lateral)	10.120	0.081	-0.269	0.000	0.058	0.011
AntMedial	0.880	P(Medial)	8.698	-0.004	0.049	0.043	0.000	-0.014

Subject 4 PerfectStride +5mm
Apriori Model (Fz, Fx(+), Fx(-), My(+), My(-))

Pressure Region	R^2	Y(hat)	Const.	Fz	Fx(+)	Fx(-)	My(+)	My(-)
Distal Tibia	0.936	P(DistTib)	-8.753	0.041	0.000	0.097	0.091	-0.042
Notch	0.953	P(Notch)	12.810	0.025	0.000	-0.331	0.000	0.117
Gastroc (Lateral)	0.985	P(GastrLateral)	34.847	0.026	0.160	-0.284	-0.080	0.110
Gastroc (Medial)	0.990	P(GastrMedial)	26.884	0.043	0.292	-0.231	-0.108	0.061
Popliteal	0.990	P(Popliteal)	29.696	0.037	0.246	-0.249	-0.097	0.077
AntLateral	0.979	P(Lateral)	5.600	0.062	-0.123	0.000	0.000	0.012
AntMedial		P(Medial)	0.000	0.000	0.000	0.000	0.000	0.000

*No variables were entered into the equation for the Anterior Medial pressure area.

Subject 4 PerfectStride -5mm
Apriori Model (Fz, Fx(+), Fx(-), My(+), My(-))

Pressure Region	R^2	Y(hat)	Const.	Fz	Fx(+)	Fx(-)	My(+)	My(-)
Distal Tibia	0.920	P(DistTib)	4.069	0.066	-0.294	0.000	0.000	-0.071
Notch	0.881	P(Notch)	-2.398	0.024	0.000	0.072	0.000	0.012
Gastroc (Lateral)	0.851	P(GastrLateral)	20.216	0.033	0.000	0.000	0.000	0.000
Gastroc (Medial)	0.961	P(GastrMedial)	16.931	0.058	0.193	-0.031	-0.097	0.000
Popliteal	0.953	P(Popliteal)	15.205	0.053	0.203	0.000	-0.083	0.000
AntLateral	0.962	P(Lateral)	5.338	0.054	-0.163	0.155	0.000	-0.029
AntMedial	0.812	P(Medial)	8.251	0.003	0.016	0.013	0.000	-0.003

Table 6-14D-P. Regression Models for Subject 4 (PerfectStride)

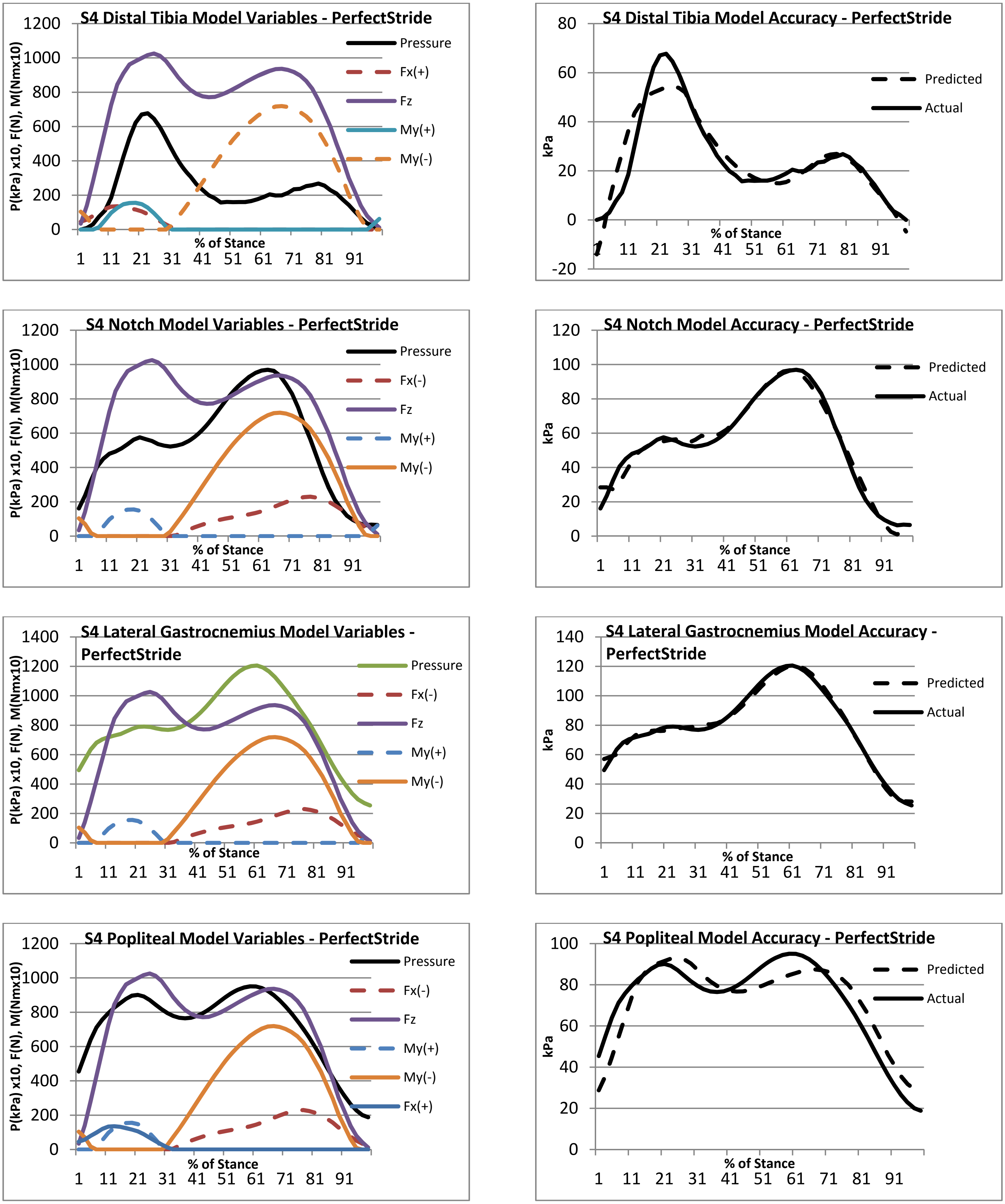

Figure 6-4C-P. Subject 4 Model Variables and Accuracy (PerfectStride)

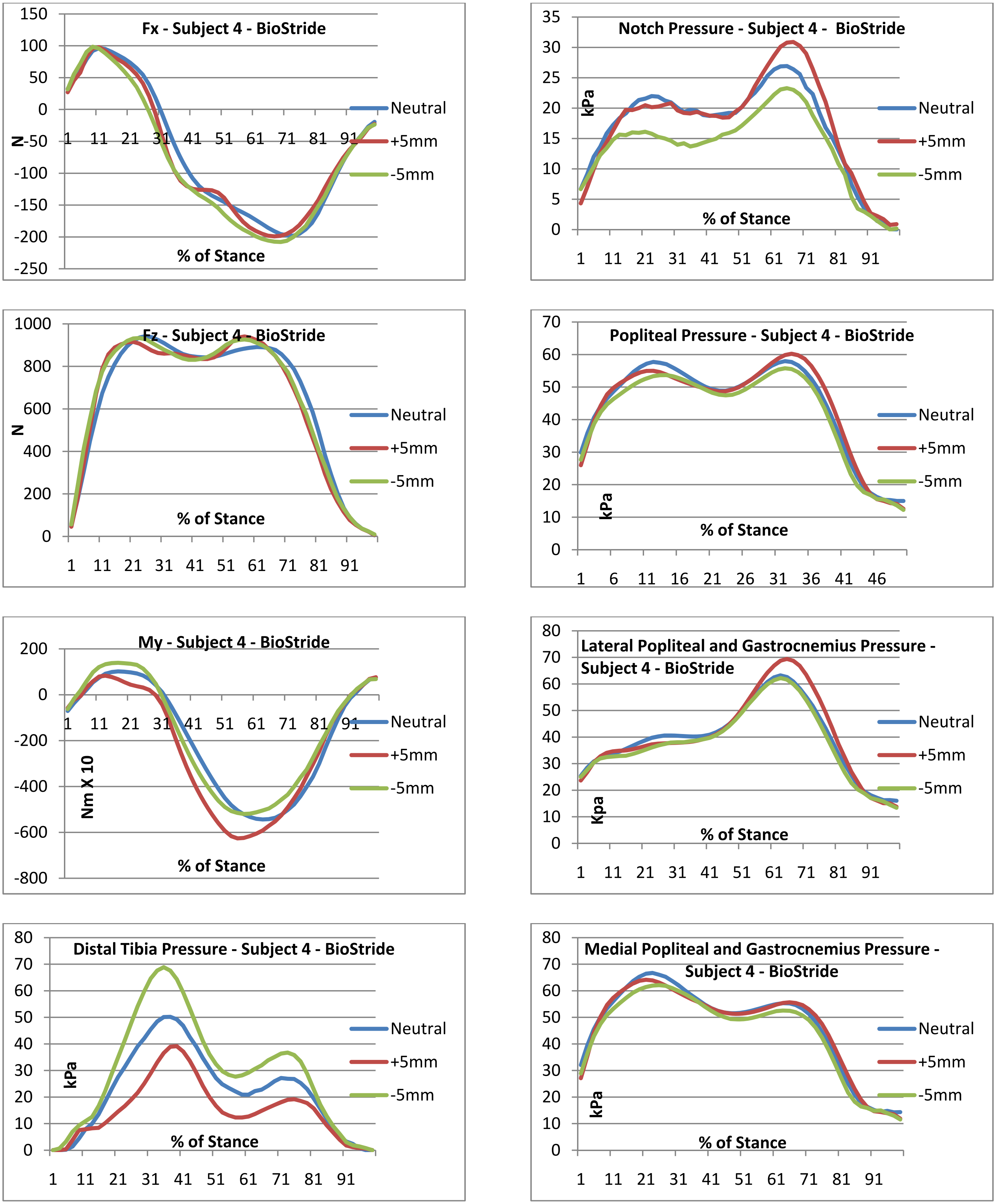

Figure 6-14B-B. Forces, Moments, and Pressures- S4 BioStride

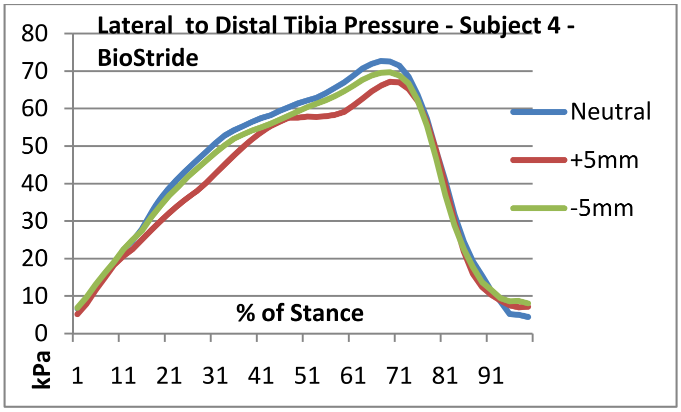

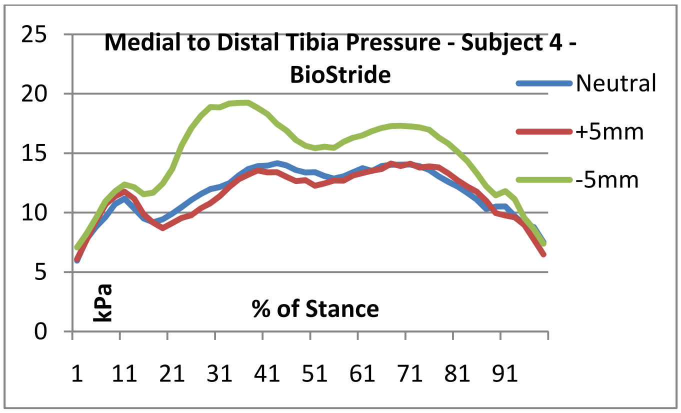

Figure 6-14B-B, Continued

SUBJECT 4 - BioStride			
	-5 mm	**Neutral Alignment**	**+ 5mm**
Fx+ (N)			
Interval of Maximum Value	5	6	6
Maximum Value	98.6	96.4	97.7
Difference from Neutral Alignment		XXXX	
Significance of Difference from Neutral Alignment	NS	XXXX	NS
Significance of Difference between +5 mm and -5mm		NS	
Fx- (N)			
Interval of Maximum Value	35	37	34
Maximum Value	207.9	198.0	199.1
Difference from Neutral Alignment		XXXX	
Significance of Difference from Neutral Alignment	NS	XXXX	NS
Significance of Difference between +5 mm and -5mm		NS	
Fz 1st Peak (N)			
Interval of Maximum Value	12	13	11
Maximum Value	933.4	941.8	915.0
Difference from Neutral Alignment		XXXX	-26.8
Significance of Difference from Neutral Alignment	NS	XXXX	0.0027
Significance of Difference between +5 mm and -5mm		0.0090	
Fz 2nd Peak (N)			
Interval of Maximum Value	29	31	29
Maximum Value	926.4	890.6	940.4
Difference from Neutral Alignment		XXXX	49.8
Significance of Difference from Neutral Alignment	NS	XXXX	0.0061
Significance of Difference between +5 mm and -5mm		NS	
My+ (NmX10)			
Interval of Maximum Value	9	9	7
Maximum Value	139.2	101.8	83.0
Difference from Neutral Alignment	37.4	XXXX	
Significance of Difference from Neutral Alignment	0.0079	XXXX	NS
Significance of Difference between +5 mm and -5mm		0.0000	
My- (NmX10)			
Interval of Maximum Value	29	32	28
Maximum Value	519.7	543.7	626.0
Difference from Neutral Alignment		XXXX	82.3
Significance of Difference from Neutral Alignment	NS	XXXX	0.0000
Significance of Difference between +5 mm and -5mm		0.0009	
Distal Tibia Pressure (kPa)			
Interval of Maximum Value	18	19	20
Maximum Value	68.9	50.2	39.1
Difference from Neutral Alignment	18.7	XXXX	
Significance of Difference from Neutral Alignment	0.0157	XXXX	NS
Significance of Difference between +5 mm and -5mm		0.0002	
Notch Pressure (kPa)			
Interval of Maximum Value	33	33	34
Maximum Value	23.3	26.9	30.9
Difference from Neutral Alignment	-3.6	XXXX	4.0
Significance of Difference from Neutral Alignment	0.0332	XXXX	0.0242
Significance of Difference between +5 mm and -5mm		0.0000	

SUBJECT 4 - BioStride			
	-5 mm	**Neutral Alignment**	**+ 5mm**
Popliteal Pressure 1st Peak (kPa)			
Interval of Maximum Value	14	12	12
Maximum Value	53.7	57.7	55.0
Difference from Neutral Alignment	-4.0	XXXX	-1.3
Significance of Difference from Neutral Alignment	0.0014	X XXX	0.0180
Significance of Difference between +5 mm and -5mm		NS	
Popliteal Pressure 2nd Peak (kPa)			
Interval of Maximum Value	32	32	33
Maximum Value	55.8	58.0	60.2
Difference from Neutral Alignment		XXXX	
Significance of Difference from Neutral Alignment	NS	XXXX	NS
Significance of Difference between +5 mm and -5mm		0.0070	
Lateral Popliteal and Gastrocnemius Pressure (kPa)			
Interval of Maximum Value	32	32	33
Maximum Value	62.2	63.2	69.4
Difference from Neutral Alignment		XXXX	6.2
Significance of Difference from Neutral Alignment	NS	XXXX	0.0482
Significance of Difference between +5 mm and -5mm			
Medial Popliteal and Gastrocnemius Pressure (kPa)			
Interval of Maximum Value	13	12	11
Maximum Value	62.1	66.7	64.1
Difference from Neutral Alignment	-4.6	XXXX	
Significance of Difference from Neutral Alignment	0.0022	X XXX	NS
Significance of Difference between +5 mm and -5mm		0.0449	
Lateral to Distal Tibia Pressure (kPa)			
Interval of Maximum Value	35	34	35
Maximum Value	69.7	72.7	67.2
Difference from Neutral Alignment		XXXX	
Significance of Difference from Neutral Alignment	NS	XXXX	NS
Significance of Difference between +5 mm and -5mm		NS	
Medial to Distal Tibia Pressure (kPa)			
Interval of Maximum Value	18	35	36
Maximum Value	19.2	14.0	14.1
Difference from Neutral Alignment	5.2	XXXX	
Significance of Difference from Neutral Alignment	0.0001	X XXX	NS
Significance of Difference between +5 mm and -5mm		0.0002	

Table 6-14A-B. Significant Differences for Subject 4 Forces, Moments, and Pressures (BioStride).

Significant Differences Between Neutral Alignment and Plus and Minus 5 mm – Subject 4 - BioStride																		
			Pressure Measurements															
			Distal Tibia		**Notch**		**Popliteal 1st Peak**		**Popliteal 2nd Peak**		**Lateral Pop**		**Medial Pop**		**LatDist Tib**		**MedDist Tib**	
			+5mm	**-5mm**	**+5mm**	**-5mm**	**+5mm**	**-5mm**	**+5mm**	**-5mm**	**+5mm**	**-5mm**	**+5mm**	**-5mm**	**+5mm**	**-5mm**	**+5mm**	**-5mm**
Transducer Measurements		**Difference** **N, NmX10, kPa**		↑ +18.7	↑ +4.0	↓ -3.6	↓ -1.3	↓ -4.0			↑ +6.2			↓ -4.6				↓ 19.2
Fx+	**+5mm**																	
	-5mm																	
Fx-	**+5mm**																	
	-5mm																	
Fz 1st Pk	**+5mm**	↓ -26.8			↓↑		↓↓				↓↑							
	-5mm																	
Fz 2nd Pk	**+5mm**	↑ +49.8			↑↑		↑↓				↑↑							
	-5mm																	
My+	**+5mm**																	
	-5mm	↑ +37.4		↑↑		↑↓		↑↓						↑↓				↑↓
My-	**+5mm**	↑ +82.3			↑↑		↑↓				↑↑							
	-5mm																	

Table 6-14B-B. Summary of Significant Differences for Subject 4 (BioStride)

Note: In the cells of the matrix, the first arrow indicates a significant change in the transducer variable, and the second arrow indicates a significant change in the peak pressure measurement (t-test, $p \leq 0.05$); upward pointing arrows represent an increase in the magnitude of the variable with the perturbation compared to the initial neutral alignment, and downward pointing arrows represent a decrease in the magnitude of the variable with the perturbation.

Subject 4 - BioStride						
Alignment	**Pressure Window**	**Variables in Regression**	**Variables Added to Regression for Neutral Alignment at p ≤ 0.005 to enter**	**Variables Removed from Regression for Neutral Alignment at p ≤ 0.005 to enter**	**Maximums Separated by 2 or More Time Intervals**	
Neutral	Distal Tibia	Fz, Fx+, My-, My+				
	Notch	Fz, My-, Fx+				
	Popliteal	Fz, Fx+, My+				
	Lat Gastrocnemius	Fz, My-, Fx-				
	Med Gastrocnemius	Fz, Fx+, Fx-, My-, My+				
	Lat Dist Tibia	Fz, Fx-, Fx+, My-				
	Med Dist Tibia	Fx-, Fz, My-, My+				
+5 mm	Distal Tibia	*Fz↑, Fx+, *My-↑		My+	*Fz↑, *My-↑	
	*Notch↑ *Fz	↑, Fx-	Fx-	Fx+, *My-↑ *Fz	↑, Fx-	
	Popliteal *	Fz↑		Fx+, My+	*Fz↑	
	*Lat Gastroc↑ *Fz	↑, Fx-, Fx+	Fx-	*My-↑ *Fz	↑, Fx-	
	Med Gastrocnemius	*Fz↑, Fx+, My+, *My-↑		Fx-	*Fz↑, *My-↑	
	Lat Dist Tibia	*Fz↑, Fx-, Fx+		*My-↑ *Fz	↑,	
	Med Dist Tibia	Fx-, *Fz↑, *My-↑		My+	*Fz↑, Fx-, *My-↑	
-5 mm	*Distal Tibia↑	Fz, Fx+, My-, *My+↑			Fz, *My+↑	
	*Notch↓	Fz, My-, Fx+			Fz,	
	*Popliteal↓ Fz			Fx+, *My+↑ P,	Fz,	
	Lat Gastrocnemius	My-, Fz		Fx-	Fz,	
	*Med Gastroc↓ Fz,	Fx-, *My+↑		Fx+, My-	Fz, Fx-, *My+↑	
	Lat Dist Tibia	Fz, Fx-, Fx+		My-	Fz, Fx-,	
	Med Dist Tibia	*Fz, Fx+	Fx+	Fx-, *My+↑, My-	P, Fz,	

Table 6-14C-B. Model Structural Changes with Perturbations for Subject 4 (BioStride)

Note: An asterisk (*) indicates a statistically significant difference in maximum values from neutral alignment at $p \leq 0.05$ and a difference that is at least 5% of the value for the neutral alignment and therefore of possible clinical relevance; an upward arrow (↑) indicates an increase in the magnitude of the maximum value and a downward arrow (↓) indicates a decrease in the magnitude of the maximum value. There are 50 time intervals during stance, and 2 intervals represent 4% of stance. P stands for maximum pressure in the column indicating 2 or more intervals between maximum values

Subject 4 BioStride Neutral
Apriori Model (Fz, Fx(+), Fx(-), My(+), My(-))

Pressure Region	R^2	Y(hat)	Const.	Fz	Fx(+)	Fx(-)	My(+)	My(-)
Distal Tibia	0.944	P(DistTib)	3.923	0.056	-0.288	0.000	-0.084	-0.051
Notch	0.940	P(Notch)	0.696	0.019	0.047	0.000	0.000	0.012
Gastroc (Lateral)	0.965	P(GastrLateral)	20.321	0.021	0.000	-0.099	0.000	0.070
Gastroc (Medial)	0.987	P(GastrMedial)	21.300	0.047	0.121	-0.137	-0.081	0.030
Popliteal	0.952	P(Popliteal)	15.488	0.043	0.135	0.000	-0.075	0.000
AntLateral	0.990	P(Lateral)	3.613	0.051	-0.160	0.042	0.000	0.025
AntMedial	0.923	P(Medial)	7.749	0.005	0.000	0.029	-0.017	-0.007

Subject 4 BioStride +5mm
Apriori Model (Fz, Fx(+), Fx(-), My(+), My(-))

Pressure Region	R^2	Y(hat)	Const.	Fz	Fx(+)	Fx(-)	My(+)	My(-)
Distal Tibia	0.703	P(DistTib)	4.062	0.033	-0.262	0.000	0.000	-0.024
Notch	0.895	P(Notch)	0.627	0.020	0.000	0.042	0.000	0.000
Gastroc (Lateral)	0.893	P(GastrLateral)	8.317	0.022	0.129	0.172	0.000	0.000
Gastroc (Medial)	0.970	P(GastrMedial)	17.157	0.048	0.133	0.000	-0.010	-0.115
Popliteal	0.916	P(Popliteal)	16.903	0.043	0.000	0.000	0.000	0.000
AntLateral	0.963	P(Lateral)	2.078	0.039	-0.107	0.148	0.000	0.000
AntMedial	0.856	P(Medial)	7.332	0.003	0.000	0.036	0.000	-0.005

Subject 4 BioStride -5mm
Apriori Model (Fz, Fx(+), Fx(-), My(+), My(-))

Pressure Region	R^2	Y(hat)	Const.	Fz	Fx(+)	Fx(-)	My(+)	My(-)
Distal Tibia	0.909	P(DistTib)	6.812	0.076	-0.352	0.000	-0.195	-0.078
Notch	0.918	P(Notch)	1.259	0.013	0.042	0.000	0.000	0.015
Gastroc (Lateral)	0.914	P(GastrLateral)	15.738	0.022	0.000	0.000	0.000	0.040
Gastroc (Medial)	0.964	P(GastrMedial)	18.331	0.054	0.000	-0.079	-0.055	0.000
Popliteal	0.940	P(Popliteal)	14.292	0.043	0.000	0.000	0.000	0.000
AntLateral	0.977	P(Lateral)	1.909	0.044	-0.123	0.133	0.000	0.000
AntMedial	0.826	P(Medial)	10.279	0.008	-0.059	0.000	0.000	0.000

Table 6-14D-B. Regression Models for Subject 4 (BioStride)

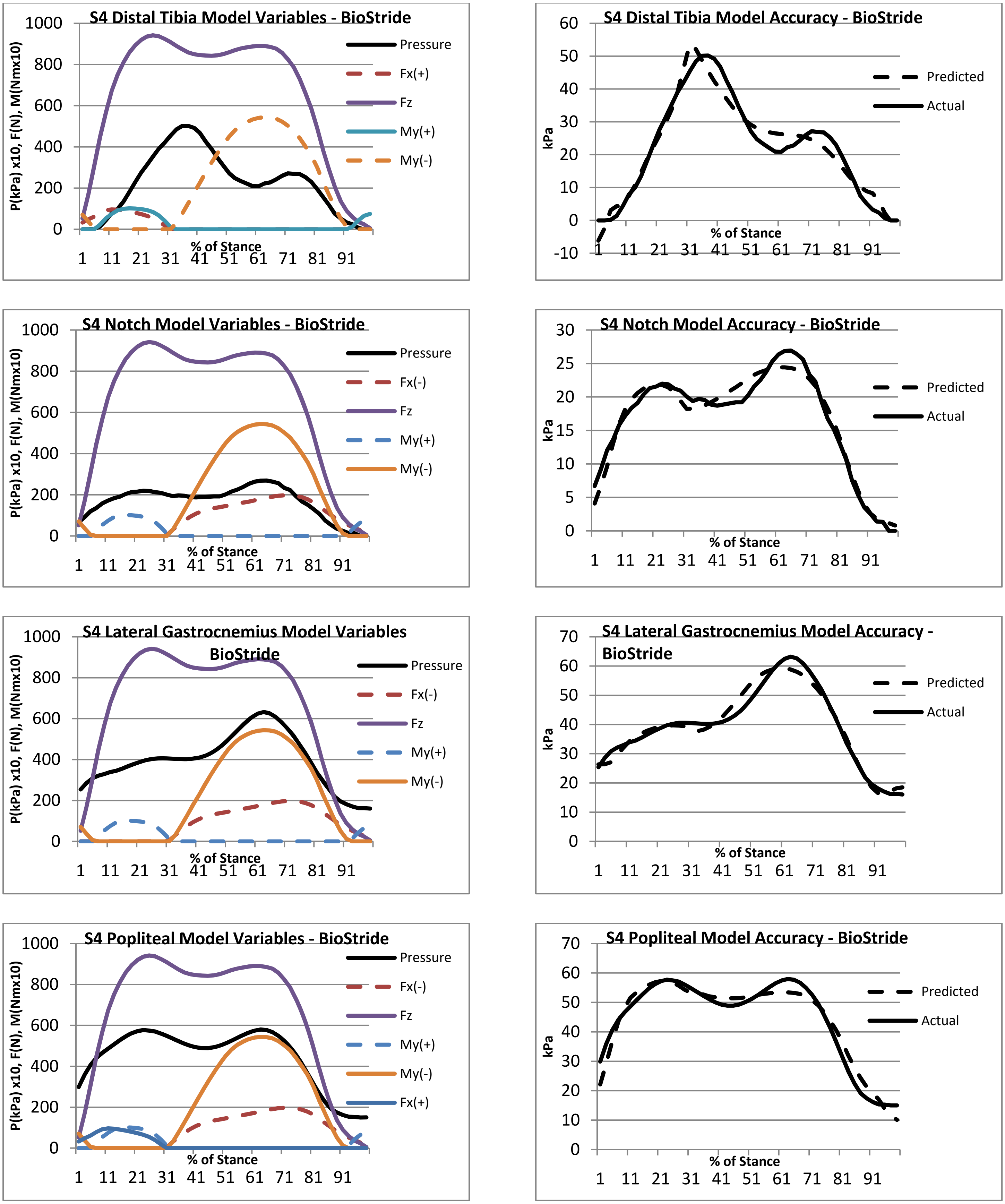

Figure 6-4C-B. Subject 4 Model Variables and Accuracy (BioStride)

7. Analysis of Subjective Data

The State-of-the-Science review found that no research study to date has undertaken a scientific approach to the measurement of alignment perception. Studies that reported on the range of acceptable alignments appeared to make the assumption that acceptance changes dramatically with a small incremental change in alignment. In the studies, the range of acceptable alignments was presented without discussion of how acceptability was measured (8, 14, 20, 26, 42, 51). The published results implied that researchers viewed acceptability as a zero-one (0 or 1) phenomenon; an alignment was either completely acceptable or completely unacceptable to the amputee. In some cases, the judgment of acceptability was made by the prosthetist. Previous research indicated that pressure changes occur gradually with small perturbations in alignment (23, 46, 52). According to the theory of psychophysics, there should be a gradual change in the perception of pressure magnitude with small changes in pressure. For purposes of research, acceptability should be conceived of as a stochastic variable, with probabilities that vary as alignment changes. With gradual changes in pressure, there also should be changes in the amputee's subjective expectation that the alignment will be unacceptable. With increasing pressure, the probability that an alignment will be perceived as unacceptable should approach 1.0.

The study attempted to obtain measures of subjective perceptions of pressure. Subjective data were collected to enable comparison of feet and activities, and also to compare perceptions of alignments. For feet and activities, subjects were asked the location in the socket where they most noticed pressure and during which phase of gait (Figure 7-1). They were then asked to estimate the amount of pressure using a Borg Scale that had been adapted to record pressure sensation (Figure 7-2). During data collection on alignment perturbation, for each alignment subjects were asked if the alignment was acceptable and how certain they were of this (Figure 7-3). They then were asked if there were any locations in the socket where they were experiencing high pressure, and if so, during which phase of gait this was noticed using the question in F1gure 7-1. They then were asked to report the magnitude using the Borg Scale in Figure 7-2. Subjects were shown or given large cards with the questions and answer selections on them.

For the locations where pressure seems to be greater, at what point in time do you most notice the pressure increase? Please select one of the following:

1. Nearer the beginning of stance, when most of my weight is mainly on the heel of my prosthetic foot
2. Nearer the end of stance, when most of my weight is mainly on the toes of my prosthetic foot
3. About equally at both the beginning and the end
4. In between when my foot is flat on the ground
5. It varies or is hard to tell

Figure 7-1. Question on Phase of Stance when Pressure is Noticeable

Comparison of Feet and Activities

Analysis of the data involved a comparison of perceived pressures for each pair of feet used by a subject with the significant differences of the forces and moments for the pair of feet, which were reported in Chapter 4. Because the regression coefficients were found to vary from subject to subject and were estimated for only one foot of each pair, they could not be used in the comparisons. The pressure windows found to have the most stable regression models across all the subjects and feet were the notch and gastrocnemius, for which My- entered all but one of the neutral alignment regression equations with a positive sign, indicating that an increase in My- lead to an increase in pressure. The one exception was Subject 1, for whom the pressure sensor malfunctioned for the notch; this was the only subject for whom My- also did not appear in the neutral alignment model for the gastrocnemius. For this reason, the relationship between significant differences in My- and differences in pereeived pressures at the notch and gastrocnemius region were examined. Subjective responses are shown in Table 7-1, which compares the pair of feet used by a subject for each activity. Table 7-2 indicates the relationship between subjective pressures and significant differences in My- as presented in Chapter 4.

Please select a number between 0 and 11 that matches the amount of PRESSURE you are experiencing at the location specified. It may be easiest to start with a verbal expression and then choose a number.

0	**Nothing at all**	**"No Pressure"**
0.3		
0.5	**Extremely weak**	**Just noticeable**
1	**Very weak**	
1.5		
2	**Weak**	**Light**
2.5		
3	**Moderate**	
4		
5	**Strong**	**Heavy**
6		
7	**Very strong**	
8		
9		
10	**Extremely strong (almost the maximum)**	
11		
*****	**The maximum I can tolerate**	

Figure 7-2. Borg Scale of Perceived Pressure

For Subject 1, The TruStep and the Renegade were compared. Subject 1 was asked to evaluate pressure in each region of the socket for each activity. Based on the magnitude of the reported perceived pressures, the TruStep was judged to produce pressures that were "extremely weak" (0.5), "very weak" (1), or between "weak" and "very weak" (1.5) at the notch and gastrocnemius for all activities. The scores for the Renegade suggest it was perceived to produce slightly less pressure for the activities- between "nothing at all" and "extremely weak" (0.3), at the notch, with nothing reported for the gastrocnemius. With the TruStep, the notch was reported most often to produce noticeable pressure for level walking, going up stairs, up ramps, walking in a circle with the prosthetic foot inside and outside, and walking across a grassy slope with the prosthetic foot uphill. Sometimes this was reported for the loading phase of gait (heel contact), sometimes for the propulsive phase, and sometimes throughout gait. With the Renegade, the notch was mentioned four times, and the magnitudes of the reported pressures were lower. The gastrocnemius region was mentioned three times for the TruStep, but not for the Renegade. Table 7-2 indicates that there were consistent relationships between perceived changes in pressure and My- measurements obtained from the transducer for some regions of the socket but not for other regions. In agreement with significant differences in My-, the TruStep pressures were perceived to be greater than the Renegade pressures at the notch for level walking at a self-selected comfortable speed, going up a ramp, going up steps, and walking in a circle. They were perceived to be greater at the gastrocnemius for going up a ramp and walking in a circle in agreement with the transducer measurement of My-. However, very large significant differences in My- associated with going down steps (100.4% increase with the TruStep) were not reported as perceived pressure differences at either the notch or gastrocnemius, and perceived differences in pressure for walking across a grassy slope with the prosthetic foot uphill were not

Subject: 1						
	Foot: TruStep			**Foot: Renegade**		
	Location Phase		Magnitude	Location Phase		Magnitude
SSCS	Notch Loading		1.5	Notch Loading		0.3
Up Stairs	Notch Throug	hout	0.5	Notch Throug	hout	0.3
Down Stairs	Distal Tibia Popliteal	Throughout Throughout	1 1	Distal Tibia	Throughout	0.5
Up Ramp	Gastrocnemius Notch	Propulsion Propulsion	1 1	NA		0
Down Ramp	Popliteal	Loading	1	NA		0
Circle – Foot Inside	Gastrocnemius Notch	Propulsion Loading	0.5 0.5	PTB Loading		0.3
Circle – Foot Outside	Gastrocnemius Notch	Propulsion Loading	0.5 0.5	Notch Lateral Distal	Loading Throughout	0.3
Foot Upslope	Notch	Loading	1	NA		0
Foot Downslope	Lateral Distal	Throughout	1.5	NA		0

Subject: 2						
	Foot: Carbon Copy 2			**Foot: SACH**		
	Location	**Phase**	**Magnitude**	**Location**	**Phase**	**Magnitude**
SSCS	Distal Tibia	Loading	3	Distal Tibia	Loading	3
Up Stairs	Popliteal	Propulsion	5	Distal Tibia Gastrocnemius	Throughout Throughout	3
Down Stairs	Distal Tibia	Propulsion	3	Distal Tibia	Throughout	3
Up Ramp	Notch Distal Tibia	Throughout Throughout	3 3	Notch Distal Tibia	Throughout Throughout	3 3
Down Ramp	Gastrocnemius Popliteal	Throughout Throughout	3 Gastrocne	mius Popliteal	Throughout Throughout	3 3
Circle – Foot Inside	Lateral Distal	Loading	3	Lateral Distal	Loading	3
Circle – Foot Outside	Distal Tibia	Loading	3	Distal Tibia	Loading	3
Foot Upslope	Distal Tibia	Loading	3	Distal Tibia	Loading	3
Foot Downslope	Distal Tibia Notch	Throughout Throughout	3 3	Distal Tibia Notch	Throughout Throughout	3 3

Table 7-1. Perceptions of Pressure for Different Activities and Feet

Subject: 3						
	Foot: Flexfoot			Foot: SACH		
	Location	Phase	Magnitude	Location	Phase	Magnitude
SSCS Lateral	Distal Distal Tibia Lateral Prox	Throughout Loading Throughout	4 3 3	Distal Tibia Lateral Prox	Propulsion Propulsion	3 3
Up Stairs	Lateral Prox	Throughout	3	Distal Tibia Lateral Prox	Propulsion Propulsion	4.5 4
Down Stairs	Distal Tibia	Propulsion	4	Lateral Prox	Throughout	3
Up Ramp	Medial Prox Lateral Prox	Midstance Throughout	4 3	Lateral Prox Medial Prox Lateral Distal	Throughout Throughout Midstance	4 4 3
Down Ramp	Distal Tibia Gastrocnemius	Loading Propulsion	4 3	Distal Tibia Lateral Prox	Propulsion Throughout	6 5
Circle – Foot Inside	Lateral Distal	Midstance	3	Notch Lateral Prox	Propulsion Propulsion	3 3
Circle – Foot Outside	Distal Tibia Lateral Prox	Propulsion Propulsion	3 3	Distal Tibia Lateral Prox	Propulsion Loading	4 4
Foot Upslope	Lateral Prox	Foot flat	3	Lateral Prox Lateral Distal Popliteal	Throughout Throughout Propulsion	4.5 4 3
Foot Downslope	Distal Tibia Lateral Distal Lateral Prox	Propulsion Midstance Throughout	3 3 3	Lateral Prox Lateral Distal Medial Distal Popliteal Notch Gastrocnemius	Throughout Midstance Throughout Loading Loading Propulsion	4 3 3 3 3 3

Subject: 4						
	Foot: PerfectStride			Foot: BioStride		
	Location	Phase	Magnitude	Location	Phase	Magnitude
SSCS NA				NA		
Up Stairs	Notch	Propulsion 2		Gastrocnemius Propulsion		3
Down Stairs	Distal Tibia	Propulsion	2	NA		
Up Ramp	Distal Tibia	Propulsion	2	NA		
Down Ramp	NA			NA		
Circle – Foot Inside	Gastrocnemius Midstance		2.5	NA		
Circle – Foot Outside	NA			NA		
Foot Upslope	Medial Prox	Midstance	2	NA		
Foot Downslope	Medial Distal	Midstance	2	NA		

Table 7-1. Perceptions of Pressure for Different Activities and Feet, Continued

Subject: 4						
	Foot: SACH			Foot:		
	Location	**Phase**	**Magnitude**	**Location**	**Phase**	**Magnitude**
SSCS NA						
Up Stairs	Gastrocnemius	Propulsion	3.5			
Down Stairs	NA					
Up Ramp	Distal Tibia	Propulsion	2			
Down Ramp	NA					
Circle – Foot Inside	Lateral Distal	Throughout	3			
Circle – Foot Outside	Distal Tibia	Propulsion	2.5			
Foot Upslope	Lateral Distal	Throughout	3			
Foot Downslope	Gastrocnemius	Loading	2			

Table 7-1. Perceptions of Pressure for Different Activities and Feet, Continued

associated with any significant differences in My-. However, the perceived pressure differences may have been due to other forces or moments acting on the socket.

For Subject 2, a SACH foot was compared to the Carbon Copy 2. Nearly all pressures for both feet were rated as "moderate", a 3 on the Borg scale. The notch was identified as experiencing noticeable pressure for going up a ramp and across a grassy slope with the prosthetic foot on the downhill side. The gastrocnemius was identified as experiencing noticeable pressure when going down a ramp. But both feet produced subjective magnitude 3 pressures as reported by the subject, even though there were large significant differences in the maximum values of My- for nearly every activity, with the higher values being associated with the Carbon Copy 2.

For Subject 3, a SACH foot was compared to a Flex Foot. Although there were large significant differences in My- for all activities except going up and down steps, with the Flex Foot producing the larger moments, Subject 3 did not report any perceived differences at the notch, and only one perceived difference for the gastrocnemius region when going down a ramp.

Subject 4 compared three feet in the experiment: a SACH foot, the PerfectStride, and the BioStride. For the PerfectStride, all pressures for all activities were reported as "weak" (2) or between "weak" and "moderate" (2.5). The only region and activity for which Subject 4 reported pressure with the BioStride was at the gastrocnemius when going up stairs, at a magnitude of 3 (moderate). For the SACH foot, reported subjective pressure was "weak" (2) at the gastrocnemius when walking across a grassy slope with the foot downhill, and the notch was not mentioned. Comparing the PerfectStride foot to the SACH foot, the transducer measurements of My- were significantly greater for the PerfectStride for four activities, but Subject 4 reported a perceived difference at the notch only for going up steps and at the gastrocnemius region only for walking with the prosthetic foot on the inside of the circle. The subject reported the SACH foot as producing more pressure at the gastrocnemius region when going up steps and walking across a grassy slope with the prosthetic foot downhill, even thought the PerfectStride had a significantly greater moment associated with the first activity and there was no significant difference between the feet for the second activity. Comparing the SACH to the BioStride, there were no significant differences in My- for any of the activities. As reported above, the subject reported greater perceived pressure from the SACH foot at the gastrocnemius for two activities. Comparing the PerfectStride to the BioStride, the PerfectStride exhibited significantly higher moments for all five activities, but Subject 4 reported consistent pressure increases at the notch for only two activities – going up steps, and walking in a circle with the prosthetic foot on the inside.

Activity	Foot Exhibiting Significantly Greater My- and Increase in Magnitude (Nm X 10), %	Foot for Which Pressure was Reported at Notch and Subjective Magnitudes	Foot for Which Pressure was Reported at Gastrocnemius and Subjective Magnitudes
S1 (Renegade vs TruStep)			
SSCS	TruStep (88.0), 10.1	TruStep (1.5 vs 0.3)	
Up Ramp	TruStep (71.9), 7.7	TruStep (1 vs no mention)	TruStep (1 vs no mention)
Down Ramp			
Up Steps	TruStep (96.5), 16.8	TruStep (0.5 vs 0.3)	
Down Steps	TruStep (170.4), 100.4		
Slope-Foot Uphill		TruStep (1 vs 0)	
Slope –Foot Downhill			
Circle-Foot Inside	TruStep (85.3), 11.0	TruStep (0.5 vs 0.3)	TruStep (0.5 vs no mention)
Circle-Foot Outside	TruStep (84.6), 10.5	TruStep (0.5 vs 0.3)	TruStep (0.5 vs no mention)
S2 (SACH vs Carbon Copy2)			
SSCS	CC 2 (152.8), 15.8		
Up Ramp	CC 2 (201.6), 22.2	Both Equal (3 vs 3)	
Down Ramp	CC 2 (88.3), 12.0		Both Equal (3 vs 3)
Up Steps	CC 2 (232.5), 42.7		
Down Steps			
Slope-Foot Uphill	CC 2 (140.8), 15.5		
Slope –Foot Downhill	CC 2 (203.5), 23.9	Both Equal (3 vs 3)	
Circle-Foot Inside	CC 2 (136.6), 17.4		
Circle-Foot Outside	CC 2 (137.8), 15.8		
S3 (SACH vs FlexFoot)			
SSCS	Flex Foot (70.1), 12.4		
Up Ramp	Flex Foot (116.9), 21.6		
Down Ramp	Flex Foot (121.2), 28.5		FlexFoot (3 versus no mention)
Up Steps			
Down Steps			
Slope-Foot Uphill	Flex Foot (151.7), 30.9		
Slope –Foot Downhill	Flex Foot (112.8), 22.1		
Circle-Foot Inside			
Circle-Foot Outside	Flex Foot (83.7), 15.5		

Table 7-2 Significant Differences My- and Perceptions of Pressure

Activity	Foot Exhibiting Significantly Greater My- and Increase in Magnitude (Nm X 10), %	Foot for Which Pressure was Reported at Notch and Subjective Magnitudes	Foot for Which Pressure was Reported at Gastrocnemius and Subjective Magnitudes
S4 (SACH vs PerfectStride)			
SSCS PerfectStride	(38.1), 6.1		
Up Ramp	PerfectStride (76.0), 11.5		
Down Ramp			
Up Steps	PerfectStride (140.8), 44.3	Perfect (2 vs no mention)	SACH (3.5 vs no mention)
Down Steps			
Slope-Foot Uphill			
Slope –Foot Downhill			SACH (2 vs no mention)
Circle-Foot Inside	Perfect-Stride (80.5), 14.4		Perfect (2.5 vs no mention)
Circle-Foot Outside			
S4 (SACH vs BioStride)			
SSCS			
Up Ramp			
Down Ramp			
Up Steps			SACH (3.5 vs 3)
Down Steps			
Slope-Foot Uphill			
Slope –Foot Downhill			SACH (2 vs no mention)
Circle-Foot Inside			
Circle-Foot Outside			
S4 (PerfectStride vs BioStride)			
SSCS PerfectStride	(76.8), 13.1		
Up Ramp	PerfectStride (64.4), 9.5		
Down Ramp	PerfectStride (54.0), 12.3		
Up Steps	PerfectStride (132.0), 40.4	Perfect (2 vs no mention)	BioStride (3 vs no mention)
Down Steps	PerfectStride (133.9), 34.4		
Slope-Foot Uphill			
Slope –Foot Downhill	PerfectStride (94.2), 16.6		
Circle-Foot Inside	PerfectStride (108.6), 20.5	Perfect (2 vs no mention)	
Circle-Foot Outside			

Table 7-2, Continued

In summary, the subjective tasks administered for the activities that compared feet did not appear to provide results that were consistent with the measurements from the transducer for the five activities. It is believed that several factors underlie this. First, the subjective measurements involving use of the Borg scale may have exceeded subject capabilities or caused fatigue. Repeating the same questions for each foot and activity (eight regions of the socket X nine walking events X 2 feet = 144 reports of pressure) probably caused subject mental fatigue. The Principal Investigator detected this, and shortened the task to involve reporting only those regions of the socket where pressure was noticed. As a result, it was difficult to obtain good and complete subjective measurements. Second, the ways in which My- contributed to the generation of pressure may have varied with the feet and activities. The results obtained for the models in Chapter 6 imply this.

Comparison of Alignment Perturbations

After each alignment, including neutral alignment and both perturbations, subjects were asked if the alignment was acceptable, and how sure they were of this. The questions and responses subjects were asked to select from are shown in Figure 7-3. Subjects were then asked to identify regions of perceived high pressure within the socket, the phase of gait when the high pressure was noticed using the categories shown in Figure 7-1, and to judge the magnitude of the pressures using the Borg scale shown in Figure 7-2.

Does this alignment feel like it would be acceptable for you to use?

Yes **No** **I don't know**

How certain are you?

1. VERY SURE
2. FAIRLY SURE
3. SOMEWHAT SURE
4. NOT COMPLETELY SURE

Figure 7-3. Question on Acceptability of Alignment

Responses are shown in Table 7-3and Table 7-4 compares subjective pressures to measured pressures. The neutral alignment was judged acceptable for all the subjects except Subject 1. [Subject 3 will be discussed separately below.] The degree of certainty was "Very Sure" for Subject 2 and Subject 4 for the PerfectStride and BioStride feet, and only "Fairly Sure" for the SACH used by Subject 4. The +5 mm alignment was judged acceptable for Subjects 2, 3, and 4 for all three feet. However, the strength of the judgment was only "Fairly Sure" for the BioStride and SACH feet. Those who judge it unacceptable were "Very Sure". The -5 mm alignment was judged acceptable for Subjects 1 and 4 for the BioStride and SACH foot. The level of certainty was reduced for the PerfectStride and BioStride. It increased to "Very Sure" for the SACH foot used by Subject In summary, there was at least one acceptable alignment for each of the subjects and feet. There were at least two acceptable alignments for Subjects 3 and 4. 4. Subject 4 judged all three alignments acceptable for the PerfectStride and BioStride feet.

Table 7-3 indicates the location in the socket where the subject commented on noticing high pressure. Locations varied with the subject and the foot. The last column of the table indicates the phase of stance during which the pressure was noted. Identification of the notch was accompanied by a judgment that pressure occurred during the propulsion phase (Subject 1) or throughout stance (Subject 3). Perception of the highest notch pressure during propulsion was consistent with the pressure data for Subject 1, but Subject 3 exhibited pronounced peaking at the notch around 68% of stance. Noticeable pressure in the gastrocnemius region was reported by Subject 3 around midstance, and by Subject 4 with the PerfectSride during propulsion. Again, the maximum measured gastrocnemius pressures for Subject 3 occurred at 70% of stance and at 62% of stance for Subject 4 when using the PerfectStride. Subject 2 reported high pressure in the popliteal region during midstance; measured pressures peaked at 20% and 64% of stance. Subject 3 reported high pressure in the popliteal region at loading response, and the first peak occurred at 28% of stance. Subject 2 reported high pressure at the distal tibia throughout stance, and pressures were generally consistent throughout stance, increasing slightly at around 78% of stance. Subject 3 reported high pressure at the distal tibia during propusion at an alignment of +5 mm and during loading response at an alignment of -5 mm. Maximum measured pressures occurred at 26%-28% of stance during loading response and were roughly twice as large as those occurring during propulsion. Subject 4 reported high pressure at the distal tibia during midstance with the SACH foot. Maximum measured pressures occurred during 28% of stance. In summary, subjects tended to be slightly inaccurate in judging when peak pressures occurred. It may be too challenging a task to identify the point in time when peak pressures actually occur.

Table 7-4 examines the relationship between reported pressures and the magnitude of the measured pressures. For Subject 1, there was a consistent mapping at the notch as measured by pressures in the region below and lateral to the notch (sensors in the notch and distal tibia failed to work) and the reported magnitudes of pressure. Subjective magnitudes were reported as 0.3, 0.3 to 0.5 and 3, and measured pressures were 74.8, 78.4, and 81.3 kPa, respectively. Both pressure changes for $\pm$5 mm perturbations around the neutral alignment were statistically significant, though small. Subject 2 reported noticing pressure in the popliteal region for the +5 mm perturbation, but there were no significant changes in measured pressures from the neutral alignment. At the distal tibia, Subject 2 reported an increase in perceived pressure with the-5mm perturbation, and there was an increase in measured pressure but it was not significant. Subject 3 reported the most pressure points. For the neutral alignment, pressure awareness was reported for the popliteal region and distal tibia. At the popliteal region, neutral alignment pressures were significantly higher than for both perturbations. For the distal tibia, pressures for the neutral alignment were higher than for either perturbation, but not significantly higher. For the +5 mm perturbation, pressure was noticed at the gastrocnemius and again at the distal tibia. At the gastrocnemius, the +5 mm pressures were higher, but not significantly higher. For the -5 mm perturbation, pressures were noticed at the notch and distal tibia. At the notch, the -5 mm pressures were significantly lower than for the neutral alignment, where pressure had not been noticed for the neutral alignment. Subject 4 reported relatively few points of noticeable pressure. For the PerfectStride foot, pressure was noticed at the gastrocnemius region for the – 5mm alignment. Pressure measurements showed a non-significant decrease from the neutral alignment. For the SACH foot, pressure was noticed at the distal tibia for the neutral alignment. Measured pressures at the neutral alignment were higher than for either perturbation, the difference being significant for the +5 mm perturbation. In summary, there were more consistencies than inconsistencies between regions of the socket where pressure was noticed and measured pressures for those regions.

An interesting finding was that in several cases subjective reports agreed with trends in measured pressures although the measured pressures were not significantly different. It is possible to speculate on whether the use of a 0.05 level of significance is too conservative for evaluating differences in pressure measurements that are perceived subjectively. A hypothesis that might merit investigation is that people use higher subjective probabilities when evaluating areas sensitive to pressure. If one accepts this possibility and reinterprets the results, it suggests that Subject 2 decided the -5 mm perturbation was unacceptable because of a small pressure increase at the distal tibia even though the differences was not statistically significant. The subject reported a level of confidence of "Very Sure" for the unacceptability of the alignment. However, the opposite conclusion would have to be drawn for the +5 mm perturbation at the popliteal region, where there was a non-significant decrease in pressure but the alignment was felt to be not acceptable at the "Very Sure" level of confidence. For Subject 4 and the -5 mm alignment of the PerfectStride foot at the gastrocnemius region, the subject was "Somewhat Sure" that they "Did Not Know" if the alignment was acceptable, although the pressure, while less than for the neutral alignment, was not significantly less; this would appear to refute the claim that a lower level of confidence would reconcile subjective and objective data. At the distal tibia for the SACH foot, Subject 4's response for acceptability would appear to support the higher level of confidence when the +5 mm and neutral alignments are compared; the +5 mm alignment produced significantly lower pressures, and pressure at the distal tibia was not noticed. The level of confidence in the alignment was rated as "Fairly Sure" that it was acceptable. However, for the -5 mm perturbation, while the distal tibia pressure was lower, it was not significantly lower; yet Subject 4 was "Very Sure" that the alignment was acceptable.

Signal Detection

One of the hypotheses of the proposal was that perception of pressure and alignment acceptability is probabilistic and can be explained best by the Theory of Signal Detection, which is a theoretically useful way to conceptualize perception and judgment of pressure, pain, and force. The Theory of Signal Detection incorporates three basic variables in a probabilistic model of judgments: 1.) the magnitude of the signal (i.e., pressure); 2.) the ability of the subject to detect differences in signal strength (sensitivity to changes in pressure); and 3.) the relative benefits and costs to the subject of correctly concluding that a signal is absent when it is absent and correctly perceiving that a signal is present when it is present (how much discomfort will be experienced for the activities of the amputee).

The initial data collection plan was to vary the alignment randomly five times for each setting, requiring a total of 15 alignments. It was planned to use the fifteen alignments to fit a Signal Detection Model. For Subject 1, concerns about the pressure sensors caused the researcher to omit asking about acceptability. Further, due to other time commitments of Subject 1, there was not sufficient time to repeat the perturbations 12 more times. Data were then collected for Subject 3. The order in which recruitment took place was the order assigned to the Subjects. Subject 2, although recruited prior to Subject 3, was not able to participate in data collection until after data had been obtained from Subject 3. For Subject 3, the three alignments, neutral and ±5 mm, were repeated four additional times each in random order without disclosing the direction of the alignment. The sequence was selected by drawing the twelve remaining alignment positions randomly. If the same two alignments were drawn in sequence, the alignment of the subject's foot was moved in a direction away from the current alignment and then returned so as not to reveal to the subject that the same alignment was being used consecutively. Following each of the fifteen alignment perturbations, Subject 3 was asked to report on the acceptability of the alignment. Results are shown below and indicate that judgments did include the kind of error needed to fit a Signal Detection model. The +5 mm alignment was judged unacceptable 60% of the time, unacceptable 20% of the time, and uncertain 20% of the time. The neutral and -5 mm alignments were judged unacceptable 40% of the time and acceptable 60% of the time.

Subject 3	**Is the Alignment Acceptable? (Number of Trials)**		
Alignment	**No**	**Yes**	**Don't Know**
+5 mm	3 1		1
Neutral	2 3		0
-5 mm	2 3		0

Once it was discovered that subjects were finding the repetitive nature of the perturbations boring and causing them to lose interest in data collection, the procedure was modified. Unless there is some degree of uncertainty on the part of the subject who is responding on whether or not a signal is present, and this uncertainty is reported and used to calibrate a Receiver Operating Curve (ROC), a signal detection model cannot be fitted to data without taking a very large number of observations. After Subjects 1 and 3, it became apparent that it was unrealistic to assume amputees would be willing to tolerate a large number of judgment tasks. Procedures were modified. The modification involved performing the three alignments only once, asking the same question about the acceptability of the alignment, and then asking the subjects how certain they were of their judgment. These were the steps followed for Subjects 2 and 4, with results shown in Table 7-3 and discussed above. This approach does not produce enough data to fit a Signal Detection model, but does give some indication of whether one could be fitted to perturbation data if the perturbations could be performed. The data indicate that Subject 2 expressed maximum certainty for all judgments and it is unlikely that a Signal Detection model could be fit if the perturbations were repeated. Subject 4 did express some uncertainty for five out of nine alignments, and repetition of the perturbations might produce data reflecting uncertainty to allow the fitting of a model.

Alignment Setting of Foot	Is Alignment Acceptable?	Certainty of This?	High Pressure Location	Pressure Magnitude	Phase of Gait
Subject: 1					
Foot: Renegade					
+5 mm	No	-	Notch	3	Propulsion
Neutral	No	-	Notch	0.3-0.5	Propulsion
-5 mm	Yes	-	Notch	0.3	Propulsion
Subject: 2					
Foot: SACH					
+5 mm	No	Very Sure	Popliteal	3	Midstance
Neutral	Yes	Very Sure	-		-
-5mm	No	Very Sure	Distal Tibia 5		Throughout Stance
Subject: 3					
Foot: SACH					
+5 mm	Yes	-	Gastrocnemius Distal Tibia	2 2	Midstance Propulsion
Neutral	Yes	-	Popliteal Distal Tibia	2 2	Loading Response Propulsion
-5 mm	No	-	Notch Distal Tibia	2 2.5	Throughout Stance Loading Response
Subject: 4					
Foot: PerfectStride					
+5 mm	Yes	Very Sure	-	-	-
Neutral	Yes	Very Sure	-	-	-
-5 mm	Don’t Know	Somewhat Sure	Gastrocnemius	2.5	Propulsion
Foot: BioStride					
+5 mm	Yes	Fairly Sure	-	-	-
Neutral	Yes	Very Sure	Medial Proximal	2.5	Throughout Stance
-5 mm	Yes	Fairly Sure	-	-	-
Foot: SACH					
+5 mm	Yes	Fairly Sure	-	-	-
Neutral	Yes	Fairly Sure	Distal Tibia	2	Midstance
-5 mm	Yes	Very Sure	-	-	-

Table 7-3 Perception of Pressure for Alignments and Acceptability of Alignment

Alignment Setting of Foot	High Pressure Location Identified by Subject	Pressure, kPa, (% change from Neutral Significant at p ≤ 0.05)	Comparison of Measured Pressures at Perceived High Pressure Locations	Subjective Pressure Magnitude
Subject: 1				
Foot: Renegade				
+5 mm	Notch[1]	81.3 (+2.9)	Pressure increased significantly from neutral	3
Neutral	Notch	78.4	Pressure lies between perturbations	0.3-0.5
-5 mm	Notch	74.8 (-3.6)	Pressure decreased significantly from neutral	0.3
Subject: 2				
Foot: SACH				
+5 mm	Popliteal	116.4	Pressure decreased from neutral but not significantly	3
Neutral	-			
-5mm	Distal Tibia	37.1	Pressure increased from neutral but not significantly	5
Subject: 3				
Foot: SACH				
+5 mm	Gastrocnemius Distal Tibia	97.1 146.1	Pressure increased from neutral but not significantly Pressure decreased from neutral but not significantly	2 2
Neutral	Popliteal Distal Tibia	144.3 160.4	Pressure significantly higher than for both perturbations[3] Pressure higher than for both perturbations, but not significantly	2 2
-5 mm	Notch Distal Tibia	65.0 (-50.9) 151.7	Pressure decreased significantly from neutral Pressure decreased from neutral but not significantly	2 2.5
Subject: 4				
Foot: PerfectStride				
+5 mm	-			-
Neutral	-			-
-5 mm	Gastrocnemius	75.7 (-20.1)	Pressure decreased from neutral but not significantly	2.5
Foot: BioStride				
+5 mm	-			-
Neutral	Medial Proximal[2]			2.5
-5 mm	-			-
Foot: SACH				
+5 mm	-			
Neutral	Distal Tibia	87.0	Pressure was higher than for both perturbations, +5 mm significantly lower by 36.0%	2
-5 mm	-			

Table 7-4. Comparison of Subjective High Pressure Locations and Measured Pressures

Notes: 1. Lateral to notch, 2. Medial proximal pressure measurements were not recorded, 3. +5 mm lower by 40.1% and -5 mm lower by 46.0%

8. Clinical Applications

The project initially envisioned use of the transducer in a military rehabilitation facility such as Walter Reed or the Center for the Intrepid after data had been collected and analyzed, and the instrumentation proved. However, the IRB process and difficulty recruiting subjects caused both money and time to run out before this could be undertaken. The IRB process necessary to do clinical evaluation might have taken another eight months beyond the point the project was at on 20 October 2010. However, the transducer has been demonstrated to provide potentially useful data of a type not previously available to clinicians, and the GUI is effective at processing data from the transducer. A clinician with a scientific background could be trained to use it. The transducer is easy to mount on the pylon of a prosthesis, and transducer data can be collected within approximately half an hour. This study found that level walking at a self-selected comfortable speed provides data adequate to distinguish between the performance of different feet, and the transducer and GUI can be used in any clinical setting where there is sufficient length of unrestricted walking space to obtain ten good steps.

The pressure models appear highly specific to individuals, alignments, and feet, and likely would not be of clinical value except as a diagnostic tool for difficult cases where discomfort is preventing use of a prosthesis, and surgical intervention or other forms of treatment are not indicated. With current pressure sensing technology the collection of pressure data is very challenging, and most practitioners would probably abandon doing this after attempting it. A possibility for future R&D would be the development of a pressure sensor designed for the notch and surrounding region of the socket at perhaps a high level of resolution that is easy to use and integrated with the transducer. The ability to place the sensor inside negative pressure sockets and have it stretch under a sleeve or liner where it crosses the knee would also make pressure measurement with FSR sensor arrays more conducive to clinical use.

One discovery that was made late in data analysis was that division of the My moment by Fz, the vertical force along the direction of the pylon that is analogous to the vertical ground reaction force, provides curves that may reveal information about how prosthetic foot performance varies among different types of feet along with information about how amputees use the performance characteristics of the feet to gain benefit from them. The ratio of My/Fz represents two characteristics of foot function. First, the number reflects an “effective moment arm” for the vertical load; the distance from the pylon through which the force Fz would have to be applied in order to produce moment My. The concept of heel and toe lever arm is a paradigm applied routinely when undertaking alignment in a clinical setting, Moving the foot forward increases the length of the forefoot lever arm, and moving it backwards increases the length of the heel lever arm. The second foot characteristic reflected in the ratio is the amount of My moment that the subject is obtaining from the foot per unit of force along the pylon in the Z direction. This is a function of foot design as well as the motivation of the amputee to generate a moment through the application of pressure at the notch. Since Fz varies in the time domain, creating a curve having a bimodal appearance very similar to and reflecting the vertical ground reaction force, the timing of maximum Fz values together with the ability of the foot to generate a moment at these times may have a strong influence on the performance of the foot during gait.

Figure 8-1 plots the curves of My/Fz for the different alignment perturbations, and Figure 8-2 shows the curves for the neutral alignments of all the SACH feet on one graph and all of the energy storing feet on one graph. Points of potential interest on the graphs include the maximum value of the My/Fz curve for loading response (effective moment arm), the interval during which the maximum value occurs, the interval during which the curve crosses the horizontal axis and moment is zero, the maximum value during propulsion and the interval in which it occurs, the shape of the curve as the maximum value during propulsion is approached, the shape of the curve during energy release after the maximum value, and the way in which the curves shift or do not shift with alignment perturbations. For example, the curves for the SACH foot clearly indicate the effect of the stiff heel plug for Subject 4, creating a high moment per unit of load along the pylon. The flat appearance of the curve for both the PerfectStride and BioStride during propulsion reflects the design of the foot - possibly the convex keel since both feet share this design. The curves for Subject 2 show the neutral alignment and -5 mm alignment to be virtually indistinguishable and the +5 mm curve to be noticeably different; the subject found the +5 mm alignment to be unacceptable (though the subject also judged the -5 mm alignment unacceptable). Subject 3 curves show the -5 mm curve to be noticeably different from the neutral alignment curve and the +5 mm curve which appear highly similar; the -5 mm alignment was judged as not acceptable whereas the +5 mm alignment was judged acceptable. Many other pieces of valuable information may exist in the curves. More research would be needed to examine their utility. These data can be obtained easily in a clinical setting using the transducer and GUI.

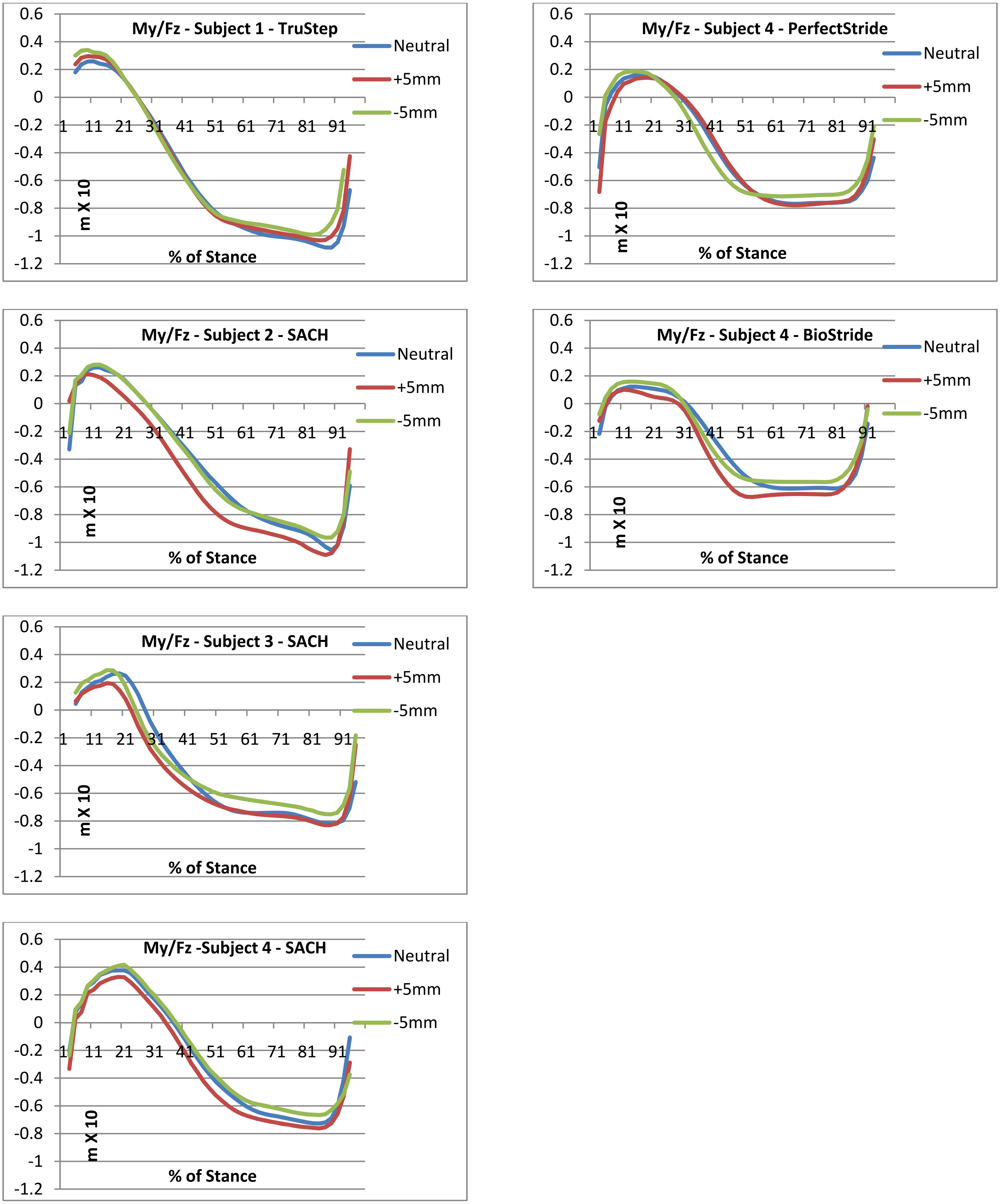

Figure 8-1. Plot of My/Fz for Perturbations

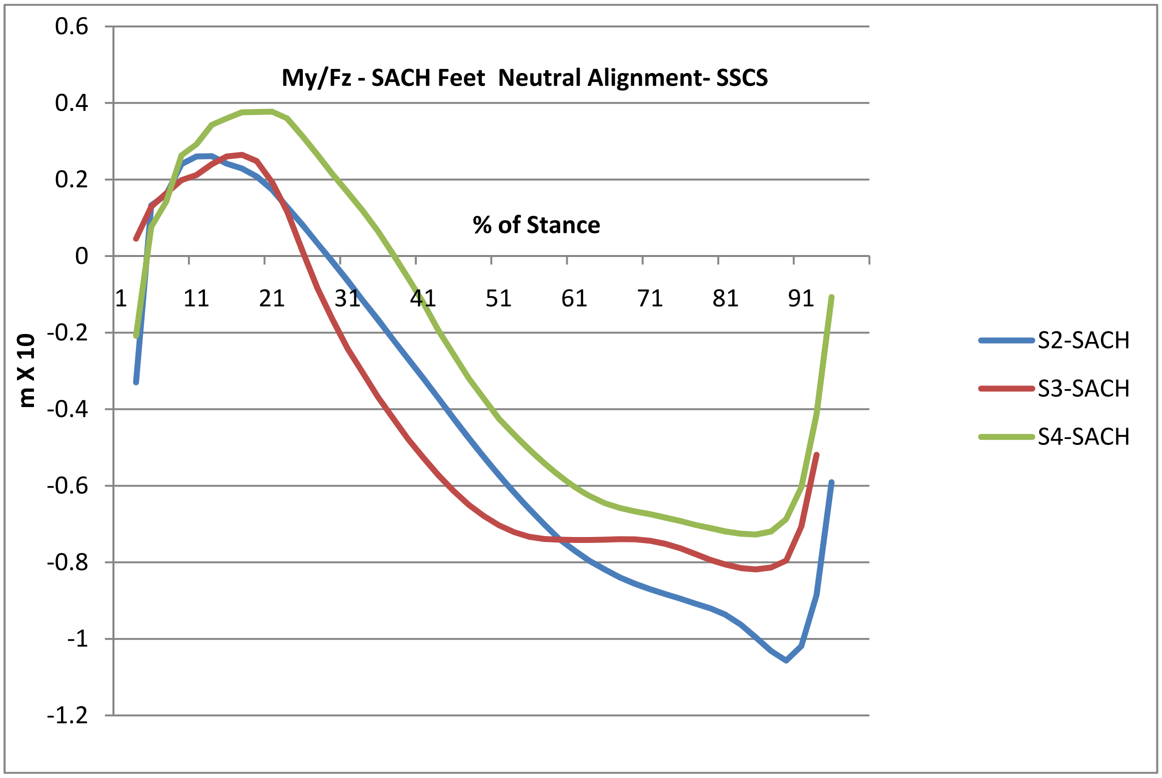

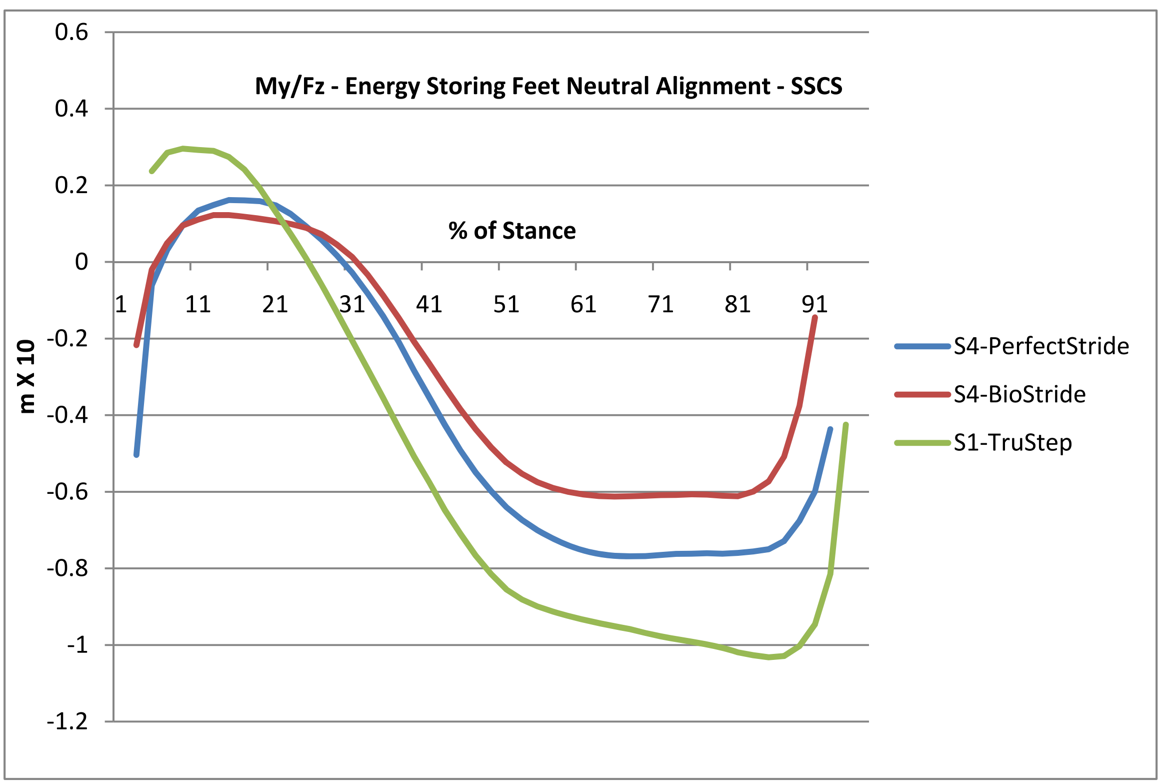

Figure 8-2. Grouped My/Fz Curves for SACH and Energy Storing Feet

Key Research Accomplishments

Key research accomplishments were as follows:

- Demonstration of how a commercially produced transducer (JR3) used in robotics can be adapted to measure the forces and moments that are generated by the residual limb inside a socket and transmitted to the pylon in response to the prosthetic components occurring below the socket, including the foot;
- Development of a portable, self-contained instrumentation package that allows the transducer to be used without the need to tether the amputee to non-mobile instrumentation for data collection
- Development of a GUI for a commercially produced transducer (JR3) that allows the forces and moments that occur immediately distal to the socket to be measured, processed, and exported in EXCEL- ready files in a format that allows statistical comparisons of feet and activities.
- Incorporation in the GUI of a capability for importing pressure measurements taken by Tekscan's F-Socket and producing exportable files in an EXCEL-ready format that allows integration of the pressure data with the transducer measurements so that models can be developed which estimate pressure as a function of the forces and moments, or so that pressures patterns can be compared
- Successful demonstration of the use of the transducer and GUI to compare feet, activities, and subjects for a convenience sample of transtibial amputees
- Successful demonstration of the use of the transducer, Tekscan F-Socket, and GUI to develop models of extremely high accuracy which estimate pressure inside the sockets of transtibial prostheses as a function of transducer measurements
- Examination of how the models of pressure vary across alignment perturbations, feet, and subjects
- Identification of level walking at a self-selected comfortable speed as the activity which best distinguishes between different feet when using forces and moments distal to the socket of a transtibial prosthesis
- Identification of the notch as being the region of the socket for which pressure is associated most logically and consistently with the design characteristics of the prosthetic foot
- Identification of the negative moment about the Y axis as the transducer measurement which most strongly influences pressure at the notch of a transtibial prosthesis and may possibly offer the most insight into the effect of alignment or foot type on gait outcomes
- Identification of the vertical force along the pylon, Fz, as being the variable with the most pervasive influence on intra-socket pressure in a transtibial prosthesis
- Development of a new way to measure foot performance for potential use in the clinic by utilizing the ratio of the moment about the Y axis of the transducer to the force along the direction of the pylon, My/Fz
- Development of a rapid method for measuring the alignment of a transtibial socket with inexpensive lasers that emphasizes the notch as the origin for describing socket location and angular alignment with respect to the foot.

Reportable Outcomes

At present, there are no reportable outcomes. Journal papers are yet to be written.

Conclusions

The research was successful in achieving the following goals:
1. Demonstrating how a commercially produced transducer can be adapted to provide new ways of measuring prosthetic foot and alignment performance in the clinic. The total hardware package for the system costs approximately $7,000. The system is also highly mobile. Because it is self-contained, it can be taken out of doors and into extreme environments. The normal activities of daily living use only about 25% of the loading capability of the transducer.
2. Development of a GUI which greatly reduces the work the user must undertake to utilize the transducer to develop data bases for further analysis of feet, activities, and subjects.
3. Development of a GUI which can be used to prepare data bases for modeling intra-socket pressures as a function of the forces and moments measured by the transducer distal to the socket.
4. Demonstrating the use of the transducer and GUI to evaluate and compare prosthetic feet, activities, and subjects in a manner not previously possible. The analyses show how that the feet, activities, and subjects vary with respect to the forces and moments transmitted to the socket. The measurements can take place anywhere a power outlet exists.
5. Development of highly accurate models of the relationship between the forces and moments measured by the transducer and intra-socket pressures.
6. Identification of a new performance measure that might assist in characterizing the performance of prosthetic feet and assist the clinician to better select and prescribe feet from among the wide and somewhat confusing variety of feet on the market.
7. Development of a way to measure the alignment of a transtibial prosthesis quickly and easily in a clinical setting.

The transducer provides data much less expensively than the traditional motion capture laboratory, and its low cost combined with the relative ease of using it in a clinical setting suggests that it may have great potential for bringing science into the clinic. It may, in fact, produce data more relevant to clinical practice in prosthetics than the motion capture laboratory. The data may give clinicians new insight into how amputees ambulate and use their prosthetic feet. It may lead to the development of new concepts and ways of organizing and interpreting the performance characteristics of the bewildering array of prosthetic feet on the market. These concepts and organizational strategies may lead to greater efficiency and cost savings, and better clinical decision-making.

Further R&D is needed to determine the clinical usefulness of the transducer measurements. The models of pressure provide good insight into the complex ways in which prosthetic feet influence the pressures that occur inside the socket during level walking at a self-selected comfortable speed, but the pressure measurements are very challenging to obtain. The research provided evidence that pressures at the notch of the socket may offer information on how effectively amputees are using specific types of prosthetic feet and how well the feet are aligned. Further research is needed to verify this. Socket angular perturbations were not examined, and experiments using the transducer should be designed and undertaken to examine this.

An important goal of R&D should be to improve pressure measurement technology. Improvements that are needed include development of sensors that are better able to resist the extreme pressure changes that occur at the brims of sockets, which break the fine electrical connections that lead from the individual sensors to the handle. If further research shows that notch pressure provides useful information on alignment and foot performance, then pressure sensors might be designed that measure only pressures at and around the notch, conform to the compound curves of the socket at this location, and do not break easily at the edge of the brim. An ability to place sensor leads under sleeves and inside gel liners without restricting the motion of the amputee at the knee would also be of benefit.

The GUI could be modified in ways which make it easier to use. If the system were to be made commercially available, the code would need to be reviewed and several improvements made. Work is currently underway to find ways to better organize the pressure data and produce output files. One suggested area of improvement would be to develop an algorithm and code for automatically identifying the beginning and ending points of steps within the GUI. The procedures followed in this study (Chapter 3) could be used as a model.

The subjective measurements produced mixed results. Some findings were consistent with the pressure measurements and some were not. It is noted that subjective measurements had a low priority compared to collecting data from the transducer and pressure sensors during the experiment. The subjective measurements taken during the experiments tended to occur within a context where the primary concern made visible to the subjects was obtaining the data from the pressure sensors and the transducer for different activities, feet, and perturbations. To collect good subjective data, experiments would need to be designed with the collection of subjective data as the primary goal. The experiments would need to take into account the psychological fatigue that can result from repeated requests to make subjective judgments about pressure sensation.

A convenience sample of only four subjects was utilized. To provide strong evidence for many of the preliminary findings of this study, more subjects are needed, and they should be selected to meet whatever criteria are relevant to the hypotheses of the study. For example, a study to compare two feet might use ten or twenty subjects and limit the activities to level walking at a self-selected comfortable speed or walking up and down a ramp. Two alignment perturbations might be examined in addition to the neutral alignment, with no pressure measurements being taken.

In summary, the project can be viewed as highly successful. It achieved all the goals of the proposal with one exception: it was not tested in a true clinical setting. This does not detract from the overall contribution of the work. The research identified new approaches to measuring the performance of prosthetic components below the socket and demonstrated how the measurements can be undertaken and analyzed. Clinical application need not be far in the future if research similar to that suggested in the previous paragraph is undertaken.

References

1. Andres RO, Stimmel SK. Prosthetic alignment effects on gait symmetry: a case study. *Clinical Biomechanics* 1990:5, p88-96.

2. Berme N, Purdey CR, Solomonidis SE. Measurement of prosthetic alignment. *Prosthet Orthot Int.* 1987:2 p73-75.

3. Beyaert C, Grumiller C, Martinet N, Paysant J, Andre J-M. Compensatory mechanism involving the knee joint of the intact limb during gait in unilateral below-knee amputees. *Gait & Posture*. 2008:

4. Breakey JW. Theory of integrated balance: the lower limb amputee. *J Prosthet Orthot*. 1998:10 p42-44.

5. Blumentritt S. A new biomechanical method for determination of static prosthetic alignment. *Prosthet Orthot Int*. 1997:21 p107-113.

6. Blumentritt S, Schmalz T, Jarasch R, Schnieder M. Effects of sagittal plane prosthetic alignment on standing trans-tibial amputee knee loads. *Prosthet Orthot Int*. 1999:23 p231-238.

7. Burnfield JM, Bontrager MS, Boyd LA, Rao SS, Mulroy SJ, Gronley JK, Perry J. Effect of prosthetic malalignment on EMG and intra-socket pressures in an individual with a transtibial amputation. *Gait & Posture*. 1999:9 p137-138.

8. Chow DHK, Holmes AD, Lee CKL, Sin SW. The effect of prosthesis alignment on the symmetry of gait in subjects with unilateral transtibial amputation. *Prosthet Orthot Int*. 2006:30 p114-128.

9. Fang L, Xiaohong J, Wang R. Modeling and simulation of muscle forces of trans-tibial amputee to study effect of prosthetic alignment. *Clin Biomech*. 2007:22 p1125-1131.

10. Fridman A, Ona I, Isakov E. The influence of prosthetic foot alignment on trans-tibial amputee gait. *Prosthet Orthot Int*. 2003:27 p17-22.

11. Geil MD, Lay A. Plantar foot pressure responses to changes during dynamic trans-tibial prosthetic alignment in a clinical setting. *Prosthet Orthot Int*. 2004:28 p105-114.

12. Hannah RE, Morrison JB, Chapman AE. Prosthesis alignment: effect on gait of persons with below-knee amputations. *Arch Phys Med Rehabil*. 1984:65 p159-162.

13. Hansen AH, Childress DS, Knox EH. Prosthetic foot roll-over shapes with implications for alignment of trans-tibial prostheses. *Prosthet Orthot Int*. 2000:24 p205-215.

14. Hansen AH, Meier MR, Sam M, Childress DS, Edwards ML. Alignment of trans-tibial prostheses based on roll-over shape principles. *Prosthet Orthot Int*. 2003:27 p89-99.

15. Hansen AH, Childress D. Effects of adding weight to the torso on roll-over characteristics of walking. *J Rehab Res Dev*. 2005:42 p381-390.

16. Hobson DA. A powered aid for aligning the lower-limb modular prosthesis. *Bull Pros Res*. 1972:10 p159-163.

17. Isakov E, Mizrahi J, Susak Z, Ona I, Hakim N. Influence of prosthesis alignment on the standing balance of below-knee amputees. *Clin Biomech*. 1994:9 p258-262.

18. Kerr G, Saleh M, Jarrett MO. An angular alignment protractor for use in the alignment of below-knee prostheses. *Prosthet Orthot Int*. 1984:8 p56-57.

19. Klute GK, Berge JS, Orendurff MS, Williams RM, Czerniecki JM. Prosthetic intervention effects on activity of lower-extremity amputees. *Arch Phys Med Rehabil*. 2006:87 p717-722.

20. Lin M-C, Wu Y-C, Edwards M. Vertical alignment axis for transtibial prostheses: a simplified alignment method. *J Formosa Med Assoc*. 2000:99 p 39-44.

21. Mizrahi J, Susak Z, Seliktar R, Najenson T. Alignment procedure for the optimal fitting of lower limb prostheses. *J Biomed Eng*. 1986:8 p229-234.

22. Ozyalcin H, Yorulmazel Z, Sesli E. Role of pedography in manufacturing and rehabilitation of lower extremity prostheses. *Gait & Posture*. 1994:2 p241-242 & p249-250.

23. Pearson JR, Holmgren G, March L, Oberg K. Pressures in critical regions of the below-knee patellar-tendon-bearing prosthesis. *Bull Prosth Res*. 1973:10 p52-76.

24. Pinzur MS, Cox W, Kaiser J, Morris T, Padwardham A, Vrbos L. The effect of prosthetic alignment on relative limb loading in persons with trans-tibial amputation: a preliminary report. *J Rehab Res Dev*. 1995:32 p373-378.

25. Reed RD, Sanders JE, Marks RJ. Neural network aided prosthetic alignment. *Proc IEEE International Conference on Systems, Man and Cybernetics; Intelligent Systems for the 21st Century*, Vancouver, BC, Oct 22-25, 1995. 1995 p505-508.

26. Reisinger KD, Casanova H, Wu Y, Moorer C. Comparison of a priori alignment techniques for transtibial prostheses in the developing world – a pilot study. *Disab & Rehabil*. 2007:29 p863-872.

27. Reynolds DP, Lord M. Interface load analysis for computer-aided design of below-knee prosthetic sockets. *Med Biol Eng Comput*. 1992:30 p419-426.

28. Rossi SA, Doyle W, Skinner HB. Gait initiation of persons with below-knee amputation: the characterization and comparison of force profiles. *J Rehabil Res Dev*. 1995:32 p120-127.

29. Saleh M, Bostock S. An aid to alignment in the below-knee amputee. *J Bone Joint Surg*. 1988:70B p497.

30. Sanders JE, Daly CH, Boone DA, Donaldson TF. An angular alignment measurement device for prosthetic fitting. *Prosthet Orthot Int*. 1990:14 p143-144.

31. Sanders JE, Daly CH, Burgess EM. Clinical measurement of normal and shear stresses on a trans-tibial stump: characteristics of wave-form shapes during walking. *Prosthet Orthot Int*. 1993:17 p38-48.

32. Sanders JE, Daly CH, Burgess EM. Interface shear stresses during ambulation with a below-knee prosthetic limb. *J Rehabil Res Dev*. 1992:29 p1-8.

33. Sanders JE, Daly CH, Cummings WR, Reed RD, Marks RJ. A measurement device to assist amputee prosthetic fitting. *J Clin Eng*. 1994:19 p63-71.

34. Sanders JE, Miller RA, Berglund DN, Zachariah SG. A modular six-directional force sensor for prosthetic assessment: a technical note. *J Rehab Res Dev*. 1997:34 p 195-202.

35. Sanders JE, Bell DM, Okaumura RM, Dralle AJ. Effects of alignment changes on stance phase pressures and shear stresses on transtibial amputees: measurements from 13 transducer sites. *IEEE Trans Rehab Eng*. 1998:6 p21-31.

36. Sanders JE, Daly CH. Interface pressures and shear stresses: sagittal plane angular alignment effects in three trans-tibial amputee case studies. *Prosthet Orthot Int*. 1999:23 p21-29.

37. Schmalz T, Blumentritt S, Jarasch R. Energy expenditure and biomechanical characteristics of lower limb amputee gait: the influence of prosthetic alignment and different prosthetic component. *Gait & Posture*. 2002:16 p255-263.

38. Seliktar R, Mizrahi J, Susak Z. Computer aided dynamic alignment of below knee prostheses. *Proceedings of the IFIP-IMIA Working Conference on the Use of Computers in Aiding the Disabled*, Hiafa, Israel,. 1981: p87-97.

39. Silver-Thorn MB, Childress DS. Generic, geometric finite element analysis of the transtibial limb and prosthetic socket. *J Rehab Res Dev*. 1997:34 p171-186.

40. Silver-Thorn MB, Steege JW, Childress DS. A review of prosthetic interface stress investigations. *J Rehab Res Dev*. 1996:33 p253-266.

41. Seelen HAM. Effects of prosthesis alignment on pressure distribution at the stump/socket interface in transtibial amputees during unsupported stance and gait. *Clin Rehabil*. 2003:17 p787-796.

42. Sin SW, Chow DHK, Cheng JCY. Significance of non-level walking on transtibial prosthesis fitting with particular reference to the effects of anterior-posterior alignment. *J Rehab Res Dev*. 2001:38 p1-6.

43. Sin SW, Chow DHK, Cheng JCY. A new alignment jig for quantification and prescription of three-dimensional alignment for the patellar-tendon bearing trans-tibial prosthesis. *Prosthet Orthot Int*. 1999:23 p225-230.

44. Summers GD, Morrison JD, Cochrane GM. Foot loading characteristics of amputees and normal subjects. *Prosthet Orthot Int*. 1987:11 p33-39.

45. van Velzen JM, Houdijk H, Polomski W, van Bennekom CAM. Usability of gait analysis in the alignment of trans-tibal prostheses: a clinical study. *Prosthet Orthot Int*. 2005:29 p255-267.

46. Winarski DJ, Pearson JR. Least-squares matrix correlations between stump stresses and prosthesis loads for below-knee amputees. *Trans of the ASME J Biomech Eng*. 1987:109 p238-246.

47. Winarski DJ, Pearson JR. Analytical description of minimum energy expenditure surfaces. *Trans of the ASME J Biomech Eng*. 1988:110 p386-391.

48. Winter DA, Sienko SE. Biomechanics of below-knee amputee gait. *J Biomech*. 1988:21 p361-367.

49. Xiaobing L, Xiaohong J, Peng D, Lidan F. Influence of shoe-heel height of the trans-tibial prosthesis on static standing biomechanics. *Proc 2005 IEEE Engineering in Medicine and Biology 27th Annual Conference*, Shanghai, China, Sept 1-4. 2005: p5227-5229.

50. Xiaohong J, Xiaobing L, Peng D, Ming Z. The influence of dynamic trans-tibial prosthetic alignment on standing plantar foot pressure. *Proc 2005 IEEE Engineering in Medicine and Biology 27th Annual Conference*, Shanghai, China, Sept 1-4. 2005: p6916-6918.

51. Zahedi MS, Spence WD, Solominidis SE, Paul JP. Alignment of lower-limb prostheses. *J Rehab Res Dev*. 1986:23 p2-19.

52. Zhang M, Turner-Smith AR, Tanner A, Roberts VC. Clinical investigation of the pressure and shear stress on the transtibial stump with a prosthesis. *Med Eng & Physics*. 1998:20 p188-198.

53. Parker K, Naumann S, Morris A, Cribbs D. Effects of trans-tibial amputee alignment changes on dynamic socket loads. *Gait & Posture*. 1999:9 p135-136.

54. Zahedi MS, Spence WD, Solomonidis SE, Paul JP. Repeatability of kinetic and kinematic measurements in gait studies of the lower limb amputee. *Prosthet Orthot Int*. 1987:11 p55-64.

55. Berme N, Lawes P, Solomonidis S, Paul JP. A shorter pylon transducer for measurement of prosthetic forces and moments during amputee gait. *Engineering Medicine*. 1975:4 p6-8.

56. American Academy of Orthotists and Prosthetists. State-of-the-Science Evidence Report Guidelines.

57. Kapp SL. "Visual analysis of prosthetic gait." In *Atlas of Amputations and Limb Deficiencies*, 3rd ed,, (Smith D, Michael JW, Bowker JH, editors). American Academy of Orthopedic Surgeons. Rosemont, IL. 2004: Chapt 31, p385-394.

58. Kerr G, Saleh M, Jarrett MO. An angular alignment protractor for use in the alignment of below-knee prostheses. *Prosthet Orthot Int*. 1984:8 p56-57.

59. Neumann ES. Measurement of socket discomfort – Part II: signal detection. *J Prosthet Orthot*. 2001:13 p111-122.

60. Hansen AH, Sam M, Childress DS. The effective foot length ratio: a potential tool for characterization and evaluation of prosthetic feet. *J Prosthet Orthot*. 2004:16 p 41-45.

61. Neumann ES. State-of-the-Science Review of Transtibial Prosthesis Alignment Perturbations. *J Prosthet Orthot*. 2009:21 (4) p174-193.

61. Gard SA, Childress DS. What determines the vertical displacement of the body during normal walking. *J Prosthet Orthot.* 2001:13 p64-67.

62. Miller LA, Childress DS. Analysis of a vertical compliance prosthetic foot. *J Rehabil Res Dev*. 1997:34(1) p 52-57.

63. Nielsen DH, Shurr DG, Golden JC, Meier K. Comparison of energy cost and gait efficiency during ambulation in below-knee amputees using different prosthetic feet – a preliminary report. *J Prosthet Orthot*. 1989:1 p 24-31.

64. Powers CM, Boyd LA, Torburn L, Perry J. Stair ambulation in persons with transtibial amputation: An analysis of the Seattle Light Foot. *J Rehabil Res Dev*. 1997:34 p 9-18.

65. Torburn L, Schweiger GP, Perry J, Powers CM. Below knee amputee gait in stair ambulation. *Clin Orthop*. 1994:303 p 185-192.

66. Yack HJ, Nielson DH, Shurr DG. Kinetic patterns during stair ascent in patients with transtibial prostheses using three different prostheses. *J Prosthet Orthot*. 1999: 11 p 57-62.

67. MacFarlane PA, Nielson DH, Shurr DG. Gait comparisons for below-knee amputees using a Flex-Foot versus a conventional prosthetic foot. *J Prosthet Orthot*. 1991: 3 p 150-161.

68. Hafner BJ, Sanders JE, Czerniecki J, Fergason J. Energy storage and return prostheses: does patient perception correlate with biomechanical analysis? *Clin Biomech*. 2002:17 p 325-344.

69. Kirtley C. *Clinical Gait Analysis Theory and Practice*. Churchill Livingstone, Elsevier, Edinburgh, 2006.

70. Neumann ES, Wong JS, Drollinger RL. Concepts of pressure in an ischial containment socket: perception. *J Prosthet Orthot*. 2005: 17 p 12-20.

71. Borg G. *Borg's Perceived Exertion and Pain Scales*. Human Kinetics, Champaign, 1998.

72. Gesheider GA. *Psychophysics, 3rd ed*. Lawrence Erlbaum, Mahwah, 1997.

.

APPENDIX A - GUI DESIGN AND OPERATION

Logic Chart

This chapter explains, by means of a flowchart which is shown below, the steps involved in processing the transducer and Tekscan pressure data. The flowchart explains the step by step calculation of the various parameters obtained from the raw transducer data. The flowchart depicts the logic behind the code, and a similar logic was used to process both transducer and Tekscan pressure sensor data. This chapter also explains use of the software in terms of the sequence of steps to be followed. A sample data file is used.

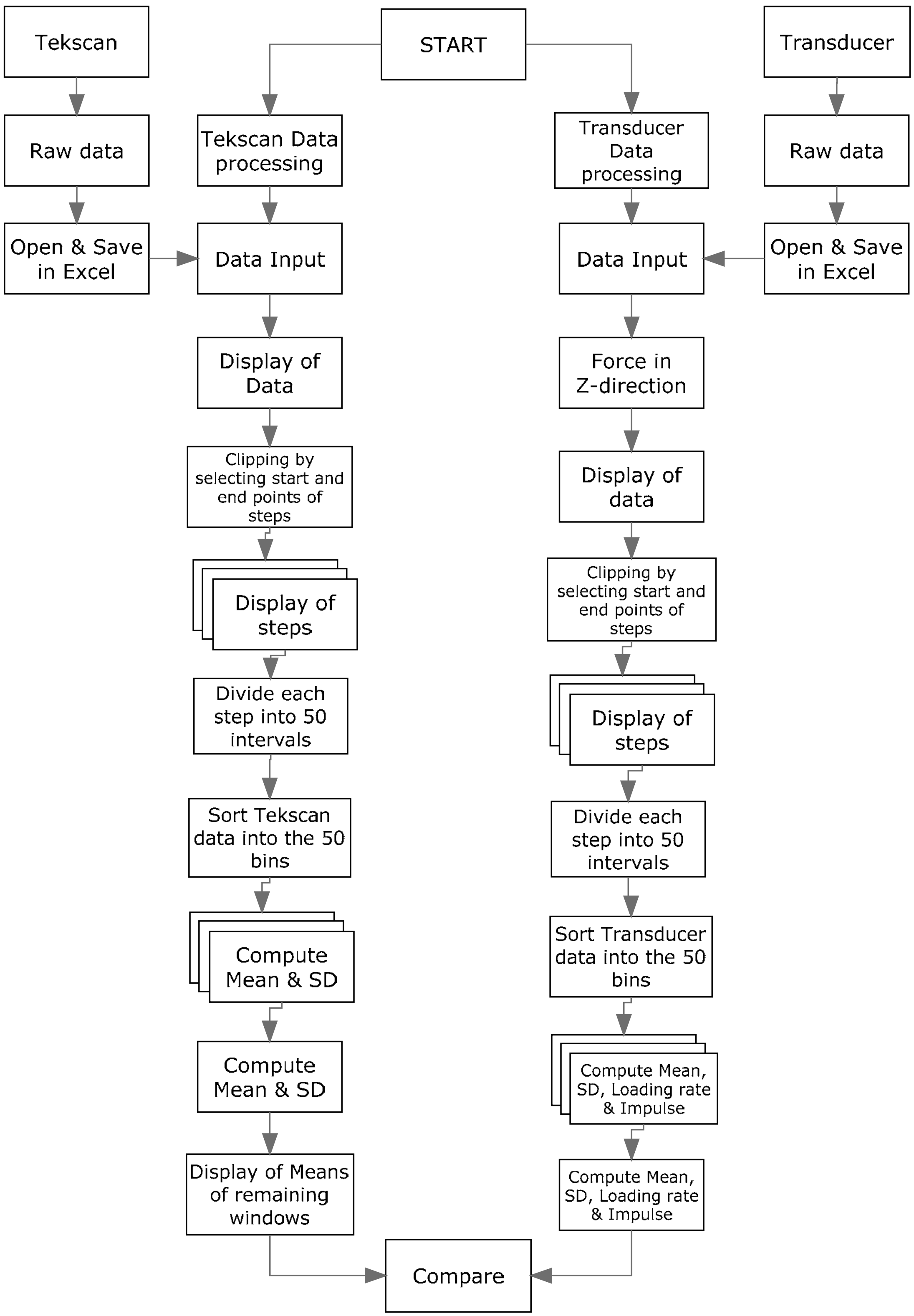

GUI Displays

This section explains the step by step procedure for using the software and obtaining the GUI displays. The text also explains how the various programs, imported files, and exported files are named and located.

The GUI itself is inside the **GUI** folder. To use the GUI on a new installation, the first requirement is to install the **MCRInstaller.exe** on the computer in which the GUI will be used. Data files from the transducer and pressure sensors will be in a format other than Excel. For the GUI to import these data successfully, the users must convert them to Excel format and save them in Excel format. When saving the transducer files in Excel format, users have to select **delimited**, then mark **space**, then click **finish** and save it in the **GUI** folder. To get the pressure data from the socket window location the Tekscan software has to be used. This is explained in the Tekscan manuals. For saving pressure sensor data files in Excel format after windowing, the user has to select **Delimited**, then **comma**, and then **finish** and save it in the **GUI** folder. After saving data files in the Excel format in the **GUI** folder the display should appear as follows:

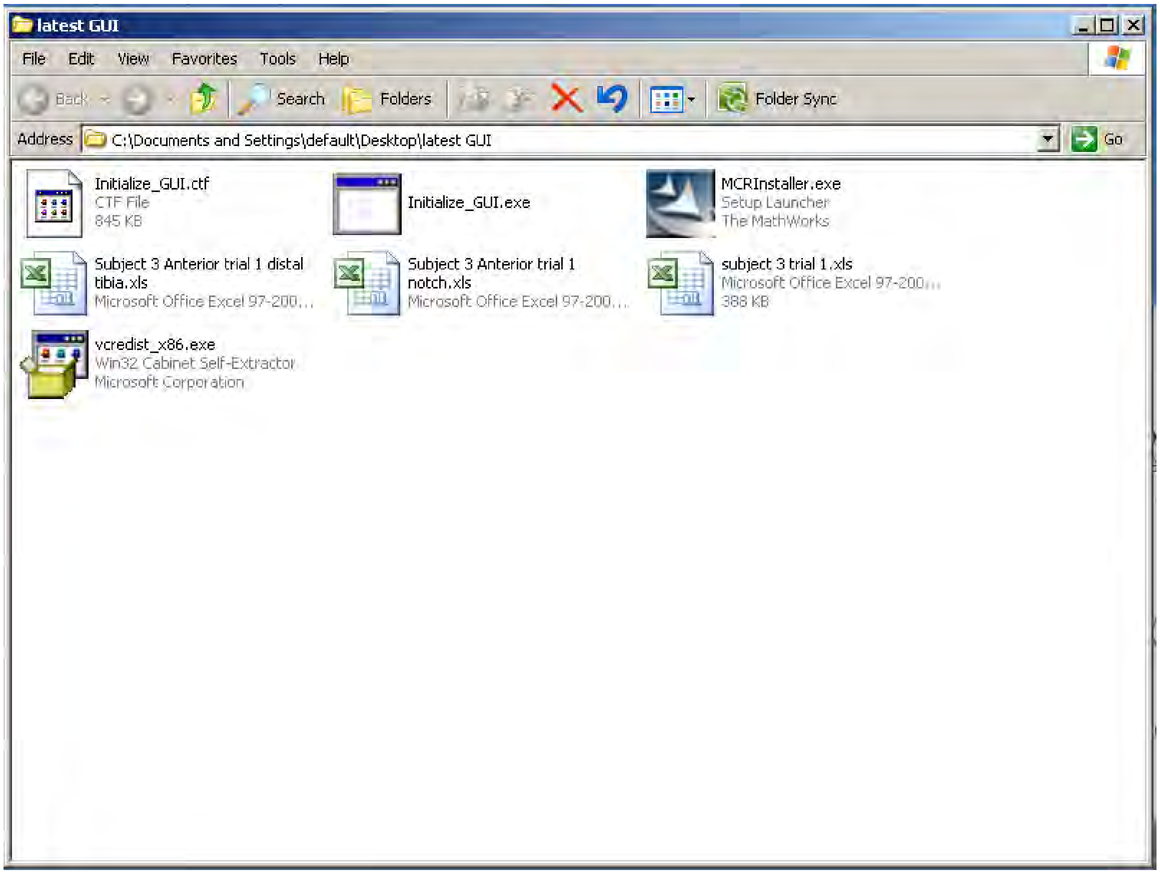

From the **GUI** folder the user has to double click on the **Initialize_GUI.exe** button to start the GUI. Then the following window will open. In this window the user has to enter the folder name into which all exported files from the GUI are to be saved.

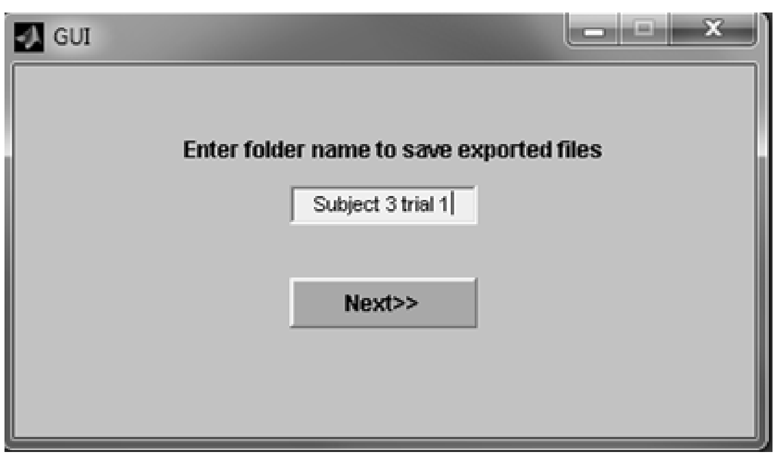

After entering the folder name the user needs to click on the **Next>>** option to go onto the following window. Here the user has to enter the side on which the prosthetic foot is located (right or left) and the weight of the subject in English pounds.

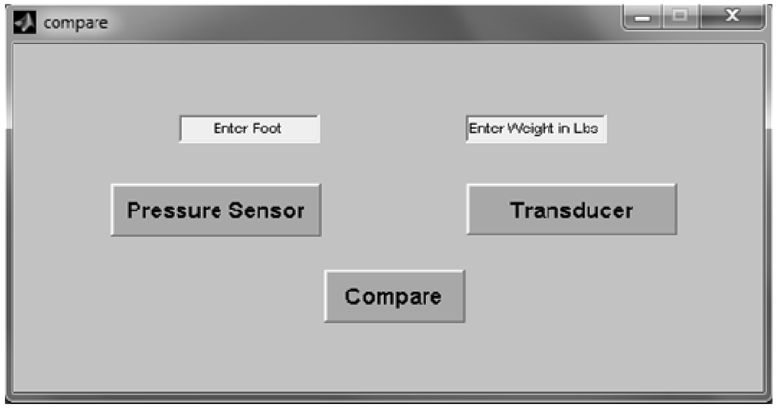

This window has three more options displayed- Pressure Sensor, Transducer and Compare. The **Pressure Sensor** option will take the user to the portion of the software in which the pressure data can be analyzed, The **Transducer** option will take the user to windows which can be used to analyze the transducer data, and the **Compare** option will compare both the transducer and pressure sensor data. First, the user has to select either **Pressure Sensor** or **Transducer** to analyze the corresponding data and only when both have been processed can the user select **Compare** for comparing the data from the two sources. Below is shown how the screen should appear for a subject weighing 159 lbs when the prosthetic foot is on the left leg.

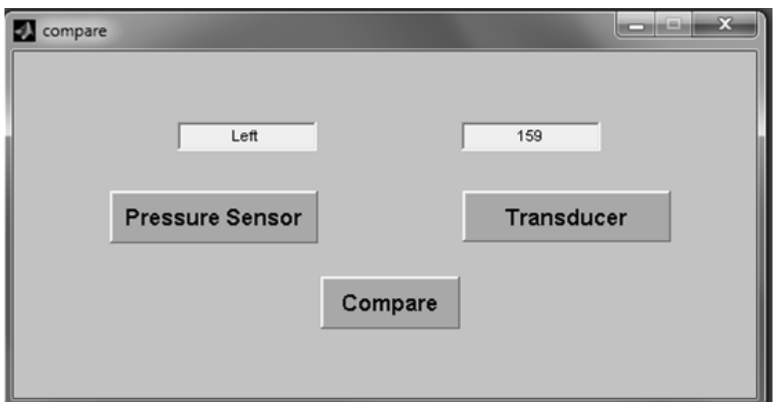

When the **Transducer** option is been selected the following window then appears.

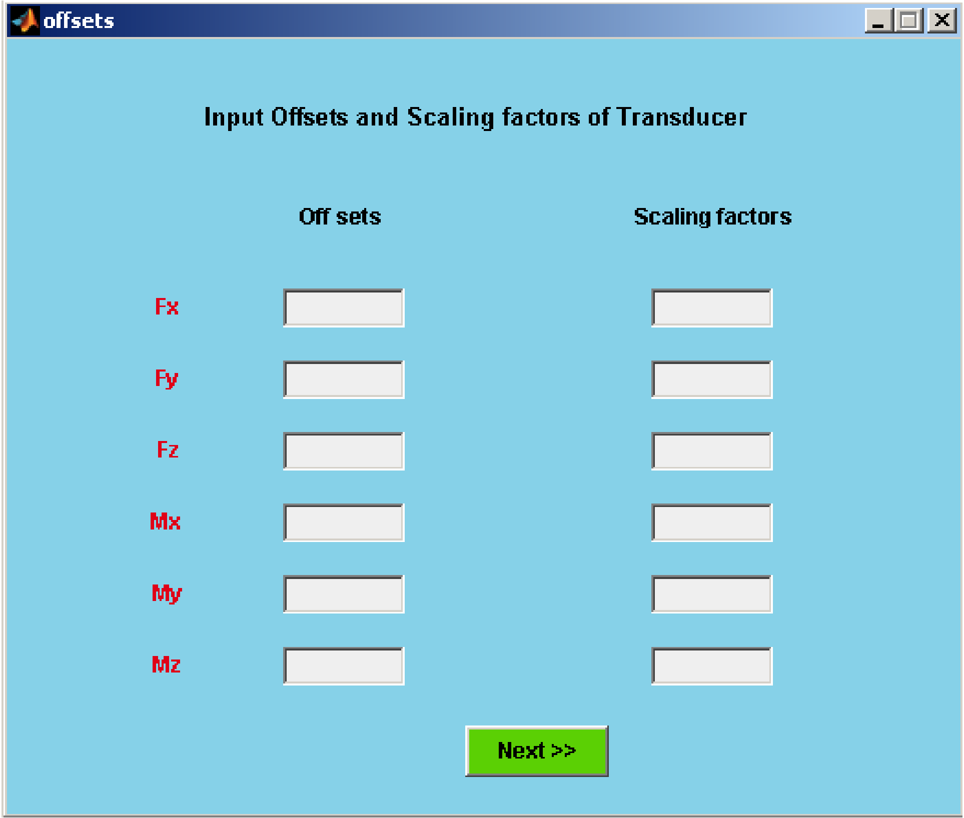

This window has text boxes for feeding the software with the transducer offsets and scaling factors for all three directions. Below is shown how the screen should appear after entering all scaling factors and offsets. These scaling factors and offsets are for the transducer used in this research.

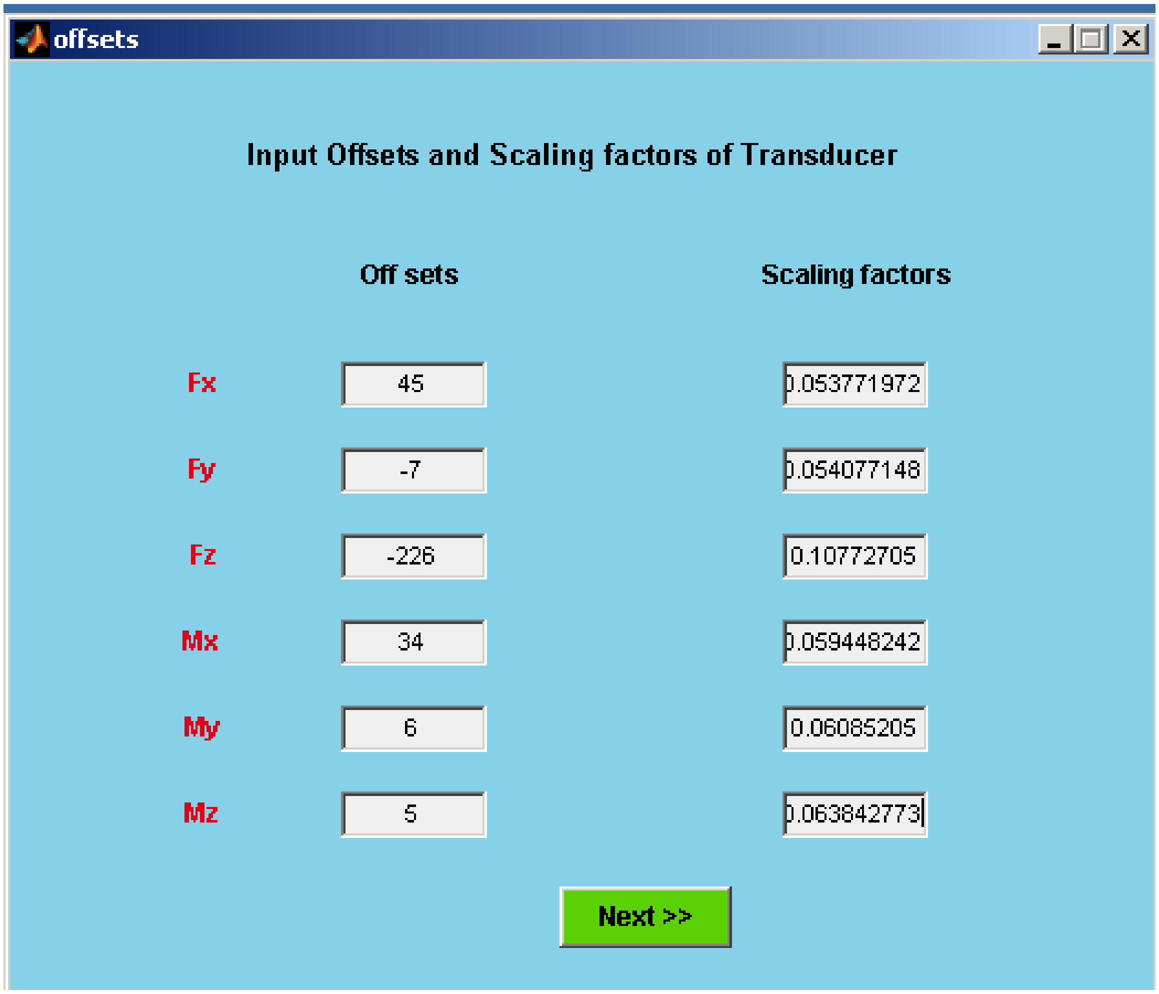

When the **Next** option is been selected the following window then appears.

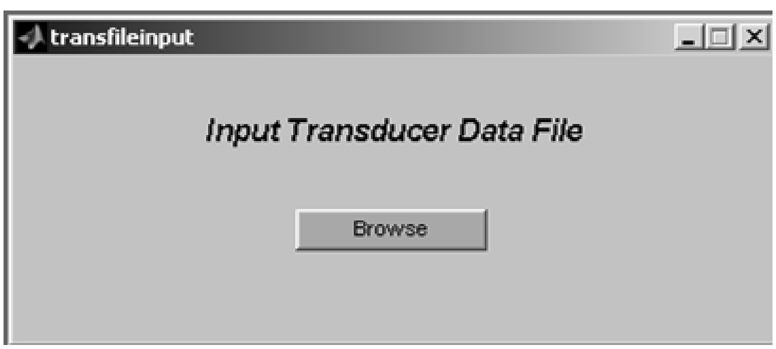

After clicking on the **Browse** button in this window, the following window will open. This window is used to select the transducer data file to be analyzed from the GUI folder.

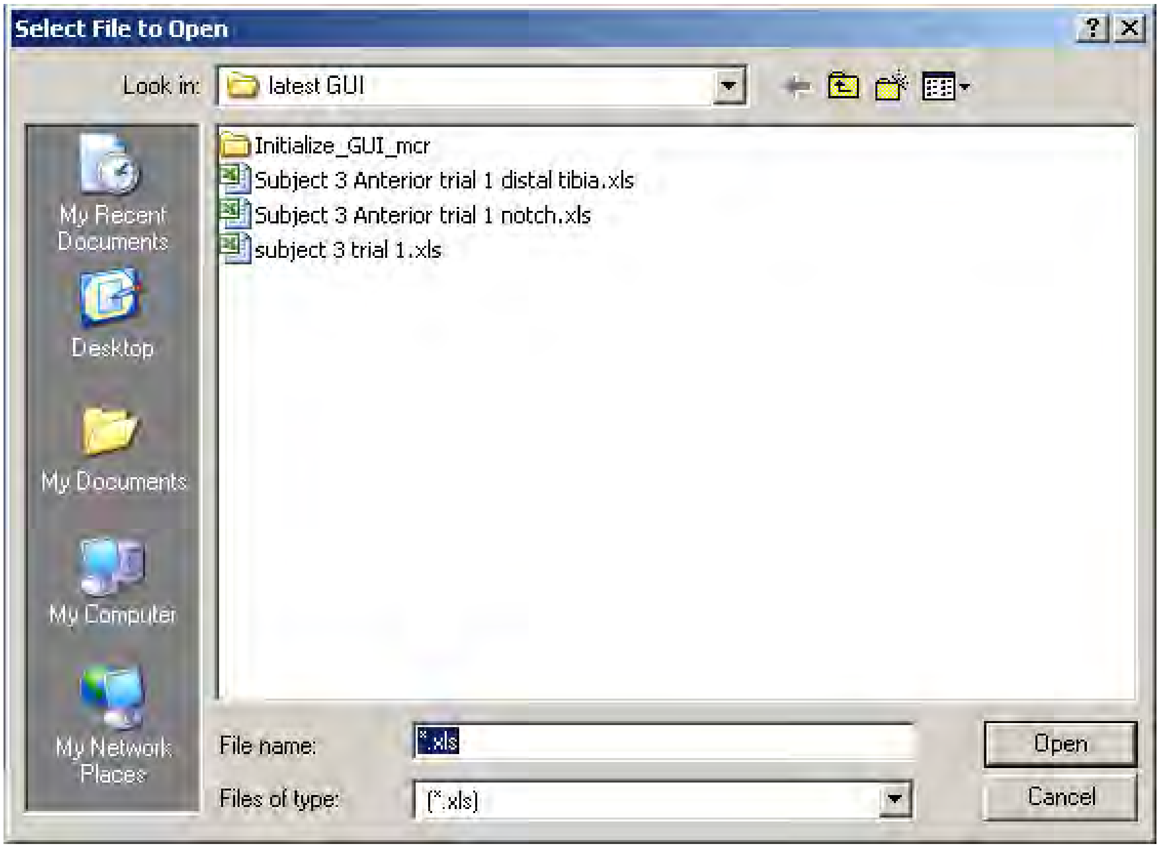

After selecting the transducer data file, **"subject 3 trial 1.xls"** in this case, the following window pops up:

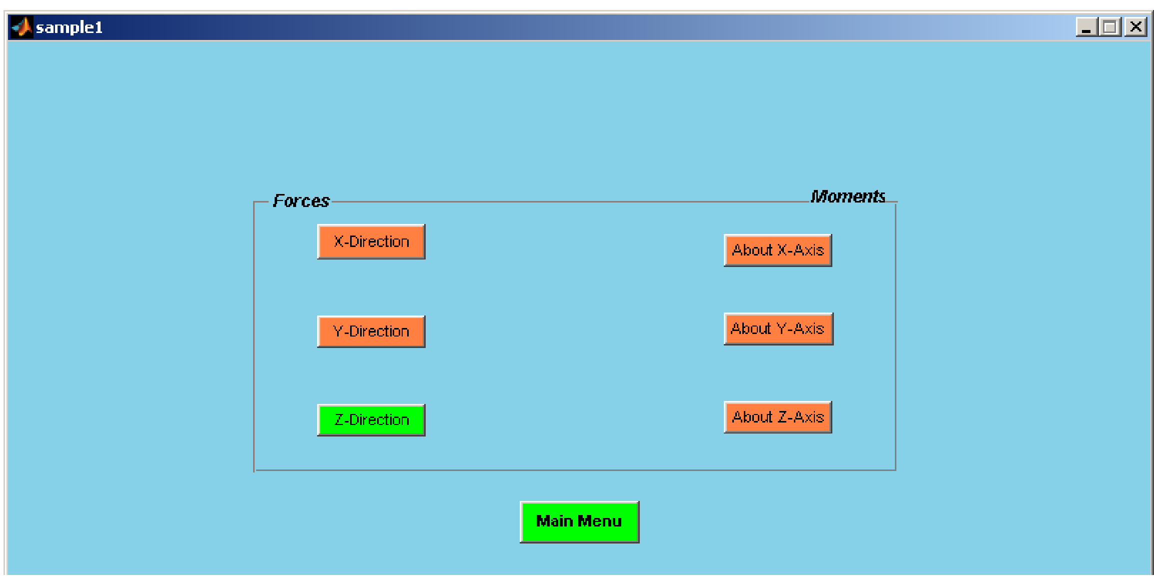

Initially the user can only select the **Z-Direction** under **Forces** to define individual steps. If the user selects other than the **Z-Direction** the GUI will ask the user to go back and select the **Z-Direction**. Selecting the **Z-Direction** will allow the user to select ten good steps to be analyzed from the trial, which frequently will consist of more than ten steps. [It is recommended that at least fifteen steps be recorded excluding steps that are different from the intended activity, such as turning around at the end of a corridor] Selecting the **Z-Direction** will open the following window which is used for identification of no more than 10 good steps for analysis. In this window the user has to enter the number of steps to be analyzed and the sampling rate of the transducer in the corresponding text boxes. This window requires the user to select the start and end points of the 10 good steps by visual inspection. The user can utilize the **Zoom in** and **Zoom out** options located in the toolbar on upper left hand side of the window to place a window on the screen around the trace of the transducer data and magnify or diminish the data for inspection. The **Data cursor** option in the same tool bar can be used for finding the x-coordinates of the data. These x coordinate data are used to define to the start and end points of each of the ten steps.

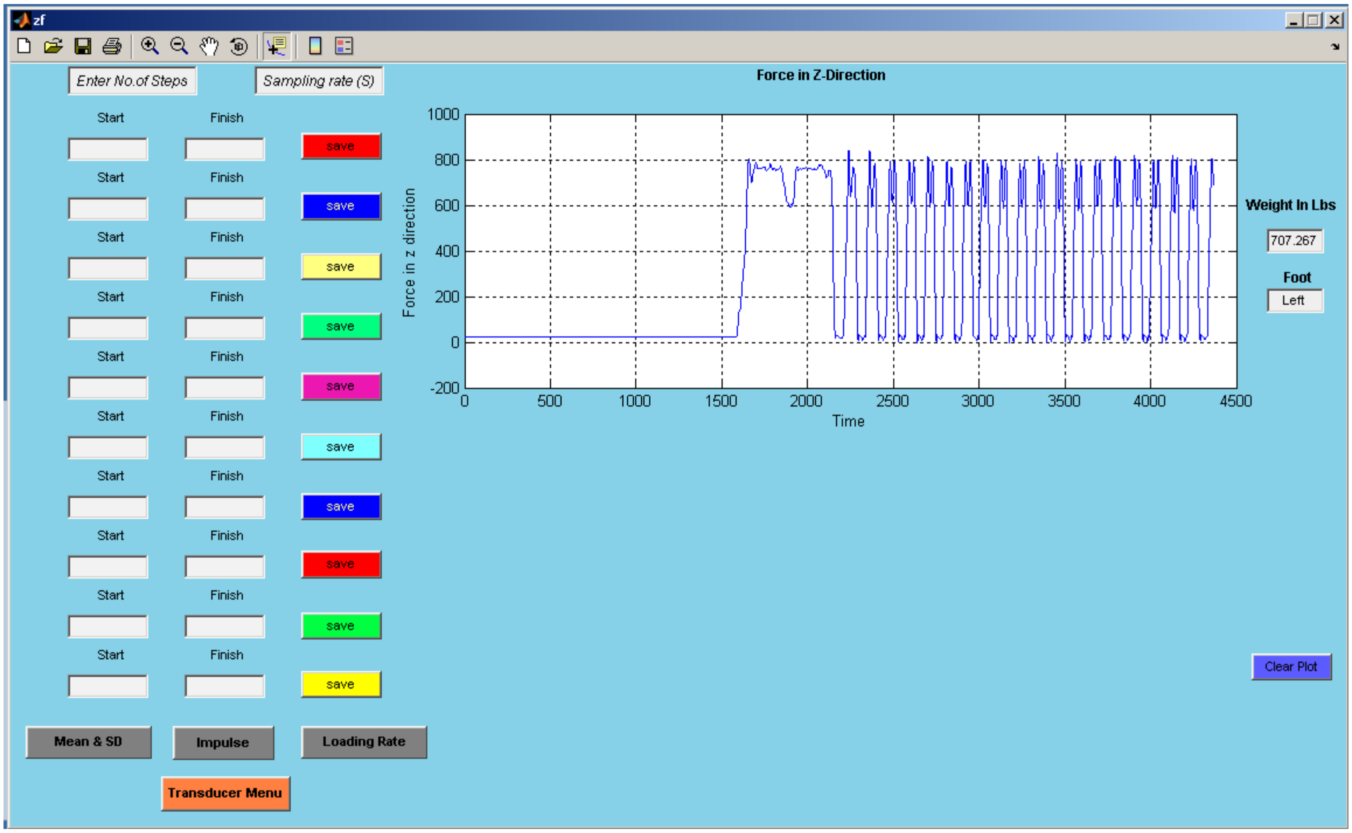

After Zooming in and using the **Data cursor**, the window can be made to look like the following display:-

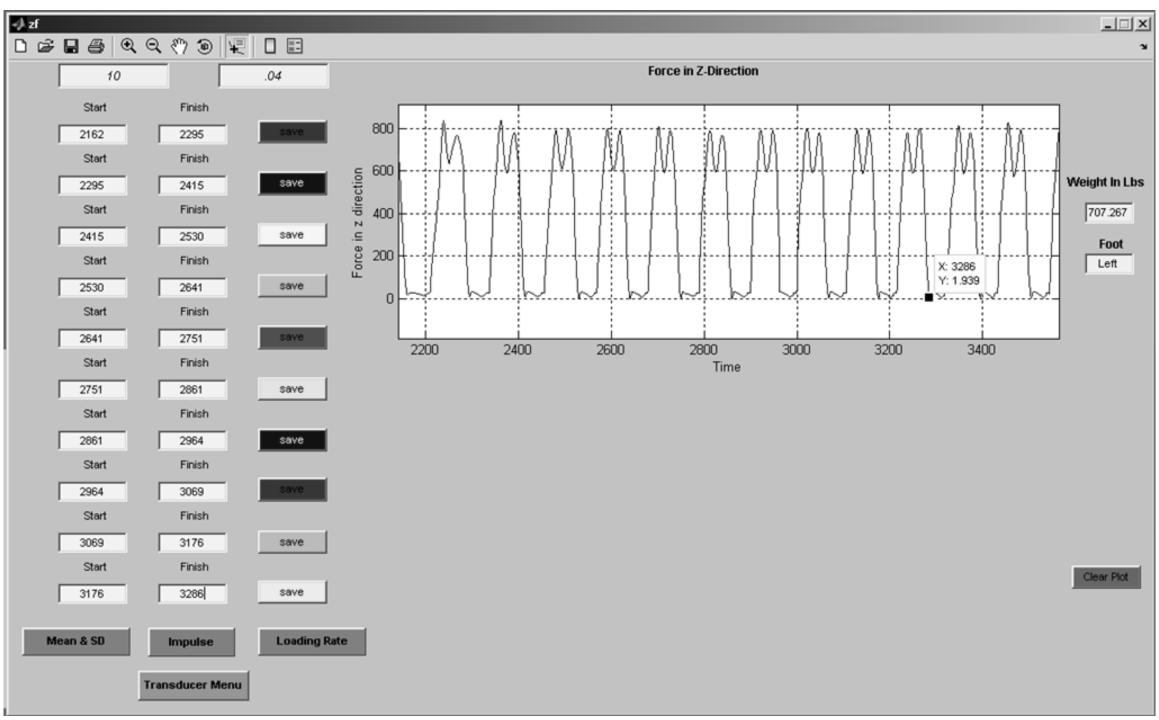

After entering the start and end points of the 10 good steps into the corresponding text boxes and clicking the respective save buttons the GUI will plot the gait cycle for the step below the main plot. The curve for each of the ten steps will be the same color as the **Save** button. The data for each single step is then sorted into 50 bins and the mean for each bin is plotted in the second plot as shown below:

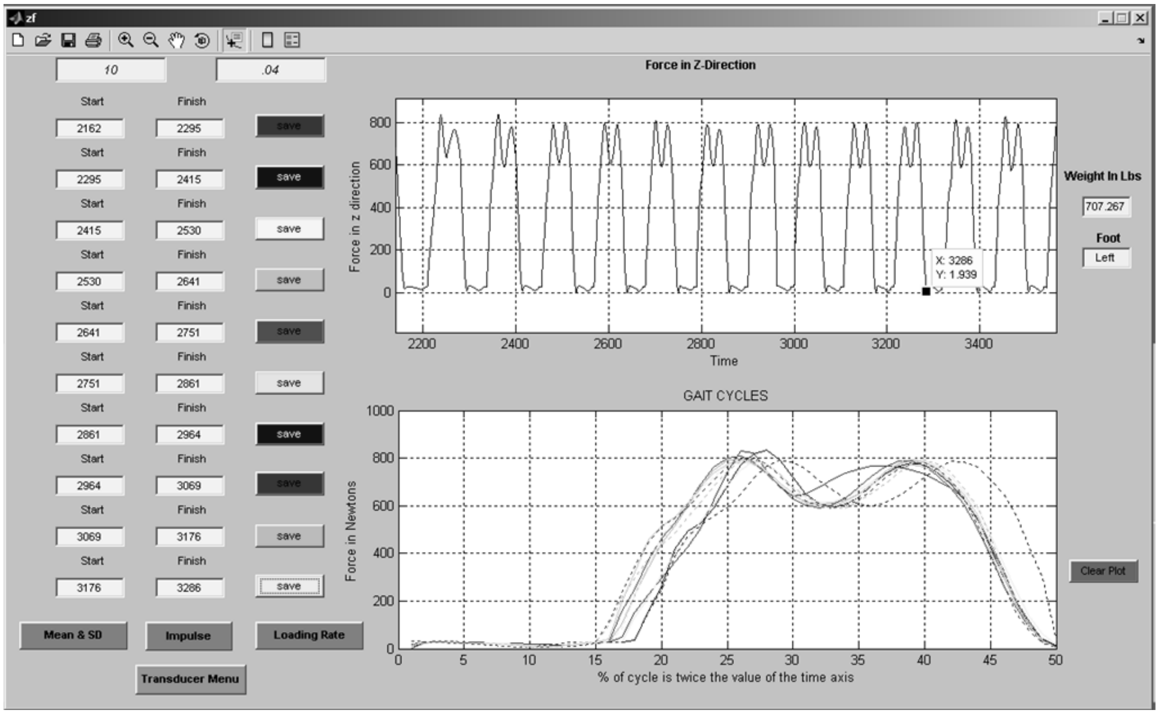

For analysis of the gait cycles, the Mean and Standard Deviations for each of the 50 intervals is computed over the ten steps by the GUI. For calculation of the means and standard deviations over the steps, the user has to click on the corresponding **Mean & SD** button at the left hand bottom of the window. The following window pops up after selecting **Mean & SD**:-

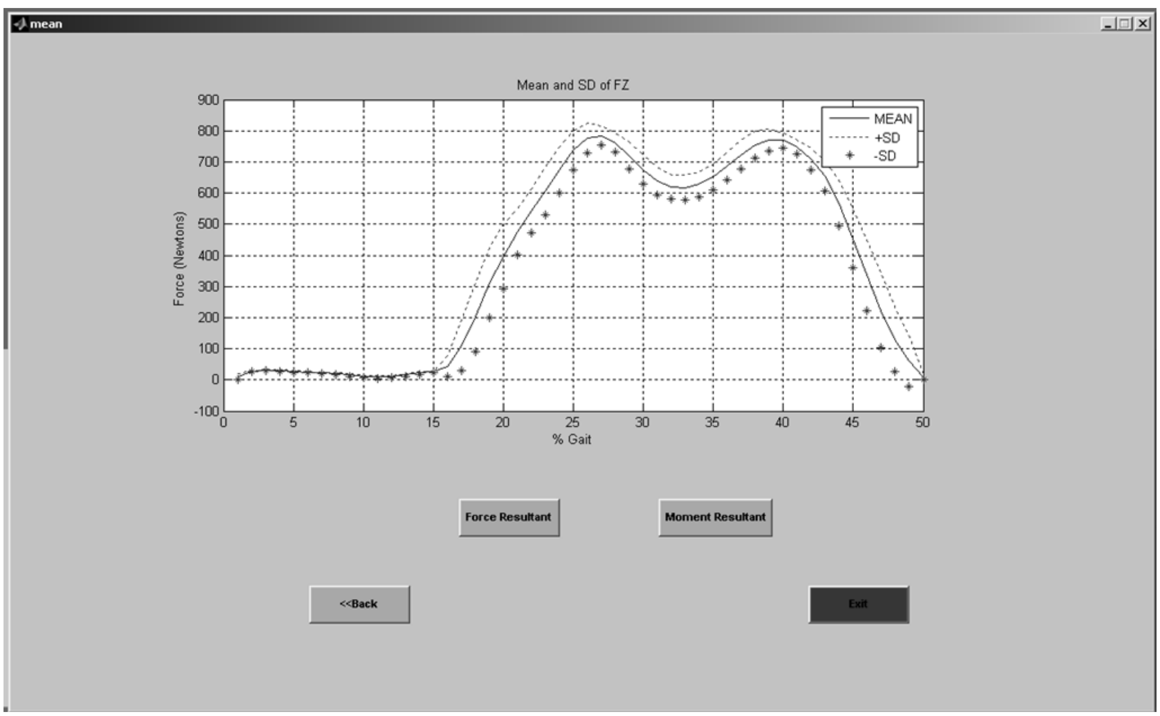

The options on this window include **Force Resultant**, **Moment Resultant**, **Back** and **Exit,** each of which takes the user to the next box. **Exit** will exit the GUI, **Back** takes the user back to the previous window, **Force Resultant** will plot the resultant of forces in X,Y,Z directions and **Moment Resultant** will plot the resultant of moments in the X,Y,Z directions. Force and Moment resultants can be obtained only after analyzing all the forces and moments along three axes. So at this time, having processed only the force along the Z axis, only the **Back** button can be used. After clicking the **Back** button the following window appears:-

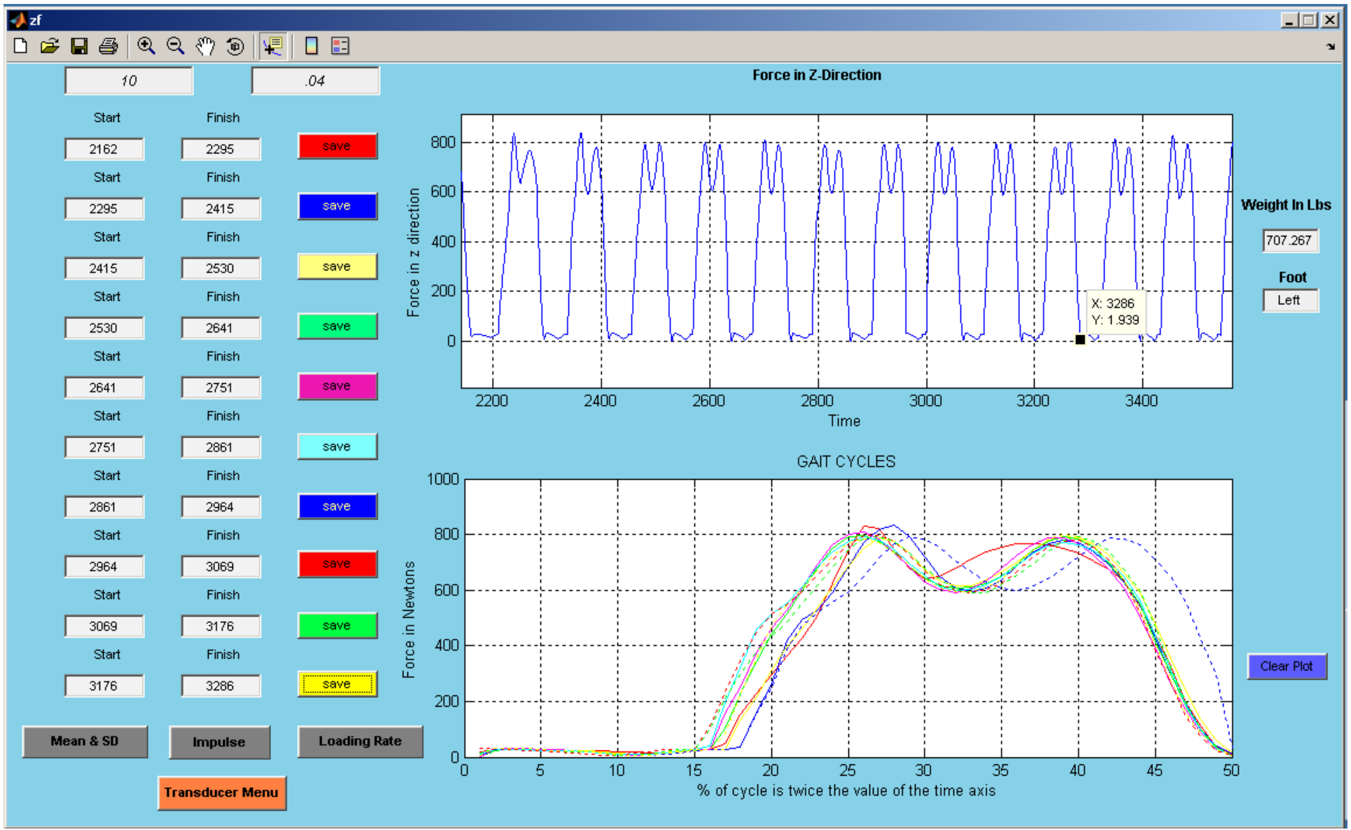

Now the user has to click on **Transducer Menu** to analyze the forces and moments along the other axes. By activating **Transducer Menu,** a window as shown below appears.

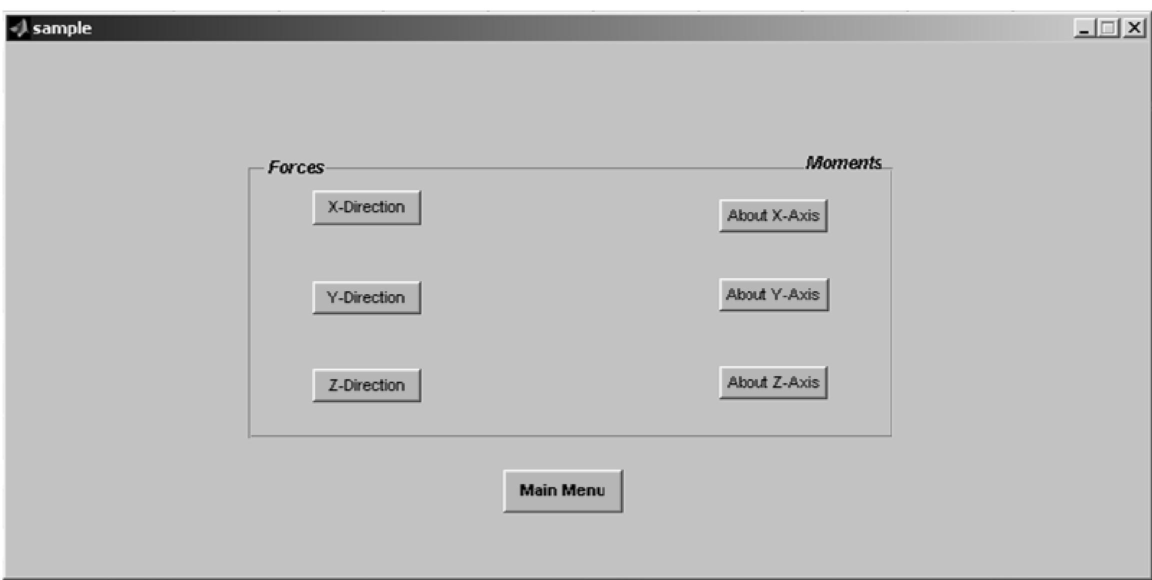

Now the user can select among the options specified in the window. All options are available to the user at this time. For explanation purposes in this chapter, the **Y-Direction** under Forces has been selected and the following window appears. The same procedure followed by the user to analyze the force in Z-direction should be used here to analyze the force in Y-direction. However, the x coordinate values used to define steps in the Fz window just explained will reappear, and these same values should be used again to break the stream of data from the transducer into the same time-wise segments so data points will match across all the forces and moments. This will ensure that the beginning and ending points of the steps will agree, and all 50 intervals will span the same points in the gait cycle. To do this, only the **SAVE** buttons for the ten steps need be clicked. The x coordinate values in the boxes should not be changed. The same procedures should be followed again for the remaining forces and moments. All windows that appear in the process are shown in the discussion that follows one after the other.

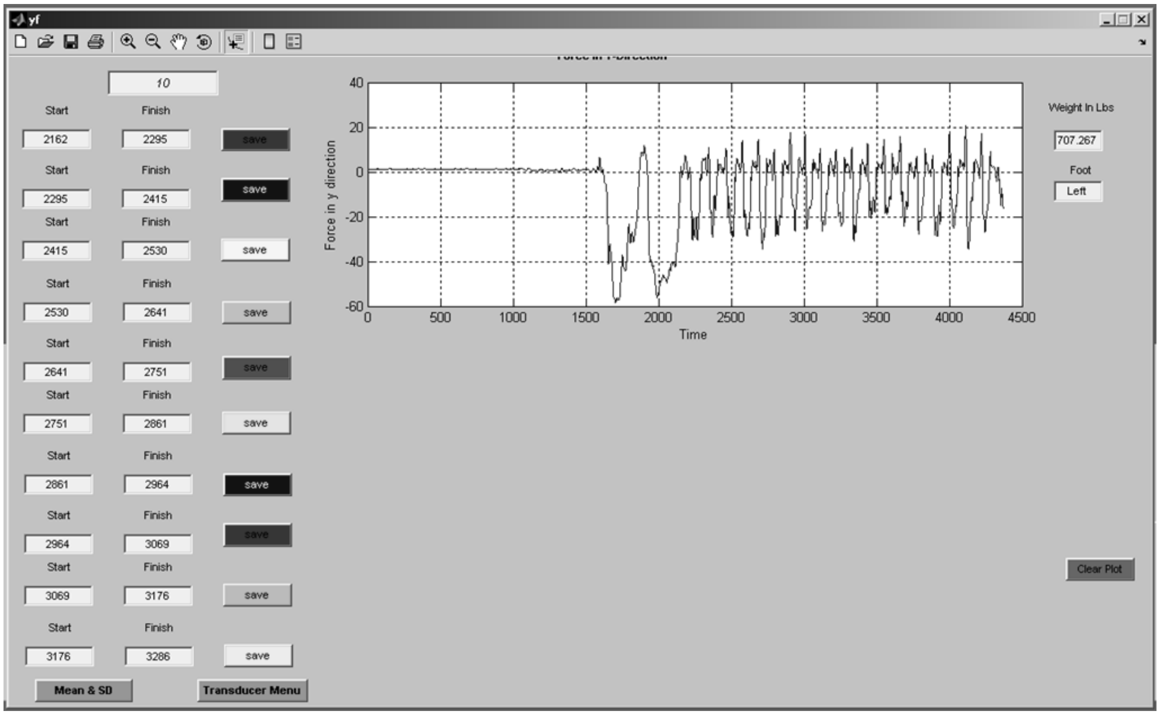

Clicking the **Save** buttons of all ten steps will produce the second plot with gait cycles.

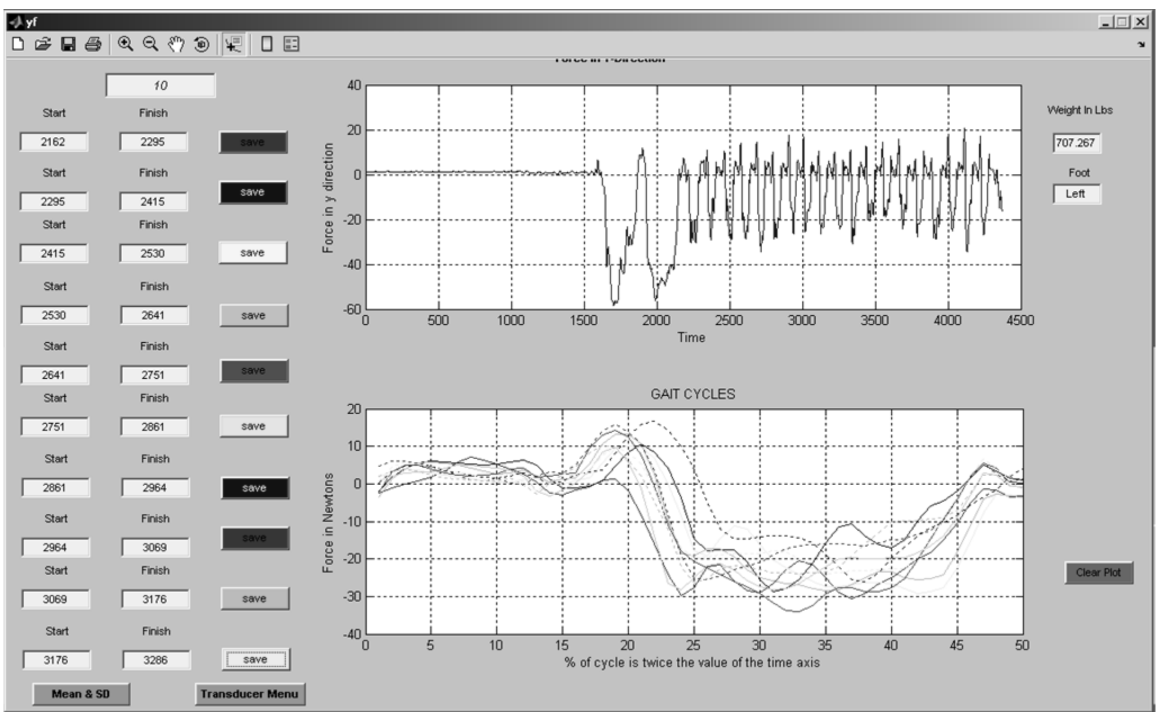

Clicking **Mean & SD** will produce the following window with the means and standard deviations plotted.

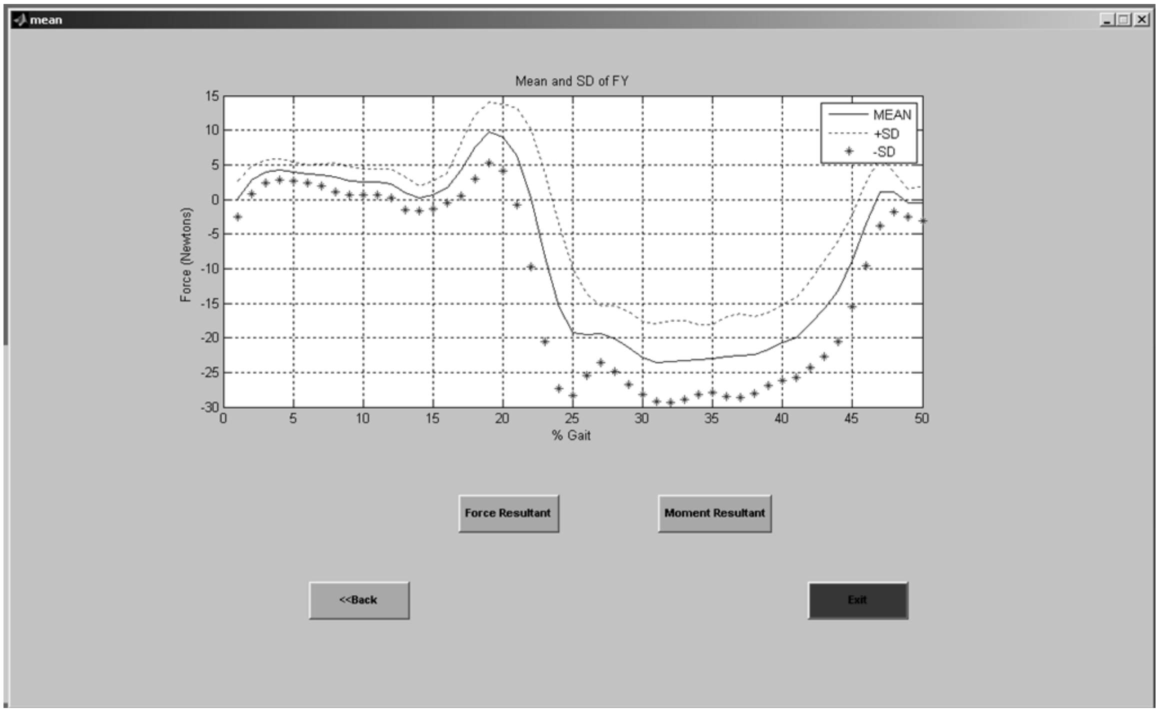

Using the **Back** button in the above screen will take the user to the Z-Direction plot window.

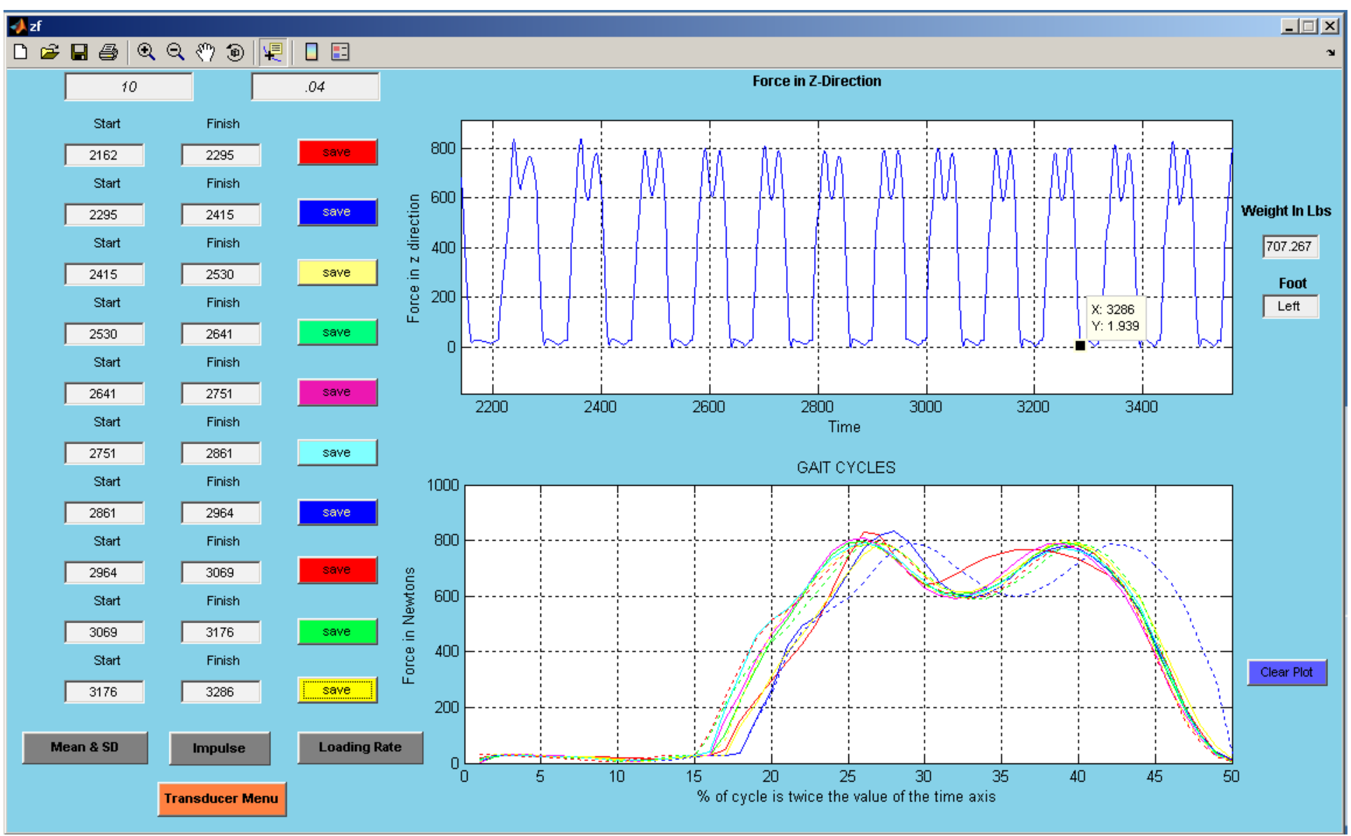

Again using the **Transducer Menu** button will let the user select the moment or force along other axes to analyze as shown below.

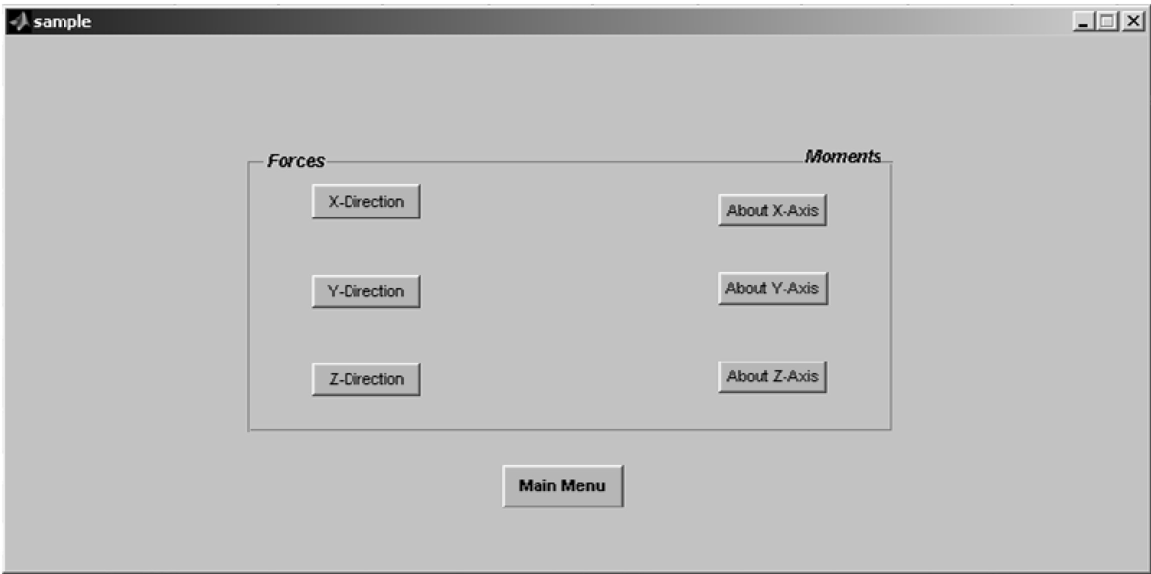

Selecting **X-Direction** under **forces** will give the user following window.

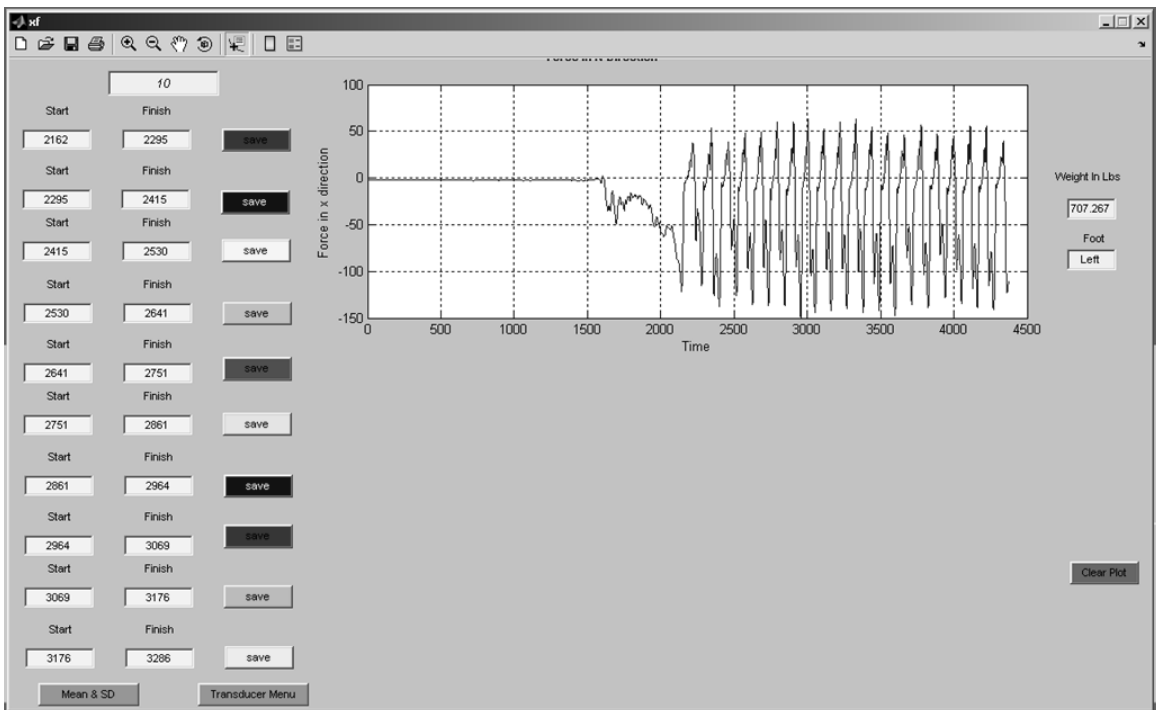

Gait cycles will be plotted as shown below in the second plot after clicking on the S**ave** buttons of all ten steps.

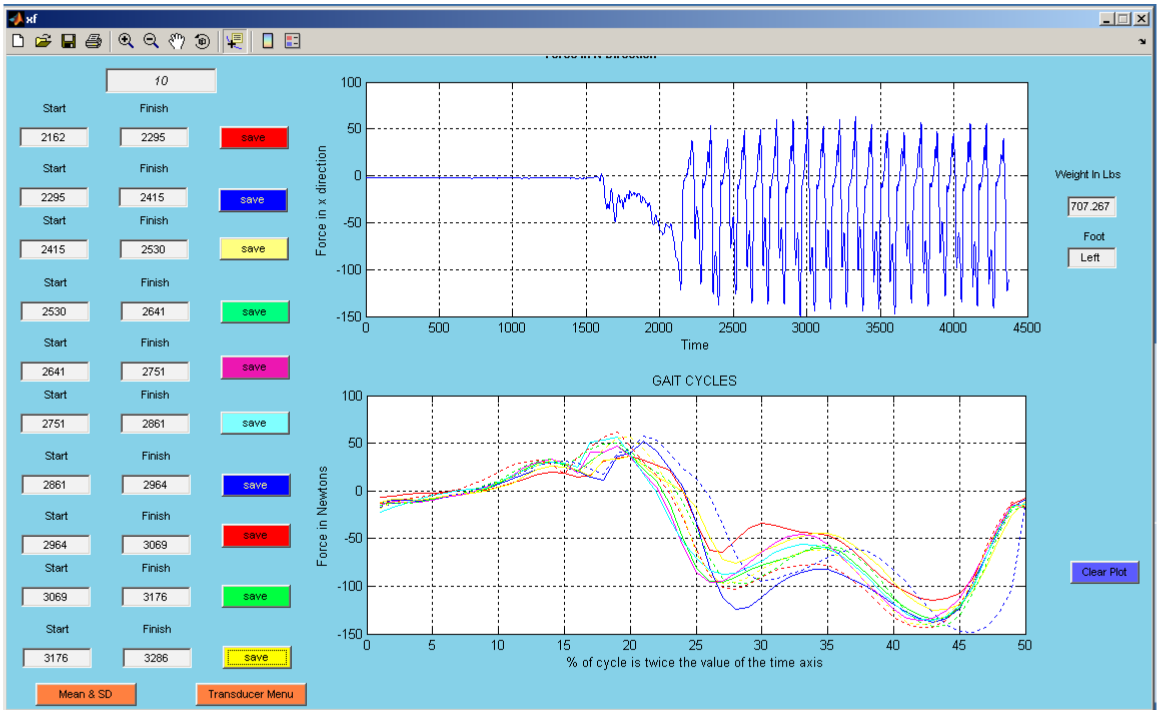

The **Mean and SD** button is used to produce the curves for the forces in the X-direction for the ten steps.

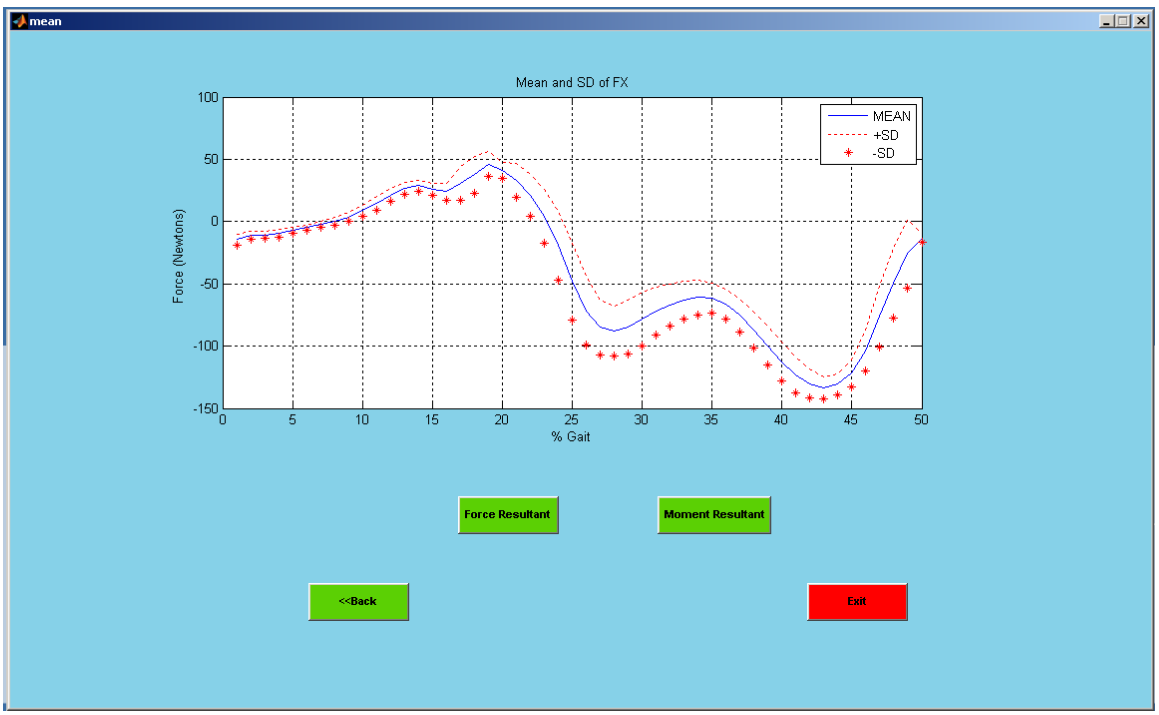

Now the user has completed processing the forces along the three axes and can use the **Force Resultant** option in the above window to obtain the following plot of the resultant force vector length computed from the magnitudes of the forces along each of the three axes. A second window indicates the angle of the resultant vector with respect to the Z axis of the transducer, which is more or less parallel to the pylon. The values shown include the projection angle of the resultant force vector with respect to the Z axis in the ZX plane and ZY planes. The following two windows show how the resultant force and its angle with the Z axis of the transducer appear.

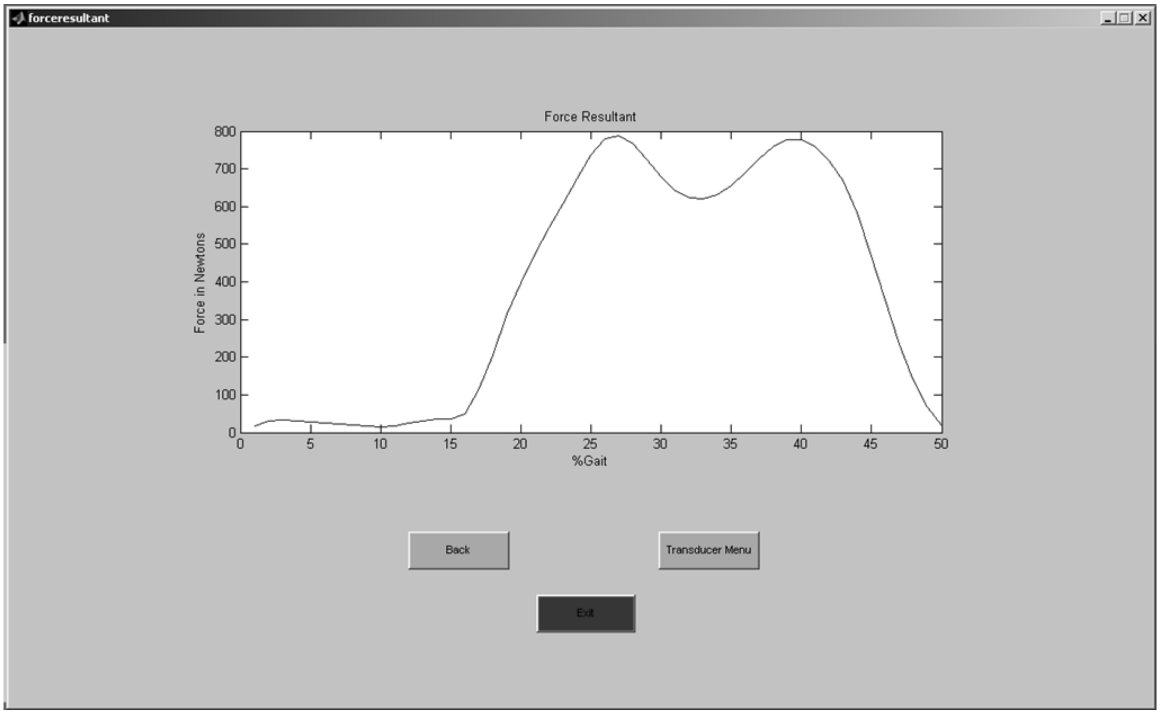
forceresultant
Force Resultant
Force in Newtons
%Gait
Back
Transducer Menu
Exit

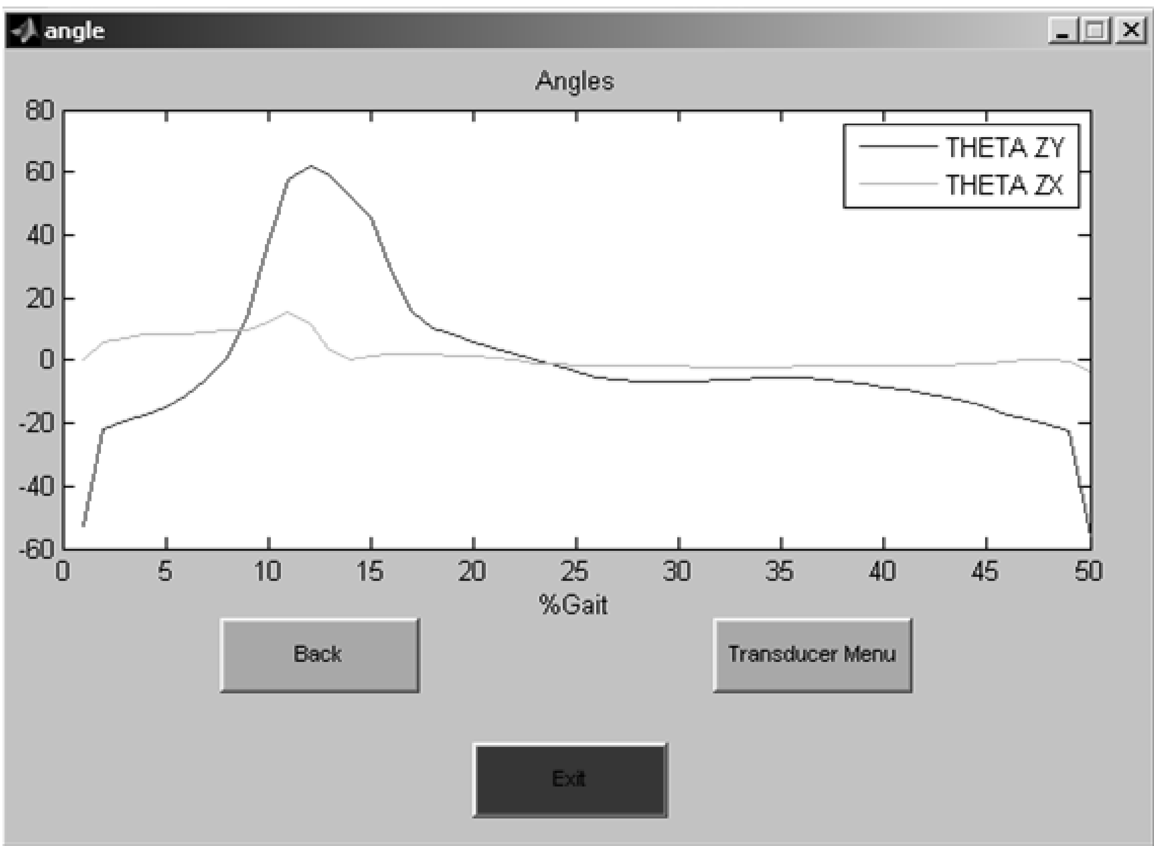
angle
Angles
THETA ZY
THETA ZX
%Gait
Back
Transducer Menu
Exit

Next, to process the data for the moments about the X,Y,Z axes the same steps must be followed. Going back to Z-direction force window again will provide the following window:-

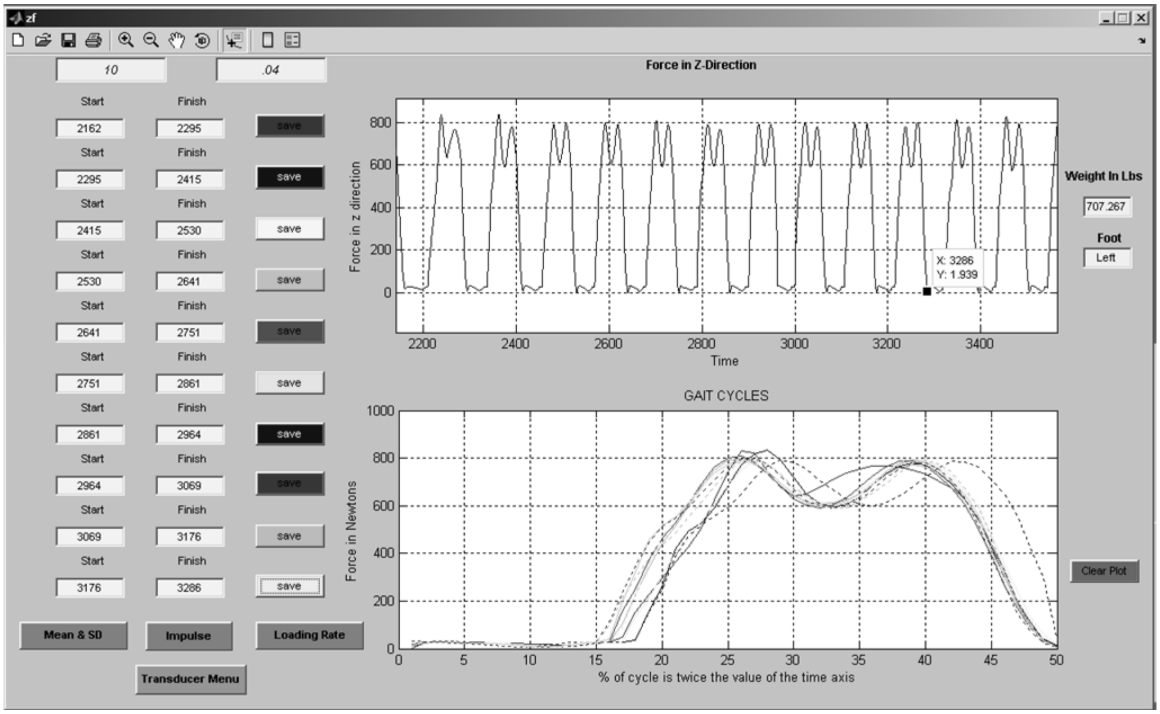

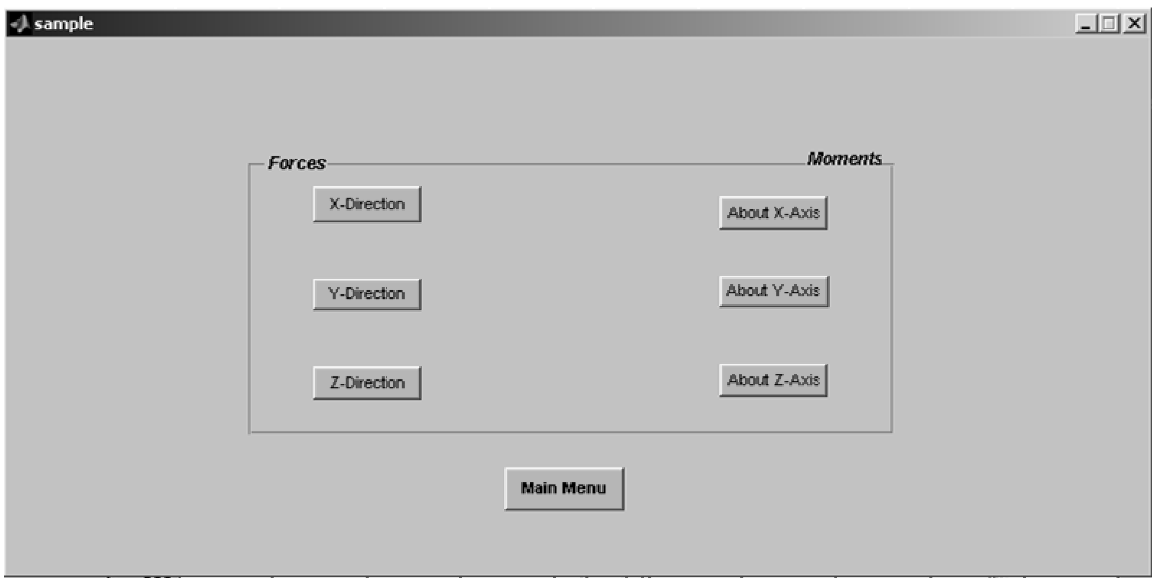

.

The user must analyze the moments in all three directions. For demonstration purposes the moment about the x-axis is selected from the **Transducer Menu**.

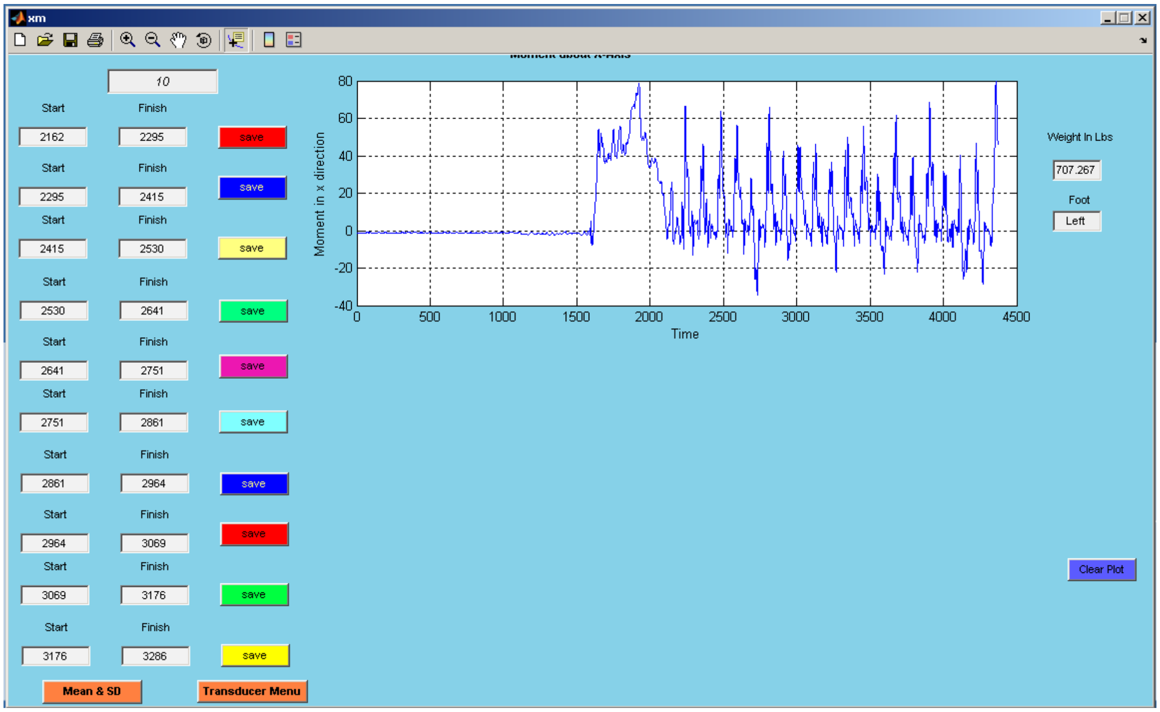

The same procedure used to analyze the force data has to be followed to analyze the moment data. However, the x coordinate (time) values defined initially for delineating individual steps for Fz have been preserved and do not need to be entered again. All windows are shown below. The first window depicts moments about the x axis.

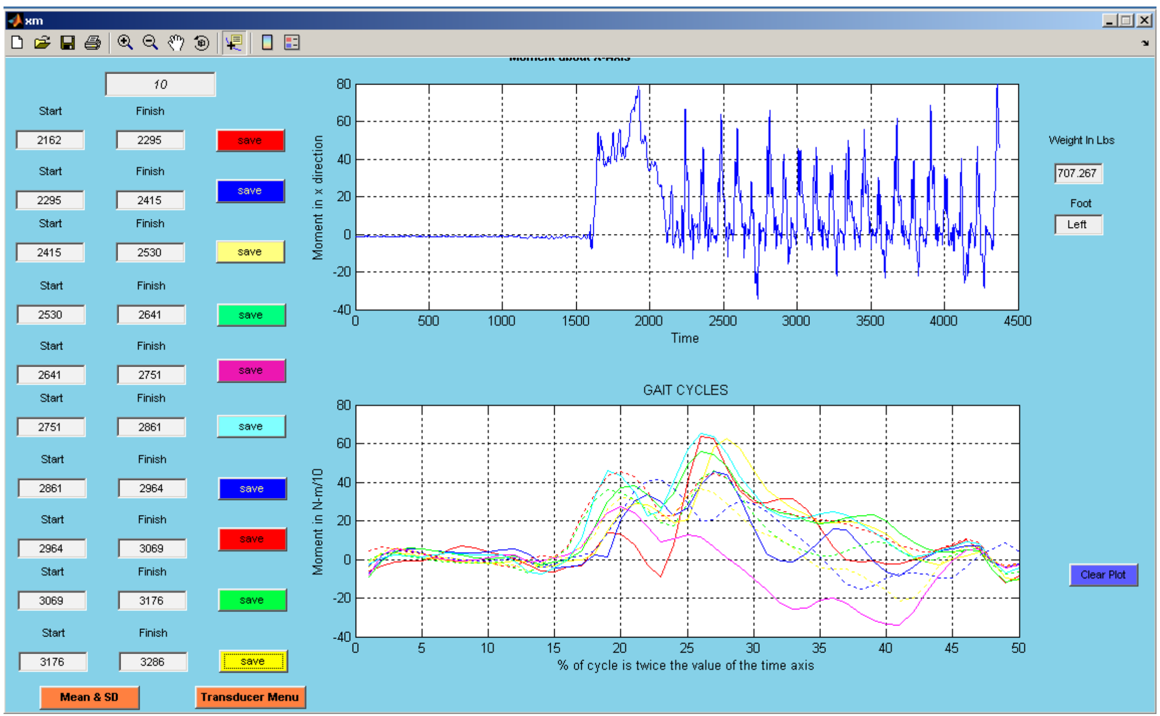

The mean and moment standard deviation of the moment about the X-axis are shown next:

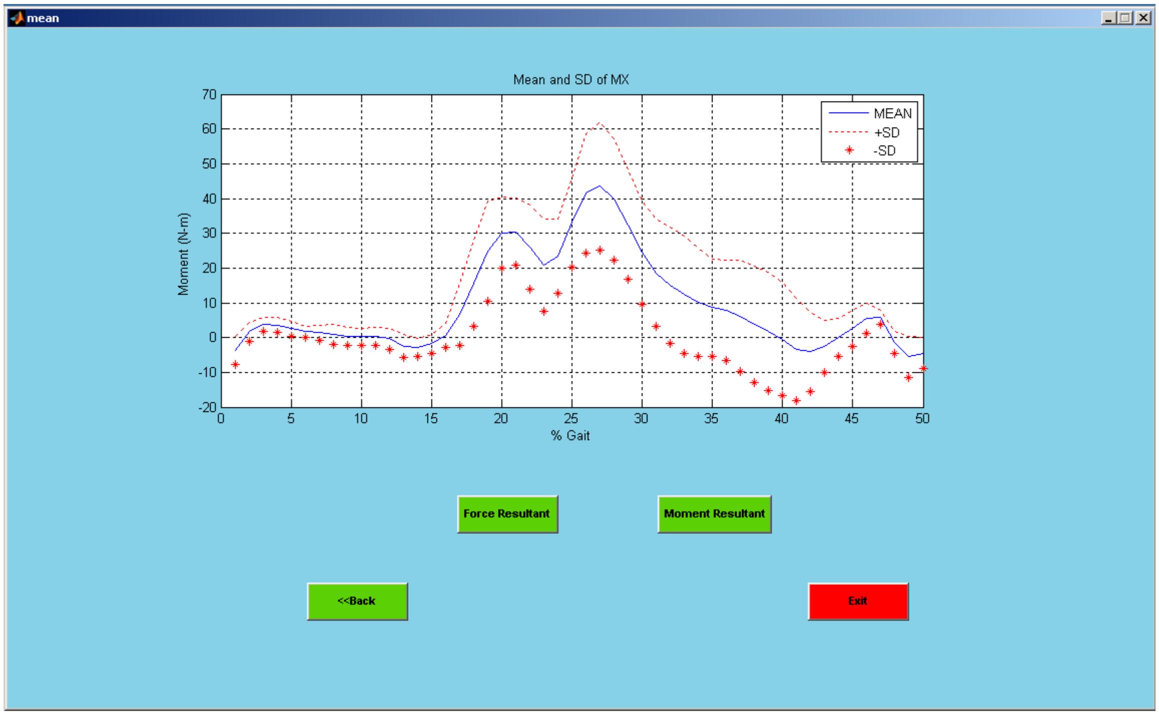

To next process the data for the moment about the Y axis, the user must go back to the original Z axis force window from the window depicting the mean and standard deviation for the moment about the X axis, and click on the **Transducer Menu** button

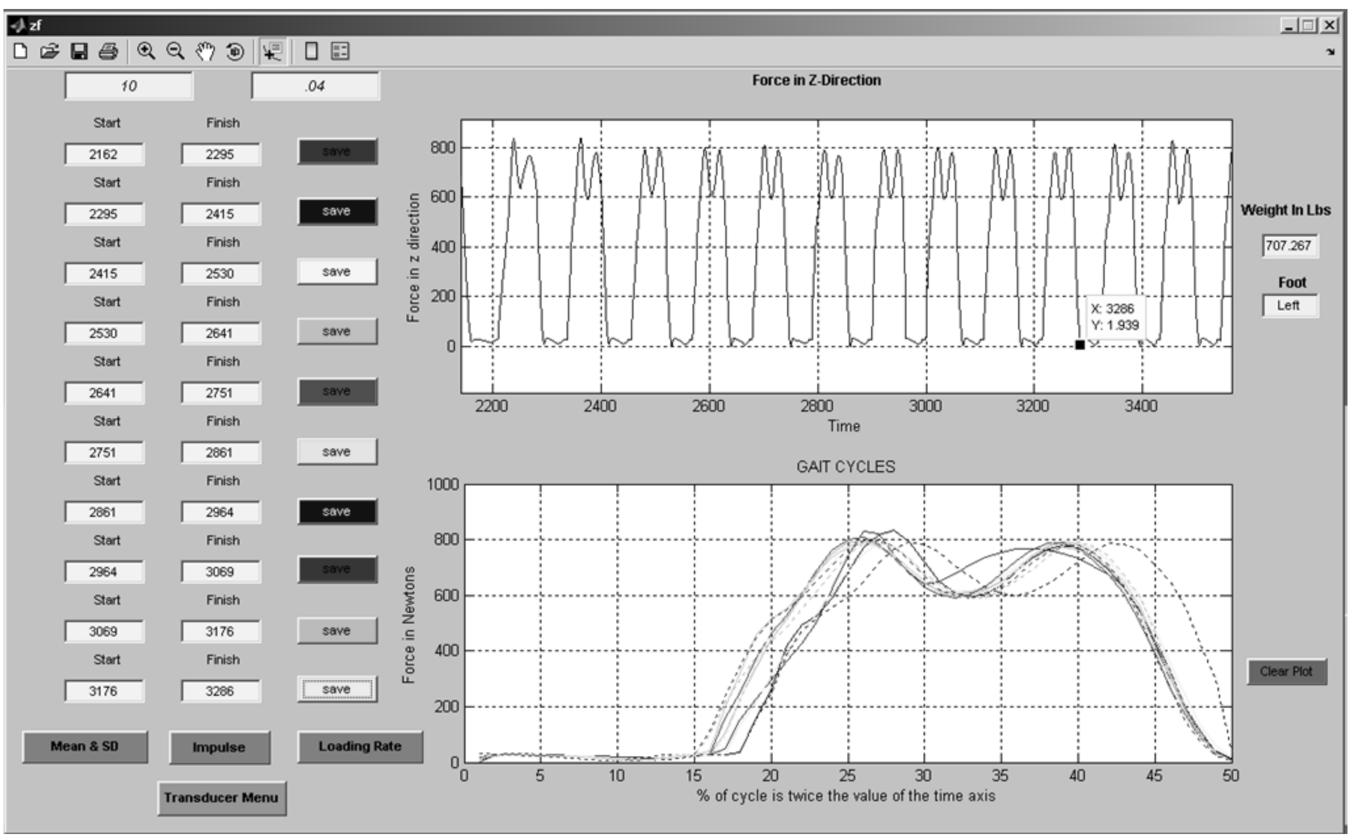

The following window shows the resulting Transducer Menu:

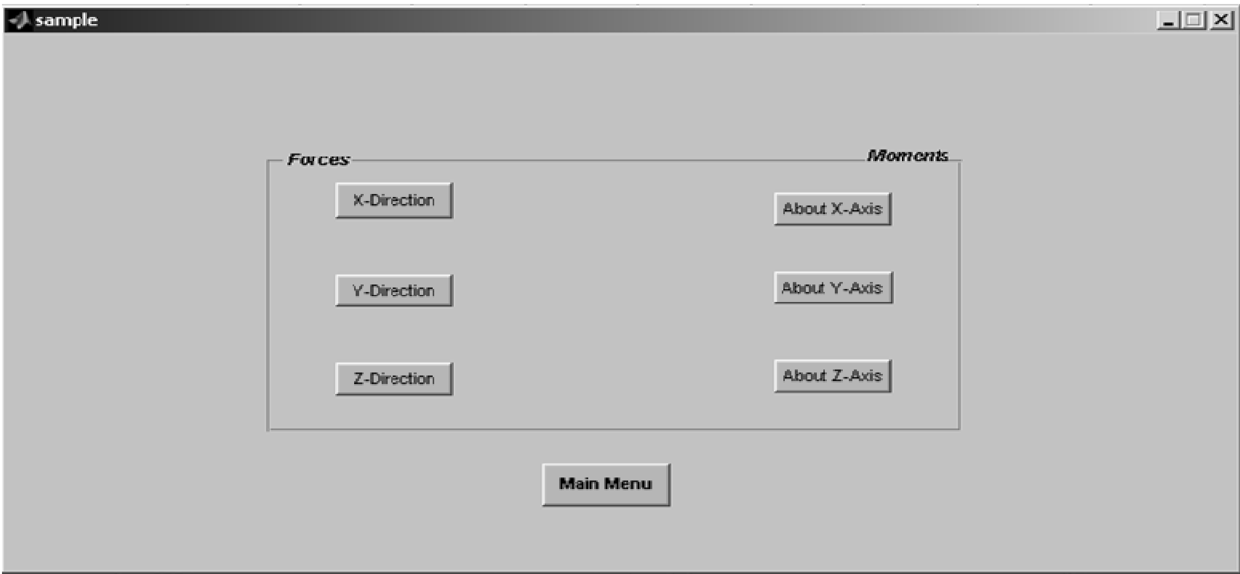

The button to analyze moments about the Y axis must be clicked:

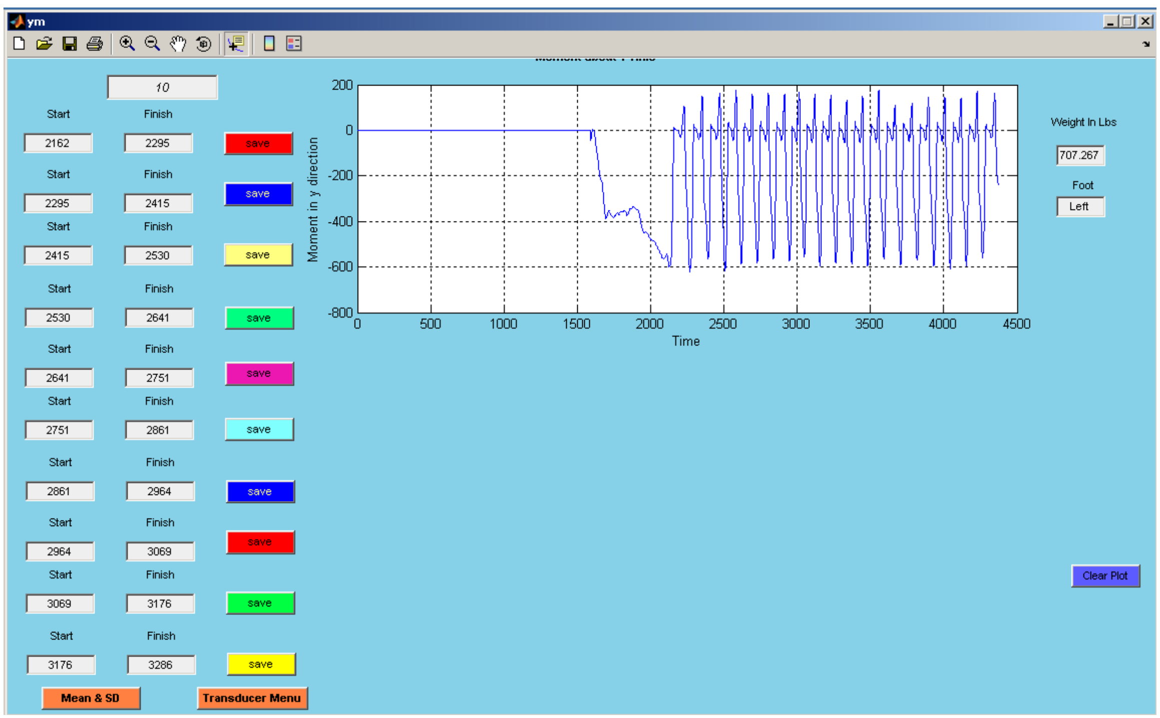

Then all the starting and ending values must be SAVED for the ten steps, which identify the gait cycles for moments about the Y axis:

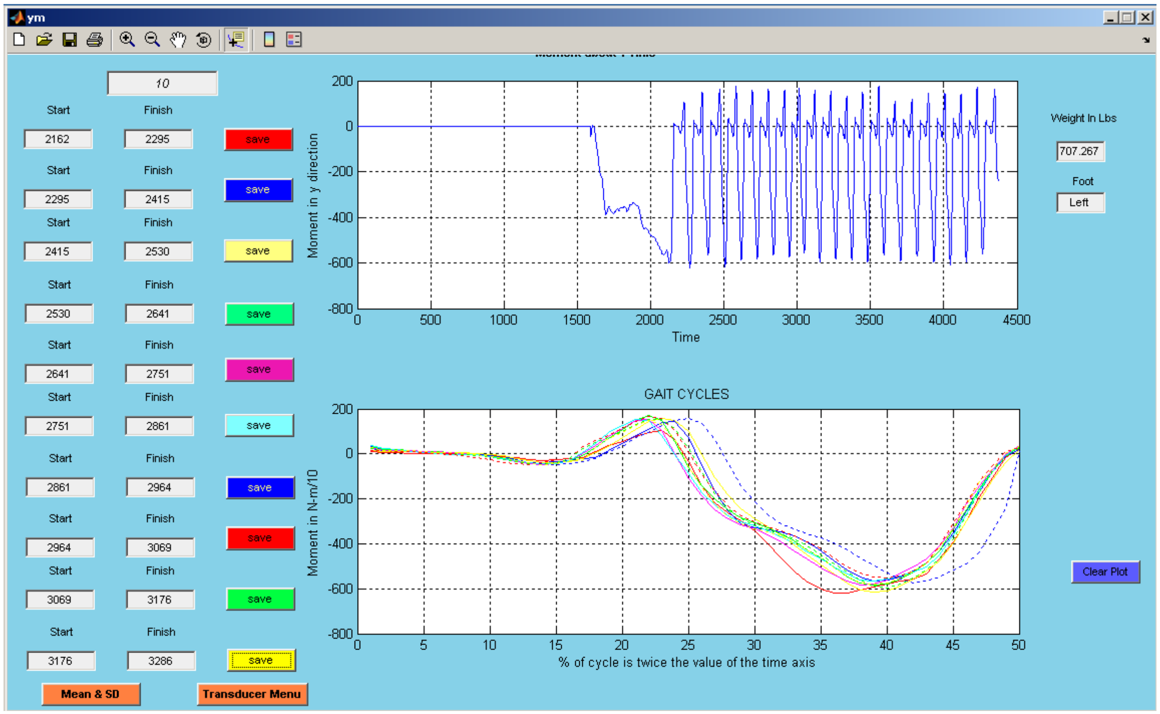

The mean and standard deviations of the moments about the Y axis must then be computed:

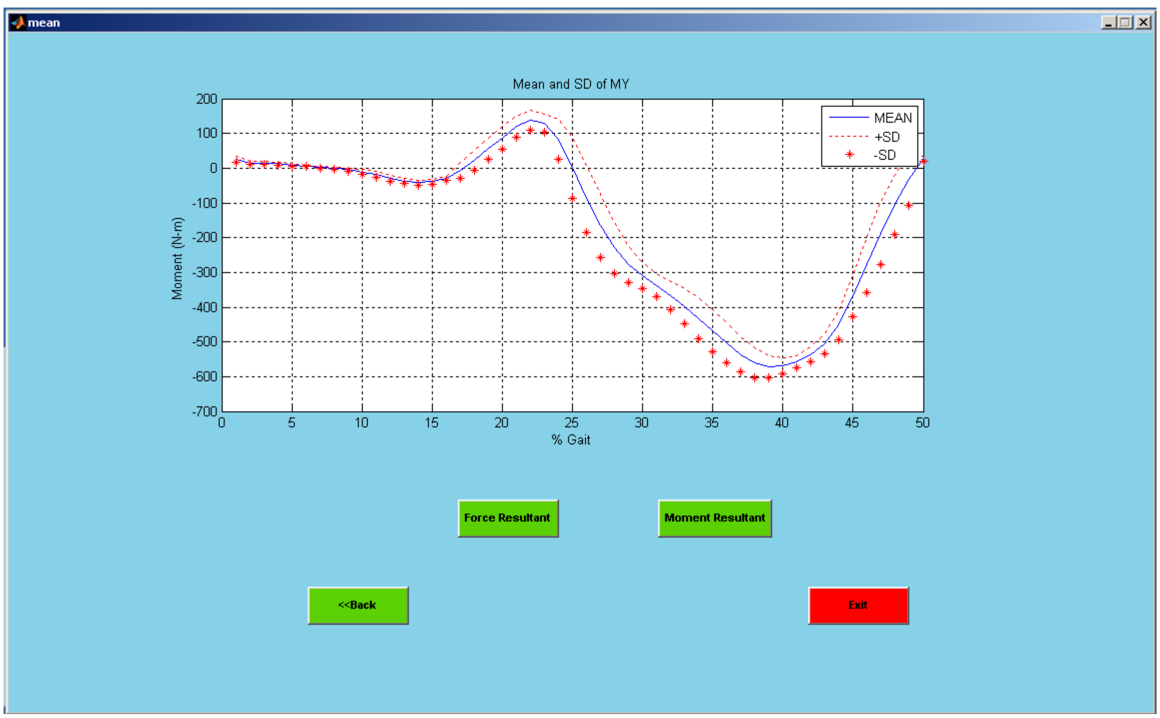

The user must then go to the original window used to first display forces in the Z direction and click on the **Transducer Menu**:

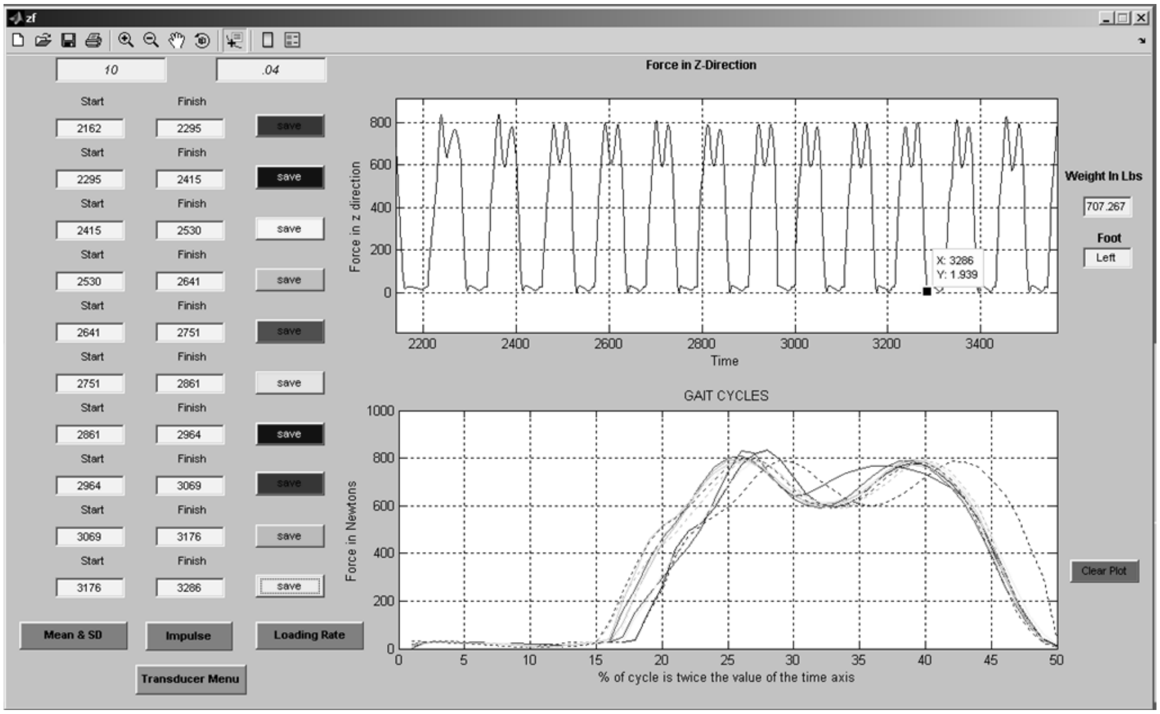

Again the Transducer Menu will appear:-

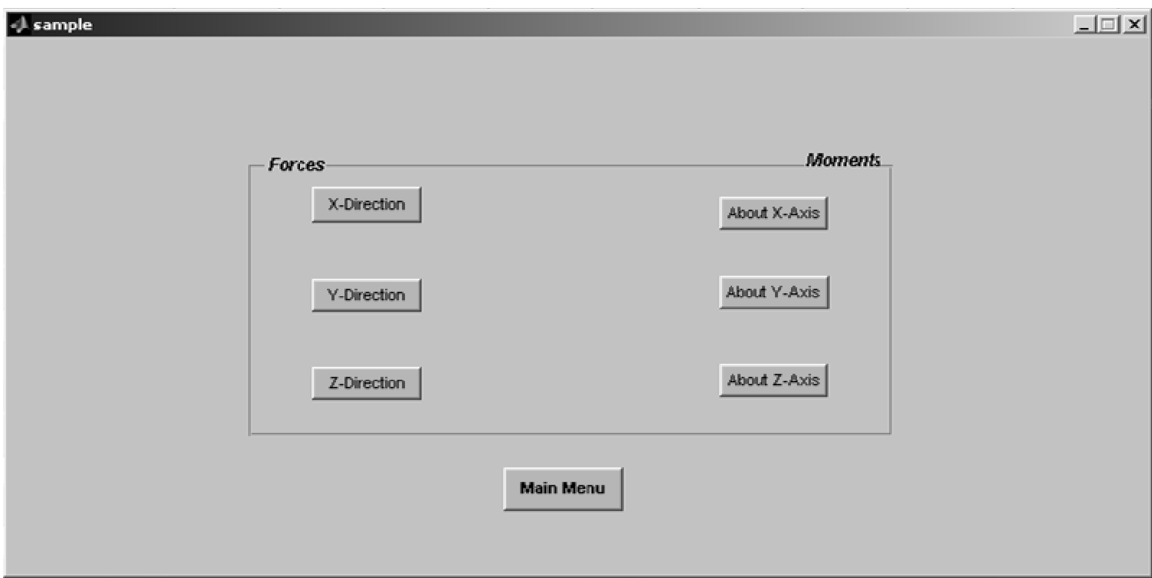

The user must request a display of moments about the Z axis:

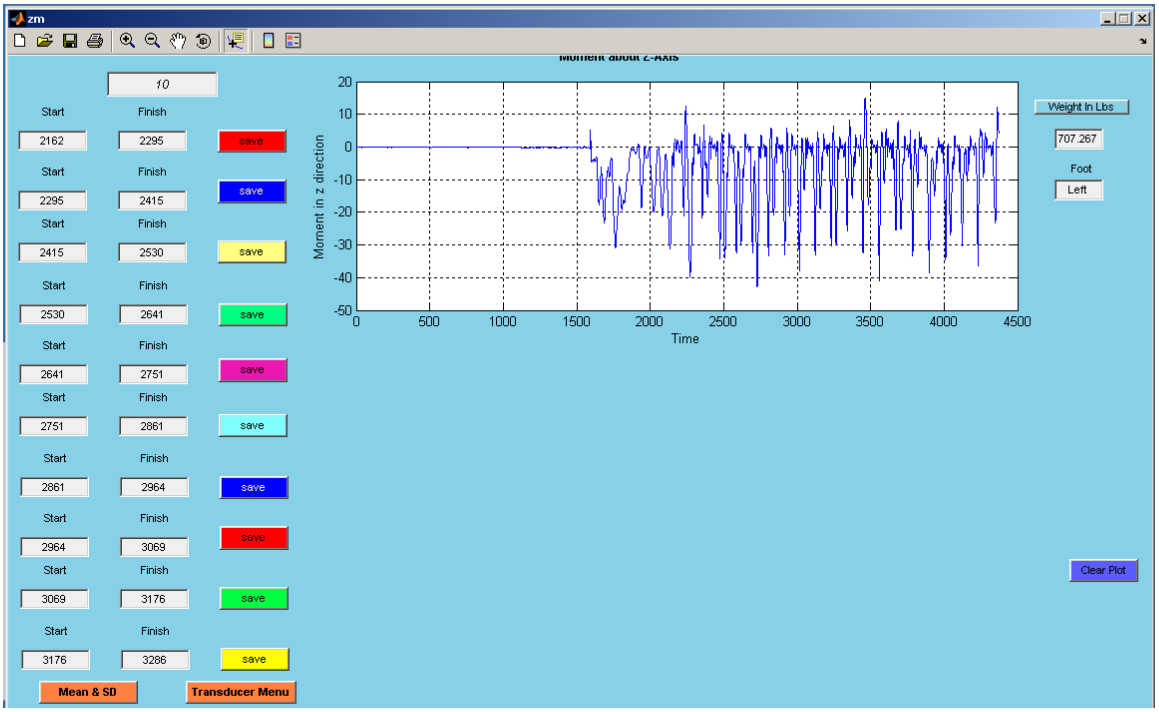

The starting and ending coordinates for the moments about the Z axis then appears:

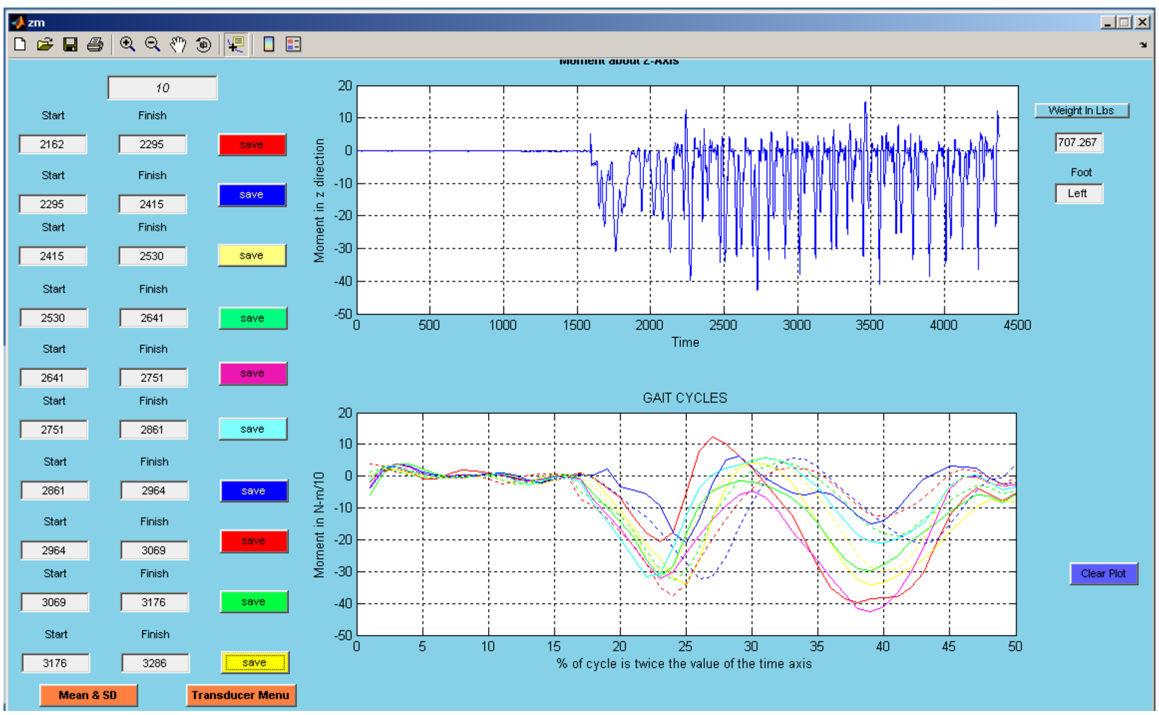

The mean and standard deviation of the moments about the Z axis are computed :

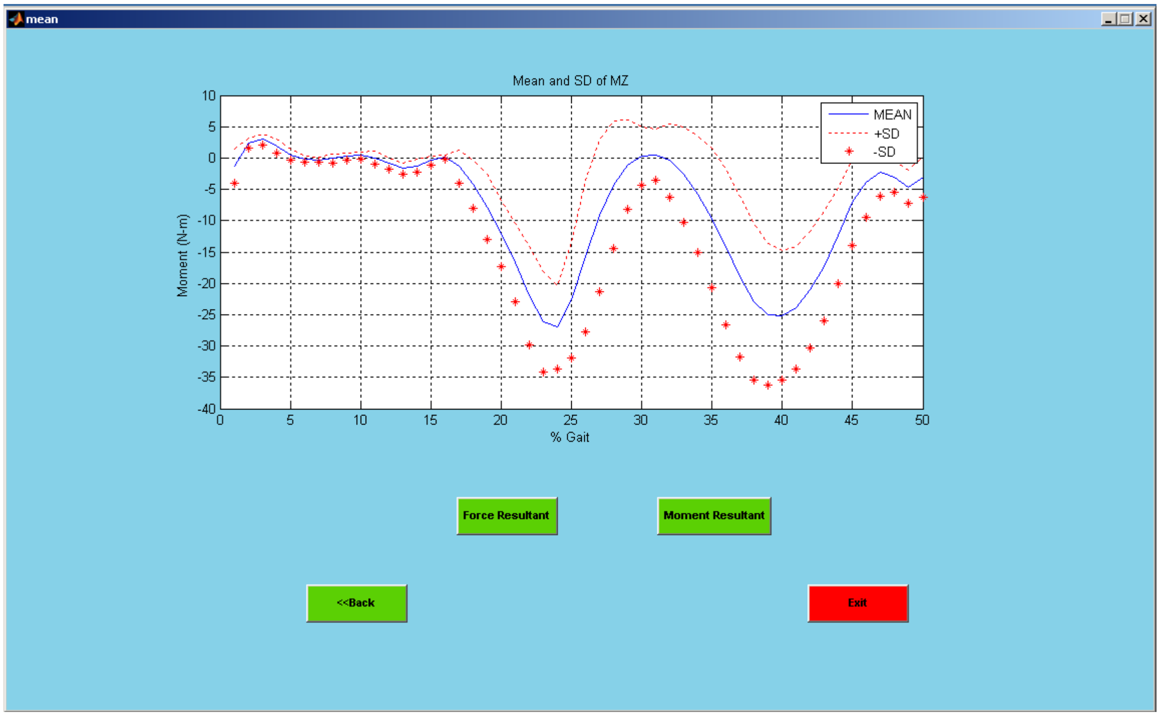

Now user can click the **Moment Resultant** button to compute the resultant of the moments about the three X, Y, Z axes since all three moments have been analyzed. Clicking on the **Moment Resultant** will produce the following windows (Resultant magnitude and resultant projection angles with respect to the Z axis in the ZX and ZY planes).

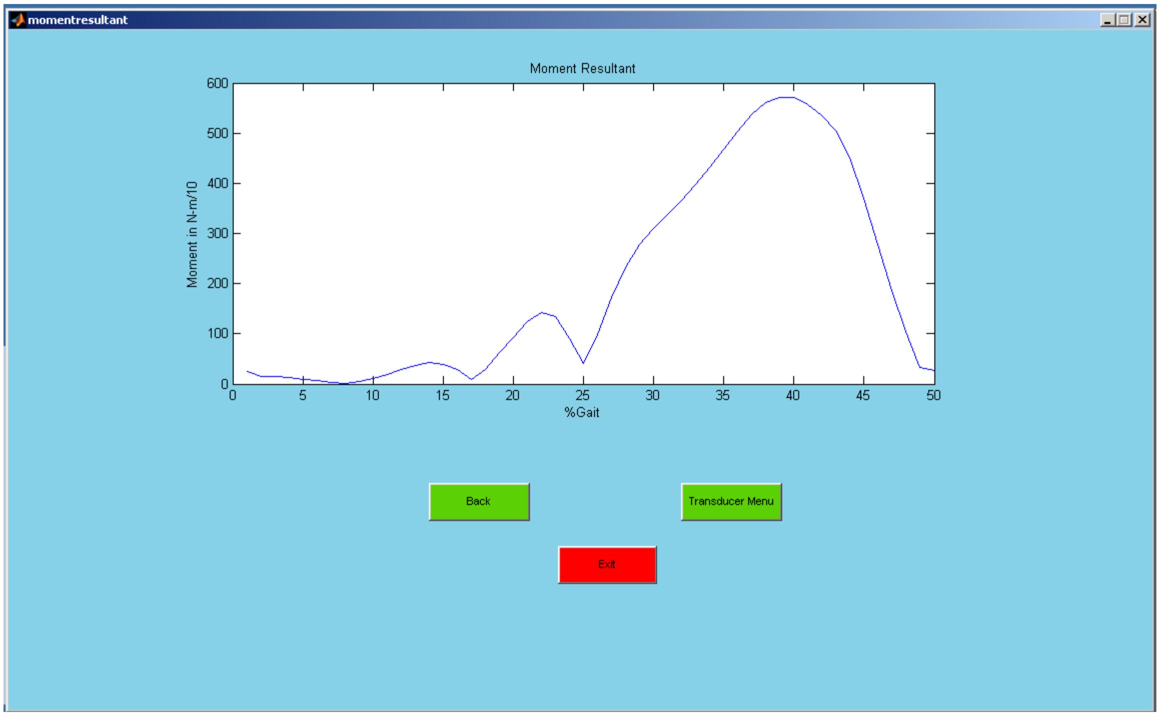

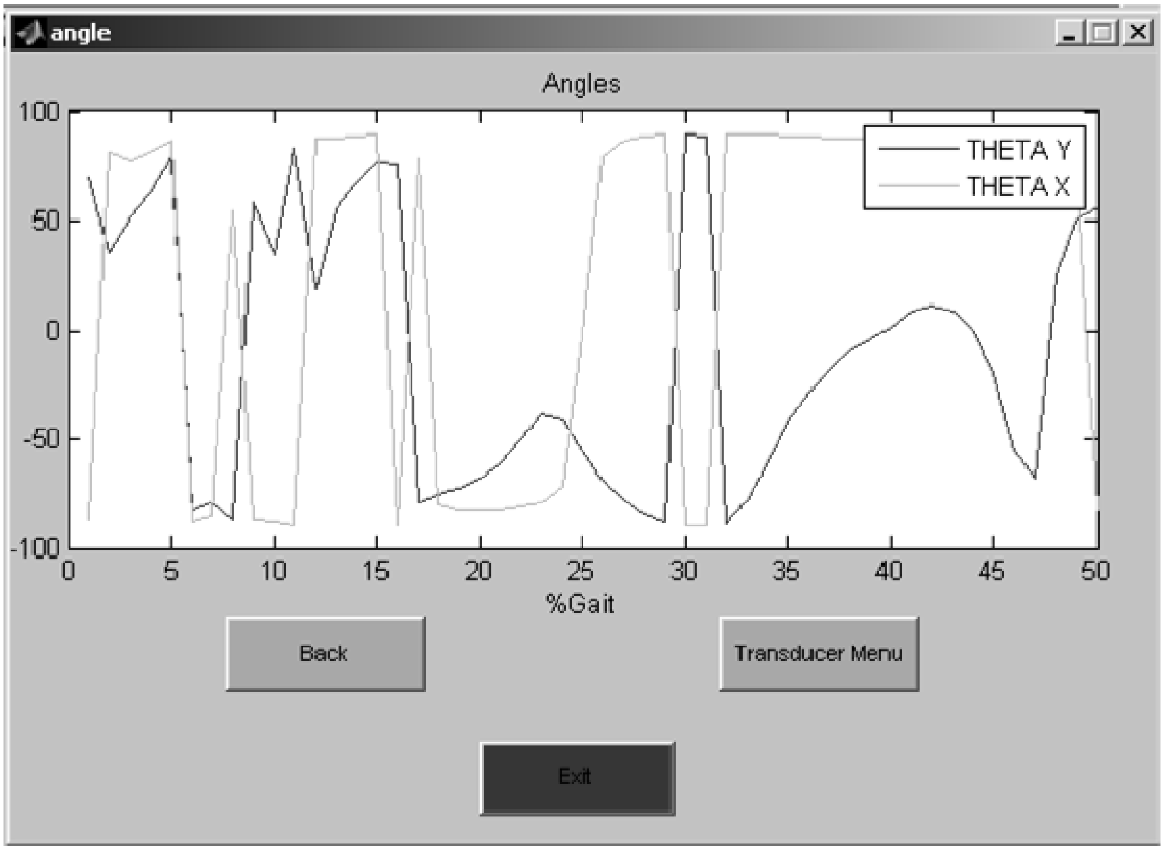

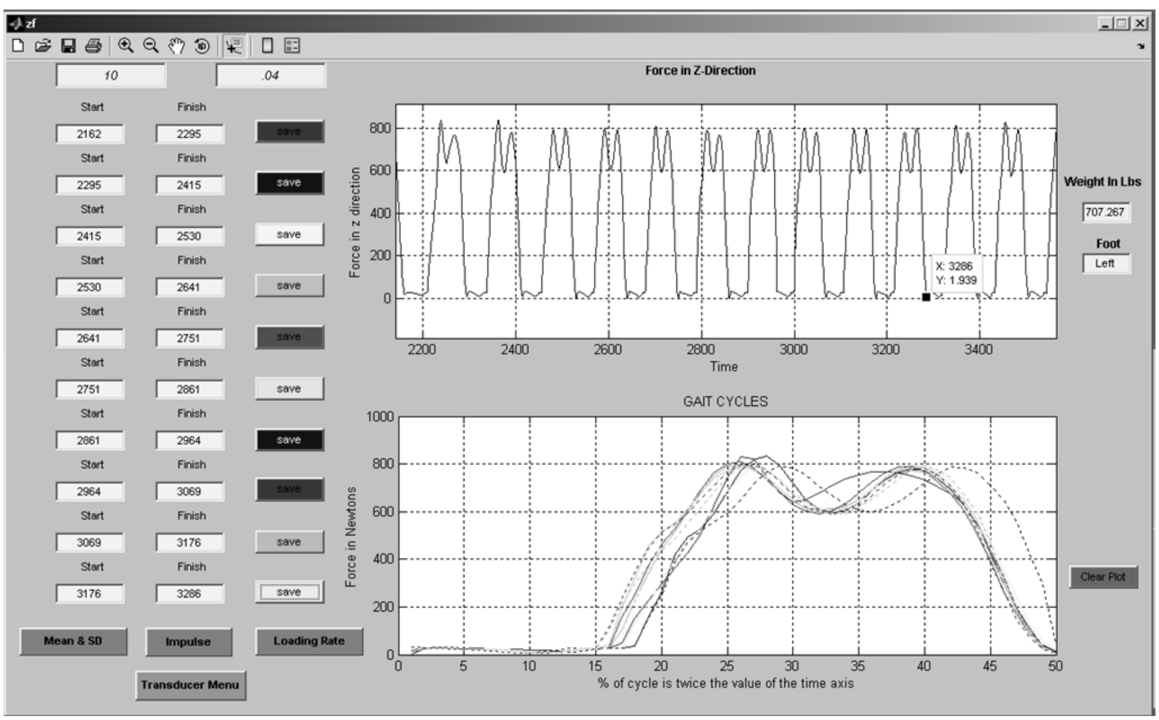

After all three forces and moments have been computed the user can calculate impulse and loading rate by using the two buttons beside the **Mean & SD** button in the above window. Impulse is broken down into three phases for calculations. The first phase corresponds to foot loading, the second to midstance or rollover, and the third to the propulsive phase. For demonstration purposes the impulse for Fz has been selected. After selecting **Impulse** the following window appears in which the user has to input the x coordinate values for the four points defining the three impulse segments. These points are obtained from the plot of the force (in this case Fz) for each step.

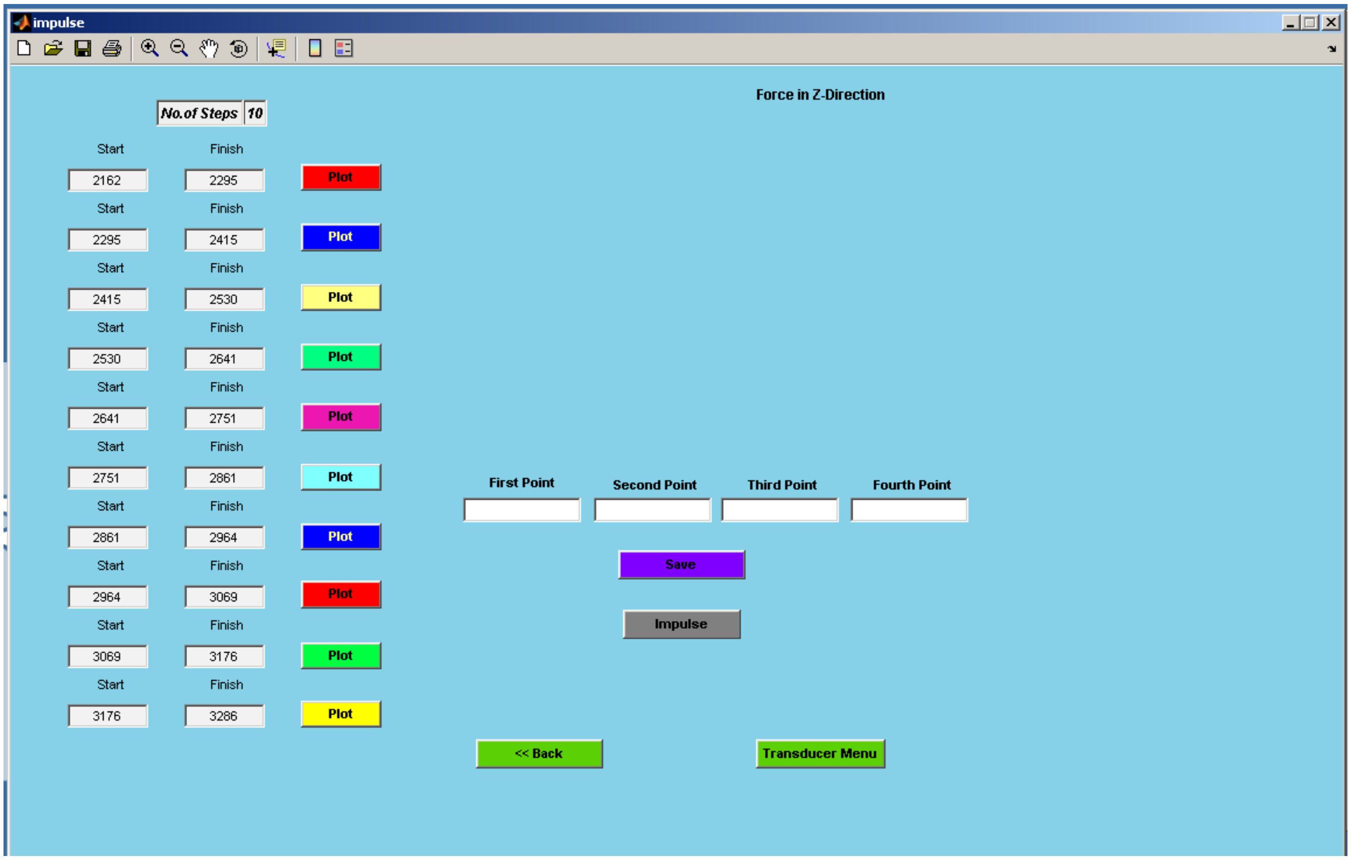

The user has to click the **Plot** button beside the start and finish buttons in the window to look at the original data for the step. With the use of zoom and data cursor the values of the four points can be entered.

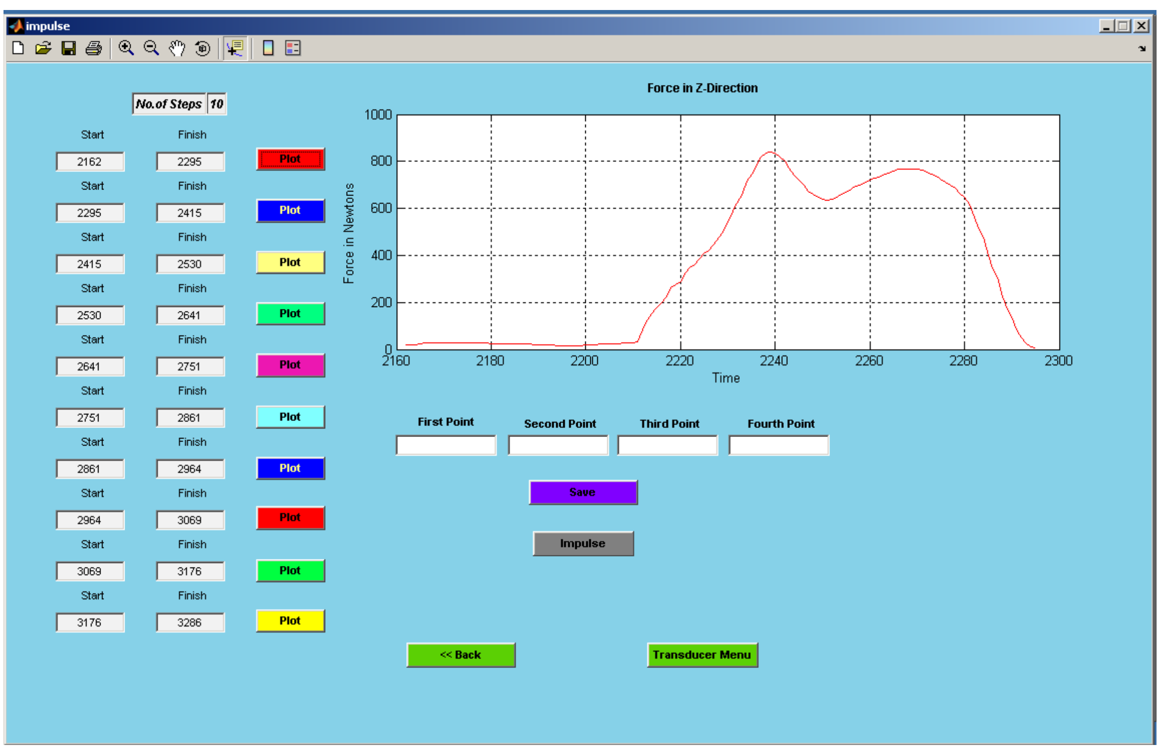

After entering the four points the user has to click the **Save** button under the four text boxes. The GUI will then calculate the three impulses and the total impulse and save it in the program for export.

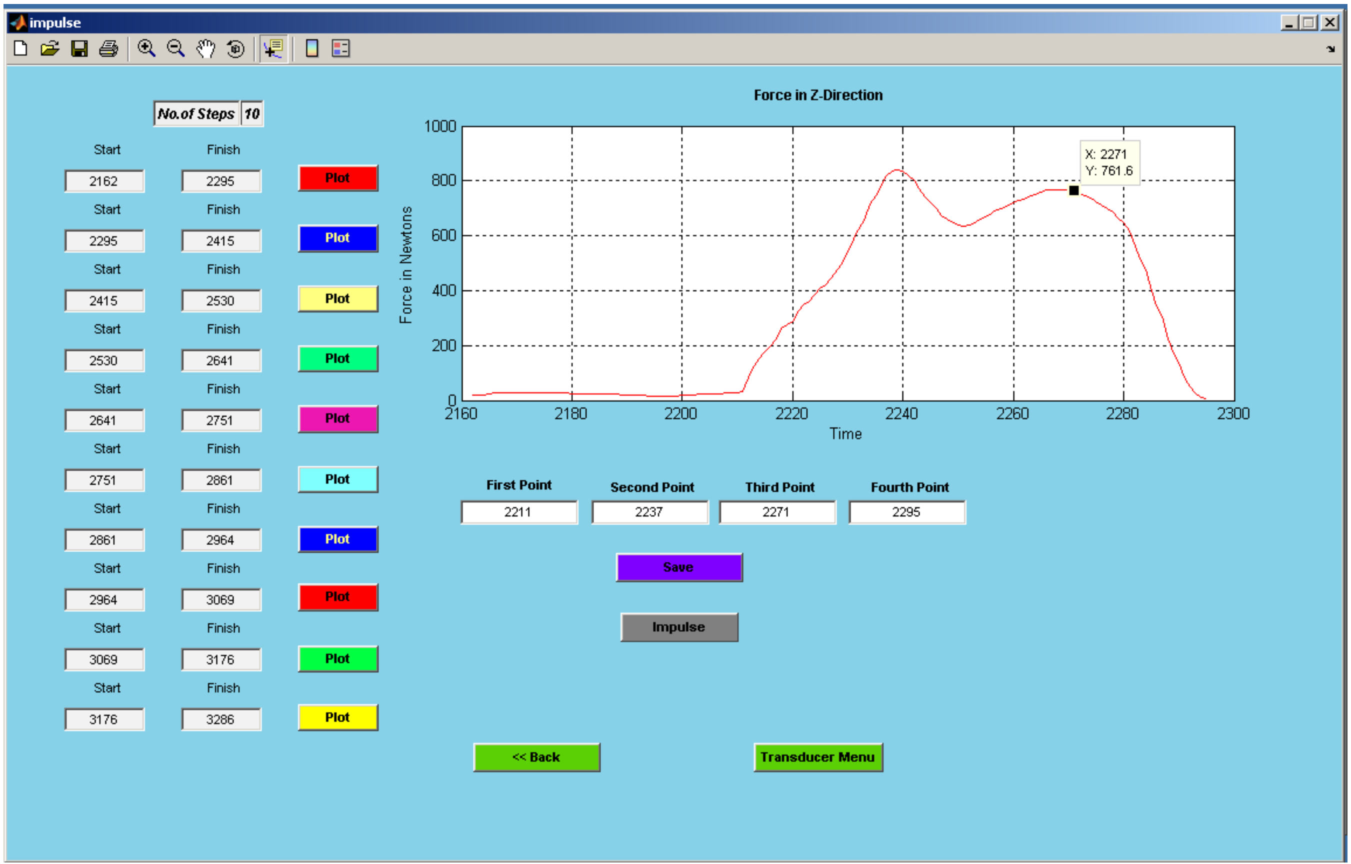

Once the user is done the **next plot** button has to be clicked to display the second step.

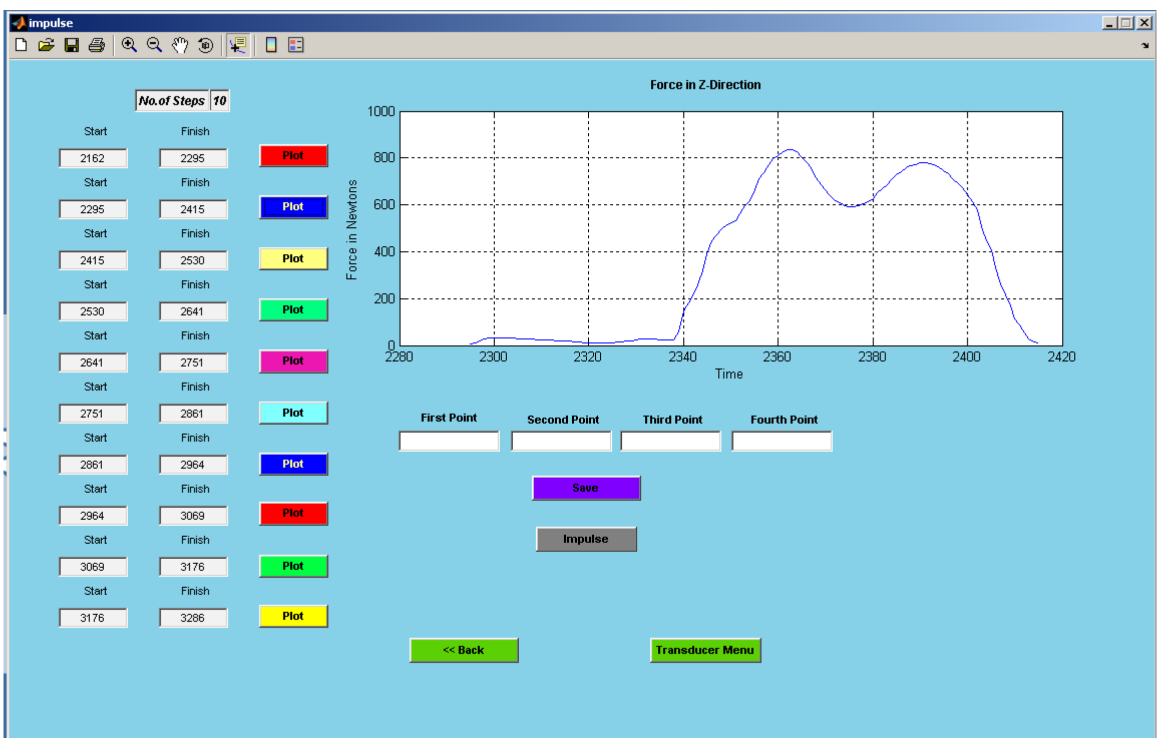

The same procedure has to be followed to calculate the impulses for the three separate phases and total impulse, and then all these steps repeated for the remaining steps. Once all 10 steps are done the user has to click on the **Impulse** button just below the **Save** button. It will display the total impulse below the **Impulse** button as shown below.

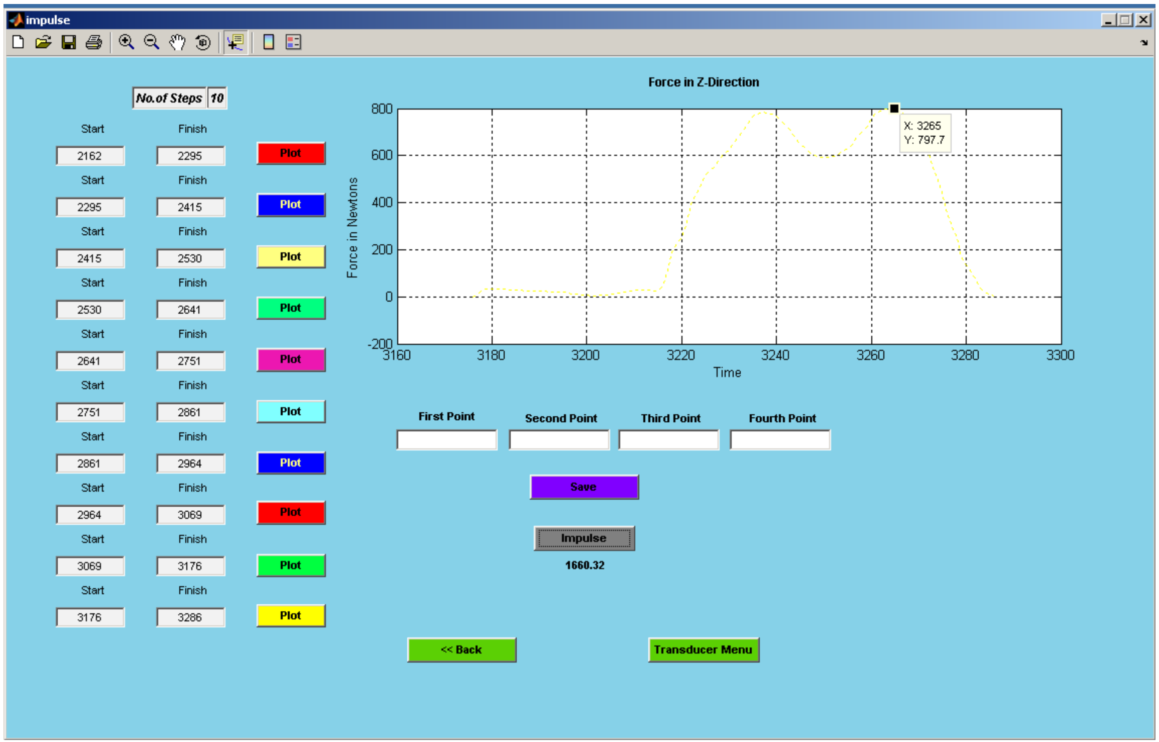

To calculate Loading Rate the user has to click on the **Back** button on the above window, which causes the following window to appear:-

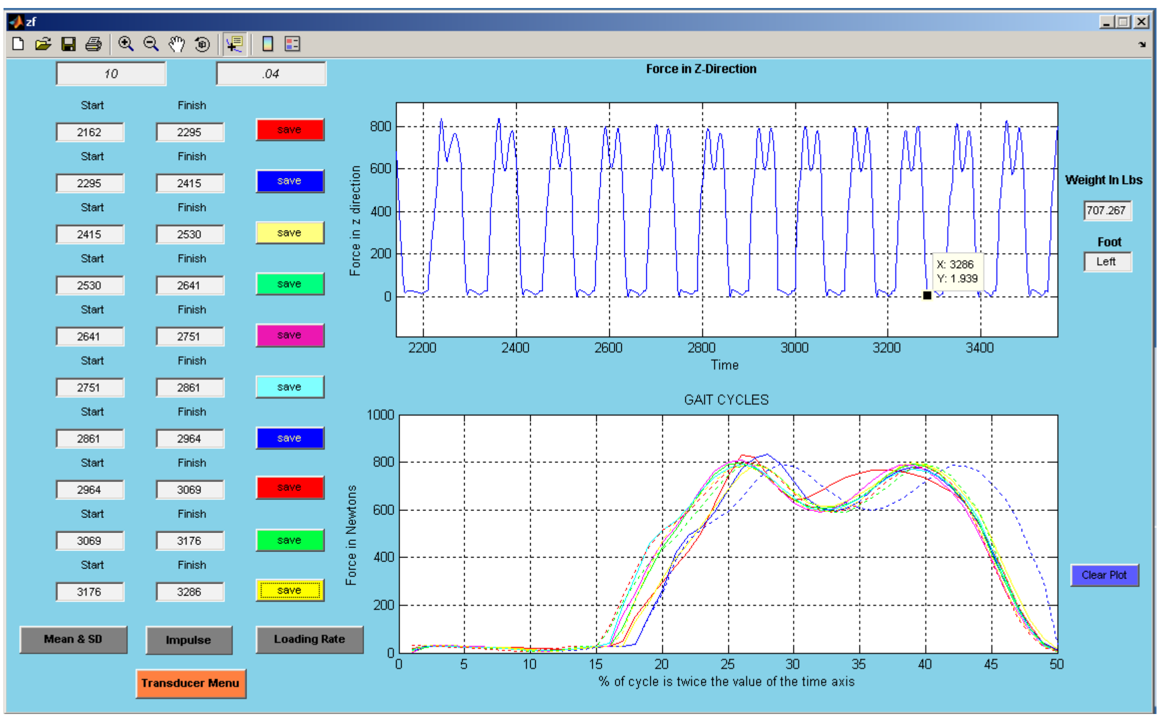

Now the user has to click on the **Loading Rate** button to bring up the loading rate window.

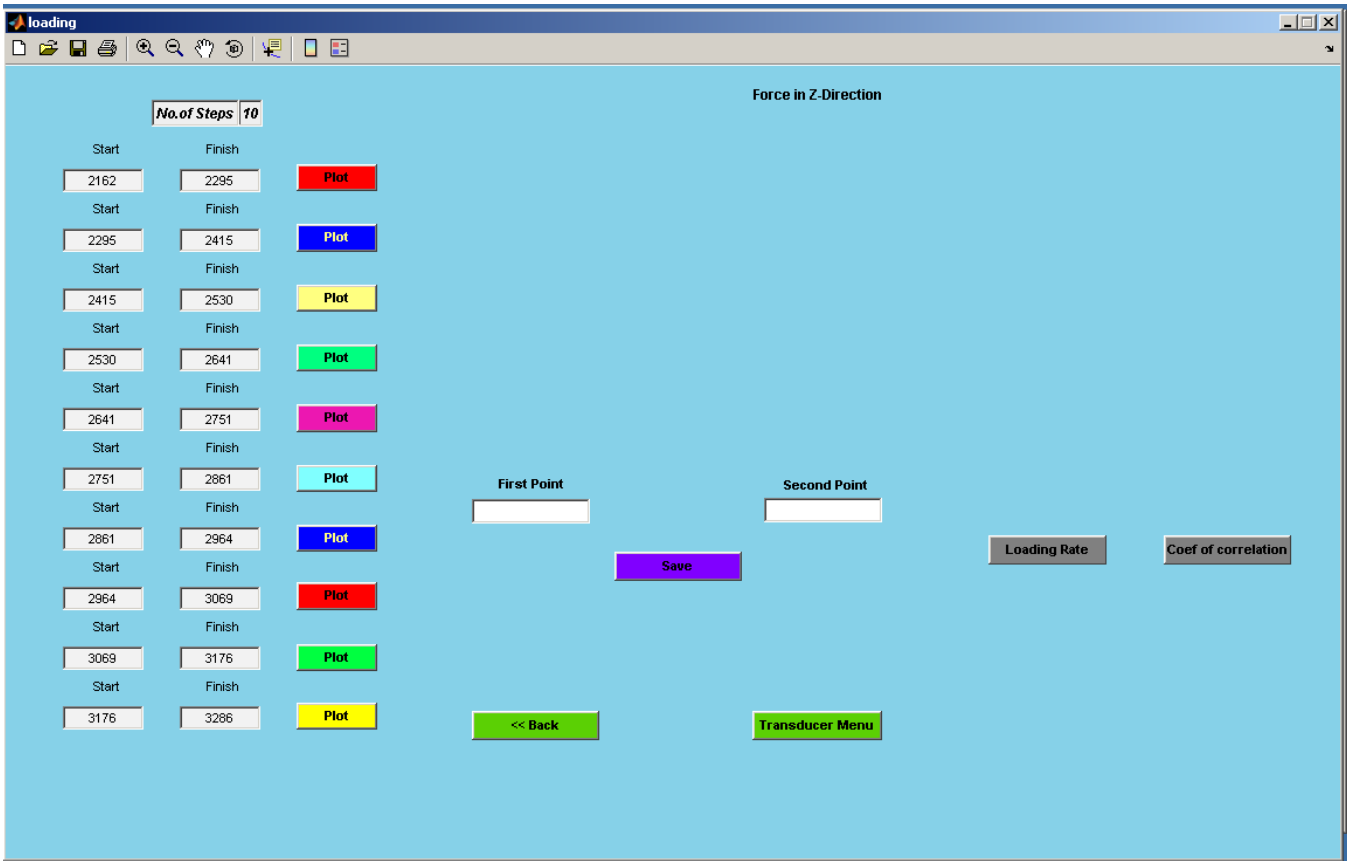

Computing the loading rate involves almost the same procedure as computing the impulse. After clicking on the **Plot** button, the following window and the corresponding step data will be displayed.

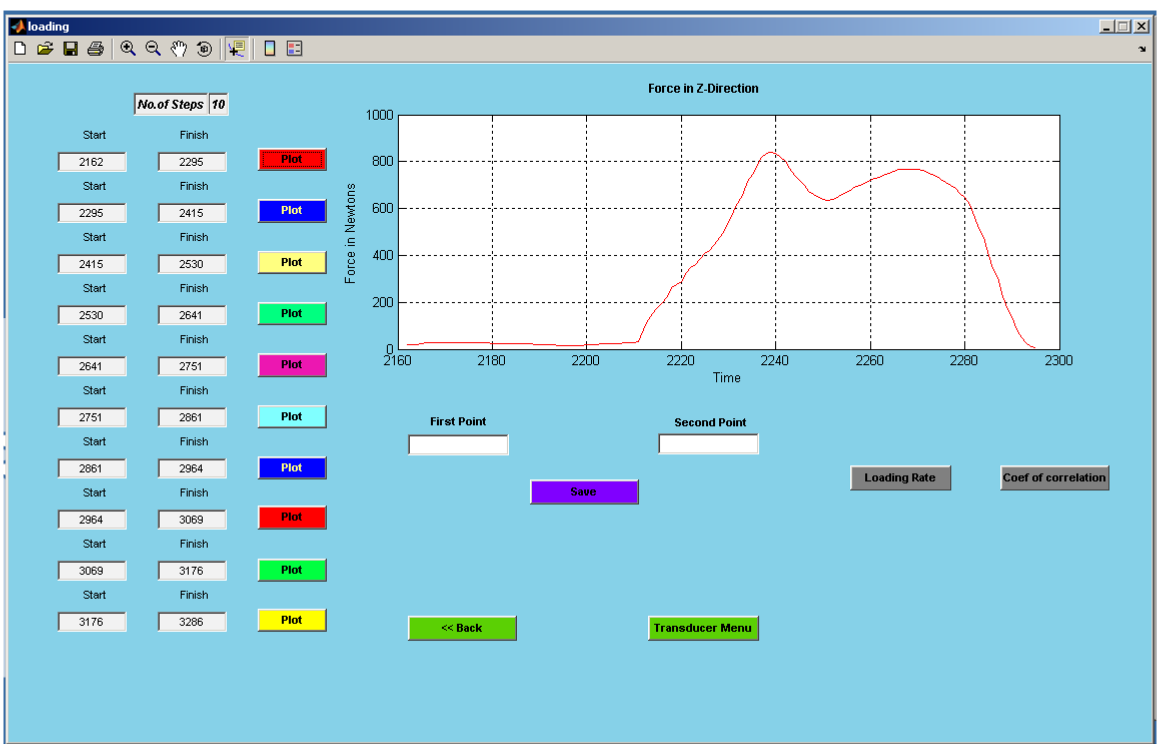

The user has to enter the two points in time to be the starting and ending points for calculating the loading rate. Then the **Save** button must be clicked as shown in the following window.

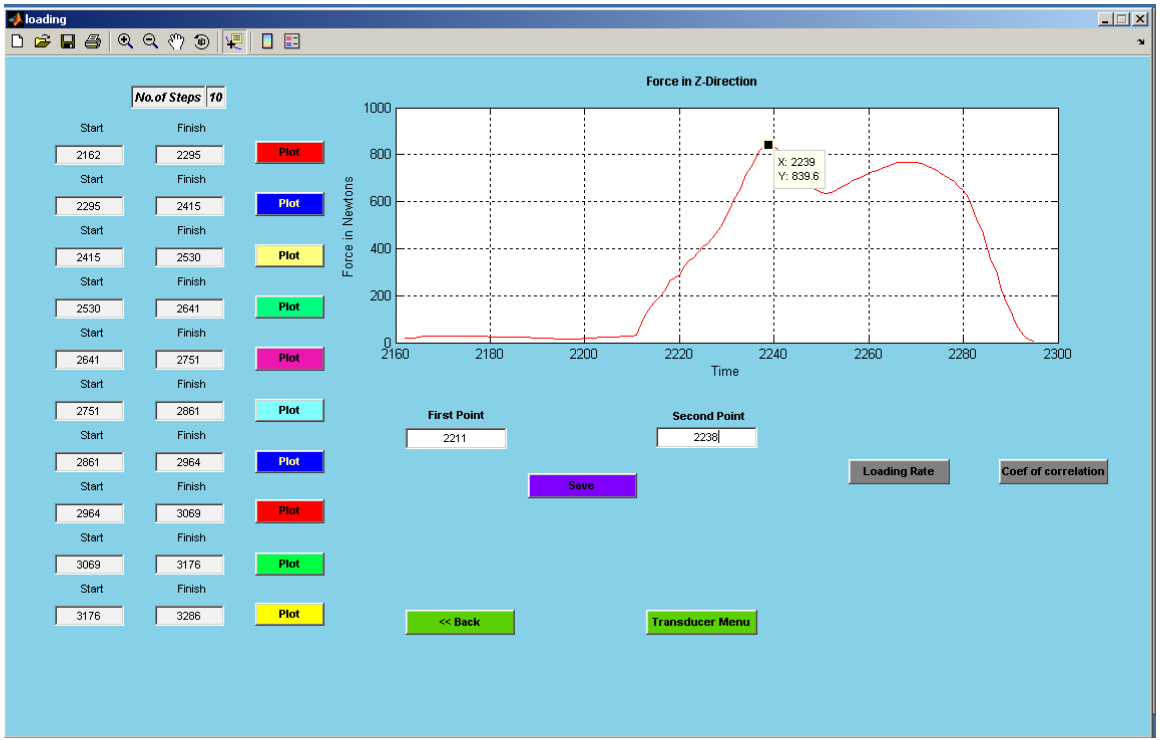

Once user is done with this first step in the sequence of steps recorded by the transducer, he or she should click the **Plot** button, which will display the second step.

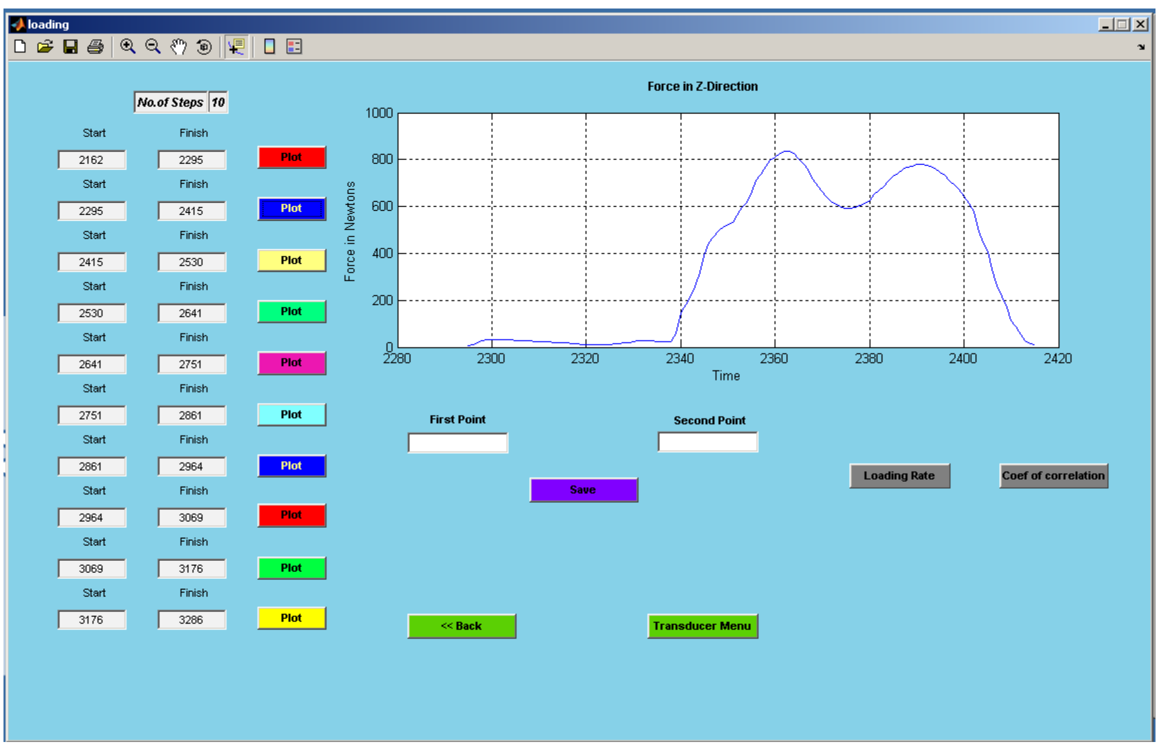

The same procedure has to be followed for calculating the loading rate of the second and remaining steps. After all ten steps are entered in this manner, the user has to click on the **Loading Rate** button and the **Coeff. of Correlation** button, which will compute the mean loading rate over all ten steps as shown below:-

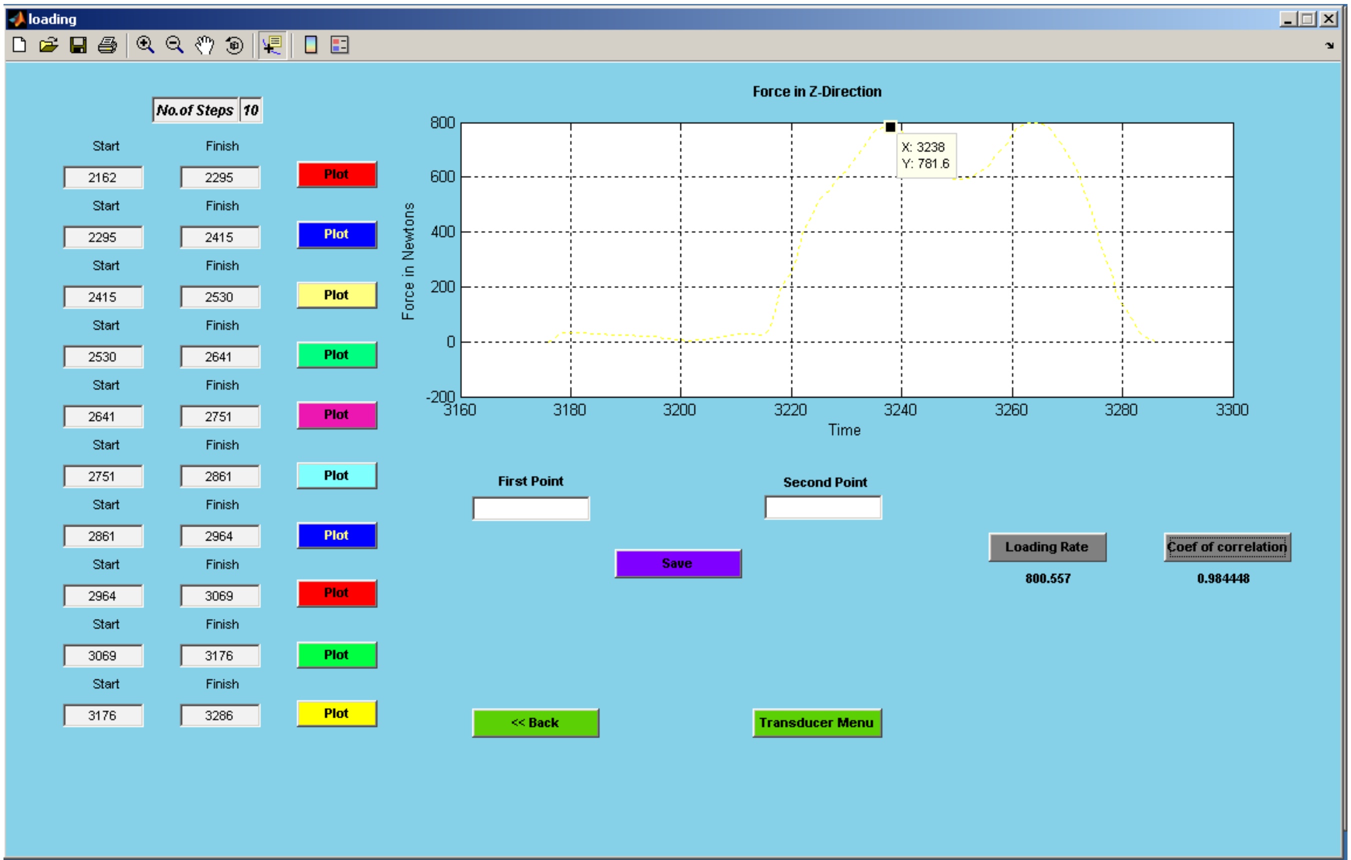

After the loading rate calculations are completed, the pressure sensor data can be analyzed. This is described in the next section

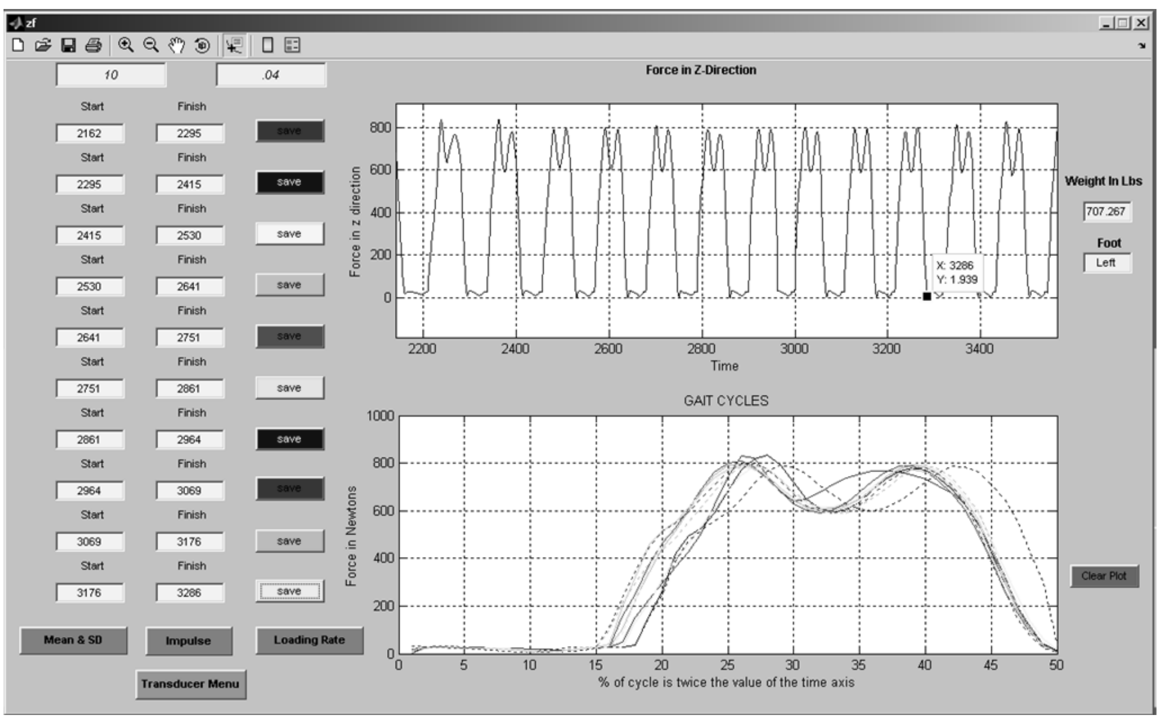

Pressure Data
Before the Tekscan pressure data can be imported into the GUI, the pressure sensor data must be windowed. The method for doing this is explained in the Tekscan manuals. For this chapter, it is assumed that the procedures have been carried out, and a file exists within the **GUI** folder in Excel format. To integrate the socket pressure data into the GUI analysis software the user has to go to the transducer menu and from there to the **Main Menu**. The button for doing this is shown below.

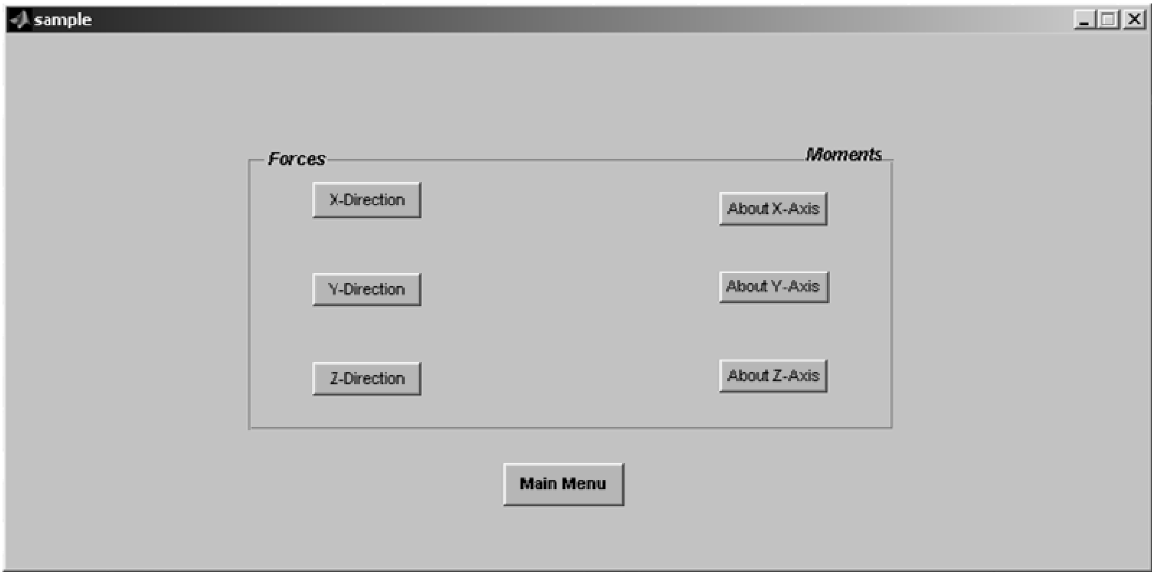

After clicking this button, the main menu will appear as shown below.

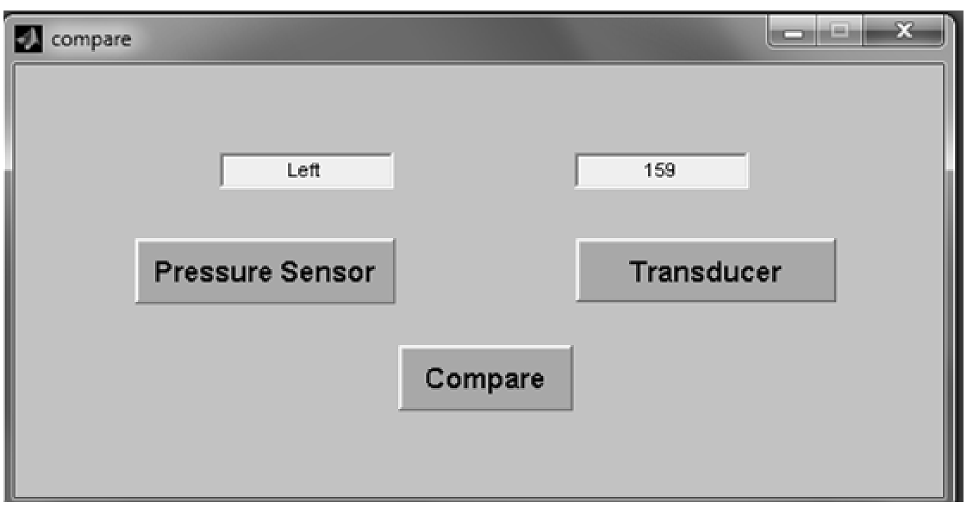

Next the user should select the **Pressure Sensor** option to analyze the pressure data. After selecting the **Pressure Sensor** option the following window appears in which the user has to enter the number of pressure windows exported using the Tekscan software. The full window for the entire array should be included as one of these.

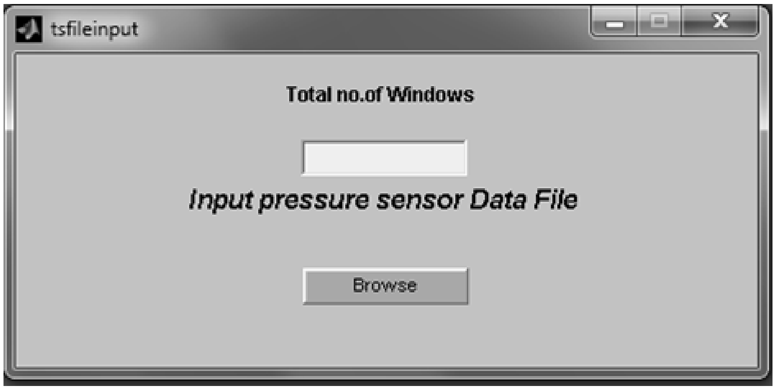

After entering the number of windows, selecting the **Browse** option opens the following window and allows the user to select the pressure data file, which needs to have all the windowed pressure data produced from the Tekscan software.

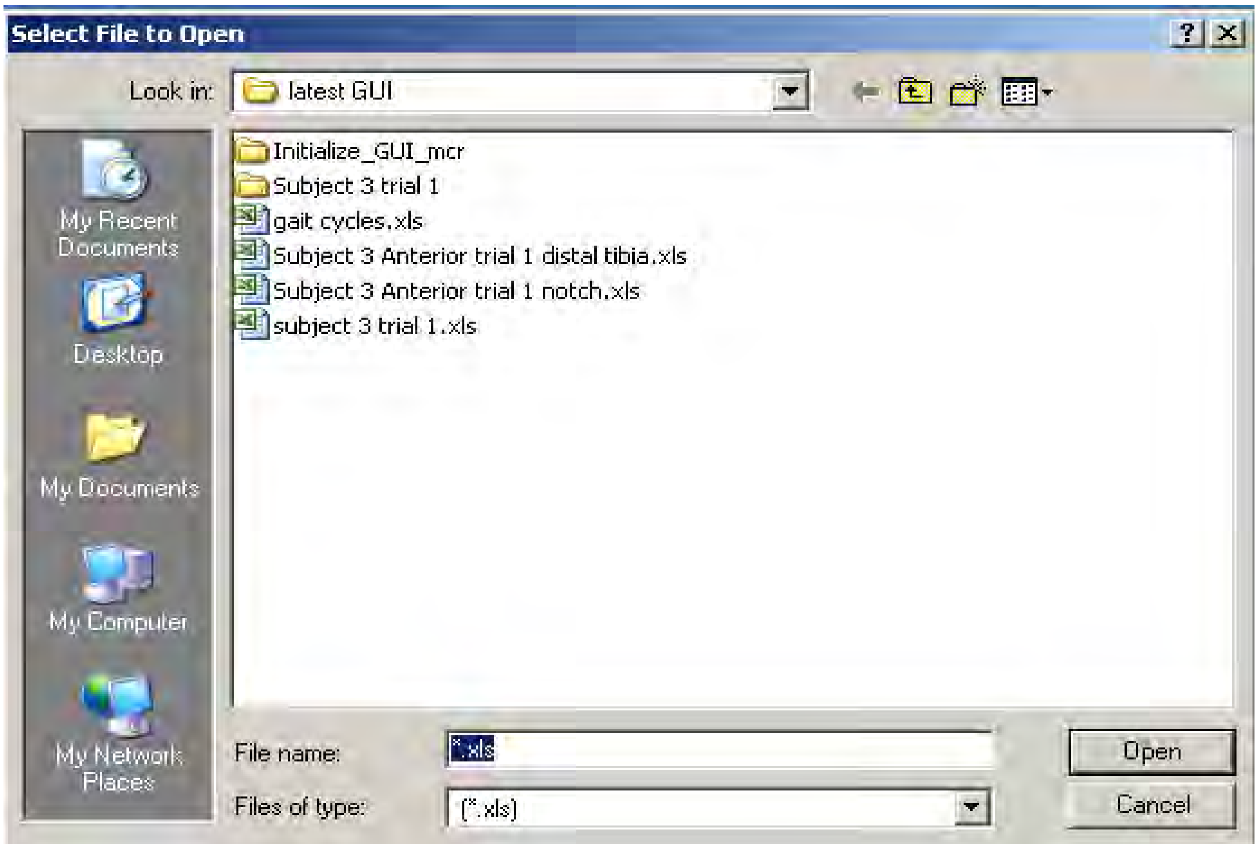

After selecting the pressure data file, the windowed pressure data will be displayed as shown below:

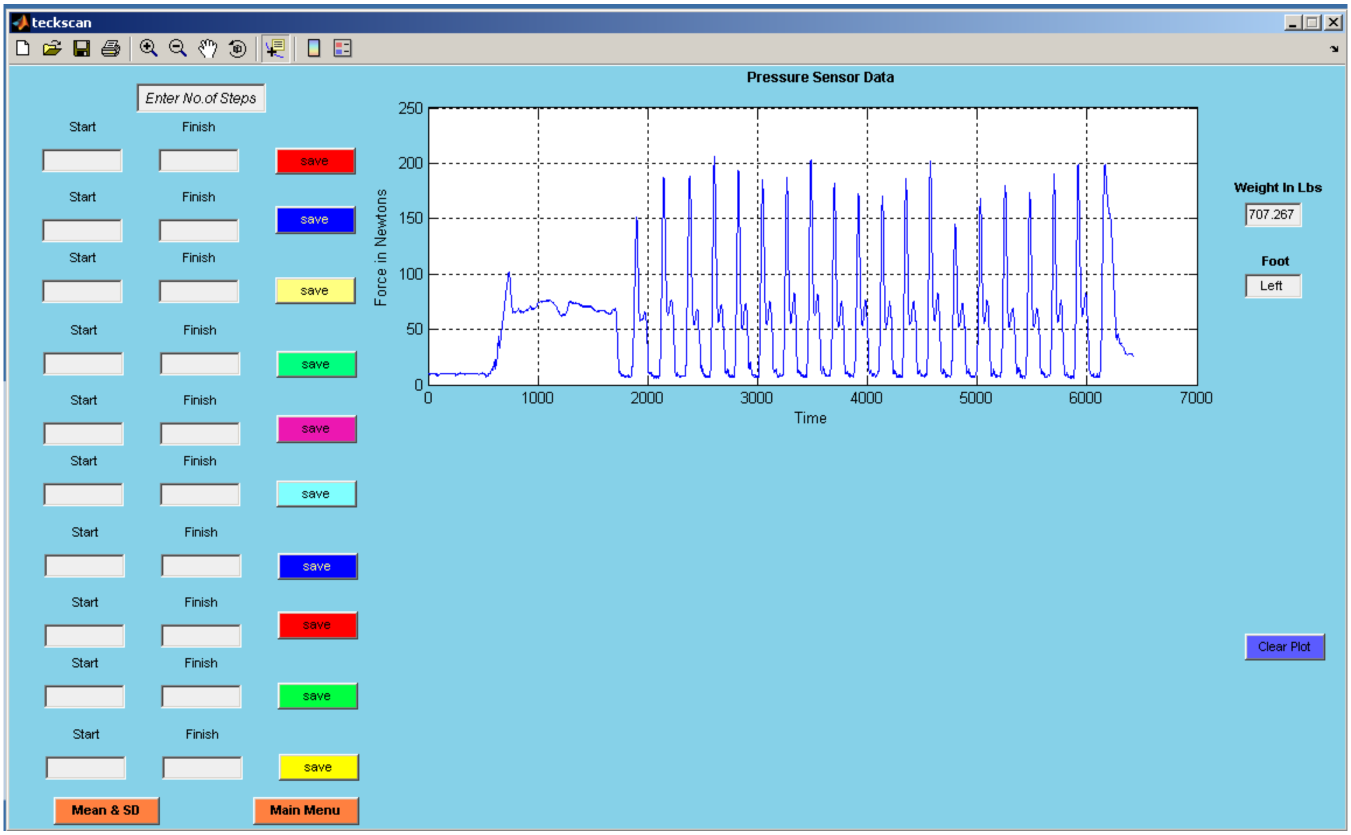

Similar to the processing of transducer data the user has to select the time domain x coordinate values of the start and end points for each step and enter them into the corresponding text boxes using the **Zoom** and **Data cursor** options from the toolbar located at the top of the window.

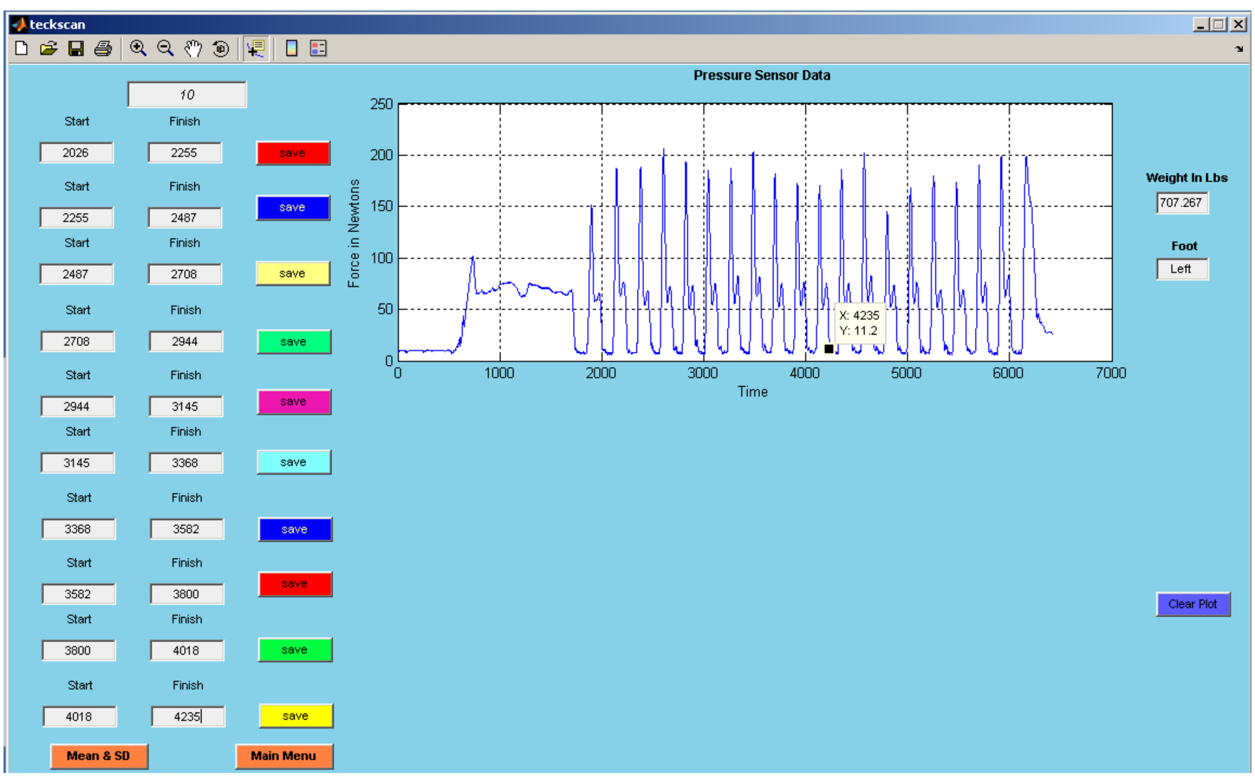

After entering the start and end points of all ten steps the user has to click on the **Save** buttons to obtain a plot that overlays all of the pressures for the ten steps, as shown in the window below:

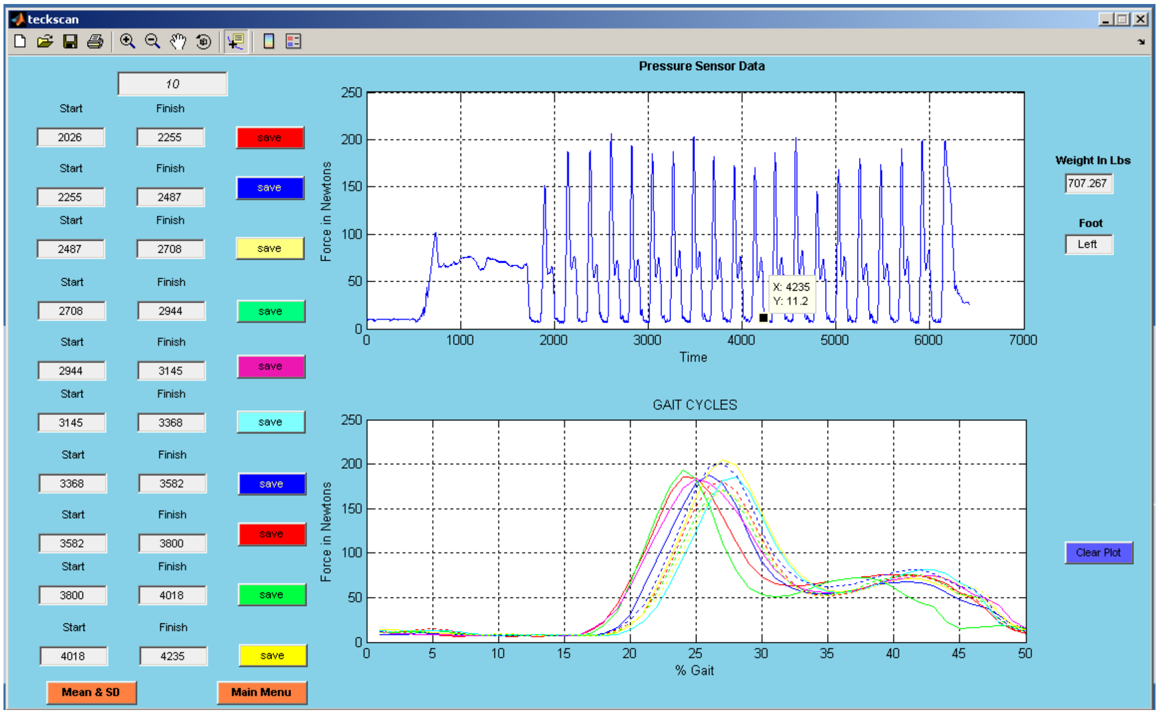

The mean and standard deviation of the ten steps can be calculated using the **Mean & SD** button in the window and the following plot will be displayed.

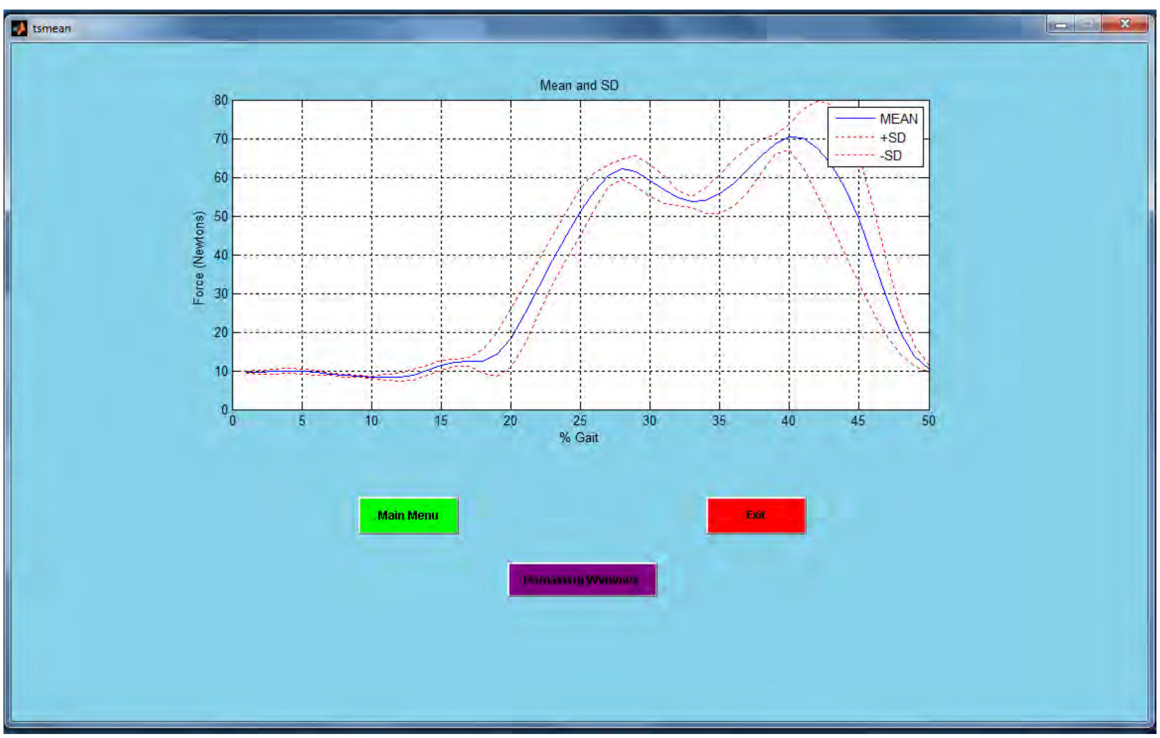

Next the user has to click on the **Remaining Windows** button to analyze the mean of remaining windows as shown in the following window.

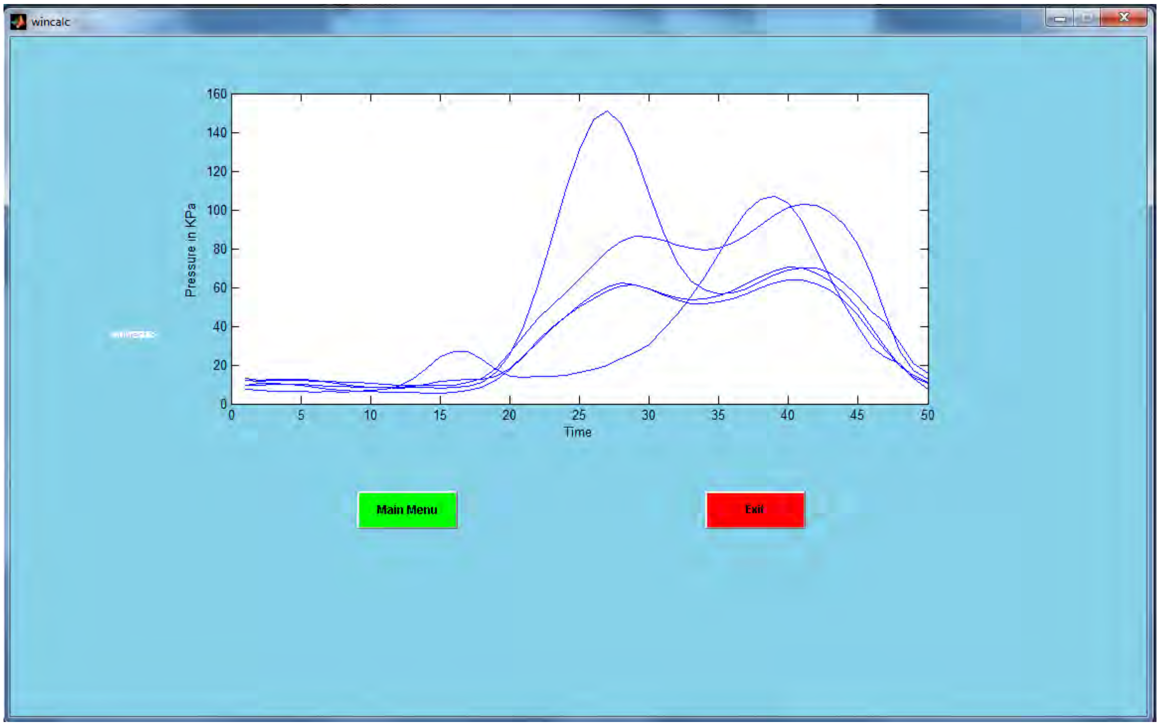

Next the user has to go back to the **Main Menu** in order to compare the transducer data and pressure data.

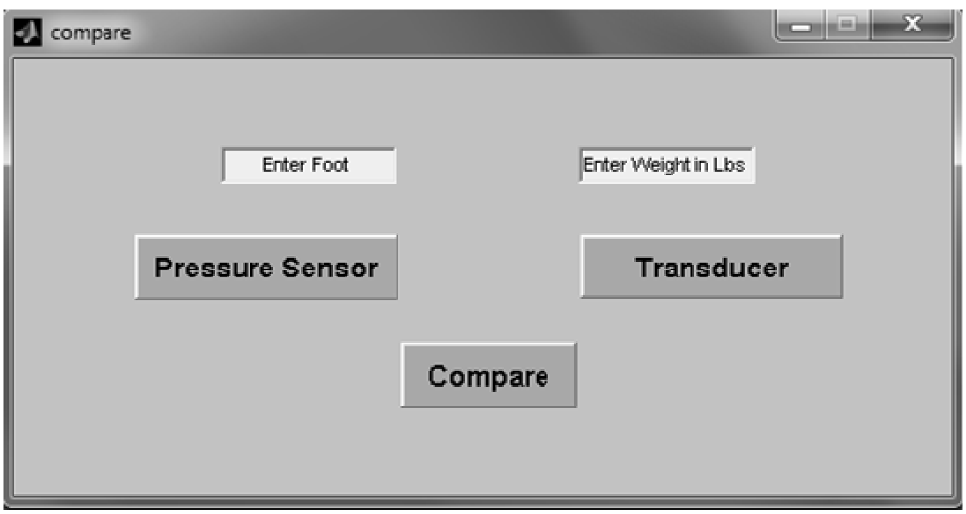

Clicking on the **Compare** button will open the following window showing the pressure data plotted in kPa and the display buttons which allow different options for selecting a particular force or moment from the transducer data.

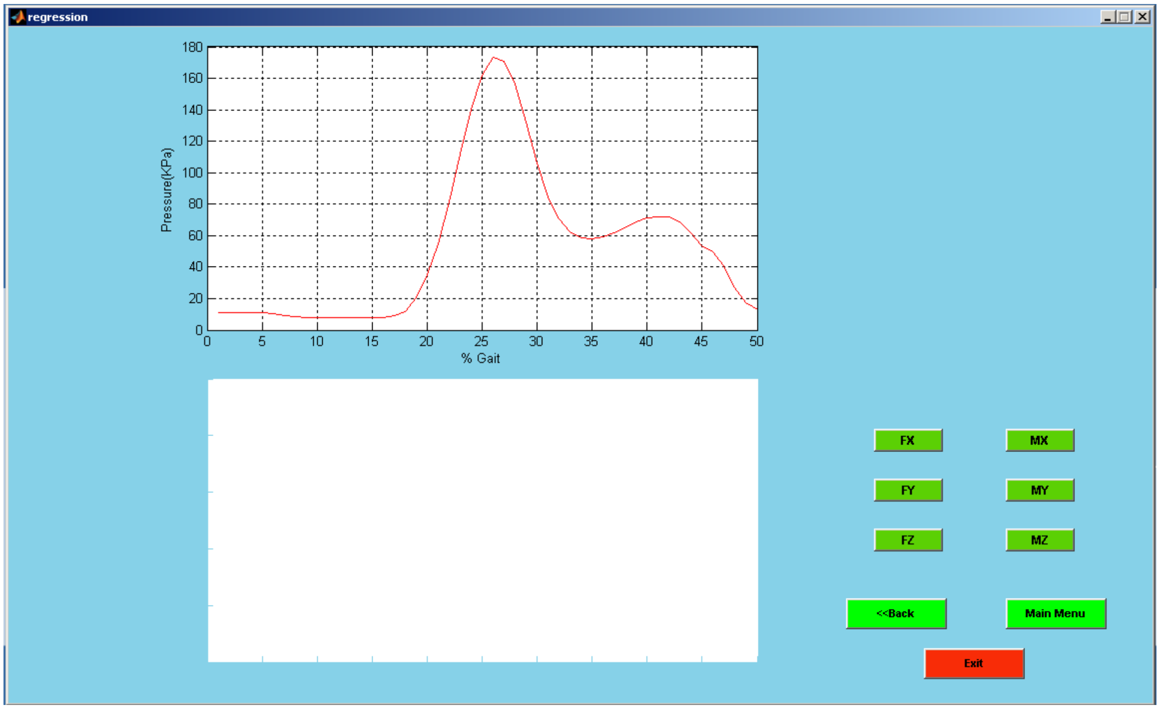

A plot of the force or moment will be displayed in the second window. If the user has selected FX, from the options provided, the plot will appear as below. [Note that in the following plots, the pressure curve displayed in the upper plot area does not change.]

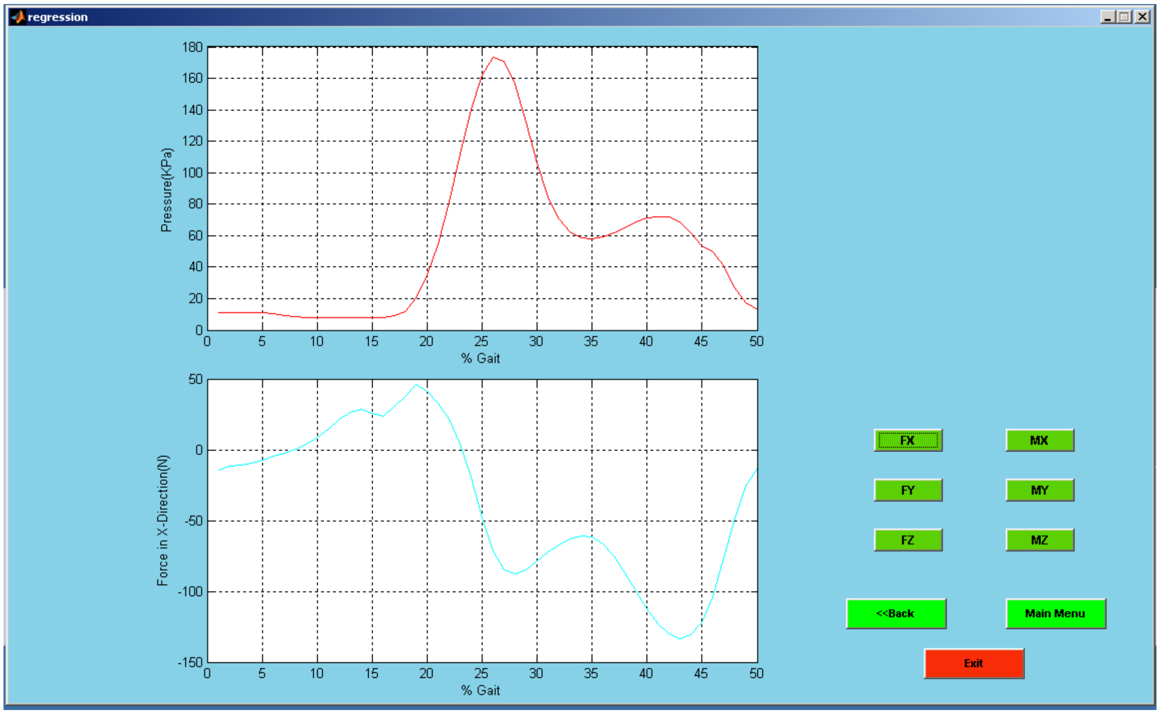

If the user selects **FY,** the following plot will be displayed in the lower plot area.

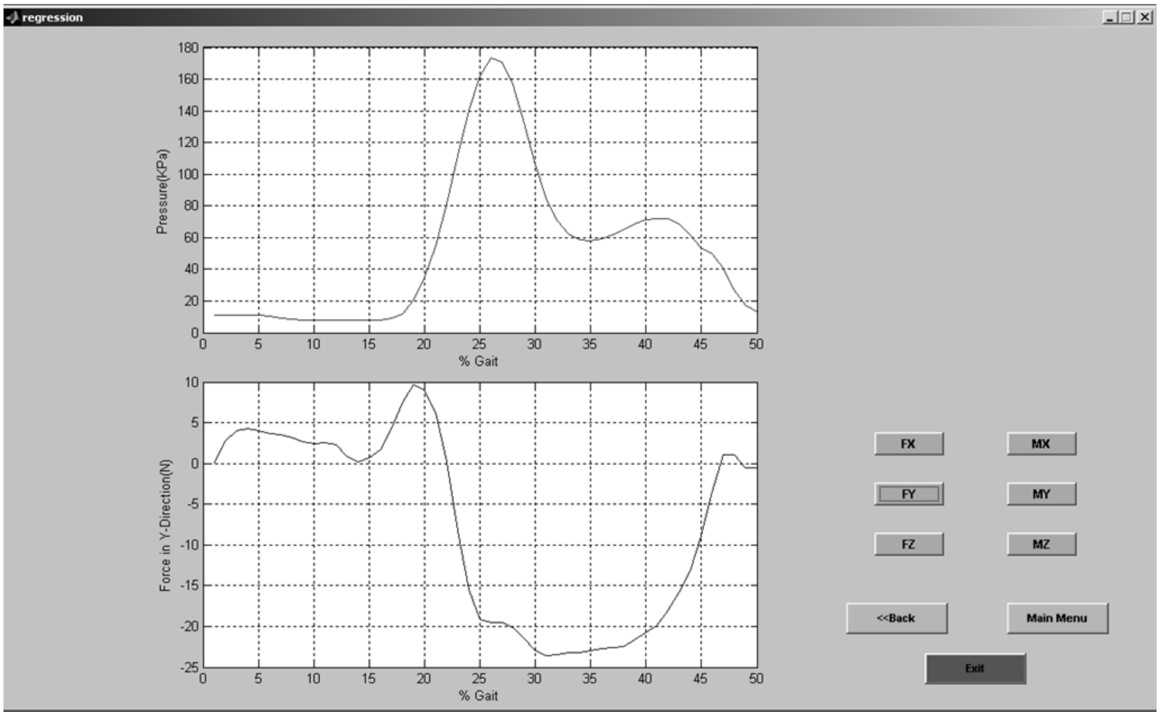

If the user selects **FZ,** the following plot will be displayed in the lower plot area.

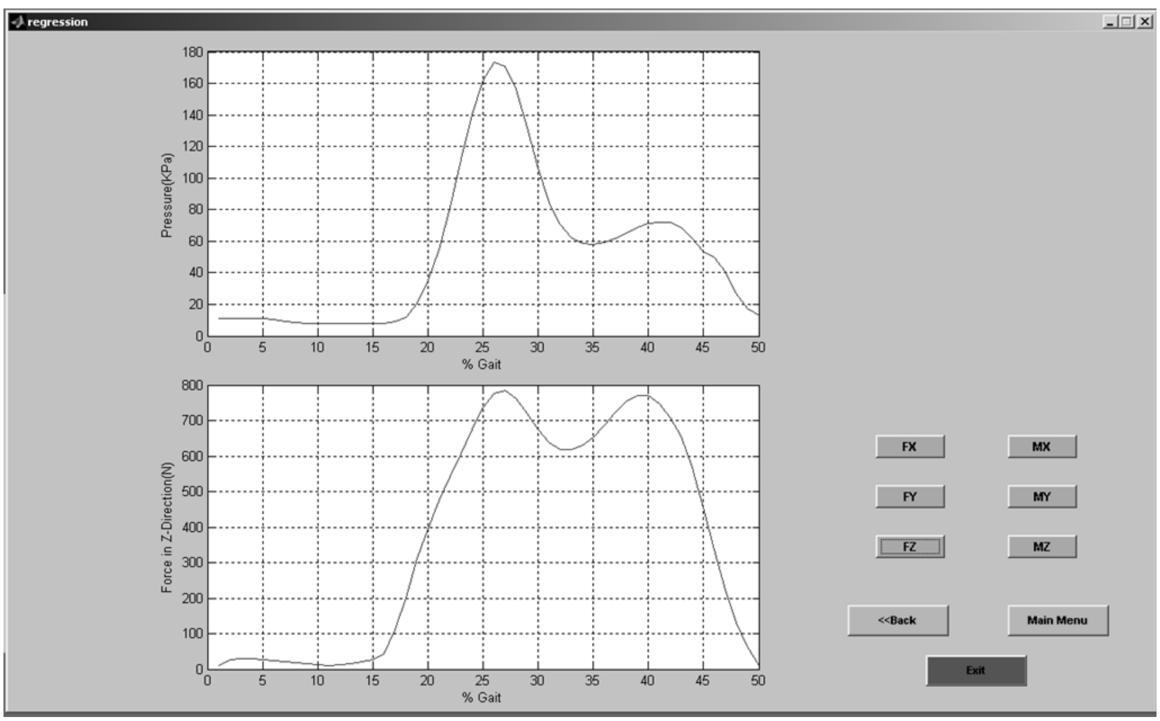

The following plot will be displayed in the lower plot area if the user selects **MX** from the options provided.

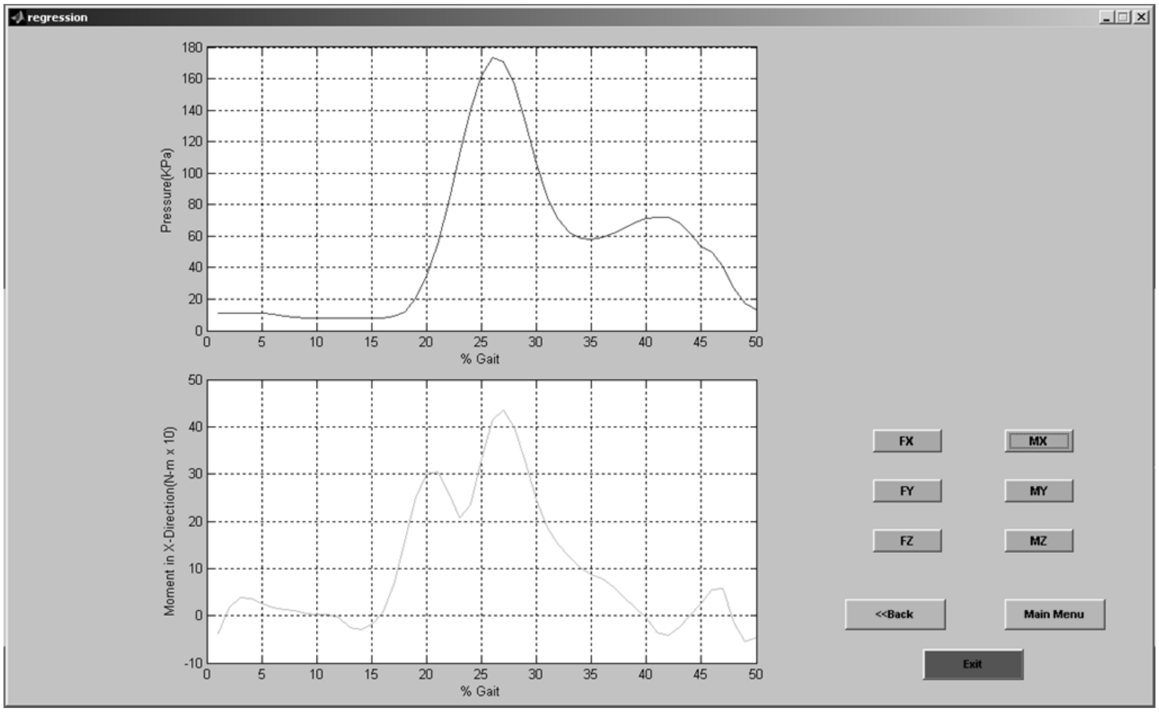

The following plot will be displayed in the lower plot area if the user selects **MY** from the options provided.

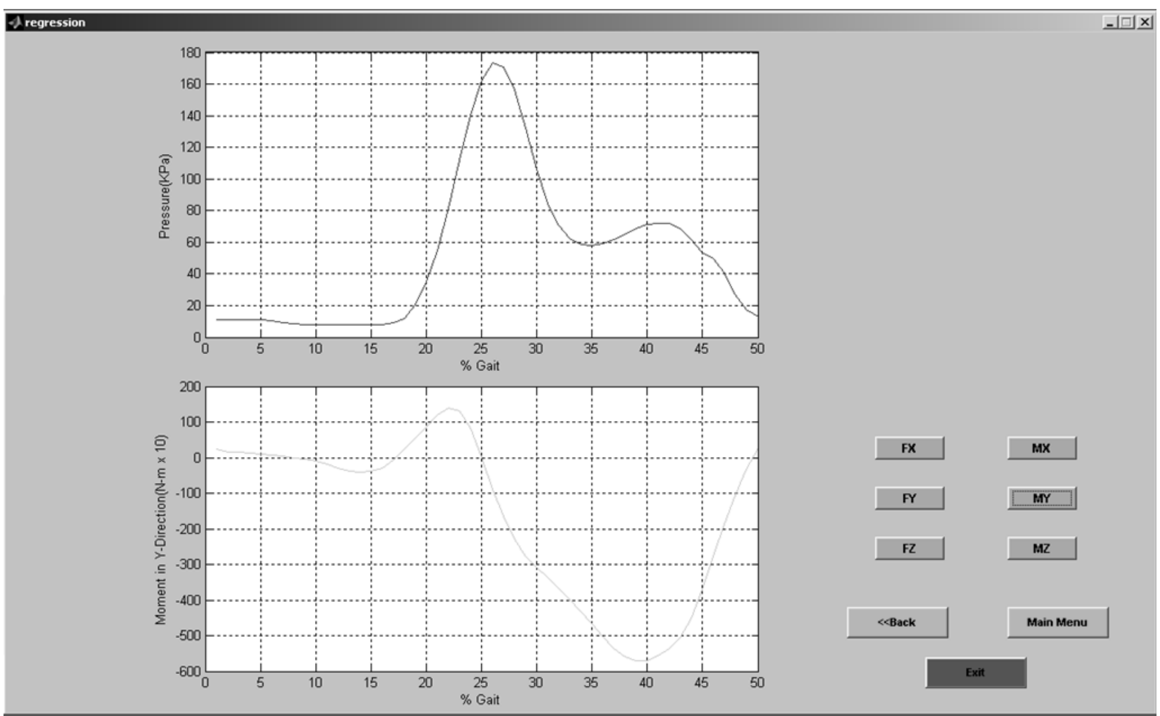

The following plot will be displayed in the lower plot area if the user selects **MZ** from the options provided.

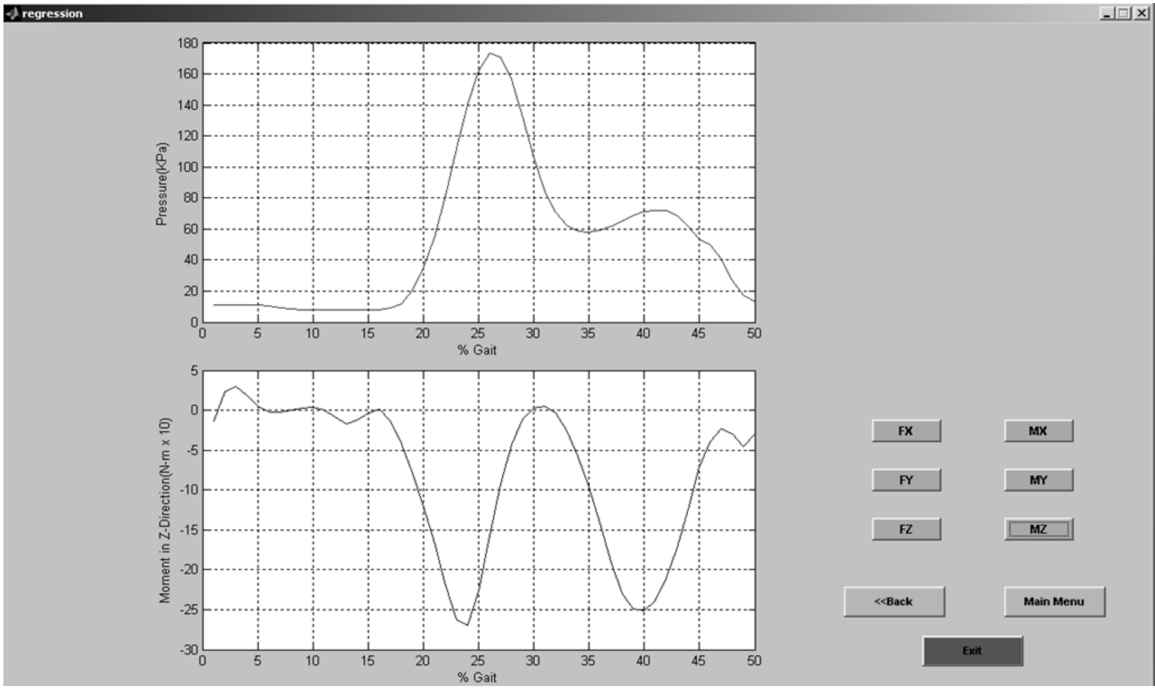

After comparing both the transducer data and the pressure data, the user has to return to the main menu to export all the files.

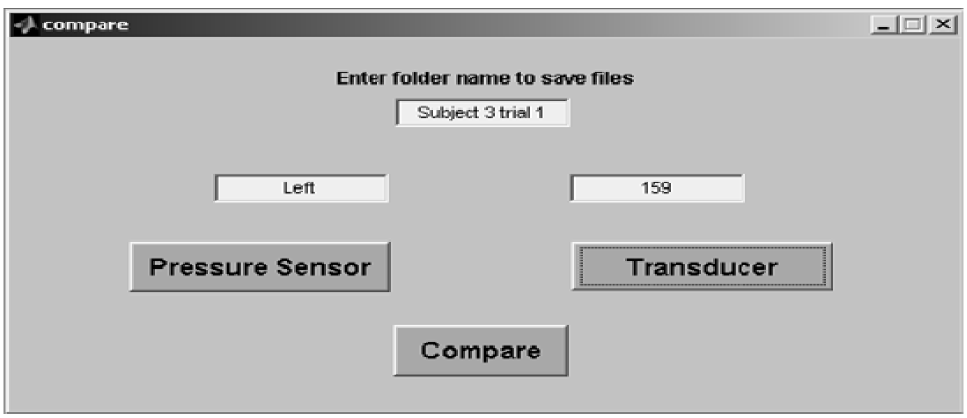

After saving these files, the **GUI** folder will appear as follows:

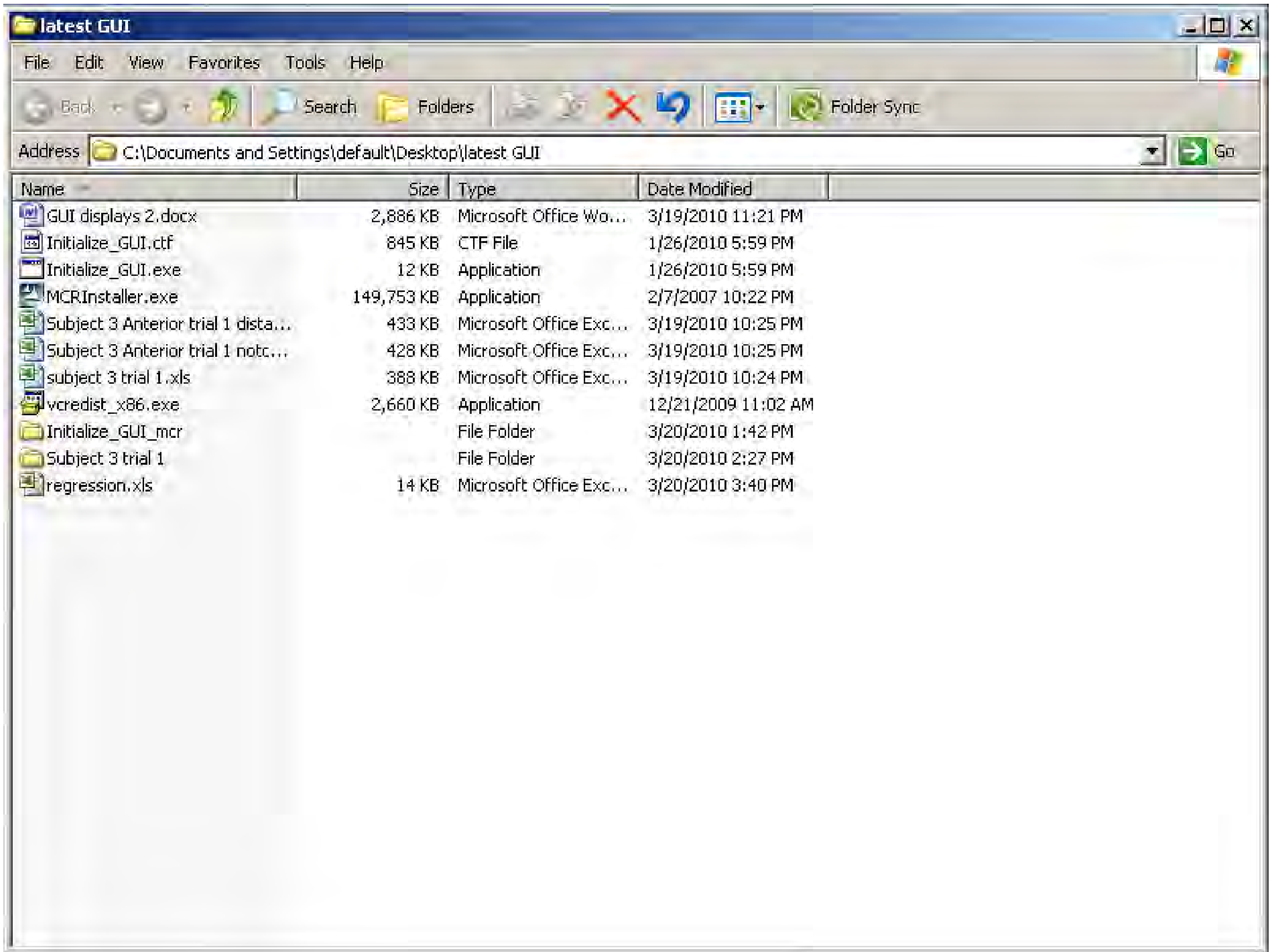

Before using the pressure sensor option of the GUI the user has to export all windowed data from Tekscan software following the instructions provided by Tekscan. Below are the offsets and scaling factors for the transducer used in the research.

TRANSDUCER OFF SETS AND SCALING FACTORS

Offset		Scaling Factor
Fx	+45	881/16384 = 0.053771972
Fy	-7	886/16384 = 0.054077148
Fz -	226	1765/16384 = 0.10772705
Mx	+34	974/16384 = 0.059448242
My	+6	997/16384 = 0.06085205
Mz +5		1046/16384 = 0.063842773

Appendix B – A Notch Center Approach to the Measurement of Alignment for Transtibial Prostheses

The alignment method developed for this study bases all measurements on the notch, rather than the center of the socket. Reasons for this are

1. Loads are transmitted from the prosthetic foot to the knee via the tibia. The tibia is located at the anterior of the residual limb where skin is thin, and near the anterior wall of the socket, not at the center of the socket. The notch is the portion of the socket closest to the center of the load bearing surfaces of the tibia and the femur
2. The angular orientation of the tibia relative to the bottom of the foot is of mechanical importance. The angular orientation of the tibial relief of the socket is the best indicator of the angular orientation of the tibia, and this angular orientation occurs directly below the notch.
3. The notch was shown in the pressure models to have a consistent relationship to the My- moment generated at the transducer. The My- moment reflects both the gait preferences of the subject and the mechanical design of the foot.
4. It is relatively easy to measure the position of the notch and angular orientation of the tibia in three dimensions using lasers. It is not easy to determine the center of the socket because it varies with the longitudinal dimension of the residual limb, is hidden from view, and requires careful positioning of a rod inside the socket if the angular orientation of the limb is to be measured as the center of the socket.

This approach to measuring socket alignment was developed because one of the subjects presented with a socket that initially appeared to have a foot that was outset with respect to the socket. Inspection of the socket and alignment revealed that the tibia was nearly centered over the adaptor and foot, but the bulk of the soft tissues were medial to the tibia, and the resulting appearance made the prosthesis appear to be mis-aligned. Figure B-1 below illustrates the socket.

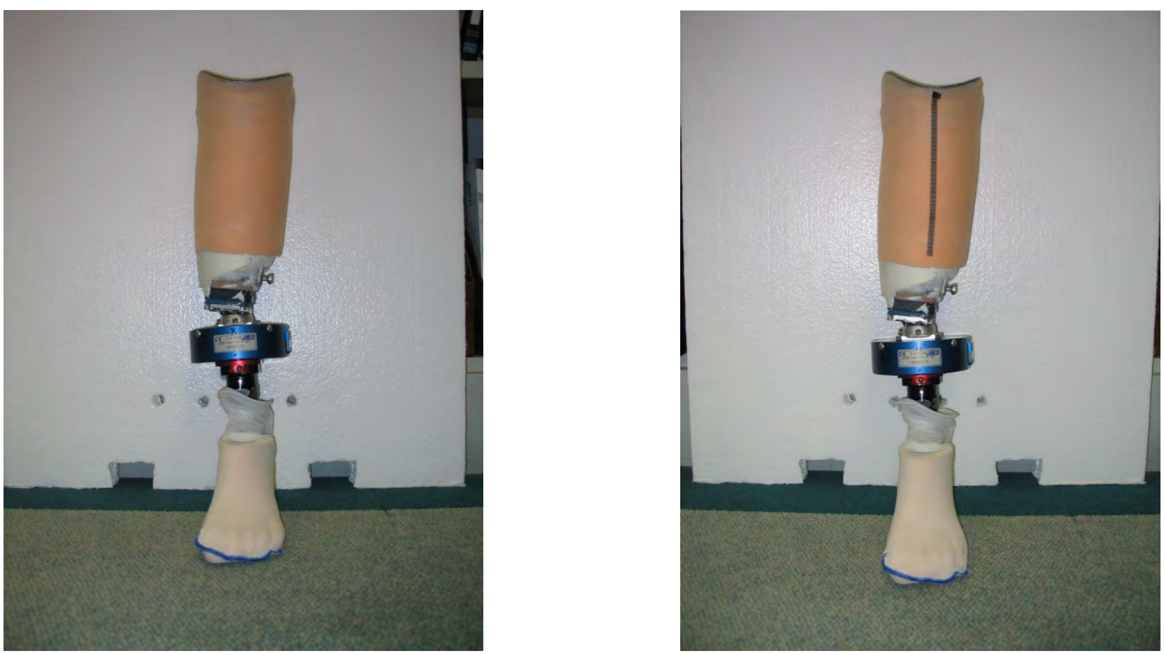

Figure B-1. Left: Prosthesis appears to have an outset foot. Right: Tape indicating the location of the tibia shows it to be nearly centered on the foot.

The procedure for measuring the alignment requires a rectangular flat horizontal surface on which a large sheet of graph paper can be taped, vertical back and side walls, and an inexpensive laser mounted on a tripod. For the study, a sheet of plywood approximately 2 ft X 2 ft was used for the horizontal surface. Lightweight Styrofoam 2 ft X 4 ft insulating panels, purchased at a building supply store, were used for the back and side walls. Large stamped metal book ends, purchased at a business supply store, were modified to provide clamps to hold the Styrofoam panels in place at right angles to each other and horizontal surface. A single piece of tape placed at the top of the sheets by the corner keeps them aligned and perpendicular to each other. Sheets of 18 inch by 24 inch graph paper with ruling were taped to the flat surface taking care to orient the ruled grid lines parallel to the side and back walls. This is important because the laser measurements rely upon use of laser lines that are parallel to the walls. The surface must be leveled using blocks or leveling screws so that the graph paper is horizontal.

The location of the tibial crest is determined by inspecting the socket. This requires examining the inside of the socket, running the fingers over the relief, and establishing the location of the tibial crest on the exterior of the socket with thin, dark tape such as drafting tape. The prosthesis is placed on the graph paper with the toe pointing toward the front and the two vertical walls located at the posterior of the foot and either the medial or lateral side of the foot. The heel of the foot is elevated to the correct height to ensure that the top of the foot is level; for example, if the heel height is 3/8 inch, then the lift should be 3/8 inches thick. The blocks used to elevate the heel should not extend beyond the edge of the area where the foot comes into contact with them. As the last step in the measurement procedure, the outline of the foot will need to be traced on the graph paper, and it is important that the outline at the heel be traced. Blocks should not extend into the area where the outline will be traced. Allen wrenches are inserted into the socket adaptor to help visually orient the foot on the graph paper. The Allen wrenches are viewed from above and the foot rotated to line the shafts of the wrenches up with the axes of the graph paper. The Allen wrenches must be viewed from directly above because they will not be horizontal when inserted into the Allen screws. If they are viewed from an angle, and not from directly above, it will be difficult to determine when they are parallel to the grid lines. When the foot is oriented correctly on the graph paper the Allen wrenches should be parallel to the ruled grid lines on the paper, so that the axes of the Allen screws are parallel to the ruled lines. This orients the prosthesis so that the socket flexion-extension and abduction-adduction axes are parallel to the ruled grid lines of the graph paper. A weight is placed on the forefoot of the prosthetic foot so that the foot rests flat on the graph paper. A small heavy sack works well, but any heavy object such as a brick that does not distort or damage the foot will also work. A properly oriented foot has the following characteristics: the forefoot is flat on the horizontal surface and stable, with the heel elevated to the correct height to make the top of the foot parallel to the graph paper, and the axes used to flex and extend the socket are parallel to the grid lines of the graph paper. The axes should then also be parallel to the posterior wall of the measurement unit, and the posterior wall should be perpendicular to both the graph paper and adjacent wall. The alignment will be measured with the foot in this position. If the pylon is not vertical when the foot is in this position, this is acceptable and will be reflected in the measurements of the notch location. This orientation of the foot assumes that all measurements should be made with the bottom of the forefoot horizontal and flat on the base.

A small, inexpensive laser construction level with level bubbles mounted on a short tripod, a 1-meter metric rule, and a protractor or level with angular measurement capabilities are used to take all the measurements. These can be obtained for under $100. Measurements can be taken in any order. Following is the order in which measurements were taken for this study.

1. The location of the notch in the horizontal plane (medial-lateral location) is established by rotating the laser line to the vertical position and moving the tripod left or right in front of the foot so that the line is simultaneously visible on both the graph paper and the notch. It is important that the laser line remains parallel to the grid lines on the graph paper. The laser line must be vertical, which should be the situation if the laser unit has been rotated in the manner described in its operating manual and the unit has been leveled correctly using its leveling bubbles before rotation. The tripod is moved to a position where the vertical laser line bisects the notch and its projection on the graph paper is parallel to the grid. The location of the projected line on the graph paper is marked on the graph paper.

2. The elevation of the notch is determined using the metric rule. Without moving the tripod, the laser unit is rotated so the line is again horizontal, and its angular orientation is changed using the head of the tripod until the line bisects the notch. The metric rule is placed to the immediate left or right of the prosthetic foot in line with the notch so that the intersection of the laser line with the rule can be observed. It is important that the rule not be positioned anterior or posterior to the notch so that the laser line intersects the rule at the same height as the notch. This can be done most accurately if the location of the notch along the anterior-posterior axis is established first (Step 3 below). The height is recorded on the graph paper.
3. The laser level and tripod are moved to the side of the horizontal surface and aimed at the side of the prosthesis. The laser unit is rotated so that the line is vertical, and the tripod is shifted left or right so that the vertical laser line just grazes the notch and is parallel to the grid lines on the graph paper. This can be determined by holding a sheet of cardboard on the far side of the notch and noticing the appearance of the line on the paper. The notch will block the laser line if it is too far posterior, and not reveal any blocking if the laser line is too far anterior. The laser unit is shifted until it just grazes the notch and begins to block the line. The red line of the laser should just graze the notch and illuminate it with diffused light. The laser is then rotated back to produce a horizontal line and leveled using its leveling bubbles. The laser unit is then rotated back to the vertical position again, and the previous steps repeated until all three of the following conditions are met: a.) the laser unit is level, b.) the vertical laser line just grazes the notch, and c.) the projected vertical laser line is parallel to the grid lines of the graph paper. When these conditions have been met, the location of the projected laser line on the graph paper is marked. The intersection of this line with the line established on the graph paper in step1 defines the center of the notch with respect to the foot.
4. The flexion of the socket is measured next. The laser unit is rotated until the line parallels the tape attached to the front of the socket that marks the tibial crest. The projection of this line can be seen on the opposite wall of the unit. Since the projection of the line on the graph paper must be parallel to the grid, and the tripod may have to be shifted left or right, care must be taken to ensure that the laser unit remains leveled. It is most accurate if the laser line just grazes the tape on the notch, and this can be achieved using the methods described for Step 3 above. While this may seem challenging, if the surfaces on which one is working are level, it requires only a few iterations. Once the rotated line just grazes the tape, the projection of the line is parallel to the grid lines on the graph paper, and the laser unit is level, the projection of the laser line on the side wall is marked with thin tape. The tape allows measurement of the angle of this line with respect to vertical using the protractor or an electronic level. If a cosmetic cover distorts the angle, then a straight object like a rule or dowel must be placed inside the socket to approximate the angle of the tibia. Small pieces of putty or Play Dough may be used to secure the object to the socket wall. It must be parallel to the tibia as defined by the interior wall of the socket.
5. The adduction-abduction of the socket with respect to the vertical is determined by returning the laser unit and tripod to the anterior of the socket as in step 1 above. The laser unit is rotated until its line bisects the tape on the anterior of the socket that marks the location of the tibial crest. Again, a series of iterations may be necessary to meet the following requirements: a.) the laser unit is level, b.) the angled laser line just bisects the tape on the tibial crest, and c.) the projected laser line is parallel to the grid lines of the graph paper. Once these conditions have been met, the projection of the laser line on the back wall is marked with thin tape. As mentioned in step 4, this tape line will be used to measure the angle of the line with respect to the vertical.
6. The locations, heights, or angles of any other components for which measurements are desired should be taken using similar procedures.
7. The vertical projection of the foot on the graph paper is recorded. This requires care because the edges of the foot are curved, and it is easy to inadvertently angle the pencil or marker when tracing the outline of the foot. If this becomes a problem, one solution is to attempt to trace the points where the foot contacts the graph paper by angling the pencil or pen, and then attempt to trace the vertical projection of the foot as carefully as possible for comparison. To make the tracing, the weight will have to be removed from the forefoot and the prosthesis steadied so that the foot does not change position.

When the preceding measurements have been completed, the prosthesis is removed from the alignment measurement unit and the location of the notch is translated to a foot-based coordinate system.

8. A line crossing the outline of the heel at its thickest point that is approximately perpendicular to the long axis of the foot is constructed and its midpoint is marked on the graph paper. A line crossing the outline of the forefoot at its thickest point that is approximately perpendicular to the long axis of the foot is constructed and its midpoint marked on the graph paper. A line connecting these two midpoints is constructed and extended to the edges of the foot. The line should appear to bisect the heel and approximately bisect the second toe. Its length should be very close to the known length of the foot.

9. The location of the notch in the coordinate system of the graph paper is determined by extending the two lines established with the lasers in Steps 1 and 3 above. Their intersection is marked on the graph paper. A perpendicular line is then constructed from this point to the line bisecting the foot that was established in Step 8. The point where the perpendicular line intersects the foot bisector is the location of the notch with respect to the longitudinal anterior-posterior axis of the foot, and the length of the perpendicular line is the offset of the notch from the longitudinal anterior-posterior axis. This foot-based coordinate system allows determination of the point of application of notch pressure with respect to the forefoot, which the regression models show as related to the negative My moment created by interaction between the mechanical design of the forefoot and the gait characteristics of the amputee. It can be reported as the per cent of the length of the foot bisector line as measured from the heel.

10. The following measurements can then be taken from the graph paper and tape placed on the walls of the alignment measurement unit: a.) the angle of the foot bisector with the axes of the Allen screws that control socket flexion and extension (internal or external rotation of the foot with respect to the adaptor; b.) the flexion-extension angle of the socket with respect to the Allen screws that control socket angular orientation in the sagittal plane; and c.) the adduction-abduction angle of the socket with respect to the Allen screws that control socket angular orientation in the frontal plane.

The table below reports the neutral alignment measurements for the three SACH feet and TruStep foot used in the perturbation experiment.

	Subject 1	**Subject 2**	**Subject 3**	**Subject 4**
Type of Foot	TruStep (Left)	SACH (Left)	SACH (Left)	SACH (Right)
Heel Height	3/8 inch	3/8 inch	3/8 inch	3/8 inch
Length	27 cm	27 cm	23 cm	27 cm
Notch Longitudinal Location, %[1]	52.2 50	.7	46.5	51.9
Notch Offset[2]	2 mm lateral	8 mm lateral	4 mm medial	5 mm lateral
Foot rotation[3]	3.6° external	1.1° external	2.0° internal	7° external
Notch Height	46.5 cm	51.0 cm	48.5 cm	47.5 cm
Flexion-Extension Angle of Tibia[4]	15° flexion	6° flexion	5° flexion	5° flexion
Abduction-Adduction Angle of Tibia[4]	0°	4° adduction	0°	7° adduction

Table B-1. Subject Transtibial Prosthesis Neutral Alignment

Notes: 1. Per cent of distance along foot bisector from heel; 2. Perpendicular distance from line bisecting the foot; 3. Angle from axis of socket abduction-adduction; 4. Flexion means an orientation of the tibia to the posterior from vertical at the notch (socket flexion), and extension means a tilting of the tibia to the anterior from vertical from the notch (socket extension). Adduction means a tilting of the tibia to the medial side from the notch (socket adduction means the same thing – the brim is tipped lateral at the adaptor) and abduction means a tilting of the tibia to the lateral side from the notch (socket abduction means the same thing – the brim is tipped medial at the adaptor).

The figures on the next page illustrate the alignment measurement procedures.

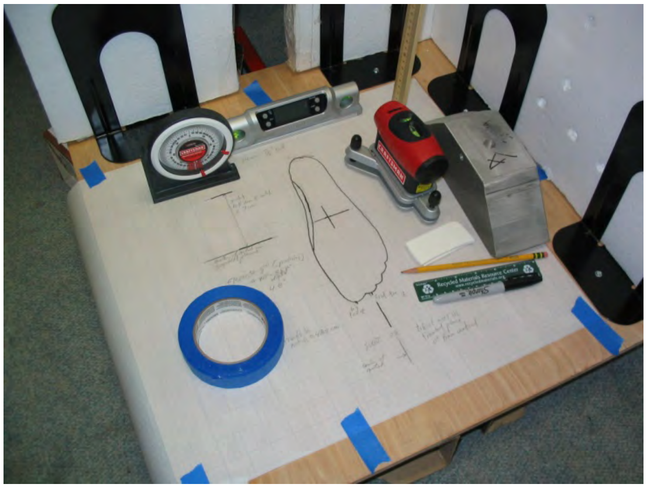

A.

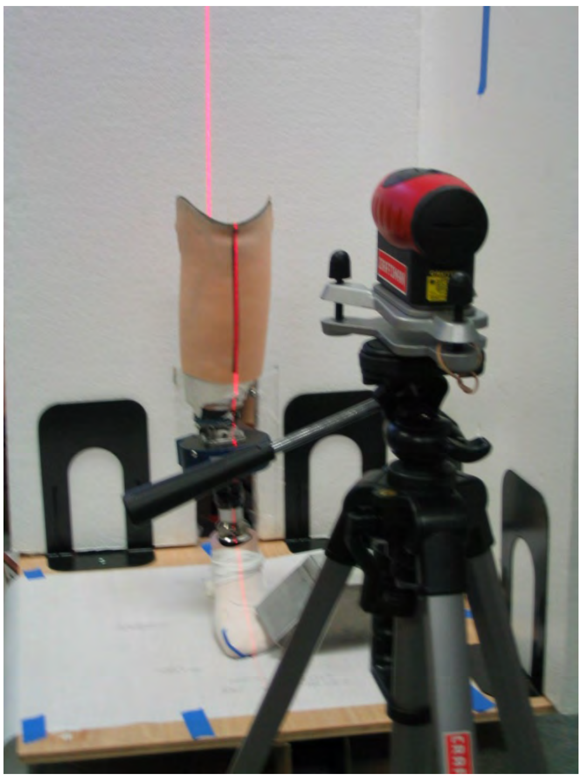

B.

C.

Figure B-2. Alignment Procedures

A. Set up showing vertical walls, instruments that are used, weight to keep foot flat on the graph paper, and the outline of the foot. The + marks the location of the notch as projected to the horizontal plane. The vertical walls are lightweight Styrofoam held to the base with modified book ends.

B. Measurement of the medial-lateral location of the notch center in the frontal plane. The abduction-adduction angle of the tibia would be measured by rotating the laser unit and placing tape on the back wall along the laser line.

C. Measurement of the flexion-extension angle of the tibia. A straight object such as a rule or stick may need to be placed inside the socket if a cosmetic cover prevents the use of external tape to identify the flexion-extension angle. Note the tape placed on the side wall to facilitate measurement of the angle.